Unravelling lateral root initiation using genome editing in *Arabidopsis*

Ghent University
Faculty of Sciences

MSc. Nick Vangheluwe

Thesis submitted as partial fulfilment of the requirements for the degree of
Doctor (Ph.D) in Sciences: Biochemistry and Biotechnology

Academic year 2020-2021

Promoter:
Prof. Dr. Tom Beeckman

VIB-UGent Center for Plant Systems Biology
Root Development Group
Technologiepark 71, 9052 Ghent, Belgium

Examination board

-standing on the shoulders of giants-

Objectives and scope

Research questions on the initiation of lateral root development in *Arabidopsis*

Root branching through lateral root formation is an important component of the adaptability of the root system of plants to its environment. Regular spacing of lateral roots as well as initiation and development of lateral root primordia is tightly regulated. In the model plant, *Arabidopsis*, lateral roots arise from a subset of pericycle cells adjacent to the xylem-pole in the primary root that were specified into lateral root founder cells. The first visible event of lateral root initiation in *Arabidopsis* is the simultaneous migration of nuclei in neighbouring founder cells. Subsequent cell cycle activation is essential for founder cells in the pericycle to undergo formative divisions resulting in the development of a lateral root primordium.

Despite the detailed description of cellular events taking place during lateral root initiation in *Arabidopsis*, important questions remain about the molecular mechanisms controlling these events. This PhD research aims to address three research questions:

- What are the molecular mechanisms controlling asymmetric cell divisions in the xylem-pole pericycle?
- What is the function of components of the cell cycle machinery in formative cell divisions?
- What are the molecular mechanisms regulating the nuclear migration event in the xylem-pole pericycle?

In view of the complexity of the molecular control on lateral root initiation, the high number of potential regulators involved and the contribution of different tissue layers, solid genetic tools are a necessity to further unravel this process. The recent development of CRISPR technology for genome editing in plants by generating targeted inheritable or somatic mutations opens new avenues to conduct loss-of-function studies. This PhD research will address the abovementioned research questions by developing and employing CRISPR-based genome editing tools for a detailed functional analysis of genes during lateral root initiation. The obtained insights in the molecular control of lateral root initiation will contribute to develop genetic strategies to improve the root system of crops for agricultural purposes. In addition, the adoption of new technologies impacts not only scientific research, but also society and this PhD dissertation highlights the importance of science communication.

Summary

Initiation of lateral root development in *Arabidopsis*, one step at a time

Lateral root formation is a major determinant of root systems architecture. In *Arabidopsis*, lateral roots arise from a subset of cells situated in the pericycle at the xylem poles. These cells undergo - prior to a nuclear migration event - tightly coordinated (asymmetric) cell divisions to generate cell diversity and tissue patterns, resulting in the development of a new lateral root primordium.

In the root development research group of prof. Dr. Tom Beeckman, we are devoted to unravelling the genetic blueprint of lateral root development. Over the past years our knowledge on the different steps of lateral root formation has expanded tremendously. However, the molecular mechanisms directing the different biological processes essential for the early stages of lateral root organogenesis including nuclear migration and formative cell divisions are largely unknown. Although a plethora of mutant collections are available for the model plant *Arabidopsis thaliana*, loss-of-function studies have been hampered because of a lack of knockout mutants, genetic redundancy or genes involved in fundamental processes.

This PhD research aims to identify and study putative molecular components underlying the biological processes involved in lateral root initiation through a forward genetic EMS mutagenesis screen and genome editing with CRISPR.

In Chapter 1, we introduce the current state-of-the-art for lateral root development and elaborate on the technological advancements of CRISPR genome editing to facilitate loss-of-function studies.

In Chapter 2, we describe the functional analysis of *MITOGEN ACTIVATED PROTEIN KINASE 6* (*MPK6*) as signalling component of the *GOLVEN 6* (*GLV6*) peptide signalling pathway to study the molecular mechanisms controlling the first asymmetric cell divisions essential for lateral root initiation.

In Chapter 3, we analyse the role of multiple *CYCLIN-DEPENDENT KINASES* (*CDKs*) during lateral root initiation through a CRISPR-based lateral root specific knockout system (CRISPR-TSKO) that we have developed through collaboration.

In Chapter 4, we investigate the function of *NUCLEAR MIGRATION 1* (*NMig1*) in the process of nuclear migration as this process is observed at the onset of lateral root initiation in two neighbouring xylem-pole pericycle cells preceding the first asymmetric cell division.

In Chapter 5, we synthesize and discuss the obtained scientific results and contextualize our observations in the current state of available knowledge on lateral root initiation. Finally, we reflect upon future prospects and share societal implications of the PhD research.

Samenvatting

Initiatie van zijwortelontwikkeling in *Arabidopsis*, stap voor stap

Zijwortelvorming is een bepalende factor van de architectuur van het wortelsysteem. In *Arabidopsis* ontstaan zijwortels uit een aandeel van cellen gelokaliseerd in de pericyclus ter hoogte van de xyleem polen. Deze cellen ondergaan - voorafgaand aan een migratie van de kernen – gecoördineerde (asymmetrische) celdelingen die diversiteit aan cellen en weefselpatronen genereren resulterend in de ontwikkeling van een zijwortelprimordium.

In de onderzoeksgroep van prof. Dr. Tom Beeckman genaamd 'Wortelontwikkeling' verrichten we onderzoek om de genetische informatie voor zijwortelontwikkeling te ontrafelen. De afgelopen jaren is onze kennis over de verschillende stappen van zijwortelvorming omvangrijk toegenomen. Daarentegen is er weinig kennis over de moleculaire mechanismen die de verschillende biologische processen aansturen essentieel voor de eerste stappen van zijwortel orgaanvorming waaronder nucleaire migratie en celdelingen. Er is een uitgebreid aanbod aan mutanten collecties voor de model plant *Arabidopsis thaliana*, desalniettemin worden verlies-aan-functie studies gehinderd doordat er geen mutanten beschikbaar zijn mede omwille van genetische overlap van functie of omdat de genen een essentiële functie coderen.

Het onderzoek in dit doctoraat heeft als doelstelling om potentiele moleculaire factoren te identificeren en bestuderen die instaan voor de biologische processen betrokken in initiatie van zijwortels door een grootschalige analyse van mutante planten en genoombewerking met CRISPR.

In Hoofdstuk 1 introduceren we de actuele kennis over zijwortelontwikkeling en voorzien we een overzicht over de technologische vooruitgang van CRISPR genoombewerking om verlies-aan-functie studies te bewerkstelligen.

In Hoofdstuk 2 beschrijven we de functionele analyse van *MITOGEN ACTIVATED PROTEIN KINASE 6* waarvan ontdekt werd dat het een signalisatie factor is van de *GOLVEN* 6 peptide reactieweg en ons toelaat om de moleculaire mechanismen te bestuderen die de eerste asymmetrische celdelingen controleren die essentieel zijn voor de initiatie van zijwortels.

In Hoofdstuk 3 analyseren we de overlappende rol van verschillende *CYCLIN-DEPENDENT KINASES* gedurende de initiatie van zijwortels aan de hand van een CRISPR-gebaseerd zijwortel-specifiek systeem om genen uit te schakelen dat in samenwerking ontwikkeld werd.

In Hoofdstuk 4 onderzoeken we de functie van *NUCLEAR MIGRATION 1* in het proces van nucleaire migratie. Dit proces wordt geobserveerd bij het begin van de initiatie van zijwortelontwikkeling in twee naburige cellen van xyleempool pericyclus cellen vooraleer de eerste asymmetrische celdeling plaatsvindt.

In Hoofdstuk 5, worden de bekomen wetenschappelijke resultaten samengevat en kritisch benaderd. Bovendien kaderen we de observaties in functie van de actuele kennis over de initiatie van zijwortels. Uiteindelijk reflecteren we over toekomstperspectieven en delen we de maatschappelijke implicaties van het onderzoek verricht in het doctoraat.

Table of Contents

List of Acronyms

35S	35S promoter from the cauliflower mosaic virus
ACD	asymmetric cell division
ACR4	ARABIDOPSIS CRINKLY4
Act	activator
ACT7	ACTIN 7
AFB	AUXIN SIGNALING F-BOX
ALF4	ABERRANT LATERAL ROOT FORMATION 4
ANOVA	Analysis of Variance
ARF	AUXIN RESPONSE FACTOR
Aux/IAA	AUXIN INDUCIBLE/INDOLE-3-ACETIC ACID INDUCIBLE
AUX1	AUXIN RESISTANT 1
BAK1	BRI1-ASSOCIATED RECEPTOR KINASE
BDL	BODENLOS
BiFC	Bimolecular Fluorescence Complementation
BIN2	BRASSINOSTEROID-INSENSITIVE2
BOB	BOBBER
bp	base pair
Cas	CRISPR-associated
CDC5	CELL DIVISION CYCLE 5
CDK	CYCLIN-DEPENDENT KINASE
CEP	C-TERMINALLY ENCODED PEPTIDE
CEPR	CEP RECEPTOR
CLEL	CLE-LIKE
CRISPR	Clustered Regularly Interspaced Short Palindromic Repeats
CS domain	protein domain shared by CHORD-containing proteins and SGT1
CYC	CYCLIN
dag	days after germination
DNA	DEOXYRIBONUCLEIC ACID
Dr.	Doctor
DR5	DIRECT REPEAT 5 (synthetic auxin responsive promoter)
E2Fa	E2F TRANSCRIPTION FACTOR A
EC	European Commission
EF1a	GTP binding Elongation factor Tu family protein
ELRs	Emerged Lateral Roots
EMS	Ethyl methanesulfonate
Est	estradiol
FER	FERONIA
FLP	FOUR LIPS
g	gram
GATA23	GATA transcription factor 23
GFP	GREEN FLUORESENT PROTEIN
GL1	GLABRA1
GLV6	GOLVEN 6
GLVp	GOLVEN peptide
GMO	Genetically Modified Organism

gRNA	guideRNA
GUS	β-GLUCURONIDASE
H2B	HISTONE 2B
HAE	HAESA
HCT	HYDROXYCINNAMOYL-COA SHIKIMATE/QUINATE HYDROXYCINNAMOYL TRANSFERASE
HSL2	HAESA-LIKE 2
HSP	HEAT SHOCK PROTEIN
HTR5	HISTONE 3.3
ICK	INTERACTOR OF CDK
IDA	INFLORESCENCE DEFICIENT IN ABSCISSION
iGLV6	inducible GOLVEN6 overexpression line
indels	insertions/deletions
KIP	KINASE-INHIBITORY PROTEIN
KRP	KIP-RELATED PROTEIN
L	liter
LBD	LATERAL ORGAN BOUNDARIES-DOMAIN
lof	loss-of-function
LRIS	Lateral Root Inducible System
LRP	lateral root primordium
LRR	LEUCINE-RICH REPEAT
LRs	Lateral Roots
LTI6B	LOW TEMPERATURE INDUCED PROTEIN 6B
M	molar
m	meter
M3	Mutant generation 3
MAP4	MICROTUBULE-ASSOCIATED PROTEIN 4
MP	MONOPTEROS
MPK6	MITOGEN-ACTIVED PROTEIN KINASE 6
mRNA	messenger RNA
MSc.	Master Of Science
NAA	1-Naphthaleneacetic acid
NHEJ	NON-HOMOLOGOUS END-JOINING
NLS	Nuclear Localisation Signal
NMD	non-sense mediated decay
NMig1	NUCLEAR MIGRATION 1
NPA	Naphthylphthalamic acid
NRPD11	Non-catalytic subunit common to nuclear RNA polymerases
NST3	NAC SECONDARY WALL THICKENING PROMOTING 3
NudC	NUCLEAR DISTRIBUTION C
PAM	Protospacer Adjacent Motif
PCR	Polymerase Chain Reaction
PhD	Doctor of Philosophy
PIN	PIN-FORMED
PREPIP2	PRECURSOR OF PAMP-INDUCED PEPTIDE 2
PIPL3	PAMP-INDUCED SECRETED PEPTIDE-LIKE 3
PLT	PLETHORA

Prof.	Professor
PSB	Plant Systems Biology (VIB-UGent Center)
PTC	premature termination codon
QC	quiescent centre
qRT-PCR	quantitative real-time PCR
RALF	RAPID ALKALINIZATION FACTOR
RFP	RED FLUORESENT PROTEIN
RGF	ROOT MERISTEM GROWTH FACTOR
RGFR	RGF RECEPTOR
RGI	RGF-INSENSITIVE
RLK	RECEPTOR-LIKE KINASE
RNA	RIBONUCLEIC ACID
RPN1a	26S PROTEASOME REGULATORY SUBUNIT S2 1A
RPS5A	RIBOSOMAL PROTEIN 5A
s.e.m.	standard error of mean
SD	Standard Deviation
SERK	SOMATIC EMBRYOGENESIS RECEPTOR-LIKE KINASE
sgps	suppressors of iGLV6 phenotype
SHY2	SHORT HYPOCOTYL 2
SKP2A	S-PHASE KINASE-ASSOCIATED PROTEIN 2A
SLR	SOLITARY-ROOT
SND1	SECONDARY WALL-ASSOCIATED NAC DOMAIN 1
STRING	database of known and predicted protein-protein interactions
T1	Transformed generation 1
TDIF	TRACHEARY ELEMENT DIFFERENTIATION INHIBITORY FACTOR
T-DNA	transfer DNA
TDR	TDIF RECEPTOR
THE1	THESEUS1
TIDE	Tracking of Indels by DEcomposition
TIR1	TRANSPORT INHIBITOR RESPONSE 1
TOLS2	TARGET OF LBD SIXTEEN 2
TPST	TYROSYLPROTEIN SULFOTRANSFERASE
TSKO	tissue-specific knockout
UTR	untranslated region
WOX5	WUSCHEL RELATED HOMEOBOX 5
XIP1	XYLEM INTERMIXED WITH PHLOEM 1
XVE	A chimeric transcription activator consisting of LexA (X), VP16 (V) and regulatory region of the human estrogen receptor (E)
XPP	Xylem-pole pericycle
YFP	YELLOW FLUORESCENT PROTEIN

Chapter 1: Introduction to lateral root initiation in *Arabidopsis*

Vangheluwe N. & Beeckman T.

Abstract

Lateral root initiation is a post-embryonic process that requires the specification of a subset of pericycle cells adjacent to the xylem-pole in the primary root into lateral root founder cells. The first visible event of lateral root initiation in *Arabidopsis* is the simultaneous migration of nuclei in neighbouring founder cells. Subsequent cell cycle activation is essential for founder cells in the pericycle to undergo formative divisions resulting in the development of a lateral root primordium. The plant signalling molecule auxin is a major regulator of lateral root development and our understanding of the molecular mechanisms controlling lateral root initiation has progressed tremendously. In addition, recent studies revealed that a multitude of secreted signaling peptide and their transmembrane receptors are involved in lateral root initiation. Here, we provide an overview of the visible events, cell cycle regulators, auxin signalling cascades and peptide-receptors modules related to the initiation of a new lateral root primordium. Furthermore, we highlight the potential of genome editing with CRISPR technology to analyse gene function in lateral root initiation, which provides an excellent model to answer fundamental developmental questions such as coordinated cell division, growth axis establishment as well as specification of cell fate and cell polarity.

Arabidopsis thaliana as a model plant to study root development

The *Arabidopsis* plant, like most angiosperms, develops an extensive root system designed to function in the anchorage of the plant, absorption of water and mineral ions and interaction with microorganisms. Several properties of roots make them amenable to developmental studies: the root apical meristem is accessible and not embedded by developing organs or primordia, the root contains no pigment and is therefore essentially transparent and there are relatively few differentiated cell types in roots. In addition, root morphogenesis in many plants occurs in a continuous and relatively uniform pattern without significant developmental transitions and cell files are easy to observe in longitudinal sections and their origin can be traced back to the meristem (Schiefelbein, 1994). Our understanding of root morphology and development in *Arabidopsis* has largely originated from studies of the seedling root system.

The remarkably simple anatomy of the *Arabidopsis* primary root has its origin in the embryonic root primordia. Upon germination, the cells in the root meristem initiate a program of regulated cell division and expansion. Since there are no morphogenetic cell movements in plants, the final form of the root is primarily controlled by three parameters: the timing of cell division, the orientation of the plane of cell division and the degree and direction of cell expansion. The ability of a root to grow in a continuous fashion is dependent on the regulation of cell division and expansion as well as maintenance of a stem cell population within the meristem. The ultimate architecture of the plant root system depends on environmental conditions as well as genetic factors. Root growth can be profoundly affected by a variety of external stimuli, including gravity, light, temperature, moisture, aeration and physical obstacles (Koevoets et al., 2016). These stimuli can alter the cell division activity, the direction or degree of cell expansion, the amount of root branching, or the structure of root cells.

Lateral root development enables root branching

Root branching is commonly known to occur by the formation of lateral roots, roots formed from internal layers along another root axis. However, the first rooting plant lineage, lycophytes, were not able to generate lateral roots. Instead, dichotomous branching of the root tip, involving the formation of two new root apical meristems, allowed these plants to shape their root system architecture (Hetherington & Dolan, 2017). Hence, lycophytes are able to have root branches only at the root tips. Evolution of root branching is accompanied by an increase in plasticity (Motte & Beeckman, 2019). Some ferns have a number of fixed cells referred to as merophytes that are maintained along the root and are competent to form a lateral root (Gifford, 1983; Gunning et al., 1978; Hou & Hill, 2004; Piekarska-Stachowiak & Nakielski, 2013). In the model fern *Ceratopteris richardii*, two out of three successive merophytes have the competence to form a lateral root, resulting in a regular branching pattern (Hou & Hill, 2004; Hou et al., 2004). Hence, lateral roots of ferns contribute to an increased capacity to explore the substrate, but their fixed positioning still restricts the plasticity of their root system.

14

In *Arabidopsis* lateral roots arise from the pericycle

In seed plants, lateral roots are initiated endogenously along the main root axis from a specific subset of pericycle cells, also called lateral root founder cells (De Rybel et al., 2010; Dubrovsky et al., 2008; Malamy & Benfey, 1997). The pericycle is composed of two different types of cells, cells located in front of the two phloem poles and cells situated in front of the two xylem poles, each with different cytological features and cell fates (Beeckman et al., 2001; Himanen et al., 2004; Laplaze et al., 2005; Parizot et al., 2008). Remarkably, xylem-pole pericycle cells are in a division-competent stage while being part of the differentiated part of the primary root (Beeckman et al., 2001; Dubrovsky et al., 2000). In addition, these cells display physiological and genetic characteristics that resemble those of root meristem cells and can be the source for massive induction of lateral roots (Himanen et al., 2002; Parizot et al., 2008). Our understanding of the mechanisms controlling lateral root development has progressed tremendously through studies in *Arabidopsis*, which were recently reviewed in Banda et al. (2019) and Du & Scheres (2018). Lateral root formation can be divided into four steps: lateral root positioning, lateral root initiation, lateral root development & patterning and lateral root emergence (Du & Scheres, 2018). Newly formed lateral roots consist of *de novo* patterned root tissues and meristems resembling those in the primary roots that ensure their continuous growth.

Initiation of lateral roots is marked by coordinated migration of nuclei -and cell divisions

The first visible event of lateral root initiation is the simultaneous migration of nuclei of neighbouring pericycle lateral root founder cells towards the common cell wall followed by an asymmetric anticlinal cell division giving rise to two small daughter cells and two larger flanking cells which is referred to as a Stage I lateral root primordium (De Rybel et al., 2010; Malamy & Benfey, 1997) (Figure 1). Asymmetric cell divisions are formative divisions that generate daughter cells of distinct identity and are essential in enabling post-embryonic organogenesis (Kajala et al., 2014). In mutants with impaired lateral root formation, no simultaneous polar movement of nuclei in lateral root founder cells could be observed (De Rybel et al., 2010). These observations revealed that the coordinated nuclear migration of two neighbouring xylem-pole pericycle nuclei might be a prerequisite for proper primordium initiation and formation of lateral roots.

The next division occurs periclinally in an outward manner and yields a two-layered (Stage II) lateral root primordium (Malamy & Benfey, 1997). Subsequently, series of anticlinal and periclinal cell divisions and differentiation steps lead to cell diversity and tissue patterns, resulting in the development of a dome-shaped lateral root primordium that progressively acquires the same tissue organisation as the root meristem and eventually emerges through overlying tissues of the primary root. Distinct lateral root primordium stages (I-VII) have been classified based on anatomical analysis considering the number of cell-layers that the lateral root primordium comprises or based on its position through the overlaying tissues (Figure 2) (Malamy & Benfey, 1997; Péret et al., 2009). Intriguingly, it was shown that the tissues in the primary root overlaying a lateral root primordium influence the shape and development of the primordium (Banda et al., 2019; Lucas et al., 2013; Vermeer et al., 2014). (Banda et al., 2019; Lucas et al., 2013; Vermeer et al., 2014). The growing LRP needs to deal with the

mechanical constraints imposed by surrounding tissues. Endodermal cells need to change shape and lose volume to accommodate the expansion of the LRP. It was shown that endodermal feedback is required for the execution of the formative divisions and for the growth of the LRP through this persistent cell layer (Vermeer et al., 2014).

Lateral root founder cells are specified in the pericycle

GATA23 is the earliest known marker for lateral root founder cell specification that was identified by meta-analysis of transcriptomic data sets for lateral root initiation (De Rybel et al., 2010; Parizot et al., 2010). *GATA23* is expressed in xylem-pole pericycle cells before the first asymmetric division. Moreover, it was shown that *GATA23* expression is controlled by an auxin signalling mechanism (De Rybel et al., 2010). Xylem-pole pericycle cells pass through a developmental window for lateral root initiation in which, at minimum auxin concentration, these cells have a high probability of becoming specified founder cells (Dubrovsky et al., 2008). The endodermis assists in the transition from the founder cell stage to the lateral root initiation phase via an auxin reflux pathway between endodermal cells and the adjacent founder cells (Benková et al., 2003; Marhavý et al., 2013). Next, when a local auxin concentration maximum is reached, several auxin signalling components interact together and the founder cells proceed to lateral root initiation (De Rybel et al., 2010; De Smet et al., 2007).
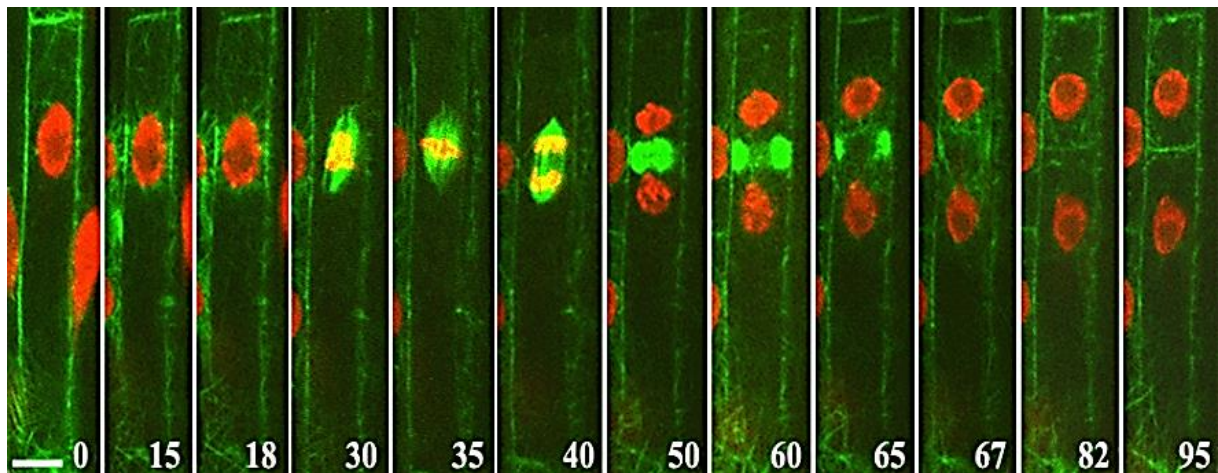

Figure 1. Time lapse from lateral root founder cell specification to asymmetric cell division in a single xylem-pole pericycle cell. Sequential images of the cellular events preceding the first asymmetric division using a *p35S::H2B-RFP × p35S::GFP-MAP4* double reporter line that marks nuclei (in red) and microtubules (in green). Polar migration of the nucleus in a lateral root founder cell is followed by an asymmetric anticlinal cell division resulting in a short and a long daughter cell. Time (in minutes) is indicated in the right bottom corner. Scale bar: 10 µm. Courtesy of Prof. Dr. Valya Vassileva (Bulgarian Academy of Sciences).
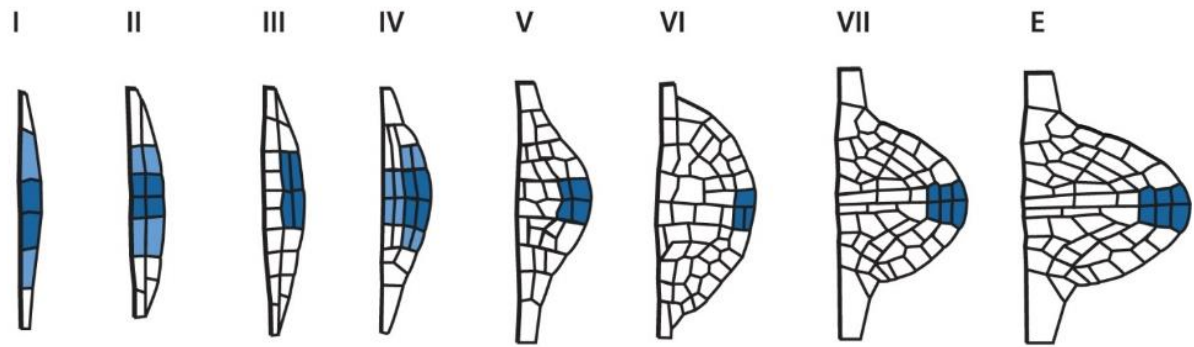
Figure 2. Schematic overview of distinct lateral root primordium stages in *Arabidopsis* according to Malamy & Benfey, 1997. Cells coloured in blue indicate auxin response according to the synthetic *DR5* reporter (Ulmasov et al., 1997). Roman numeral indicates lateral root primordium stage. Modified from Péret *et al*., 2009.

Auxin acts as a common integrator to many endogenous and environmental signals regulating lateral root development (Lavenus et al., 2013). A *plethora* of auxin 'signalling modules' act sequentially during lateral root development and control various steps of lateral root formation from priming to initiation, patterning, and emergence. An auxin response module is defined as a pair of strongly interacting Aux/IAA proteins and AUXIN RESPONSE FACTORS (ARFs) which regulate together a subset of primary auxin response genes (De Smet, 2010). The properties of this auxin response depend on the cellular auxin concentration, F-box (TIR1 and AFB1-5) affinity for auxin and for the Aux/IAA target protein, Aux/IAA–ARF interaction, as well as ARF activity and affinity for the promoter of its target genes.
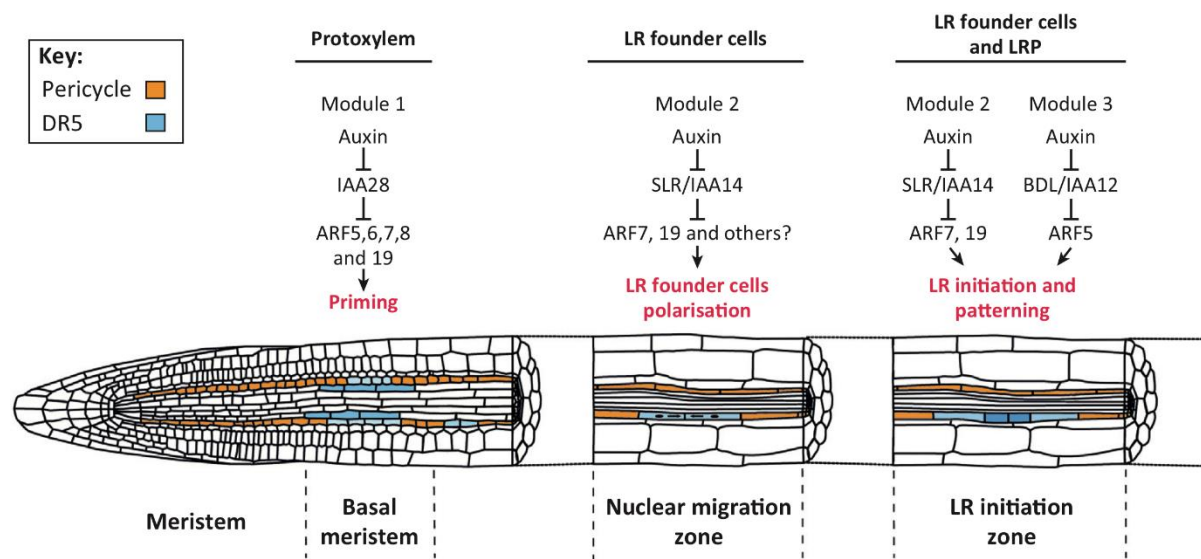

Figure 3. Auxin regulates different stages of lateral root development through multiple auxin-signalling modules in *Arabidopsis*. Lateral root founder cell priming involves the IAA28–ARF5,6,7,8,19 and IAA3-ARF7 module (Module 1) in the basal meristem (De Rybel et al., 2010; Orosa-Puente et al., 2018). After priming, cells at prebranch sites maintain an increased auxin response, which was revealed through analysis of the *pDR5:LUCIFERASE* reporter (De Smet et al., 2007; Moreno-Risueno et al., 2010; Xuan et al., 2015; Xuan et al., 2016). Lateral root founder cells start to accumulate auxin, which triggers their polarisation and subsequent lateral root initiation (De Rybel et al., 2010). The IAA14/SOLITARY-ROOT–ARF7-ARF19 module (Module 2) regulates the polarisation of lateral root founder cell pairs, which leads to coordinated nuclear migration towards the common cell walls (De Rybel et al., 2010; Goh et al., 2012). Both the IAA14/SLR–ARF7,19 and the IAA12/BDL–ARF5 modules (Modules 2 and 3 respectively) are necessary for triggering lateral root initiation which starts with an asymmetric anticlinal division of lateral root founder cells (Fukaki et al., 2005; Fukaki et al., 2002; Vanneste et al., 2005). These modules also regulate the morphological and histological patterning of the lateral root primordium (Benková et al., 2003; De Smet et al., 2008; Hirota et al., 2007). Figure modified from Lavenus *et al*. (2013).

Developmental decisions on the distribution of lateral roots take already place in the distal zone of the primary root tip, in the basal meristem region which represents a transition zone between the apical meristem and the elongation zone. Studies using *DR5*-based reporters suggest that periodic auxin response, along with oscillating waves of gene expression, functions as an endogenous clock-like mechanism (De Rybel et al., 2010; De Smet et al., 2007; Moreno-Risueno et al., 2010; Orosa-Puente et al., 2018; Xuan et al., 2015; Xuan et al., 2016). Following an auxin response maximum in the protoxylem cell file, the neighbouring xylem-pole pericycle cells are 'primed' and form pre-branch sites, providing them with the competence to develop lateral roots. The mechanism through which the 'priming information' is transmitted from the protoxylem to the overlaying xylem-pole pericycle has not been characterised yet. However, it was shown that expression of *GATA23* is dependent on the IAA28–ARF7/19 auxin module (De Rybel et al., 2010). In addition, transactivation of *GATA23* in xylem-pole pericycle cells in the *iaa28* gain-of-function mutant is able to rescue the dominant *iaa28* lateral root mutant phenotype (De Rybel et al., 2010). These observations suggest that an IAA28-dependent auxin signalling mechanism controls *GATA23* expression, regulating lateral root founder cell specification prior to lateral root initiation (Figure 3).

Auxin regulates and coordinates both founder cell divisions and founder cell polarity/identity specification during lateral root initiation. The auxin response increases in founder cell pairs a few hours before initiation of lateral root organogenesis (Dubrovsky et al., 2008). Disturbing the auxin response in founder cells using polar auxin transport inhibition is sufficient to block initiation, whereas artificial auxin production in single xylem-pole pericycle cells triggers initiation, indicating that auxin accumulation is necessary and sufficient for lateral root initiation (Casimiro et al., 2001; Dubrovsky et al., 2008). Moreover, coordinated regulation of auxin influx and efflux carriers including AUXIN RESISTANT 1 (AUX1) and PIN-FORMED (PIN) in the lateral root primordium and surrounding tissues are needed to establish an auxin gradient essential for lateral root initiation (Figure 2) (Benková et al., 2003; Laskowski et al., 2008; Marhavý et al., 2013).

In *solitary-root* (*slr*)-*1*, a dominant negative mutant of *SLR*/*IAA14*, lateral root initiation is blocked at the G1-to-S transition and no nuclear migration in paired founder cells can be observed. Moreover, the defects in *slr-1* cannot be restored by exogenous auxin application. The *arf7arf19* double mutant phenocopies *slr-1* and IAA14 interacts with ARF7 and ARF19 indicating that auxin stimulates lateral root initiation through the SLR/IAA14–ARF7,19 signalling module (Figure 3). Following the first asymmetric division, the small daughter cells exhibit an auxin maximum, which is accompanied by BODENLOS/IAA12–MONOPTEROS/ARF5 -dependent signalling (De Smet et al., 2010). It was shown that the hemizygous gain-of-function *bdl* mutants and weak loss-of-function *mpS319* mutants display abnormalities in pericycle divisions and lateral root positioning (De Smet et al., 2010). Taken together, a second auxin-signalling module involving BDL/IAA12 and MP/ARF5 regulates lateral root initiation together with SLR–ARF7–ARF19 (Figure 3). It has been proposed that auxin plays an instructive role for the structural and functional patterning of the lateral root primordium similar to the shoot and root apical meristems (Benková et al., 2003). However, exactly how this auxin gradient actually governs cell identities and divisions is still poorly understood.

The pericycle in *Arabidopsis* is a heterogeneous tissue with diarch symmetry composed of two cell-types with distinct cell division ability (Parizot et al., 2008). Phloem-pole pericycle cells are mitotically inactive, whereas xylem-pole-pericycle cells retain stem cell activity after leaving the primary root meristem and thus maintain a division-competent state essential for lateral root formation (Beeckman et al., 2001; Himanen et al., 2004; Parizot et al., 2008). It was shown that the nuclear protein ABERRANT LATERAL ROOT FORMATION 4 (ALF4) is required to maintain xylem-pole pericycle cells in a mitosis-competent state (DiDonato et al., 2004; Dubrovsky et al., 2008).

The onset of lateral root initiation coincides with the occurrence of a series of anticlinal, asymmetric divisions in the xylem-pole pericycle. Hence, cell cycle activation is inherently connected with lateral root initiation. The transition of xylem-pole pericycle cells from G1 to S and subsequent cycle progression are stimulated by auxin. These 'primed' cells reactivate the cell cycle only when they reach the lateral root initiation zone, which indicates that activating cell cycle-related genes alone is not sufficient to initiate a new lateral root (Casimiro et al., 2003; Vanneste et al., 2005). Moreover, disturbing the auxin response through inhibition of polar auxin transport or impaired auxin signalling is sufficient to inhibit cell divisions necessary for lateral root initiation (Casimiro et al., 2001; Himanen et al., 2002; Vanneste et al., 2005). Activation and progression through the major phases of the cell cycle are governed by the control of CYCLIN-DEPENDENT-KINASES (CDKs). Several highly conserved components of the cell cycle have been demonstrated to be important for lateral root initiation (Kajala et al., 2014). For instance, LATERAL ORGAN BOUNDARIES-DOMAIN (LBD) 18 and LBD33 lateral root regulatory protein dimers mediate lateral root initiation by direct binding to the promoter of *E2Fa*, which encodes a transcriptional activator of cell cycle genes (Berckmans et al., 2011). *E2Fa* is expressed during lateral root initiation and promotes the first asymmetric cell divisions (Berckmans et al., 2011; De Smet et al., 2010).

Asymmetric cell divisions are formative divisions that generate daughter cells of distinct identity. These divisions are coordinated by either extrinsic or intrinsic regulatory mechanisms and are fundamentally important in plant development (Kajala et al., 2014). In intrinsic asymmetric cell divisions, there is unequal segregation of identity determinants within the cell. To mediate an intrinsic asymmetric cell division in plants, the position of the pre-prophase band and hence the orientation of the cell division plane have to be regulated and coordinated with cell identity-determinant distribution. Extrinsic asymmetric divisions are also referred to as 'niche-controlled' asymmetric cell divisions. The generation of daughter cells with distinct identities is referred to as the 'asymmetric' property of these cell divisions. In some cases, distinctly specified daughter cells are then the precursors for a cell type population that will proliferate. In others, the initial cell retains its ability to proliferate. Asymmetric cell divisions in all plant species are considered to be formative because they establish axis and organ polarity, tissue patterning and morphogenesis. How asymmetric cell divisions are regulated during development and in different cell types in both the root and the shoot of plants was elaborately reviewed in Kajala et al. (Kajala et al., 2014).

The auxin-mediated G1 to S transition is inhibited by the INTERACTOR OF CDK/KINASE-INHIBITORY PROTEIN (KIP)-RELATED PROTEIN (ICK/KRP) family of proteins, hence, preventing lateral root initiation (Himanen et al., 2002; Ren et al., 2008). Loss-of-function mutants of *KRP2* display increased lateral root density, whilst overexpression of *KRP2* results in a large reduction in lateral root density (Himanen et al., 2002; Ren et al., 2008; Sanz et al., 2011). KRP2 interacts with the CDKA;1–CYCD2;1 complex and results in accumulation in the nucleus of the inactive complex (Ren et al., 2008). Upon auxin treatment, reduced *KRP2* expression and increased KRP2 protein turnover result in a transient increase in CDKA;1–CYCD2;1 activity and subsequent cell division, which promotes lateral root initiation (Sanz et al., 2011). Other D-type cyclins such as *CYCD4;1* and *CYCD3;1* are also shown to be involved in lateral root initiation (Himanen et al., 2002; Nieuwland et al., 2009). In addition, A2-type cyclins are involved in early G2 to M transition of the cell cycle during lateral root initiation. The triple *cyca2;234* mutant displays a delay in the expression of mitotic regulators, while auxin signalling and G1 to S regulatory genes remain unaffected (Vanneste et al., 2011).

The F-box protein S-PHASE KINASE-ASSOCIATED PROTEIN 2A (SKP2A) positively regulates lateral root initiation (Jurado et al., 2010; Jurado et al., 2008). Auxin binds directly to SKP2A and mediates the proteolysis of cell cycle-repressing transcription factors in an TIR1-AFB auxin receptor-independent pathway. Overexpression of *SKP2A* in the *tir1* mutant induces lateral root initiation and *skp2a* mutants display an auxin-resistant root growth phenotype. In contrast, a close homologue SKP2B, negatively regulates the cell cycle and lateral root development as it represses founder cell divisions (Manzano et al., 2012).

In summary, strict control of cell division is regulated by highly conserved inhibiting and activating components of the cell cycle and is required for lateral root organogenesis.

Small peptides are emerging as key signalling molecules in coordinating various aspects of plant development and are usually recognized by the extracellular domains of transmembrane proteins belonging to the receptor-like kinase family, and SERK family receptor-like kinases function as coreceptors for the peptide–receptor-like kinase pair activation via peptide-induced heterodimerization and phosphorylation. More than 1000 signalling peptides have been predicted in the genome sequence of *Arabidopsis* indicating that peptide-derived intercellular communication is an important signalling mechanism in plants (Lease & Walker, 2006). To date, the identified receptors for peptide signals belong to the receptor-like kinase (RLK) family, particularly the leucine-rich repeat receptor-like kinase (LRR-RLK) subfamily comprising more than 200 members in *Arabidopsis* (Wu et al., 2016; Zhang et al., 2016). Over recent years great progress has been made in the identification of receptors, structural analysis of peptide–receptor pairs, and characterization of their signalling pathways during lateral root development, which was recently reviewed in Oh *et al.* and Jourquin *et al.* (Figure 4) (Jourquin et al., 2020; Oh et al., 2018).
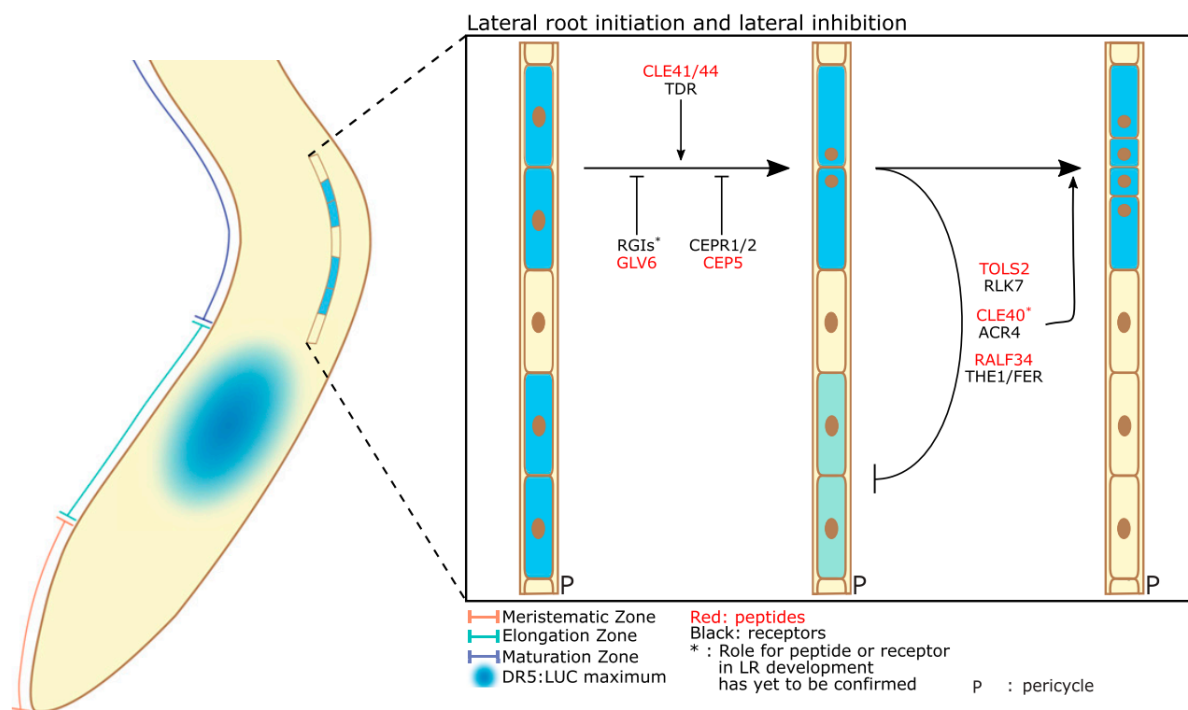

Figure 4. Peptide-receptor signalling pathways are involved in lateral root initiation and lateral inhibition in *Arabidopsis*. Overview of the peptide-receptor pairs currently known to be involved in these processes. In the maturation zone, lateral root initiation takes place, a process that is influenced by the stimulatory and inhibitory effects of multiple peptide signalling pathways. Additionally, several signalling peptides repress lateral root development in the vicinity of present primordia in a process called "lateral inhibition". Explanatory information is provided in the text below. Figure modified from Jourquin *et al.*, 2020.

GOLVEN peptides control root apical meristem size

Tyrosine sulfation is a post-translational modification of peptide hormones that is mediated by tyrosylprotein sulfotransferase (TPST) and the *Arabidopsis* genome encodes one *TPST* gene. The *tpst-1* mutant allele displays pleiotropic phenotypes including severely shortened roots with a reduced root meristem size (Matsuzaki et al., 2010). Application of synthetic and sulfated ROOT MERISTEM GROWTH FACTOR 1 (RGF1) / GOLVEN 11 (GLV11) peptides restores root meristem activity in the *tpst-1* mutant, indicating that this peptide is required for root stem cell maintenance and that sulfation of the tyrosine residue of RGF1 is crucial for its activity (Matsuzaki et al., 2010). In addition, the *rgf1rgf2rgf3* triple mutant displays a short-root phenotype similar to that of the *tpst-1* mutant (Matsuzaki et al., 2010). Three different research groups independently identified receptors for RGFs (Ou et al., 2016; Shinohara et al., 2016; Song et al., 2016). The *rgf insensitive* (*rgi*) quintuple mutants display a short primary root with a short meristem (Ou et al., 2016; Shinohara et al., 2016). The expression of root meristem-maintenance genes *PLETHORA 1* (*PLT1*) and *PLT2* is almost undetectable in *rgi* quintuple mutants, and ectopic expression of *PLT2* in the quintuple *rgi* mutant rescues the root meristem defects (Ou et al., 2016). Moreover genetic and expression analysis demonstrated that *RGF RECEPTOR* (*RGFR*) *1*, *RGFR2*, and *RGFR3* are required for producing the gradient of PLT in the proximal meristem (Shinohara et al., 2016). RGF1 induces the interaction between RGFR1 or RGFR2 and SERK1/2/BAK1 (Song et al., 2016). Taken together, these results revealed that RGF peptides regulate primary root meristem activity through PLT transcription factors by interacting with RGFRs/BAK1 receptor pairs.

Several GOLVEN family members are involved in lateral root development

Out of the 11 GLV/RGF/CLE-LIKE (CLEL) family members that are encoded in the *Arabidopsis* genome, 8 are expressed during lateral root primordium development (Fernandez et al., 2013; Ghorbani et al., 2016). These *GLV* genes are sequentially induced at different stages of primordium development with *GLV6* and *GLV10* as the earliest ones upon lateral root initiation (Fernandez et al., 2015). Overexpression of certain *GLV* genes triggers aberrant anticlinal cell divisions throughout the whole pericycle resulting in a strong reduction in emerged lateral root density (Fernandez et al., 2013; Meng et al., 2012). Application of synthetic GLV peptides mimics similar phenotypic changes compared to those produced by *GLV* overexpression (Fernandez et al., 2013). However, no changes in lateral root formation have been observed in single loss-of-function mutations in each *GLV* gene (Fernandez et al., 2013; Fernandez et al., 2015; Meng et al., 2012). RGF1 treatment greatly reduces lateral root numbers and the *rgi1,2,3,4* quadruple mutant exhibits reduced sensitivity to RGF1 in lateral root formation, indicating that the RGF1 receptor pair has a role in lateral root development (Ou et al., 2016).

GOLVEN 6 controls the asymmetry of the lateral root founder cell divisions

The function of GLV6/RGF8/CLEL2 during lateral root development has been analysed more extensively considering its expression pattern. *GLV6* is expressed in lateral root founder cells before the onset of nuclear migration (Fernandez et al., 2015). Moreover, *GLV6* overexpression and GLV6 peptide treatment trigger supernumerary anticlinal divisions

throughout the xylem-pole pericycle along the primary root axis (Fernandez et al., 2015). Ectopic expression of *GLV6* in different root tissue layers indicated that this can be almost completely phenocopied upon expression in the xylem-pole pericycle and is a lot weaker when expressed in the overlying tissues. This suggests that GLV6 peptides function as autocrine rather than paracrine signals that are produced and perceived in the founder cells as RGI1/5 are expressed in these cells as well (Fernandez et al., 2020). Furthermore, in-depth analysis revealed that the nuclear migration in founder cells is disrupted upon treatment with GLV6 peptide. As of a result, the first anticlinal cell division of lateral root founder cells loses its essential asymmetry, preventing progression of lateral root primordium development. Hence, GLV6 peptide signalling seems to be required for proper cell patterning upon lateral root initiation.

TRACHEARY ELEMENT DIFFERENTIATION INHIBITORY FACTOR positively regulates lateral root initiation

It has been demonstrated that two other peptides, CLE41 and CLE44, both encoding the same mature peptide known as TRACHEARY ELEMENT DIFFERENTIATION INHIBITORY FACTOR (TDIF) positively regulate LR initiation. TDIF and its receptor TDIF RECEPTOR (TDR) suppress vascular stem cell differentiation into xylem and stimulate lateral root initiation by regulating the transcriptional activity of the lateral root regulatory genes ARF7 and ARF19 (Cho et al., 2014; Hirakawa et al., 2008). TDIF is secreted from the phloem and perceived by TDR in xylem-pole pericycle cells (Cho et al., 2014). Treatment with TDIF increases emerged lateral root density in a TDR-dependent manner, while *tdr* loss-of-function mutants exhibit reduced emerged lateral root densities. In the presence of TDIF, TDR interacts with BRASSINOSTEROID-INSENSITIVE2 (BIN2) in the pericycle and enhances BIN2-mediated phosphorylation of ARFs to activate ARFs (Cho et al., 2014; Pérez-Pérez et al., 2002; Vert et al., 2008). Phosphorylation of ARFs attenuates the interactions between ARFs and AUX/IAA proteins, thereby enlarging the pool of available ARF7 and ARF19 transcriptional activators that promote lateral root formation (Cho et al., 2014). These data suggest that auxin-induced TDIF in the phloem travels to the pericycle where it stimulates TDR-induced activation of BIN2, which in turn attenuates the inhibitory activity of Aux/IAAs on ARF7 and ARF19, thereby mediating auxin signalling for the initiation of lateral root development.

C-TERMINALLY ENCODED PEPTIDE 5 functions during lateral root initiation

The C-TERMINALLY ENCODED PEPTIDE (CEP) family has been primarily studied for their role in nitrogen starvation responses and related inhibition of lateral root elongation, however, some members are also involved in lateral root initiation (Delay et al., 2013; Roberts et al., 2013; Roberts et al., 2016). In particular, the function of CEP5 during lateral root initiation has been studied more extensively (Roberts et al., 2016). *CEP5* is predominantly expressed in phloem-pole pericycle cells and to a lesser extent in the adjacent phloem cells located in the primary root tip starting from the elongation zone and in association with lateral root primordia. Knocking down *CEP5* expression results in increased early stage primordia, while *CEP5* overexpression and peptide treatments cause a decrease in total lateral root density, indicating a reduction in lateral root initiation events. Moreover, aberrant pericycle divisions, as well as fused and closely spaced lateral root primordia were often observed. The LRR-RLKs

CEP RECEPTOR1 (CEPR1) / XYLEM INTERMIXED WITH PHLOEM1 (XIP1) and CEPR2 function as receptors for CEP1, CEP3 and CEP5 and potentially also other members of the CEP family (Tabata et al., 2014). Loss-of-function *cepr1* mutants show reduced sensitivity to CEP5 peptide treatments, supporting the role of CEPR1 as a CEP5 receptor during lateral root development. However, the CEP5–CEPR1/XIP1 interaction occurring at phloem-pole pericycle cells seems to be an antagonistic interaction in lateral root initiation because *CEP5* overexpression reduces lateral root density in a similar manner to the *cepr1* mutant, which displays a reduction in early stage lateral root primordia (Roberts et al., 2016). On the other hand, it has been reported that *cepr1cepr2* double mutants show an increase in emerged lateral root -as well as lateral root primordium densities, suggesting that CEPRs might act as negative regulators of lateral root initiation. Follow-up experiments are required to resolve these different results.

TARGET OF LBD SIXTEEN2 controls the lateral inhibition of lateral root founder cell specification

Signalling peptides are involved in other processes as well including a lateral inhibition mechanism that prevents lateral root primordia from developing in close proximity to each other and mediates the spatial distribution of lateral roots along the primary root. It has recently been shown that TARGET OF LBD SIXTEEN2 (TOLS2), which encodes a secreted 11-amino acid peptide hormone and a close homolog called PRECURSOR OF PAMP-INDUCED PEPTIDE 2 (PREPIP2), together with their transmembrane receptor RECEPTOR-LIKE KINASE7 (RLK7), are involved in the lateral inhibition of lateral root founder cell specification (Toyokura et al., 2019). *TOLS2* is expressed in founder cells and developing lateral root primordia and its transcription is induced by auxin via the activity of the lateral root regulatory gene *LBD16* (Goh et al., 2012; Lee et al., 2009; Okushima et al., 2007). Moreover, *TOLS2* overexpression and treatment with synthetic TOLS2 or PIP2 peptides decreases the density of prebranch sites, consequently resulting in a reduction in lateral root primordium density. *RLK7* on the other hand is expressed in the pericycle but absent in founder cells and developing lateral root primordia, where *TOLS2* is expressed. Loss-of-function of *RLK7* increases prebranch site density and prebranch sites are often found in close proximity to each other, which is also observed in *tols2pip2* double mutants. Expression of the lateral root regulatory gene *PUCHI* is induced by TOLS2 in an *RLK7*-dependent manner (Toyokura et al., 2019). In agreement with this, *puchi* mutants display increased prebranch site densities and increased frequencies of paired prebranch sites (Hirota et al., 2007). Furthermore, *puchi* mutants display a reduced sensitivity to TOLS2 peptide treatments. Taken together, the TOLS2 signalling peptide seems to be involved in a lateral inhibition mechanism that prevents lateral root primordia from developing in close proximity to each other. This is achieved via the transcriptional activation of *PUCHI* in the regions flanking a founder cell pair through its receptor RLK7.

RAPID ALKALINIZATION FACTOR 34 is involved in lateral root initiation and lateral inhibition

RAPID ALKALINIZATION FACTOR (RALF) peptides affect cell growth by regulating calcium ion responses, MAPK signalling, and alkalization, and are linked to lateral root development as well (Bergonci et al., 2014; Haruta et al., 2014; Murphy et al., 2016). Loss-of-function of *RALF34* results in an increase in total lateral root primordium density, primarily due to an increased density of stage-I primordia (Murphy et al., 2016). Moreover, primordia were often

observed in close proximity to one another as well as aberrant pericycle cell divisions flanking lateral root primordia. *RALF34* is expressed in xylem-pole pericycle cells before the onset of lateral root initiation and its expression remains throughout the entire lateral root developmental process (Murphy et al., 2016). These observations suggest that RALF34 functions as a negative regulator of lateral root initiation and possibly acts to inhibit initiation in close proximity to existing primordia. *THESEUS1* (*THE1*) has been identified as a receptor for RALF34 (Gonneau et al., 2018). *THE1* is expressed throughout the stele, pericycle, and in developing lateral root primordia and *the1* loss-of-function mutants display the same phenotypic defects as *ralf34* knockdown mutants. In addition to THE1, RALF34 signalling also seems to require FERONIA, a receptor kinase that is known to perceive other RALF peptides as well (Gonneau et al., 2018; Haruta et al., 2014). This is supported by the observation that *fer* mutants display increased lateral root densities (Dong et al., 2019). However, the mechanism via which the RALF34-THE1/FER module regulates lateral root initiation has not yet been uncovered. In agreement with the inhibitory effect of RALF34 on lateral root initiation, other RALF peptides have also been found to negatively affect lateral root development, suggesting that other family members share the same function (Atkinson et al., 2013; Bergonci et al., 2014).

The receptor-like kinase ARABIDOPSIS CRINKLY4 promotes formative divisions in the lateral root primordium and represses cell divisions in surrounding pericycle cells

The receptor-like kinase *ARABIDOPSIS CRINKLY4* (*ACR4*) was identified as an auxin-inducible regulator of the first asymmetric anticlinal cell division upon lateral root initiation and is expressed specifically in the small central daughter cells as a result from the initial asymmetric cell division (De Smet et al., 2008; Yue et al., 2016). The density in lateral root initiation events is increased in *acr4* mutants (De Smet et al., 2008). Furthermore, lateral root primordia are often initiated close to one other and double-layered stretches of pericycle cells or fused primordia were observed as well. Despite the increase in total lateral root primordium density, emerged lateral root densities are reduced in *acr4*. Inversely, ectopic expression of *ACR4* in the xylem-pole pericycle cells results in an increase in emerged lateral root density (De Smet et al., 2008). Thus far, these observations suggest that ACR4 represses divisions in pericycle cells surrounding lateral root founder cells, while simultaneously promoting the correct organization of the initial founder cell divisions, thereby ensuring proper lateral root spacing and initiation. A peptide ligand for ACR4 during LR initiation has not yet been identified. However, CLE40 has been proposed as a ligand for ACR4 in the root apical meristem where the CLE40-ACR4/CLAVATA1 signalling module regulates the fate of root stem cells (Berckmans et al., 2020; Stahl et al., 2013; Stahl & Simon, 2009).

In summary, a multitude of peptide-receptor signalling pathways have been identified mediating both stimulatory and inhibitory effects on lateral root initiation. Interestingly, the involvement of signalling peptides in lateral inhibition seemingly coincides with a role during lateral root initiation. Moreover, it has become clear that multiple signalling peptides and receptors from different families are involved in the regulation of the same developmental process. Future research is required to study if different peptide-receptor pathways act redundantly and/or crosstalk occurs between these pathways.

Loss-of-function mutant alleles are indispensable in functional genomic studies

In view of the complexity of the molecular control on lateral root initiation, the high number of potential regulators involved and the contribution of different tissue layers, solid genetic tools are a necessity to further unravel this process. Loss-of-function mutant alleles have been indispensable to analyse and demonstrate the function of genes in lateral root development. In plants, knockout or knockdown lines have been generated using various techniques such as ionizing radiation, ethyl methane sulfonate treatment, T-DNA or transposon insertions in the genome, RNA interference or artificial microRNAs. In addition, engineered nucleases can be used to generate knockout lines as a result of error-prone non-homologous end-joining (NHEJ) induced upon site-specific double-strand breaks in plant genomes. In the past five years, the generation of knockout plant lines via clustered regularly interspaced short palindromic repeats (CRISPR) genome editing technology has been widely adopted by researchers, while the basic principles behind double-strand break-induced targeted mutagenesis are well known for decades (Voytas, 2013). Previous experiments demonstrated that by induction of double-strand breaks in genomes using a highly specific endonuclease, different types of genome editing can be achieved (Voytas, 2013). Distinct types of nucleases have been engineered including mega nucleases, zinc finger nucleases, transcription activator-like effector nucleases and CRISPR-associated (Cas) nucleases (Christian et al., 2010; Jasin, 1996; Jinek et al., 2012; Kim et al., 1996).

On the origin of CRISPR

The CRISPR system originates from bacteria and archaea, in which it serves as an adaptive immune response system that degrades invading foreign plasmid or viral DNA (Wiedenheft et al., 2012). The elucidation of the molecular mechanism of a type II CRISPR/Cas9 system from *Streptococcus pyogenes* has revealed a simple three-component system (Jinek et al., 2012). Cas9 is a nuclease that is able to cleave double-stranded DNA with two nuclease domains, each cleaving one of the two DNA strands. The target specificity is mediated by a short CRISPR RNA that binds directly to a stretch of 20 nucleotides on the target DNA referred to as protospacer. An additional 3-nucleotide element termed protospacer-adjacent motif (PAM) with the sequence 5'-NGG-3' downstream of the target sequence is necessary for binding and cleavage by Cas9. This means that any 23-nucleotide sequence ending in 5'-GG-3' can be targeted. The trans-activating CRISPR RNA interacts with the CRISPR RNA and facilitates the recruitment of Cas9, which results in the cleavage of the DNA target sequence 3-base pairs upstream of the PAM. Furthermore, it was shown that a direct fusion of the two RNAs to generate a chimeric guideRNA (gRNA) is functional as well (Jinek et al., 2012).

Loss-of-function mutant alleles in *Arabidopsis* can be efficiently generated with CRISPR

The first scientific report that described an effective CRISPR system to generate inheritable mutations in *Arabidopsis thaliana* was published in 2014 (Schiml et al., 2014). They used the constitutive *UBIQUITIN 4-2* promoter from *Petroselinum crispum* to drive Cas9 expression (Schiml et al., 2014) and provided a Gateway®-based cloning system to clone up to two gRNA expression cassettes in the expression vector. Cas9 is very efficient in plants at inducing

double-strand DNA breaks. Repair of DNA breaks by the error-prone NHEJ pathway ultimately results in the formation of short insertions and/or deletions (indels) at the break site (Bortesi & Fischer, 2015). These indels most often lead to frame shifts and/or early stop codons, which result in knockout mutations in the targeted gene(s). Currently, the most commonly used CRISPR system in plants is a two-component system based on Cas9 and the gRNA. However, many variations and applications have been developed which were recently reviewed in Wada *et al.* (Wada et al., 2020).

Most CRISPR efforts in plants to date have focused on generating stable and heritable mutant alleles for reverse genetics approaches, which has substantially contributed to study redundant gene families or genes for which no or limited number of mutant alleles are available in *Arabidopsis* mutant collections (Fernandez et al., 2020; Rojas-Murcia et al., 2020; Yamaguchi et al., 2017). However, this strategy is limited in case loss-of-function conveys severe pleiotropic phenotypes or even lethality. It is estimated that 10% of the approximate 25.000 protein-coding genes in the genome of *Arabidopsis* are essential (Lloyd et al., 2015). Hence, detailed functional analysis of many fundamentally important plant genes is impeded and hinders the study of their function in a developmental-specific context.

Current genetic tools comprise certain limitations for functional gene studies in a developmental-specific context

Lateral root development is a post-embryonic process that requires the specification of a subset of pericycle cells adjacent to the xylem-pole in the primary root into lateral root founder cells (De Rybel et al., 2010). Subsequently, during the process of lateral root initiation, cell fate specification and *de novo* lateral root meristem establishment is required for lateral root organogenesis (Du & Scheres, 2017; Goh et al., 2016; Laskowski et al., 1995). These processes rely on key genetic players including *PIN-FORMED*, *PLETHORA*, *AUX/IAA* and *ARF* genes that are necessary in primary root development as well (Aida et al., 2004; Benková et al., 2003; De Smet et al., 2010; Hamann et al., 2002; Schlereth et al., 2010; Tian et al., 2014). Hence, a lot of loss-of-function alleles affect primary- and lateral root development, which hampers functional analysis. Moreover, primary roots are initiated during embryogenesis and post-embryonic functional analysis of some of these common genetic players such as for instance *MONOPTEROS* are limited because they govern essential functions during embryogenesis (Schlereth et al., 2010).

Different strategies have been pursued to enable a comprehensive investigation of gene function in specific developmental or physiological processes. An approach is the use of tissue-specific gene silencing (Alvarez et al., 2006; Schwab et al., 2006). However, gene silencing is often incomplete, interfering with the interpretation of the observed phenotypes and it has been demonstrated that small RNAs can be mobile, limiting the tissue specificity in knockdown experiments (Melnyk et al., 2011). Alternatively, transgenic vectors generating dominant-negative protein versions have been developed for certain genes and expressing these mutant versions in a tissue-specific context can locally interfere with endogenous gene functions (Fukaki et al., 2005; Mitsuda et al., 2011). Other methods include the conditional knockout of genes in specific cell types or tissues using the Cre/lox-based clonal deletion (Heidstra et al., 2004; Sieburth et al., 1998). However, these approaches rely on complicated genetic engineering and are difficult to scale.

CRISPR-TSKO enables lateral root-specific loss-of-function studies

These limitations have been overcome using genome editing with CRISPR technology to generate conditional knockouts. Originally, tissue-specific promoters driving Cas9 expression have been employed with the focus on increasing the chance of obtaining heritable mutant alleles (Hyun et al., 2015; Mao et al., 2016; Yan et al., 2015). For instance, the *NST3*/*SND1* promoter was used to drive xylem-specific Cas9 expression and target the essential gene *HCT* encoding a hydroxycinnamoyl transferase in *Arabidopsis* (Liang et al., 2019). The potential of conditional gene knockouts of several essential genes in diverse plant cell types, tissues, and organs in *Arabidopsis* has recently been demonstrated (Decaestecker et al., 2019). Therefore, a versatile CRISPR tissue-specific knockout (CRISPR-TSKO) vector system was devised that allows for the specific generation of somatic DNA mutations in particular plant cell types, tissues, and organs (Decaestecker et al., 2019). Furthermore, an additional layer of conditionality was tested by integrating the CRISPR technology with an XVE-based, cell-type-specific inducible system (Siligato et al., 2016; Wang et al., 2020; Zuo et al., 2000). This inducible CRISPR system in *Arabidopsis* enables efficient generation of target gene knockouts in desired cell types and at desired times (Wang et al., 2020).

It was recently demonstrated that it is possible to knockout genes in entire lateral roots using the promoter sequence of *GATA23* (Decaestecker et al., 2019). As proof-of-concept *GFP* was targeted in *Arabidopsis* seedlings ubiquitously expressing *NLS-GFP* in the transgenic line *pHTR5:NLS-GFP-GUS* (Decaestecker et al., 2019; Ingouff et al., 2017). Fluorescence -and sequence analysis of T1 and T2 seedlings demonstrated that organ-specific *GFP* knockout in lateral roots is highly efficient via the xylem-pole pericycle-expressed Cas9 controlled by *GATA23*. Interestingly, the observation that entire lateral roots lack GFP signal, provides evidence that *GATA23*-expressing precursor cells are clonally linked to the cells that constitute lateral roots.

In a next step, *ARF7* and *ARF19* were targeted as lateral root initiation is strongly inhibited in *arf7arf19* double mutants (Decaestecker et al., 2019; Okushima et al., 2007). Surprisingly, lateral root initiation was only mildly affected when *ARF7* and *ARF19* were knocked out in *GATA23*-expressing pericycle cells (Decaestecker et al., 2019) while an *arf7arf19* mutant is not capable in producing lateral roots. This suggests that the function of ARF7 and ARF19 in lateral root founder cells is not essential for lateral root development and raises the question of when and in which cells of the primary root these ARFs are necessary for lateral root organogenesis. These experiments demonstrate that conditional knockouts enable to study the function of genes in spatial and temporal contexts of plant development. In summary, loss-of-function studies by generating inheritable or somatic mutations using genome editing opens avenues for discovering and analysing gene functions in lateral root development.

Conclusions and perspectives

Root branching through lateral root formation is an important component of the adaptability of the root system to its environment. Regular spacing of lateral roots, as well as initiation and development of lateral root primordia, is tightly regulated in *Arabidopsis*. However, lateral root development is readily influenced by external cues, ensuring the root system architecture is highly adaptable to different environmental conditions. To achieve such strict regulation while maintaining a high degree of flexibility, lateral root development relies on strong intercellular communication networks, mediated by the exchange of molecular messengers over both short and long distances.

Auxin acts as a common integrator to many endogenous and environmental signals regulating lateral root development. It was shown that auxin regulates and coordinates both lateral root founder cell divisions and founder cell polarity/identity specification during lateral root initiation. Thereafter, auxin plays an instructive role for the structural and functional patterning of the lateral root primordium. How and which molecular mechanisms auxin regulates during lateral root development are still poorly understood. However, it has been becoming increasingly clear that a multitude of secreted signalling peptides and their transmembrane receptors are involved. A plethora of peptide-receptor signalling pathways have been identified mediating both stimulatory and inhibitory effects on lateral root initiation. How signals of different peptides are integrated to result in specific developmental outputs requires further research.

Root development is primarily controlled by three intertwined parameters: the timing of cell division, the orientation of the plane of cell division and the degree and direction of cell expansion. Hence, detailed functional analysis of genes involved in these fundamentally important processes in a developmental-specific context is limited because loss-of-function results in pleiotropic phenotypes or even embryo lethality. Lateral root-specific genome editing with CRISPR technology enables the analysis of gene function specifically in root organogenesis. The advantageous properties of *Arabidopsis* root development including simple morphology, small size, transparent organ combined with genome editing will undoubtedly contribute to a better understanding of these fundamental cellular processes.

References

Aida, M., Beis, D., Heidstra, R., Willemsen, V., Blilou, I., Galinha, C., Nussaume, L., Noh, Y.-S., Amasino, R., & Scheres, B. (2004). The PLETHORA Genes Mediate Patterning of the Arabidopsis Root Stem Cell Niche. *Cell, 119*(1), 109-120. https://doi.org/https://doi.org/10.1016/j.cell.2004.09.018

Alvarez, J. P., Pekker, I., Goldshmidt, A., Blum, E., Amsellem, Z., & Eshed, Y. (2006). Endogenous and Synthetic MicroRNAs Stimulate Simultaneous, Efficient, and Localized Regulation of Multiple Targets in Diverse Species. *The Plant Cell, 18*(5), 1134. https://doi.org/10.1105/tpc.105.040725

Atkinson, N. J., Lilley, C. J., & Urwin, P. E. (2013). Identification of Genes Involved in the Response of Arabidopsis to Simultaneous Biotic and Abiotic Stresses. *Plant Physiology, 162*(4), 2028. https://doi.org/10.1104/pp.113.222372

Banda, J., Bellande, K., von Wangenheim, D., Goh, T., Guyomarc'h, S., Laplaze, L., & Bennett, M. J. (2019). Lateral Root Formation in Arabidopsis: A Well-Ordered LRexit. *Trends in Plant Science, 24*(9), 826-839. https://doi.org/https://doi.org/10.1016/j.tplants.2019.06.015

Beeckman, T., Burssens, S., & Inzé, D. (2001). The peri-cell-cycle in Arabidopsis. *Journal of Experimental Botany, 52*(suppl_1), 403-411. https://doi.org/10.1093/jexbot/52.suppl_1.403

Benková, E., Michniewicz, M., Sauer, M., Teichmann, T., Seifertová, D., Jürgens, G., & Friml, J. (2003). Local, Efflux-Dependent Auxin Gradients as a Common Module for Plant Organ Formation. *Cell, 115*(5), 591-602. https://doi.org/https://doi.org/10.1016/S0092-8674(03)00924-3

Berckmans, B., Kirschner, G., Gerlitz, N., Stadler, R., & Simon, R. (2020). CLE40 Signaling Regulates Root Stem Cell Fate. *Plant Physiology, 182*(4), 1776. https://doi.org/10.1104/pp.19.00914

Berckmans, B., Vassileva, V., Schmid, S. P. C., Maes, S., Parizot, B., Naramoto, S., Magyar, Z., Kamei, C. L. A., Koncz, C., Bögre, L., Persiau, G., De Jaeger, G., Friml, J., Simon, R., Beeckman, T., & De Veylder, L. (2011). Auxin-Dependent Cell Cycle Reactivation through Transcriptional Regulation of Arabidopsis E2F by Lateral Organ Boundary Proteins. *The Plant Cell, 23*(10), 3671. https://doi.org/10.1105/tpc.111.088377

Bergonci, T., Ribeiro, B., Ceciliato, P. H. O., Guerrero-Abad, J. C., Silva-Filho, M. C., & Moura, D. S. (2014). Arabidopsis thaliana RALF1 opposes brassinosteroid effects on root cell elongation and lateral root formation. *Journal of Experimental Botany, 65*(8), 2219-2230. https://doi.org/10.1093/jxb/eru099

Bortesi, L., & Fischer, R. (2015). The CRISPR/Cas9 system for plant genome editing and beyond. *Biotechnology Advances, 33*(1), 41-52. https://doi.org/https://doi.org/10.1016/j.biotechadv.2014.12.006

Casimiro, I., Beeckman, T., Graham, N., Bhalerao, R., Zhang, H., Casero, P., Sandberg, G., & Bennett, M. J. (2003). Dissecting Arabidopsis lateral root development. *Trends in Plant Science, 8*(4), 165-171. https://doi.org/https://doi.org/10.1016/S1360-1385(03)00051-7

Casimiro, I., Marchant, A., Bhalerao, R. P., Beeckman, T., Dhooge, S., Swarup, R., Graham, N., Inzé, D., Sandberg, G., Casero, P. J., & Bennett, M. (2001). Auxin Transport Promotes Arabidopsis Lateral Root Initiation. *The Plant Cell, 13*(4), 843. https://doi.org/10.1105/tpc.13.4.843

Cho, H., Ryu, H., Rho, S., Hill, K., Smith, S., Audenaert, D., Park, J., Han, S., Beeckman, T., Bennett, M. J., Hwang, D., De Smet, I., & Hwang, I. (2014). A secreted peptide acts on BIN2-mediated phosphorylation of ARFs to potentiate auxin response during lateral root development. *Nature Cell Biology, 16*(1), 66-76. https://doi.org/10.1038/ncb2893

Christian, M., Cermak, T., Doyle, E. L., Schmidt, C., Zhang, F., Hummel, A., Bogdanove, A. J., & Voytas, D. F. (2010). Targeting DNA Double-Strand Breaks with TAL Effector Nucleases. *Genetics, 186*(2), 757. https://doi.org/10.1534/genetics.110.120717

De Rybel, B., Vassileva, V., Parizot, B., Demeulenaere, M., Grunewald, W., Audenaert, D., Van Campenhout, J., Overvoorde, P., Jansen, L., Vanneste, S., Möller, B., Wilson, M., Holman, T., Van Isterdael, G., Brunoud, G., Vuylsteke, M., Vernoux, T., De Veylder, L., Inzé, D., Weijers, D., Bennett, M. J., & Beeckman, T. (2010). A Novel Aux/IAA28 Signaling Cascade Activates GATA23-Dependent Specification of Lateral Root Founder Cell Identity. *Current Biology, 20*(19), 1697-1706. https://doi.org/https://doi.org/10.1016/j.cub.2010.09.007

De Smet, I. (2010). Multimodular auxin response controls lateral root development in Arabidopsis. *Plant Signaling & Behavior, 5*(5), 580-582. https://doi.org/10.4161/psb.11495

De Smet, I., Lau, S., Voß, U., Vanneste, S., Benjamins, R., Rademacher, E. H., Schlereth, A., De Rybel, B., Vassileva, V., Grunewald, W., Naudts, M., Levesque, M. P., Ehrismann, J. S., Inzé, D., Luschnig, C., Benfey, P. N., Weijers, D., Van Montagu, M. C. E., Bennett, M. J., Jürgens, G., & Beeckman, T. (2010). Bimodular auxin response controls organogenesis in Arabidopsis. *Proceedings of the National Academy of Sciences, 107*(6), 2705. https://doi.org/10.1073/pnas.0915001107

De Smet, I., Tetsumura, T., De Rybel, B., Frey, N. F. d., Laplaze, L., Casimiro, I., Swarup, R., Naudts, M., Vanneste, S., Audenaert, D., Inzé, D., Bennett, M. J., & Beeckman, T. (2007). Auxin-dependent regulation of lateral root positioning in the basal meristem of Arabidopsis. *Development, 134*(4), 681. https://doi.org/10.1242/dev.02753

De Smet, I., Vassileva, V., De Rybel, B., Levesque, M. P., Grunewald, W., Van Damme, D., Van Noorden, G., Naudts, M., Van Isterdael, G., De Clercq, R., Wang, J. Y., Meuli, N., Vanneste, S., Friml, J., Hilson, P., Jürgens, G., Ingram, G. C., Inzé, D., Benfey, P. N., & Beeckman, T. (2008). Receptor-Like Kinase ACR4 Restricts Formative Cell Divisions in the Arabidopsis; Root. *Science, 322*(5901), 594. https://doi.org/10.1126/science.1160158

Decaestecker, W., Buono, R. A., Pfeiffer, M. L., Vangheluwe, N., Jourquin, J., Karimi, M., Van Isterdael, G., Beeckman, T., Nowack, M. K., & Jacobs, T. B. (2019). CRISPR-TSKO: A Technique for Efficient Mutagenesis in Specific Cell Types, Tissues, or Organs in Arabidopsis. *The Plant Cell, 31*(12), 2868. https://doi.org/10.1105/tpc.19.00454

Delay, C., Imin, N., & Djordjevic, M. A. (2013). CEP genes regulate root and shoot development in response to environmental cues and are specific to seed plants. *Journal of Experimental Botany, 64*(17), 5383-5394. https://doi.org/10.1093/jxb/ert332

DiDonato, R. J., Arbuckle, E., Buker, S., Sheets, J., Tobar, J., Totong, R., Grisafi, P., Fink, G. R., & Celenza, J. L. (2004). Arabidopsis ALF4 encodes a nuclear-localized protein required for lateral root formation. *The Plant Journal, 37*(3), 340-353. https://doi.org/10.1046/j.1365-313X.2003.01964.x

Dong, Q., Zhang, Z., Liu, Y., Tao, L.-Z., & Liu, H. (2019). FERONIA regulates auxin-mediated lateral root development and primary root gravitropism. *FEBS Letters, 593*(1), 97-106. https://doi.org/10.1002/1873-3468.13292

Du, Y., & Scheres, B. (2017). PLETHORA transcription factors orchestrate de novo organ patterning during Arabidopsis lateral root outgrowth. *Proceedings of the National Academy of Sciences, 114*(44), 11709. https://doi.org/10.1073/pnas.1714410114

Du, Y., & Scheres, B. (2018). Lateral root formation and the multiple roles of auxin. *Journal of Experimental Botany, 69*(2), 155-167. https://doi.org/10.1093/jxb/erx223

Dubrovsky, J. G., Doerner, P. W., Colón-Carmona, A., & Rost, T. L. (2000). Pericycle Cell Proliferation and Lateral Root Initiation in Arabidopsis. *Plant Physiology, 124*(4), 1648. https://doi.org/10.1104/pp.124.4.1648

Dubrovsky, J. G., Sauer, M., Napsucialy-Mendivil, S., Ivanchenko, M. G., Friml, J., Shishkova, S., Celenza, J., & Benková, E. (2008). Auxin acts as a local morphogenetic trigger to specify lateral root founder cells. *Proceedings of the National Academy of Sciences, 105*(25), 8790. https://doi.org/10.1073/pnas.0712307105

Fernandez, A., Drozdzecki, A., Hoogewijs, K., Nguyen, A., Beeckman, T., Madder, A., & Hilson, P. (2013). Transcriptional and Functional Classification of the GOLVEN/ROOT GROWTH FACTOR/CLE-Like Signaling Peptides Reveals Their Role in Lateral Root and Hair Formation. *Plant Physiology, 161*(2), 954. https://doi.org/10.1104/pp.112.206029

Fernandez, A., Drozdzecki, A., Hoogewijs, K., Vassileva, V., Madder, A., Beeckman, T., & Hilson, P. (2015). The GLV6/RGF8/CLEL2 peptide regulates early pericycle divisions during lateral root initiation. *Journal of Experimental Botany, 66*(17), 5245-5256. https://doi.org/10.1093/jxb/erv329

Fernandez, A. I., Vangheluwe, N., Xu, K., Jourquin, J., Claus, L. A. N., Morales-Herrera, S., Parizot, B., De Gernier, H., Yu, Q., Drozdzecki, A., Maruta, T., Hoogewijs, K., Vannecke, W., Peterson, B., Opdenacker, D., Madder, A., Nimchuk, Z. L., Russinova, E., & Beeckman, T. (2020). GOLVEN peptide signalling through RGI receptors and MPK6 restricts asymmetric cell division during lateral root initiation. *Nature Plants, 6*(5), 533-543. https://doi.org/10.1038/s41477-020-0645-z

Fukaki, H., Nakao, Y., Okushima, Y., Theologis, A., & Tasaka, M. (2005). Tissue-specific expression of stabilized SOLITARY-ROOT/IAA14 alters lateral root development in Arabidopsis. *The Plant Journal, 44*(3), 382-395. https://doi.org/10.1111/j.1365-313X.2005.02537.x

Fukaki, H., Tameda, S., Masuda, H., & Tasaka, M. (2002). Lateral root formation is blocked by a gain-of-function mutation in the SOLITARY-ROOT/IAA14 gene of Arabidopsis. *The Plant Journal, 29*(2), 153-168. https://doi.org/10.1046/j.0960-7412.2001.01201.x

Ghorbani, S., Hoogewijs, K., Pečenková, T., Fernandez, A., Inzé, A., Eeckhout, D., Kawa, D., De Jaeger, G., Beeckman, T., Madder, A., Van Breusegem, F., & Hilson, P. (2016). The SBT6.1 subtilase processes the GOLVEN1 peptide controlling cell elongation. *Journal of Experimental Botany, 67*(16), 4877-4887. https://doi.org/10.1093/jxb/erw241

Gifford, E. M. (1983). Concept of Apical Cells in Bryophytes and Pteridophytes. *Annual Review of Plant Physiology, 34*(1), 419-440. https://doi.org/10.1146/annurev.pp.34.060183.002223

Goh, T., Joi, S., Mimura, T., & Fukaki, H. (2012). The establishment of asymmetry in Arabidopsis lateral root founder cells is regulated by LBD16/ASL18 and related LBD/ASL proteins. *Development, 139*(5), 883. https://doi.org/10.1242/dev.071928

Goh, T., Toyokura, K., Wells, D. M., Swarup, K., Yamamoto, M., Mimura, T., Weijers, D., Fukaki, H., Laplaze, L., Bennett, M. J., Guyomarc, & h, S. (2016). Quiescent center initiation in the Arabidopsis lateral root primordia is dependent on the SCARECROW transcription factor. *Development, 143*(18), 3363. https://doi.org/10.1242/dev.135319

Gonneau, M., Desprez, T., Martin, M., Doblas, V. G., Bacete, L., Miart, F., Sormani, R., Hématy, K., Renou, J., Landrein, B., Murphy, E., Van De Cotte, B., Vernhettes, S., De Smet, I., & Höfte, H. (2018). Receptor Kinase THESEUS1 Is a Rapid Alkalinization Factor 34 Receptor in Arabidopsis. *Current Biology, 28*(15), 2452-2458.e2454. https://doi.org/https://doi.org/10.1016/j.cub.2018.05.075

Gunning, B. E. S., Hughes, J. E., & Hardham, A. R. (1978). Formative and proliferative cell divisions, cell differentiation, and developmental changes in the meristem of Azolla roots. *Planta, 143*(2), 121-144. https://doi.org/10.1007/BF00387786

Hamann, T., Benkova, E., Bäurle, I., Kientz, M., & Jürgens, G. (2002). The Arabidopsis BODENLOS gene encodes an auxin response protein inhibiting MONOPTEROS-mediated embryo patterning. *Genes & Development, 16*(13), 1610-1615. https://doi.org/10.1101/gad.229402

Haruta, M., Sabat, G., Stecker, K., Minkoff, B. B., & Sussman, M. R. (2014). A Peptide Hormone and Its Receptor Protein Kinase Regulate Plant Cell Expansion. *Science, 343*(6169), 408. https://doi.org/10.1126/science.1244454

Heidstra, R., Welch, D., & Scheres, B. (2004). Mosaic analyses using marked activation and deletion clones dissect Arabidopsis SCARECROW action in asymmetric cell division. *Genes & Development, 18*(16), 1964-1969. https://doi.org/10.1101/gad.305504

Hetherington, A. J., & Dolan, L. (2017). The evolution of lycopsid rooting structures: conservatism and disparity. *New Phytologist, 215*(2), 538-544. https://doi.org/10.1111/nph.14324

Himanen, K., Boucheron, E., Vanneste, S., de Almeida Engler, J., Inzé, D., & Beeckman, T. (2002). Auxin-Mediated Cell Cycle Activation during Early Lateral Root Initiation. *The Plant Cell, 14*(10), 2339. https://doi.org/10.1105/tpc.004960

Himanen, K., Vuylsteke, M., Vanneste, S., Vercruysse, S., Boucheron, E., Alard, P., Chriqui, D., Van Montagu, M., Inzé, D., & Beeckman, T. (2004). Transcript profiling of early lateral root initiation. *Proceedings of the National Academy of Sciences of the United States of America, 101*(14), 5146. https://doi.org/10.1073/pnas.0308702101

Hirakawa, Y., Shinohara, H., Kondo, Y., Inoue, A., Nakanomyo, I., Ogawa, M., Sawa, S., Ohashi-Ito, K., Matsubayashi, Y., & Fukuda, H. (2008). Non-cell-autonomous control of vascular stem cell fate by a CLE peptide/receptor system. *Proceedings of the National Academy of Sciences, 105*(39), 15208. https://doi.org/10.1073/pnas.0808444105

Hirota, A., Kato, T., Fukaki, H., Aida, M., & Tasaka, M. (2007). The Auxin-Regulated AP2/EREBP Gene PUCHI Is Required for Morphogenesis in the Early Lateral Root Primordium of Arabidopsis. *The Plant Cell, 19*(7), 2156. https://doi.org/10.1105/tpc.107.050674

Hou, G.-c., & Hill, J. P. (2004). Developmental anatomy of the fifth shoot-borne root in young sporophytes of Ceratopteris richardii. *Planta, 219*(2), 212-220. https://doi.org/10.1007/s00425-004-1225-6

Hou, G., Hill, J. P., & Blancaflor, E. B. (2004). Developmental anatomy and auxin response of lateral root formation in Ceratopteris richardii. *Journal of Experimental Botany, 55*(397), 685-693. https://doi.org/10.1093/jxb/erh068

Hyun, Y., Kim, J., Cho, S. W., Choi, Y., Kim, J.-S., & Coupland, G. (2015). Site-directed mutagenesis in Arabidopsis thaliana using dividing tissue-targeted RGEN of the CRISPR/Cas system to generate heritable null alleles. *Planta, 241*(1), 271-284. https://doi.org/10.1007/s00425-014-2180-5

Ingouff, M., Selles, B., Michaud, C., Vu, T. M., Berger, F., Schorn, A. J., Autran, D., Van Durme, M., Nowack, M. K., Martienssen, R. A., & Grimanelli, D. (2017). Live-cell analysis of DNA methylation during sexual reproduction in Arabidopsis reveals context and sex-specific dynamics controlled by noncanonical RdDM. *Genes & Development, 31*(1), 72-83. https://doi.org/10.1101/gad.289397.116

Jasin, M. (1996). Genetic manipulation of genomes with rare-cutting endonucleases. *Trends Genet, 12*(6), 224-228. https://doi.org/10.1016/0168-9525(96)10019-6

Jinek, M., Chylinski, K., Fonfara, I., Hauer, M., Doudna, J. A., & Charpentier, E. (2012). A Programmable Dual-RNA–Guided DNA Endonuclease in Adaptive Bacterial Immunity. *Science, 337*(6096), 816. https://doi.org/10.1126/science.1225829

Jourquin, J., Fukaki, H., & Beeckman, T. (2020). Peptide-Receptor Signaling Controls Lateral Root Development. *Plant Physiology, 182*(4), 1645. https://doi.org/10.1104/pp.19.01317

Jurado, S., Abraham, Z., Manzano, C., López-Torrejón, G., Pacios, L. F., & Del Pozo, J. C. (2010). The Arabidopsis Cell Cycle F-Box Protein SKP2A Binds to Auxin. *The Plant Cell, 22*(12), 3891. https://doi.org/10.1105/tpc.110.078972

Jurado, S., Diaz-Trivino, S., Abraham, Z., Manzano, C., Gutierrez, C., & del Pozo, J. c. (2008). SKP2A protein, an F-box that regulates cell division, is degraded via the ubiquitin pathway. *Plant Signaling & Behavior, 3*(10), 810-812. https://doi.org/10.4161/psb.3.10.5888

Kajala, K., Ramakrishna, P., Fisher, A., C. Bergmann, D., De Smet, I., Sozzani, R., Weijers, D., & Brady, S. M. (2014). Omics and modelling approaches for understanding regulation of asymmetric cell divisions in arabidopsis and other angiosperm plants. *Annals of Botany, 113*(7), 1083-1105. https://doi.org/10.1093/aob/mcu065

Kim, Y. G., Cha, J., & Chandrasegaran, S. (1996). Hybrid restriction enzymes: zinc finger fusions to Fok I cleavage domain. *Proceedings of the National Academy of Sciences, 93*(3), 1156. https://doi.org/10.1073/pnas.93.3.1156

Koevoets, I. T., Venema, J. H., Elzenga, J. T. M., & Testerink, C. (2016). Roots Withstanding their Environment: Exploiting Root System Architecture Responses to Abiotic Stress

to Improve Crop Tolerance [Review]. *Frontiers in Plant Science, 7*(1335). https://doi.org/10.3389/fpls.2016.01335

Laplaze, L., Parizot, B., Baker, A., Ricaud, L., Martinière, A., Auguy, F., Franche, C., Nussaume, L., Bogusz, D., & Haseloff, J. (2005). GAL4-GFP enhancer trap lines for genetic manipulation of lateral root development in Arabidopsis thaliana. *Journal of Experimental Botany, 56*(419), 2433-2442. https://doi.org/10.1093/jxb/eri236

Laskowski, M., Grieneisen, V. A., Hofhuis, H., Hove, C. A. t., Hogeweg, P., Marée, A. F. M., & Scheres, B. (2008). Root System Architecture from Coupling Cell Shape to Auxin Transport. *PLOS Biology, 6*(12), e307. https://doi.org/10.1371/journal.pbio.0060307

Laskowski, M. J., Williams, M. E., Nusbaum, H. C., & Sussex, I. M. (1995). Formation of lateral root meristems is a two-stage process. *Development, 121*(10), 3303. http://dev.biologists.org/content/121/10/3303.abstract

Lavenus, J., Goh, T., Roberts, I., Guyomarc'h, S., Lucas, M., De Smet, I., Fukaki, H., Beeckman, T., Bennett, M., & Laplaze, L. (2013). Lateral root development in Arabidopsis: fifty shades of auxin. *Trends in Plant Science, 18*(8), 450-458. https://doi.org/https://doi.org/10.1016/j.tplants.2013.04.006

Lease, K. A., & Walker, J. C. (2006). The Arabidopsis Unannotated Secreted Peptide Database, a Resource for Plant Peptidomics. *Plant Physiology, 142*(3), 831. https://doi.org/10.1104/pp.106.086041

Lee, H. W., Kim, N. Y., Lee, D. J., & Kim, J. (2009). LBD18/ASL20 Regulates Lateral Root Formation in Combination with LBD16/ASL18 Downstream of ARF7 and ARF19 in Arabidopsis. *Plant Physiology, 151*(3), 1377. https://doi.org/10.1104/pp.109.143685

Liang, Y., Eudes, A., Yogiswara, S., Jing, B., Benites, V. T., Yamanaka, R., Cheng-Yue, C., Baidoo, E. E., Mortimer, J. C., Scheller, H. V., & Loqué, D. (2019). A screening method to identify efficient sgRNAs in Arabidopsis, used in conjunction with cell-specific lignin reduction. *Biotechnology for Biofuels, 12*(1), 130. https://doi.org/10.1186/s13068-019-1467-y

Lloyd, J. P., Seddon, A. E., Moghe, G. D., Simenc, M. C., & Shiu, S.-H. (2015). Characteristics of Plant Essential Genes Allow for within- and between-Species Prediction of Lethal Mutant Phenotypes. *The Plant Cell, 27*(8), 2133. https://doi.org/10.1105/tpc.15.00051

Lucas, M., Kenobi, K., von Wangenheim, D., Voβ, U., Swarup, K., De Smet, I., Van Damme, D., Lawrence, T., Péret, B., Moscardi, E., Barbeau, D., Godin, C., Salt, D., Guyomarc'h, S., Stelzer, E. H. K., Maizel, A., Laplaze, L., & Bennett, M. J. (2013). Lateral root morphogenesis is dependent on the mechanical properties of the overlaying tissues. *Proceedings of the National Academy of Sciences, 110*(13), 5229. https://doi.org/10.1073/pnas.1210807110

Malamy, J. E., & Benfey, P. N. (1997). Organization and cell differentiation in lateral roots of Arabidopsis thaliana. *Development, 124*(1), 33. http://dev.biologists.org/content/124/1/33.abstract

Manzano, C., Ramirez-Parra, E., Casimiro, I., Otero, S., Desvoyes, B., De Rybel, B., Beeckman, T., Casero, P., Gutierrez, C., & C. del Pozo, J. (2012). Auxin and Epigenetic Regulation of SKP2B, an F-Box That Represses Lateral Root Formation. *Plant Physiology, 160*(2), 749. https://doi.org/10.1104/pp.112.198341

Mao, Y., Zhang, Z., Feng, Z., Wei, P., Zhang, H., Botella, J. R., & Zhu, J.-K. (2016). Development of germ-line-specific CRISPR-Cas9 systems to improve the production of heritable gene modifications in Arabidopsis. *Plant Biotechnology Journal, 14*(2), 519-532. https://doi.org/10.1111/pbi.12468

Marhavý, P., Vanstraelen, M., De Rybel, B., Zhaojun, D., Bennett, M. J., Beeckman, T., & Benková, E. (2013). Auxin reflux between the endodermis and pericycle promotes lateral root initiation. *The EMBO Journal, 32*(1), 149-158. https://doi.org/10.1038/emboj.2012.303

Matsuzaki, Y., Ogawa-Ohnishi, M., Mori, A., & Matsubayashi, Y. (2010). Secreted Peptide Signals Required for Maintenance of Root Stem Cell Niche in Arabidopsis. *Science, 329*(5995), 1065. https://doi.org/10.1126/science.1191132

Melnyk, C. W., Molnar, A., & Baulcombe, D. C. (2011). Intercellular and systemic movement of RNA silencing signals. *The EMBO Journal, 30*(17), 3553-3563. https://doi.org/10.1038/emboj.2011.274

Meng, L., Buchanan, B. B., Feldman, L. J., & Luan, S. (2012). CLE-like (CLEL) peptides control the pattern of root growth and lateral root development in Arabidopsis. *Proceedings of the National Academy of Sciences, 109*(5), 1760. https://doi.org/10.1073/pnas.1119864109

Mitsuda, N., Matsui, K., Ikeda, M., Nakata, M., Oshima, Y., Nagatoshi, Y., & Ohme-Takagi, M. (2011). CRES-T, An Effective Gene Silencing System Utilizing Chimeric Repressors. In L. Yuan & S. E. Perry (Eds.), *Plant Transcription Factors: Methods and Protocols* (pp. 87-105). Humana Press. https://doi.org/10.1007/978-1-61779-154-3_5

Moreno-Risueno, M. A., Van Norman, J. M., Moreno, A., Zhang, J., Ahnert, S. E., & Benfey, P. N. (2010). Oscillating Gene Expression Determines Competence for Periodic Arabidopsis Root Branching. *Science, 329*(5997), 1306. https://doi.org/10.1126/science.1191937

Motte, H., & Beeckman, T. (2019). The evolution of root branching: increasing the level of plasticity. *Journal of Experimental Botany, 70*(3), 785-793. https://doi.org/10.1093/jxb/ery409

Murphy, E., Vu, L. D., Van den Broeck, L., Lin, Z., Ramakrishna, P., van de Cotte, B., Gaudinier, A., Goh, T., Slane, D., Beeckman, T., Inzé, D., Brady, S. M., Fukaki, H., & De Smet, I. (2016). RALFL34 regulates formative cell divisions in Arabidopsis pericycle during lateral root initiation. *Journal of Experimental Botany, 67*(16), 4863-4875. https://doi.org/10.1093/jxb/erw281

Nieuwland, J., Maughan, S., Dewitte, W., Scofield, S., Sanz, L., & Murray, J. A. H. (2009). The D-type cyclin CYCD4;1 modulates lateral root density in Arabidopsis by affecting the basal meristem region. *Proceedings of the National Academy of Sciences, 106*(52), 22528. https://doi.org/10.1073/pnas.0906354106

Oh, E., Seo, P. J., & Kim, J. (2018). Signaling Peptides and Receptors Coordinating Plant Root Development. *Trends in Plant Science, 23*(4), 337-351. https://doi.org/https://doi.org/10.1016/j.tplants.2017.12.007

Okushima, Y., Fukaki, H., Onoda, M., Theologis, A., & Tasaka, M. (2007). ARF7 and ARF19 Regulate Lateral Root Formation via Direct Activation of LBD/ASL Genes in Arabidopsis. *The Plant Cell, 19*(1), 118. https://doi.org/10.1105/tpc.106.047761

Orosa-Puente, B., Leftley, N., von Wangenheim, D., Banda, J., Srivastava, A. K., Hill, K., Truskina, J., Bhosale, R., Morris, E., Srivastava, M., Kümpers, B., Goh, T., Fukaki, H., Vermeer, J. E. M., Vernoux, T., Dinneny, J. R., French, A. P., Bishopp, A., Sadanandom, A., & Bennett, M. J. (2018). Root branching toward water involves posttranslational modification of transcription factor ARF7. *Science, 362*(6421), 1407. https://doi.org/10.1126/science.aau3956

Ou, Y., Lu, X., Zi, Q., Xun, Q., Zhang, J., Wu, Y., Shi, H., Wei, Z., Zhao, B., Zhang, X., He, K., Gou, X., Li, C., & Li, J. (2016). RGF1 INSENSITIVE 1 to 5, a group of LRR receptor-like kinases, are essential for the perception of root meristem growth factor 1 in Arabidopsis thaliana. *Cell Research, 26*(6), 686-698. https://doi.org/10.1038/cr.2016.63

Parizot, B., De Rybel, B., & Beeckman, T. (2010). VisuaLRTC: A New View on Lateral Root Initiation by Combining Specific Transcriptome Data Sets. *Plant Physiology, 153*(1), 34. https://doi.org/10.1104/pp.109.148676

Parizot, B., Laplaze, L., Ricaud, L., Boucheron-Dubuisson, E., Bayle, V., Bonke, M., De Smet, I., Poethig, S. R., Helariutta, Y., Haseloff, J., Chriqui, D., Beeckman, T., & Nussaume, L. (2008). Diarch Symmetry of the Vascular Bundle in Arabidopsis Root Encompasses the Pericycle and Is Reflected in Distich Lateral Root Initiation. *Plant Physiology, 146*(1), 140. https://doi.org/10.1104/pp.107.107870

Péret, B., De Rybel, B., Casimiro, I., Benková, E., Swarup, R., Laplaze, L., Beeckman, T., & Bennett, M. J. (2009). Arabidopsis lateral root development: an emerging story. *Trends in Plant Science, 14*(7), 399-408. https://doi.org/https://doi.org/10.1016/j.tplants.2009.05.002

Pérez-Pérez, J. M., Ponce, M. R., & Micol, J. L. (2002). The UCU1 Arabidopsis gene encodes a SHAGGY/GSK3-like kinase required for cell expansion along the proximodistal axis. *Dev Biol, 242*(2), 161-173. https://doi.org/10.1006/dbio.2001.0543

Piekarska-Stachowiak, A., & Nakielski, J. (2013). The simulation model of growth and cell divisions for the root apex with an apical cell in application to Azolla pinnata. *Planta, 238*(6), 1051-1064. https://doi.org/10.1007/s00425-013-1950-9

Ren, H., Santner, A., Pozo, J. C. d., Murray, J. A. H., & Estelle, M. (2008). Degradation of the cyclin-dependent kinase inhibitor KRP1 is regulated by two different ubiquitin E3 ligases. *The Plant Journal, 53*(5), 705-716. https://doi.org/10.1111/j.1365-313X.2007.03370.x

Roberts, I., Smith, S., De Rybel, B., Van Den Broeke, J., Smet, W., De Cokere, S., Mispelaere, M., De Smet, I., & Beeckman, T. (2013). The CEP family in land plants: evolutionary analyses, expression studies, and role in Arabidopsis shoot development. *Journal of Experimental Botany, 64*(17), 5371-5381. https://doi.org/10.1093/jxb/ert331

Roberts, I., Smith, S., Stes, E., De Rybel, B., Staes, A., van de Cotte, B., Njo, M. F., Dedeyne, L., Demol, H., Lavenus, J., Audenaert, D., Gevaert, K., Beeckman, T., & De Smet, I. (2016). CEP5 and XIP1/CEPR1 regulate lateral root initiation in Arabidopsis. *Journal of Experimental Botany, 67*(16), 4889-4899. https://doi.org/10.1093/jxb/erw231

Rojas-Murcia, N., Hématy, K., Lee, Y., Emonet, A., Ursache, R., Fujita, S., De Bellis, D., & Geldner, N. (2020). High-order mutants reveal an essential requirement for peroxidases but not laccases in Casparian strip lignification. *bioRxiv*, 2020.2006.2017.154617. https://doi.org/10.1101/2020.06.17.154617

Sanz, L., Dewitte, W., Forzani, C., Patell, F., Nieuwland, J., Wen, B., Quelhas, P., De Jager, S., Titmus, C., Campilho, A., Ren, H., Estelle, M., Wang, H., & Murray, J. A. H. (2011). The Arabidopsis D-Type Cyclin CYCD2;1 and the Inhibitor ICK2/KRP2 Modulate Auxin-Induced Lateral Root Formation. *The Plant Cell, 23*(2), 641. https://doi.org/10.1105/tpc.110.080002

Schiefelbein, J. W., and Benfey, P.N. (1994). Root development in Arabidopsis. *Cold Spring Harbor Laboratory Press*, 335-353.

Schiml, S., Fauser, F., & Puchta, H. (2014). The CRISPR/Cas system can be used as nuclease for in planta gene targeting and as paired nickases for directed mutagenesis in Arabidopsis resulting in heritable progeny. *The Plant Journal, 80*(6), 1139-1150. https://doi.org/10.1111/tpj.12704

Schlereth, A., Möller, B., Liu, W., Kientz, M., Flipse, J., Rademacher, E. H., Schmid, M., Jürgens, G., & Weijers, D. (2010). MONOPTEROS controls embryonic root initiation by regulating a mobile transcription factor. *Nature, 464*(7290), 913-916. https://doi.org/10.1038/nature08836

Schwab, R., Ossowski, S., Riester, M., Warthmann, N., & Weigel, D. (2006). Highly Specific Gene Silencing by Artificial MicroRNAs in Arabidopsis. *The Plant Cell, 18*(5), 1121. https://doi.org/10.1105/tpc.105.039834

Shinohara, H., Mori, A., Yasue, N., Sumida, K., & Matsubayashi, Y. (2016). Identification of three LRR-RKs involved in perception of root meristem growth factor in Arabidopsis. *Proceedings of the National Academy of Sciences, 113*(14), 3897. https://doi.org/10.1073/pnas.1522639113

Sieburth, L. E., Drews, G. N., & Meyerowitz, E. M. (1998). Non-autonomy of AGAMOUS function in flower development: use of a Cre/loxP method for mosaic analysis in Arabidopsis. *Development, 125*(21), 4303. http://dev.biologists.org/content/125/21/4303.abstract

Siligato, R., Wang, X., Yadav, S. R., Lehesranta, S., Ma, G., Ursache, R., Sevilem, I., Zhang, J., Gorte, M., Prasad, K., Wrzaczek, M., Heidstra, R., Murphy, A., Scheres, B., & Mähönen, A. P. (2016). MultiSite Gateway-Compatible Cell Type-Specific Gene-Inducible System for Plants. *Plant Physiology, 170*(2), 627. https://doi.org/10.1104/pp.15.01246

Song, W., Liu, L., Wang, J., Wu, Z., Zhang, H., Tang, J., Lin, G., Wang, Y., Wen, X., Li, W., Han, Z., Guo, H., & Chai, J. (2016). Signature motif-guided identification of receptors for peptide hormones essential for root meristem growth. *Cell Research, 26*(6), 674-685. https://doi.org/10.1038/cr.2016.62

Stahl, Y., Grabowski, S., Bleckmann, A., Kühnemuth, R., Weidtkamp-Peters, S., Pinto, Karine G., Kirschner, Gwendolyn K., Schmid, Julia B., Wink, René H., Hülsewede, A., Felekyan, S., Seidel, Claus A. M., & Simon, R. (2013). Moderation of Arabidopsis Root Stemness by CLAVATA1 and ARABIDOPSIS CRINKLY4 Receptor Kinase Complexes. *Current Biology, 23*(5), 362-371. https://doi.org/https://doi.org/10.1016/j.cub.2013.01.045

Stahl, Y., & Simon, R. (2009). Is the Arabidopsis root niche protected by sequestration of the CLE40 signal by its putative receptor ACR4 *Plant Signaling & Behavior, 4*(7), 634-635. https://doi.org/10.4161/psb.4.7.8970

Tabata, R., Sumida, K., Yoshii, T., Ohyama, K., Shinohara, H., & Matsubayashi, Y. (2014). Perception of root-derived peptides by shoot LRR-RKs mediates systemic N-demand signaling. *Science, 346*(6207), 343. https://doi.org/10.1126/science.1257800

Tian, H., Jia, Y., Niu, T., Yu, Q., & Ding, Z. (2014). The key players of the primary root growth and development also function in lateral roots in Arabidopsis. *Plant Cell Reports, 33*(5), 745-753. https://doi.org/10.1007/s00299-014-1575-x

Toyokura, K., Goh, T., Shinohara, H., Shinoda, A., Kondo, Y., Okamoto, Y., Uehara, T., Fujimoto, K., Okushima, Y., Ikeyama, Y., Nakajima, K., Mimura, T., Tasaka, M., Matsubayashi, Y., & Fukaki, H. (2019). Lateral Inhibition by a Peptide Hormone-

Receptor Cascade during Arabidopsis Lateral Root Founder Cell Formation. *Developmental Cell, 48*(1), 64-75.e65. https://doi.org/https://doi.org/10.1016/j.devcel.2018.11.031

Ulmasov, T., Murfett, J., Hagen, G., & Guilfoyle, T. J. (1997). Aux/IAA proteins repress expression of reporter genes containing natural and highly active synthetic auxin response elements. *The Plant Cell, 9*(11), 1963. https://doi.org/10.1105/tpc.9.11.1963

Vanneste, S., Coppens, F., Lee, E., Donner, T. J., Xie, Z., Van Isterdael, G., Dhondt, S., De Winter, F., De Rybel, B., Vuylsteke, M., De Veylder, L., Friml, J., Inzé, D., Grotewold, E., Scarpella, E., Sack, F., Beemster, G. T. S., & Beeckman, T. (2011). Developmental regulation of CYCA2s contributes to tissue-specific proliferation in Arabidopsis. *The EMBO Journal, 30*(16), 3430-3441. https://doi.org/10.1038/emboj.2011.240

Vanneste, S., De Rybel, B., Beemster, G. T. S., Ljung, K., De Smet, I., Van Isterdael, G., Naudts, M., Iida, R., Gruissem, W., Tasaka, M., Inzé, D., Fukaki, H., & Beeckman, T. (2005). Cell Cycle Progression in the Pericycle Is Not Sufficient for SOLITARY ROOT/IAA14-Mediated Lateral Root Initiation in Arabidopsis thaliana. *The Plant Cell, 17*(11), 3035. https://doi.org/10.1105/tpc.105.035493

Vermeer, J. E. M., von Wangenheim, D., Barberon, M., Lee, Y., Stelzer, E. H. K., Maizel, A., & Geldner, N. (2014). A Spatial Accommodation by Neighboring Cells Is Required for Organ Initiation in Arabidopsis. *Science, 343*(6167), 178. https://doi.org/10.1126/science.1245871

Vert, G., Walcher, C. L., Chory, J., & Nemhauser, J. L. (2008). Integration of auxin and brassinosteroid pathways by Auxin Response Factor 2. *Proceedings of the National Academy of Sciences, 105*(28), 9829. https://doi.org/10.1073/pnas.0803996105

Voytas, D. F. (2013). Plant Genome Engineering with Sequence-Specific Nucleases. *Annual Review of Plant Biology, 64*(1), 327-350. https://doi.org/10.1146/annurev-arplant-042811-105552

Wada, N., Ueta, R., Osakabe, Y., & Osakabe, K. (2020). Precision genome editing in plants: state-of-the-art in CRISPR/Cas9-based genome engineering. *BMC Plant Biology, 20*(1), 234. https://doi.org/10.1186/s12870-020-02385-5

Wang, X., Ye, L., Lyu, M., Ursache, R., Löytynoja, A., & Mähönen, A. P. (2020). An inducible genome editing system for plants. *Nature Plants, 6*(7), 766-772. https://doi.org/10.1038/s41477-020-0695-2

Wiedenheft, B., Sternberg, S. H., & Doudna, J. A. (2012). RNA-guided genetic silencing systems in bacteria and archaea. *Nature, 482*(7385), 331-338. https://doi.org/10.1038/nature10886

Wu, Y., Xun, Q., Guo, Y., Zhang, J., Cheng, K., Shi, T., He, K., Hou, S., Gou, X., & Li, J. (2016). Genome-Wide Expression Pattern Analyses of the Arabidopsis Leucine-Rich Repeat Receptor-Like Kinases. *Molecular Plant, 9*(2), 289-300. https://doi.org/https://doi.org/10.1016/j.molp.2015.12.011

Xuan, W., Audenaert, D., Parizot, B., Möller, B. K., Njo, Maria F., De Rybel, B., De Rop, G., Van Isterdael, G., Mähönen, Ari P., Vanneste, S., & Beeckman, T. (2015). Root Cap-Derived Auxin Pre-patterns the Longitudinal Axis of the Arabidopsis Root. *Current Biology, 25*(10), 1381-1388. https://doi.org/https://doi.org/10.1016/j.cub.2015.03.046

Xuan, W., Band, L. R., Kumpf, R. P., Van Damme, D., Parizot, B., De Rop, G., Opdenacker, D., Möller, B. K., Skorzinski, N., Njo, M. F., De Rybel, B., Audenaert, D., Nowack, M. K., Vanneste, S., & Beeckman, T. (2016). Cyclic programmed cell death stimulates hormone signaling and root development in Arabidopsis. *Science, 351*(6271), 384. https://doi.org/10.1126/science.aad2776

Yamaguchi, Y. L., Ishida, T., Yoshimura, M., Imamura, Y., Shimaoka, C., & Sawa, S. (2017). A Collection of Mutants for CLE-Peptide-Encoding Genes in Arabidopsis Generated by CRISPR/Cas9-Mediated Gene Targeting. *Plant and Cell Physiology, 58*(11), 1848-1856. https://doi.org/10.1093/pcp/pcx139

Yan, L., Wei, S., Wu, Y., Hu, R., Li, H., Yang, W., & Xie, Q. (2015). High-Efficiency Genome Editing in Arabidopsis Using YAO Promoter-Driven CRISPR/Cas9 System. *Molecular Plant, 8*(12), 1820-1823. https://doi.org/https://doi.org/10.1016/j.molp.2015.10.004

Yue, K., Sandal, P., Williams, E. L., Murphy, E., Stes, E., Nikonorova, N., Ramakrishna, P., Czyzewicz, N., Montero-Morales, L., Kumpf, R., Lin, Z., van de Cotte, B., Iqbal, M., Van Bel, M., Van De Slijke, E., Meyer, M. R., Gadeyne, A., Zipfel, C., De Jaeger, G., Van Montagu, M., Van Damme, D., Gevaert, K., Rao, A. G., Beeckman, T., & De Smet, I. (2016). PP2A-3 interacts with ACR4 and regulates formative cell division in the Arabidopsis root. *Proceedings of the National Academy of Sciences, 113*(5), 1447. https://doi.org/10.1073/pnas.1525122113

Zhang, H., Han, Z., Song, W., & Chai, J. (2016). Structural Insight into Recognition of Plant Peptide Hormones by Receptors. *Molecular Plant, 9*(11), 1454-1463. https://doi.org/https://doi.org/10.1016/j.molp.2016.10.002

Zuo, J., Niu, Q.-W., & Chua, N.-H. (2000). An estrogen receptor-based transactivator XVE mediates highly inducible gene expression in transgenic plants. *The Plant Journal, 24*(2), 265-273. https://doi.org/10.1046/j.1365-313x.2000.00868.x

Chapter 2: GOLVEN peptide signaling through RGI receptors and MPK6 restricts asymmetric cell division during lateral root initiation

Fernandez A. I., Vangheluwe N., Xu K., Jourquin J., Neubus Claus L. A., Morales-Herrera S., Parizot B., De Gernier H., Yu Q., Drozdzecki A., Maruta T., Hoogewijs K., Vannecke W., Peterson B., Opdenacker D., Madder A., Nimchuk Z. L., Russinova E. & Beeckman T.

Abstract

During lateral root initiation, lateral root founder cells undergo asymmetric cell divisions that generate daughter cells with different sizes and fates, a prerequisite for correct primordium organogenesis. An excess of the GLV6/RGF8 peptide disrupts these initial asymmetric cell divisions, resulting in more symmetric divisions and the failure to achieve lateral root organogenesis. Here, we show that loss-of-function GLV6 and its homologue GLV10 increase asymmetric cell divisions during lateral root initiation, and we identified three members of the RGF1 INSENSITIVE/RGF1 receptor subfamily as likely GLV receptors in this process. Through a suppressor screen, we found that MITOGEN-ACTIVATED PROTEIN KINASE6 is a downstream regulator of the GLV pathway. Our data indicate that GLV6 and GLV10 act as inhibitors of asymmetric cell divisions and signal through RGF1 INSENSITIVE receptors and MITOGEN-ACTIVATED PROTEIN KINASE6 to restrict the number of initial asymmetric cell divisions that take place during lateral root initiation.

Authors contribution

AIF designed the project. AIF generated the *iGLV6* line, performed the EMS mutagenesis screen and analyzed EMS mutants identity with help from NV, AD, DO and TM. AIF and KX phenotypically characterized the *CRISPR glv* mutants, and generated and characterized *rgi* mutants and reporter lines. NV generated and characterized the *CRISPR glv6* mutants. NV, KX, JJ and SMH phenotypically characterized the *mpk6* mutants. JJ, SMH and HG characterized the crosstalk between auxin and GLV pathways. QY generated the *RGI4* reporter line. BoPa performed *in silico* expression analysis. LANC, NV and ER performed the MPK6 phosphorylation experiments. BrPe and ZLN generated the *CRISPR glv* mutants. KH, WV and AM synthesized the peptides. JJ and AIF performed the statistical analysis. AIF, NV and TB wrote the manuscript with input from all authors. TB provided guidance and advice on the project, the experiments and the analysis of the results.

Introduction

Root branching is a major determinant of root systems architecture. *De novo* formation of lateral roots (LRs) is the trade-off for plants to compensate their lack of mobility while still being able to search for water and nutrients in the soil. In *Arabidopsis*, LRs arise from a subset of stem cells situated in the pericycle at the xylem poles. These cells are termed LR founder cells and undergo a series of tightly coordinated cell divisions in the differentiation zone of the root to generate cell diversity and tissue patterns, resulting in the development of an LR primordium that eventually emerges from the main root body. LR formation follows a regular spacing pattern, indicating that not all xylem-pole pericycle cells become LR founder cells and start dividing. The details of LR spacing are not well understood to date. Since the whole LR formation process comprises several steps, with the first steps taking place when xylem-pole pericycle cells leave the root apical meristem, each of these constitute a regulatory check-up point for the root to adapt the number of eventually emerged LRs.

The first event currently associated with LR formation takes place in the elongation zone of the root where an oscillatory gene transcription mechanism is proposed to prime some xylem-pole pericycle cells before they reach the differentiation zone (Moreno-Risueno et al., 2010; Xuan et al., 2016). Based on the oscillation frequency of the *DR5::Luciferase* marker reporting auxin transcriptional response, it is thought that a higher number of xylem-pole pericycle cells undergo priming than the ones that later participate in the formation of an LR. Furthermore, several genetic studies have reported on the occurrence of clustered or at least closely spaced lateral root primordia in mutants affected in various regulatory genes (De Rybel et al., 2010; De Smet et al., 2010; De Smet et al., 2008; Hofhuis et al., 2013). The oversupply of such mutants with more and closely formed lateral roots argues for the existence of inhibitory mechanisms that are required to restrain the division activity of the xylem-pole pericycle cells.

On the other hand, spacing of lateral roots can be fostered by the type of division. During the so-called LR initiation process, the nuclei of adjacent LR founder cells arranged as pairs in two or three contiguous cell files, move towards the common cell wall, and both cells undergo one or two rounds of asymmetric division with an anticlinal orientation yielding smaller central daughter cells flanked by larger ones (Casimiro et al., 2001; De Rybel et al., 2010; De Smet et al., 2008). The outcome of the asymmetric divisions is a focused center of cell division activity in the small daughter cells surrounded by larger flanking cells that are less or not dividing. The initial anticlinal divisions generate a recognizable hallmark that is referred to as stage I primordium. Subsequent anticlinal and periclinal divisions generate a dome-shaped primordium that eventually becomes an LR (Lucas et al., 2013; von Wangenheim et al., 2016).

Apart from some components of the auxin signaling cascade and the LATERAL ORGAN BOUNDARIES DOMAIN16 (LBD16) transcription factor, not many elements have been identified that regulate the LR initiation step. Recently the GOLVEN/ROOT GROWTH FACTOR/CLE-like (GLV/RGF/CLEL) signaling peptide family has been implicated in the LR initiation process (Fernandez et al., 2013;Fernandez et al., 2015; Meng et al., 2012). One of its family members, GLV6/RGF8/CLEL2 (from now on referred to as GLV6), is transcribed in LR founder cells during nuclear migration which reflects the repolarization of LR founder cells preparing for asymmetric cell division (ACD). *GLV6* overexpression (*GLV6^OE^*) disturbs the initial ACD resulting in more symmetric seemingly non-formative divisions since a dome-shape primordium is rarely formed in *GLV6^OE^* roots. Consequently, *GLV6^OE^* primary roots appear "naked", without emerged LRs (ELRs). Here we show that loss-of-function (*lof*) *GLV6* and its

homologue *GLV10* result in increased ACDs during LR initiation. We provide evidence that GLV6/10 signaling likely involves perception by RGI/RGFR receptors and were able to identify MPK6 as a component of the immediate downstream signaling. We propose a model on how secreted GLV peptides may restrict initial ACDs taking place during LR initiation.

Results

The GLV signaling pathway inhibits LR initiation

Our previous work demonstrated the involvement of GLV6 in LR initiation, however, in the absence of knock-out mutants a defined role could, up to date, not be delineated (Fernandez et al., 2015). To further corroborate the GLV6 function in LR initiation we generated *GLV6* mutants using the CRISPR system. We obtained three mutant lines (*CRISPR glv6-1*, *glv6-2* and *glv6-3*) where insertions, deletions and/or gene rearrangements led to frame shifts and premature stop codons (Supplementary Table1). The remaining sequences are predicted to encode truncated proteins of 55, 37 and 106 amino acids in the *CRISPR glv6-1*, *glv6-2* and *glv6-3* mutants, respectively, instead of the 123 amino acids normally encoded by the wild-type *GLV6* gene (Supplementary Table 1). Phenotyping of these lines revealed that only *CRISPR glv6-1* had a small increase in root length, a phenotype likely intrinsic to this line and not the consequence of *GLV6* knockout. No other difference with the wild type was observed in these mutants either in primary root length or LR density (Extended Data Fig. 1a-c and Supplementary Table 2).

In contrast to the strong *GLV6* overexpression phenotype (Fernandez et al., 2015), mutating *GLV6* had no effect on root system architecture, pointing to redundancy with other *GLV* gene(s). From our previous studies, we know that *GLV10* is expressed during early lateral root formation (Fernandez et al., 2013) suggesting redundancy with *GLV6*. In agreement with this hypothesis, *GLV10* overexpression resulted in a similar LR phenotype as *GLV6* (Fernandez et al., 2013). A more detailed investigation of the *GLV10pro-NLS2XGFP* transcriptional reporter revealed indeed low *GLV10* expression at early stages of primordium formation including in LR founder cells before the first division. After the first ACD and throughout development, *GLV10* transcription was strongest in the central cells (Fig. 1a). To investigate if GLV6 and 10 are functionally redundant we analyzed an available sextuple *GLV* mutant generated by CRISPR, in which *GLV6* and *10,* as well as other *GLV* genes not transcribed in the root or transcribed at later LR developmental stages were targeted (from now on, *CRISPR glv,* see M&M)(Peterson et al., 2016). No difference in primary root length was observed in this mutant compared to wild type (Fig. 1b and Extended Data Fig. 1d). However, in contrast to the *CRISPR glv6* mutants, an increase in the total LR density was observed, mostly due to an accumulation of non-emerged primordia, especially at stage I (Fig. 1c-d and Supplementary Table 2). To test that *GLV6* and *10* are responsible for the observed phenotype, we generated a *glv6glv10* double mutant by crossing a *glv10* T-DNA *lof* mutant with the *CRISPR glv6-2* mutant. Analysis of the LR phenotype revealed a small non-significant increase in total LR density in the single *glv10* mutant that was further enhanced in the *glv6glv10* double mutant (Fig. 1e). Similar to the *CRISPR glv* mutant, non-emerged primordia, mainly at stage I, accumulated in *glv6glv10* seedlings (Fig. 1e and Extended Data Fig. 1e). Interestingly, the observed phenotype could be complemented by growing the mutants on low concentrations of GLV6 peptide (GLV6p) or GLV10p, indicating that the phenotype reflects the lack of GLV signaling (Fig. 1c-e and Extended Data Fig. 1e). These data indicate that upon *GLV6/10* knockout more pericycle cells undergo ACD giving rise to stage I primordia, pointing to a role for GLV peptides as negative regulators of LR initiation. The *glv6glv10* phenotype was somewhat weaker than the *CRISPR glv* mutant suggesting that other *GLV* genes targeted in

the latter (e.g. *GLV7*) are expressed in LR founder cells at undetectable levels in the wild type or upon knocking out *GLV6* and *10*.

During the formation of a stage I primordium one or two anticlinal ACD events can take place in the central pericycle cell file (Fernandez et al., 2015; von Wangenheim et al., 2016) before the division plane changes to produce a two-layered primordium. After the first ACD, four cells are generated (two central short and two larger flanking cells). When a second round of ACD takes place, five to six cells are produced depending whether one or both flanking cells underwent division (Fig. 1f). To understand whether GLV signaling is involved in inhibiting only the first or also subsequent ACD events we quantified the frequency of four- or five/six-celled stage I primordia. First, we observed that many of the stage I primordia were present in the mature region of the root where other primordia had developed into more advanced stages, indicating they may be arrested (20 out of 29 in the wild type, 69%, and 33 out of 51, 65%, in the *CRISPR glv* mutant). Around 2/3 of the total stage I primordia in the wild type had gone through the first ACD only while 1/3 proceeded with the second one (Fig. 1g). These data altogether suggest that not all wild-type primordia that underwent the first ACD will by default continue through the second one and point out to the existence of potential checkpoints at the transition of these two events, as well as after the second ACD. Regardless of the fact that a similar proportion of stage I primordia seemed arrested in the *CRISPR glv* mutant as in the wild type, quantification of stage I primordium cell numbers showed that the second ACD happened much more often in the *CRISPR glv* mutant, which was further confirmed in the *glv6glv10* double mutant (Fig. 1g). These data indicate that GLV signaling may not only negatively regulate the occurrence of the first ACD, but also the transition from the first to the second ACD.

In addition, we observed that occasionally two primordia/LRs formed in close proximity in the *glv* mutant seedlings (Fig. 1h and Extended Data Fig. 1f). Indeed, the frequency of such events was higher in the *CRISPR glv* and the *glv6glv10* mutants than in the wild type, suggesting extra initiation sites and/or disturbed LR initiation spacing in the mutants. Once again, this phenotype was complemented by supplementing GLV6p or GLV10p to the growth medium (Fig. 1i). Altogether, the analysis of gain- and loss-of-function phenotypes points toward a function for both, GLV6 and 10 peptides in the control of LR initiation events during the first and second ACD steps.
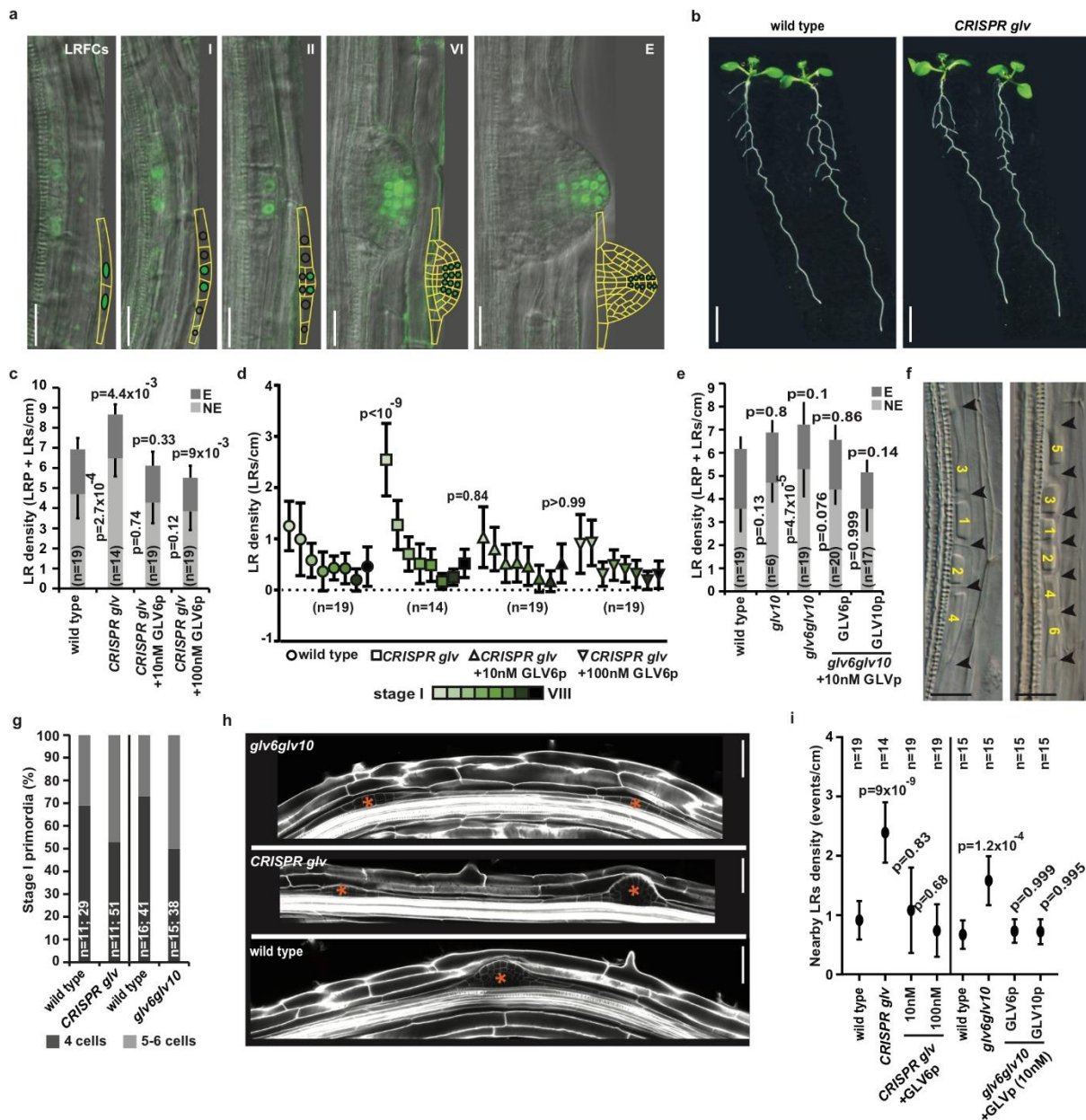
Figure 1. _CRISPR glv_ lines have defects in LR initiation. a, _GLV10pro:nls-2XGFP_ signal in LR founder cells and the forming primordium. Representative primordium stages (roman numerals indicated at the upper right side) are shown. Note that LR founder cells (LRFCs) can be recognized by the oval shape of nuclei. After division, nuclei become round. Inset shows a representation of _GLV10_ expression (green filled circles) at the different primordium stages. Empty circles indicate no _GLV10_ expression in those cells (omitted at later stages). b, _CRISPR glv_ seedlings show similar root length as wild type. c, Quantification of non-emerged primordia (NE), ELRs (E) and total LR density in the _CRISPR glv_ mutant (8 dag). Significant differences with the wild type are shown for NE and total LR density. d, Quantification of all primordium stages density in _CRISPR glv_ seedlings germinated on MS or on GLV6p at the indicated concentrations (8 dag). e, Quantification of NE, E and total LR density in the _glv6glv10_ mutant (8 dag) supplemented or not with GLV6p or GLV10p. Significant differences with the wild type are shown for NE and total LR density. f, Stage I primordia with one (left) or two (right) rounds of ACDs. Arrowheads indicate cell borders following ACDs, the resulting

daughter cells are numbered. g, Quantification of stage I primordia with one or two ACDs. The percentage of four or five/six-celled stage I primordia (n= # roots; # primordia). h, Primordia (indicated by asterisks) are often observed in close proximity in the *CRISPR glv* and *glv6glv10* mutants. i, Density of nearby LRs in *glv* mutants supplemented or not with the GLV6p or GLV10p compared to wild type. Comparison of all genotypes/treatments with the wild type was done using a Generalized Estimation Equations (GEE) model (c-e, i). See M&M for details and Supplementary Table 2 for full statistical analysis. Charts (c-e, i) represent mean values ± SD. Scale bars represent 20 µm in (a) and (f), 0.5 cm in (b) and 50 µm in (h). Representative images in (a) and (b) were observed at least twice with similar results.

51

Extended Data Fig 1. GLV6 and 10 act redundantly during LR initiation. a-c, Phenotypic characterization of *CRISPR glv6* mutants compared to wild type (8 dag, n=12). Quantification of root length (a), all primordium stages density (b) and non-emerged primordia (NE) and emerged (E) LR density (c). d, Quantification of root length in the *CRISPR glv* mutant compared to wild type. e, Quantification of all primordium stages density in the *glv6glv10* mutant germinated on MS or on 10 nM of GLV6p/GLV10p (8 dag). Charts show mean values ± SD (b, e) or s.e.m (c). Significant differences compared to wild type are shown and were determined using one-way ANOVA (a, d) or a GEE model (b-c, e). For full statistical analysis see Supplementary Table 2. n.s.: no significant differences were found between mutants and wild type. f, Example of nearby primordia frequently found in *glv* mutants. The lower picture shows a higher magnification image of the framed area in the upper picture for each genotype. Scale bars represent 50 μm.

To better understand GLV signaling during LR initiation we decided to search for downstream elements of the pathway. For this, a suppressor screening was carried out taking advantage of the lack of visible LRs in $GLV6^{OE}$ seedlings. We generated an estradiol inducible $GLV6^{OE}$ line (*iGLV6*) which offers the possibility to score mutant phenotypes both, in the presence (induced) and absence (non-induced) of *GLV6* overexpression. We confirmed the inducibility of the *GLV6* transcript in the *iGLV6* line and its capability in phenocopying the constitutive $GLV6^{OE}$ in the presence of estradiol, while having a wild-type phenotype in non-induced conditions (Fig. 2a-c and Supplementary Fig. 1a-b). Indeed in the presence of estradiol, initiation events consisting of excessive anticlinal divisions were observed in the pericycle along the whole root resulting in very few dome-shaped primordia and emerged LRs (Fig. 2b-c) (Fernandez et al., 2015). An EMS mutagenesis was then performed and *iGLV6* seedlings were screened on estradiol for the presence of LRs, indicating suppression of the $GLV6^{OE}$ phenotype (Supplementary Fig 1c). We eventually obtained five confirmed mutants and named them *suppressors of GLV6^{OE} phenotype* (*sgps*) (Fig. 2d and Supplementary Fig. 1d).

We previously reported that treatments with the GLV6p phenocopy the ectopic pericycle divisions observed in $GLV6^{OE}$ (Fernandez et al., 2015). Surprisingly, *sgp1* and *2* responded to GLV6p peptide treatment, prompting us to postulate that the mutated gene was involved in the production of bioactive mature GLV peptides (Fig. 2e). Additionally, *sgp1* and *2* showed similar root phenotypes as reported for the *tpst-1* mutant (Supplementary Fig. 2a-b) (Komori et al., 2009; Zhou et al., 2010). The tyrosylprotein sulphotransferase enzyme (TPST) catalyzes tyrosine sulfonation in plants and is encoded by a single-copy gene in *Arabidopsis*. Tyrosine sulfonation is crucial for RGF/GLV peptide bioactivity (Matsuzaki et al., 2010; Whitford et al., 2012) and accordingly, *tpst-1* mutant root phenotypes have been ascribed to a defect in the production of GLV/RGF, as well as, PSK bioactive peptides. Indeed sequencing of the *TPST* gene revealed mutations resulting in a E^{146} to K^{146} change in *sgp1*, and in a R^{195} to W^{195} change in *sgp2* (Supplementary Fig. 2c). F1 crosses of *sgp1* with *sgp2*, as well as with *tpst-1*, confirmed that they are indeed allelic (Supplementary Fig. 1e, Supplementary Fig. 2d and Supplementary Table 3). We renamed *sgp1* and *2* as *tpst-3* and *-4*, following up on previously reported *tpst* mutants nomenclature (Wu et al., 2015). The finding of *tpst* alleles validates that our screening strategy was suitable for identifying genes involved in the GLV signaling pathway.

In contrast to *sgp1* and *2*, *sgp 3* and *4* suppressed the LR phenotype caused by $GLV6^{OE}$ as well as peptide treatment, indicating that the mutated gene acts at the level or downstream of peptide ligand perception (Fig. 2d-e and Fig. 3a). Backcrossing *sgp3* and *4* to the parental *iGLV6* line, as well as with each other, showed that the mutants are recessive and allelic with regard to the suppression of the $GLV6^{OE}$ LR phenotype (Supplementary Fig. 1e and Supplementary Table 3). Next-generation sequencing revealed that both *sgp3* and *4* carried mutations in the *MITOGEN-ACTIVATED PROTEIN KINASE6* (*MPK6*) gene resulting in a change of a conserved amino acid in *sgp3* and in a premature stop codon in *sgp4* (Fig. 3b and Supplementary Fig. 3b). We confirmed the absence of signal in *sgp4*, while full length MPK6 was detected in *sgp3*, probing with anti-MPK6 antibodies (Fig. 3c). Additionally, *sgp 3* and *4*, and F1 seedlings resulting from crossing them to the *mpk6-4* T-DNA line, displayed pleiotropic root phenotypes reported earlier for *mpk6* mutants (Lopez-Bucio et al., 2014). Furthermore, an *iGLV6/mpk6-4* line showed also suppression of the LR root phenotype after estradiol induction of $GLV6^{OE}$

(Supplementary Fig. 3b-e). *sgp3* and *4* will be therefore, referred to as *iGLV6/mpk6-6* and *-7*, respectively. The *sgp5* mutant was also analyzed using next generation sequencing but the causative mutation for its suppression phenotype could not be demonstrated yet.
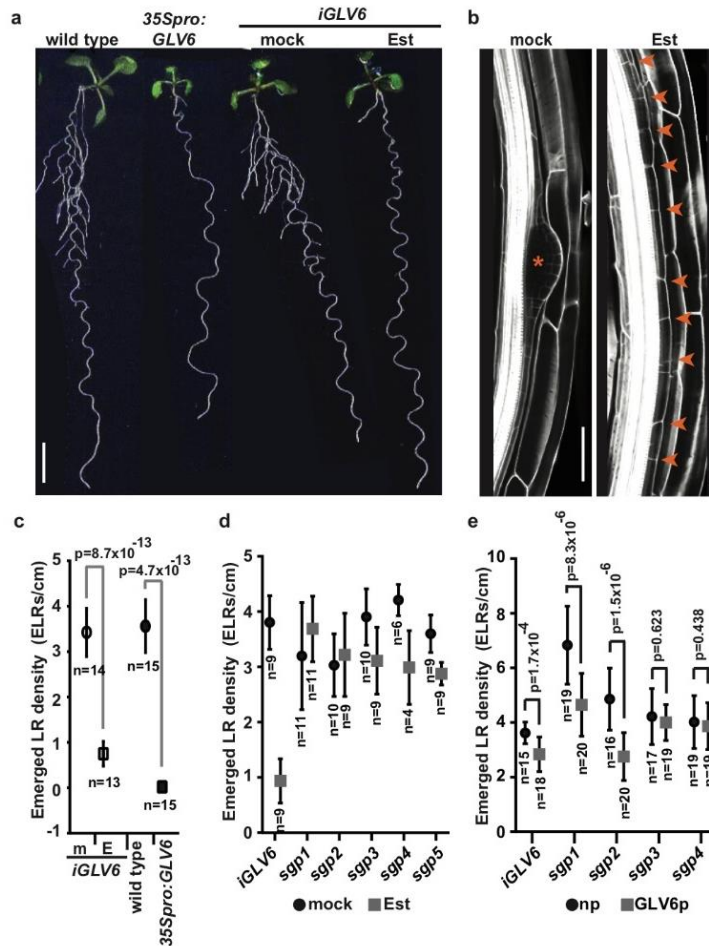

Figure 2. Identification of downstream components of GLV signaling during LR initiation. a-c, Phenotypical analysis of an estradiol inducible line (*iGLV6*) that phenocopies constitutive *GLV6^OE*. a, Phenotype of *iGLV6* 13 dag seedlings in induced (2 μM estradiol) and non-induced (mock) conditions compared to constitutive *GLV6^OE* (*35pro:GLV6*). b, Ectopic anticlinal divisions or normal primordium development in the pericycle of *iGLV6* roots in the presence or absence of estradiol, respectively. c, Quantification of ELR density in *iGLV6* and *35pro:GLV6* 13 dag seedlings compared to controls. d, ELR density in confirmed 12 dag M3 mutants germinated on estradiol or mock treatments. e, ELR density of *sgp1-4* germinated in liquid medium supplemented or not with GLV6 peptide (2 μM). m: mock, E: Estradiol, np: no peptide treatment. Charts (c-e) represent mean values ± SD. Different treatments for the same genotype are compared using a two-sided Student's *t*-test. Scale bars represent 0.5 cm in (a) and 50 m in (b).

GLV6^{OE} ectopic anticlinal pericycle divisions are suppressed in *mpk6* mutant

Mitogen-activated protein kinase (MAPK) cascades are highly conserved signaling modules downstream of peptide and receptor pairs (Xu & Zhang, 2015). We therefore, focused on the study of MPK6 as a likely downstream effector of the GLV signaling pathway in LR initiation.

First, we analyzed the occurrence of excessive pericycle anticlinal divisions, typically found when *GLV6* is overexpressed, in *iGLV6/mpk6-6* and *-7* mutants germinated on estradiol. This analysis revealed none or very few of these divisions in the presence of estradiol in the mutants (on average 0,5 excessive pericycle anticlinal division events per cm primary root). Instead, normal primordia were formed similar to those found under non-induced conditions (Fig. 3d, compare with Fig. 2b). In the *iGLV6* germinated on estradiol, initiation events consisting of one or two pericycle layer(s) that disproportionately divide anticlinally are predominantly observed, often hindering the quantification of separate initiation events. Consequently, wild-type-looking primordia, as well as ELRs, seldom develop (Fig. 3e-f). In contrast, all LR developmental stages were recognizable in the *iGLV6/mpk6-6* and *-7* mutants with or without estradiol (Fig. 3d-f). This was confirmed by studying individual initiation events after induction of LR formation through bending of the primary root. Upon gravistimulation, a primordium was formed at the outer side of the bend in the mock-treated *iGLV6* line as previously reported (Ditengou et al., 2008; Laskowski et al., 2008). When transferred to estradiol a few hours before LR initiation, only anticlinally divided pericycle cells were observed at the bend, similar to the division pattern detected in *iGLV6* line germinated on estradiol (Extended Data Fig. 2a). Performing the same experiment in the *mpk6-6*, *mpk6-7* and *mpk6-4* mutants background confirmed the suppression of the *GLV6^{OE}* phenotype by the *mpk6* mutations (Fig. 3g and Extended Data Fig. 2a).

mpk6 mutants have defects in LR initiation similar to *glv lof* mutants

The suppression of the *GLV6^{OE}* phenotype during LR initiation points to a function of MPK6 in this process. Indeed an increase in the total LR density was detected in the *iGLV6/mpk6-6* and *-7* lines with or without estradiol (Fig. 3f and Supplementary Table 2). Similarly, total LR density was increased in *mpk6-3 and -4* mutants (Fig. 3f and Supplementary Table 2) confirming earlier published results (Lopez-Bucio et al., 2014). The analysis of all primordium stages in *mpk6* mutants revealed a consistent significant increase in non-emerged primordium density, particularly at early stages, with the largest difference found at primordium stages I and II (Fig. 3e-f, Extended Data Fig. 2b and Supplementary Table 2). Taken together, our results indicate increased LR initiation events in *mpk6* mutants, which do not always proceed in development, leading to strong accumulation of non-emerged primordia. The *mpk6* mutant phenotypes resemble the increase in LR initiation observed in *glv* lines. Interestingly, primordia were also found in close proximity in the *mpk6* mutants (Fig. 3d and 3h). The corresponding phenotypes of *glv* and *mpk6 lof* mutants in the LR development process point to genes functioning in the same pathway, although the *mpk6* mutant phenotype is stronger. This is likely because MPK6 is a converging point for multiple pathways controlling LR initiation, including but not limited to, the GLV pathway.
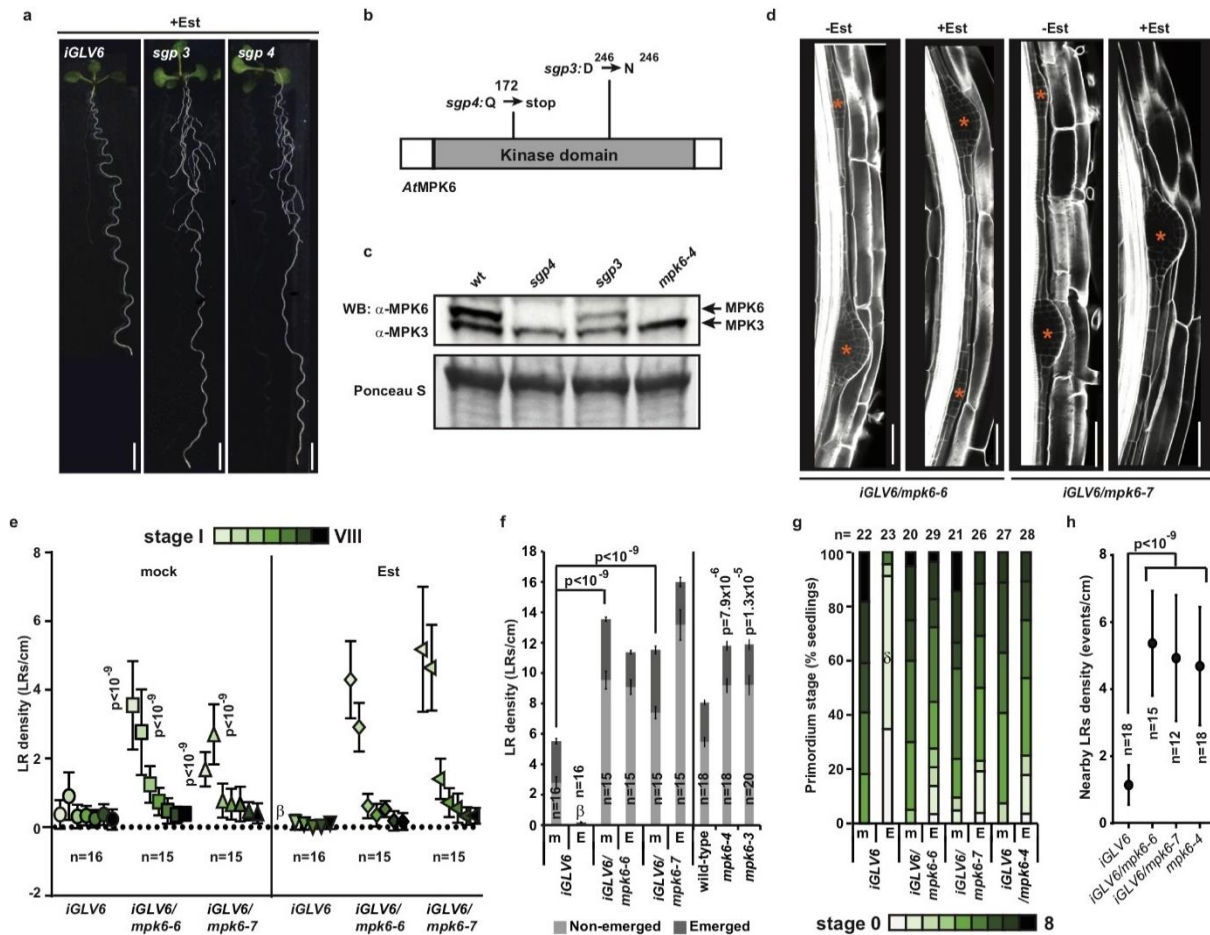
Figure 3. *mpk6* mutants suppress the LR *GLV6*^{OE} phenotype. a, ELRs are restored in *sgp3* and *4*. b, Position of the respective mutations of *sgp3* and *4* in the *MPK6* gene. c, Analysis of MPK3 and MPK6 proteins in extracts of the *sgp3* and *4* mutants using anti-MPK6/MPK3 antibodies in Western blots. Extracts from wild type and *mpk6-4* are included as controls. d, Dome-shaped primordia are observed in *mpk6* mutants with or without estradiol. Note primordia (indicated by asterisks) initiating in close proximity. e, Quantification of all primordium stages in *iGLV6/mpk6-6* and *-7* with and without estradiol (8 dag). Significant differences with the wild type in stage I and II primordia under mock conditions were recorded. f, Quantification of non-emerged primordia and total LR density in the *iGLV6/mpk6-6* and *-7* mutants with and without estradiol, and in *mpk6* T-DNA mutants germinated on MS compared to controls (8 dag). P-values correspond to analysis of total LR density. g, Quantification of primordia (stages) formed after primary root bending. Stage from 0 to 8 are color-coded. Stage 0 indicates no primordia formed at the bend. h, Quantification of nearby primordia in *mpk6* mutants without estradiol (8 dag). No significant differences were found between different *mpk6* mutants (0.5<p<1). Charts represent mean values ± SD (e, h) or s.e.m. (f). A GEE model was used (e, f, h) for comparison. For full statistical analysis see Supplementary Table 2. β: wild-type-like stage I and II primordia cannot be distinguished in these lines, only anticlinally divided pericycle cells were observed preventing the quantification of individual primordia stages. δ: Stage I and II refers in this case to one or two layered anticlinally dividing pericycle. m: mock, E, Est: Estradiol. Scale bars represent 0.5 cm in (a) and 50 µm in (d).
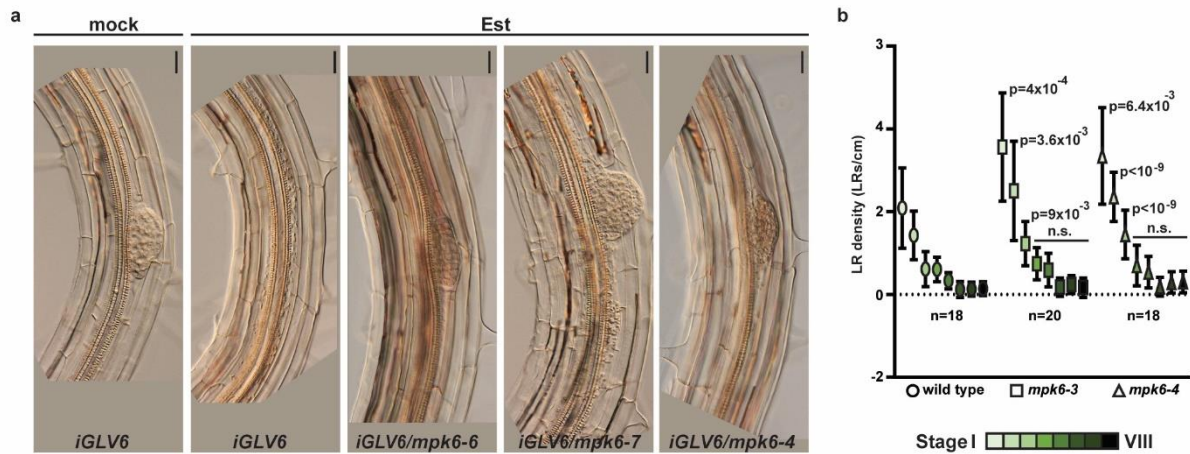
Extended Data Fig 2. Suppression of the *GLV6^OE^* phenotype and LR defects in *mpk6* mutants. a, Suppression of the *GLV6^OE^* phenotype in *mpk6* mutants after LR initiation was induced by gravistimulation of the primary root. This experiment was done three times with similar results. b, Quantification of all primordium stages in reported *mpk6* mutants compared to wild type (8 dag). Chart represents mean values ± SD. A GEE model was used. n.s.: no significant differences were found between mutants and wild type. For full statistical analysis see Supplementary Table 2. Scale bars represent 20 μm.

Based on our previous results we postulated that MPK6 conveys phosphorylation events in response to GLV peptides and thus, we tested whether GLV6p treatment induces MPK6 phosphorylation. Using anti-Phos p42/44 antibodies, rapid and transient MPK6 phosphorylation was detected in wild-type seedlings minutes after GLV6p treatment reminiscent of patterns previously reported for other ligands (Fig. 4a-b and Supplementary Fig. 4a-b) (Ortiz-Morea et al., 2016). MPK3 was also phosphorylated upon GLV6p addition, albeit to a lesser degree than MPK6.
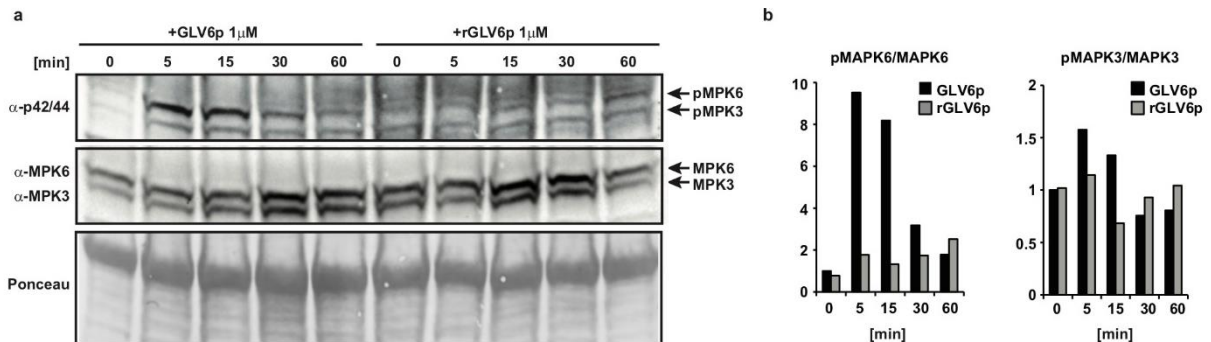

Figure 4. MPK6 phosphorylation is induced shortly after GLV6p treatment. a, Analysis of MPK3 and MPK6 phosphorylation and protein levels in extracts of seedlings treated with GLV6p or rGLV6p for the indicated time points. Representative western blot probed with anti-Phos 42/44 or anti-MPK6/anti-MPK3 antibodies and Ponceau staining as loading control. Note that MPK6/MPK3 phosphorylation is specific as rGLV6p (same amino acid composition as GLV6p but randomized amino acid sequence) did not induce protein phosphorylation. b, Quantification of the ratio between the phosphorylated MPK6 or MPK3 (pMPK6/3) and the MPK6 or MPK3 protein signal shown in (a), respectively. Fold change relative to time 0 (GLV6p) is shown. This experiment was done three times with similar results.

Recently, a family of five leucine-rich repeat receptor-like kinases (LRR RLKs) was identified by three independent groups as the receptors for RGF1/GLV11. They were named RGF1 RECEPTORS (RGFR) or RGF1 INSENSITIVE (RGI) (Ou et al., 2016; Shinohara et al., 2016; Song et al., 2016) (from now on referred to as RGI1 to 5). We wondered whether any of the RGI receptors could also serve as receptors for GLV6/10 during the LR initiation process. Based on available transcriptomic compendia generated upon induction of LR formation (Peret et al., 2012; Voss et al., 2015), *RGI1*, *4* and *5* transcription appears to be activated before stage I, *RGI 2* from stage III/IV while *RGI3* is not expressed in LRs (Supplementary Fig. 5a). Because of their early induction, *RGI1*, *4* and *5* are the most likely candidate receptors in the GLV pathway during LR initiation. Analysis of transcriptional reporters revealed *RGI1* expression in all xylem-pole pericycle cells at the beginning of the differentiation zone where no primordia have yet been formed. After primordium formation *RGI1* expression is mostly present in the cells at the base of the primordia (Fig. 5a). *RGI5* expression appeared in LR founder cells and remained in all primordium cells after the first ACD. GFP signal also appeared in the endodermal and cortical cell(s) adjacent to the forming primordium. Unfortunately, we could not detect *RGI4* expression in the mature root region likely due to very low promoter activity (Supplementary Fig. 5b). To investigate a possible function in LR initiation we examined two independent *lof*

mutant lines for each receptor but could not find differences in LR density as compared to the wild type (data not shown). Nevertheless, an increase in the percentage of 5-6 celled stage I primordia, similar to the *glv6glv10* phenotype, was observed in *rgi1* and *4* but not in *rgi5* mutants (Fig. 5b). Occasionally, stage I primordia with more than 6 cells were observed in the *rgi* mutants (Fig. 5b). This phenotype points to additional ACD taking place and is in agreement with *RGI1*, but not *RGI5*, expression in the flanks of the forming primordium.

To test whether RGI1, 4 and 5 act downstream of GLV peptides during LR initiation we analyzed the *GLV6*^{OE} LR phenotype in single, as well as, in a triple *rgi145* mutant backgrounds. Quantification of ELRs revealed a small suppression of phenotype in single *rgi* mutants compared to the wild type, while almost full suppression was observed in the triple *rgi145* mutant background (Fig. 5c, 5e and Supplementary Fig. 6a). This suggests that RGI receptors act redundantly downstream of GLV peptides during LR formation. Microscopic analysis showed that the aberrant pericycle divisions induced by GLV6 excess were also suppressed in the *rgi145* mutant and dome-shaped primordia were formed instead (Fig. 5d). Similarly, the increased pericycle anticlinal symmetric divisions and the consequent drop in ELR density induced by GLV10p treatment in the wild type was slightly reduced in *rgi1* and *rgi4* mutants, and almost completely suppressed in the *rgi145* mutant (Fig. 5f and Supplementary Fig. 6c-d). Expression of an RGI1-Venus fusion protein driven by the constitutive *RPS5A* promoter restored the small root apical meristem of the *iGLV6/rgi145* mutant without estradiol, but not the root length. This could be the consequence of only partial redundancy in RGI receptors and/or additional defects triggered by overexpressing *RGI1* (Fig. 5c and Supplementary Fig. 6e-f). The wavy root phenotype (Fernandez et al., 2015) and the reduction in ELRs caused by *GLV6*^{OE} were also (partially) recovered in the *iGLV6/rgi145/RPS5Apro:RGI1-Venus* line (Fig. 5c and 5e). Increased anticlinal symmetric pericycle divisions upon induction of *GLV6*^{OE} were observed in *iGLV6/rgi145/RPS5Apro:RGI1-Venus* roots, although they were not as continuous as in the wild type (Fig. 5d). These data indicate that RGI receptors are necessary for the LR phenotype induced by GLV excess and that RGI1 can partially complement for the *rgi145* defects in the GLV pathway.

Finally, we analyzed whether RGI receptors are necessary for the MPK6 phosphorylation triggered by GLV6p treatment. Indeed, GLV6p-induced phosphorylation of MPK6 was highly decreased in the *rgi145* triple mutant, indicating that MPK6 phosphorylation by GLV6p treatment is also dependent on the RGI receptors (Fig. 5g-h and Supplementary Fig. 4c).
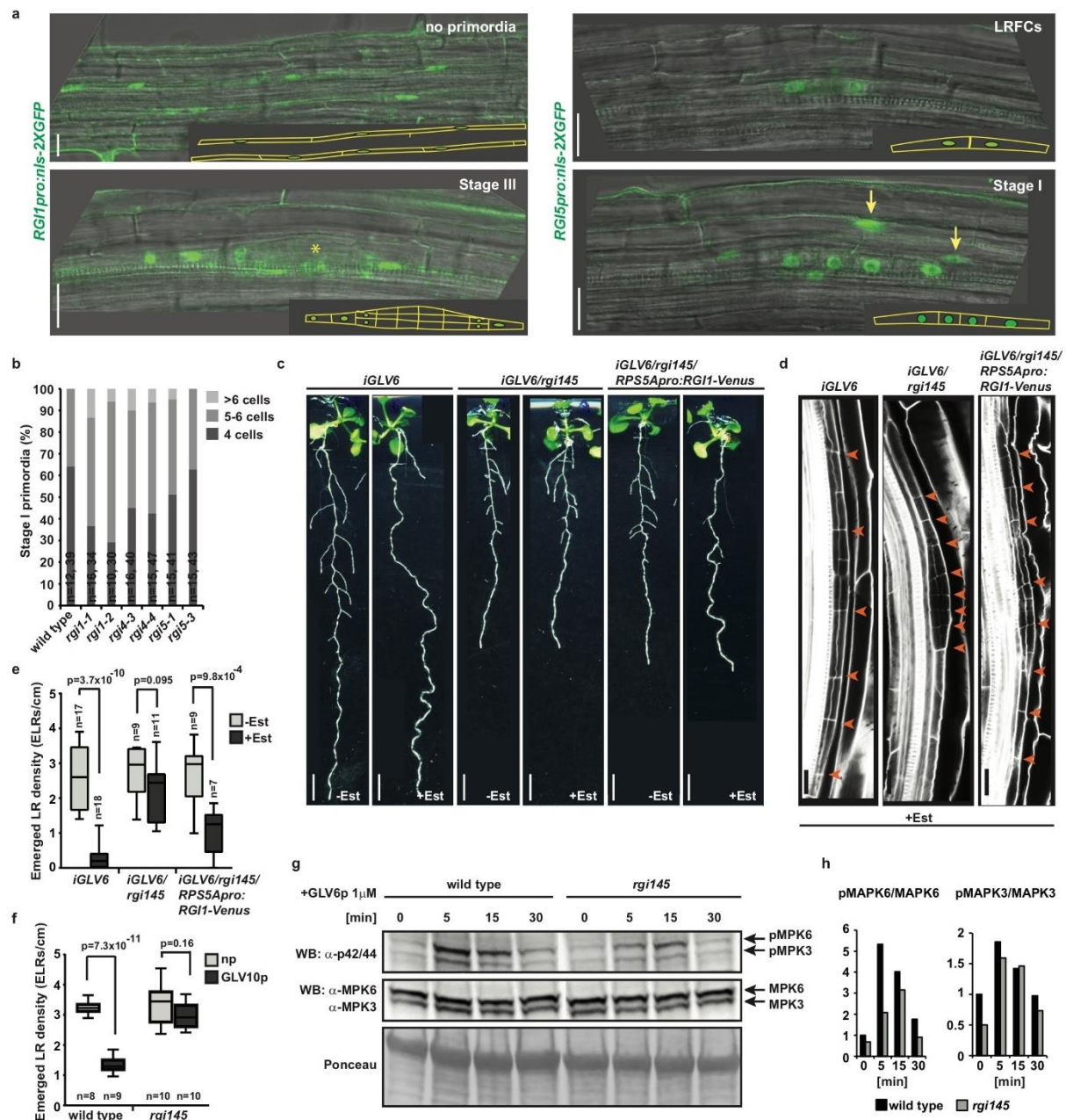
Figure 5. *GLV6^OE* phenotypes and induction of MPK6 phosphorylation are dependent on RGI receptors. a, *RGIpro:nls-2XGFP* signal in pericycle cells and during primordium formation. The beginning of the differentiation zone where no primordia have formed yet or where a primordium is developing was imaged. Primordium stages are indicated in the upper right corner. Arrows indicate GFP signal in endodermal and cortical cells in front of the forming primordium. Insets show a schematic representation of *RGI* expression. b, Quantification of stage I primordia that have undergone one or two rounds of ACDs. The percentage of four or five/six-celled stage I primordia in the wild type and the *rgi* mutants (9 dag) is shown (n= #roots; #primordia). c-d, *GLV6^OE* phenotypes: decreased ELRs and increased wavy root growth (c), and pericycle divisions (d) are suppressed in the *rgi145* and partially rescued in the *RPS5Apro:RGI1:Venus/rgi145* in the presence of estradiol. Arrowheads indicate anticlinal divisions across all pericycle layers. e, Quantification of ELRs in the *iGLV6/rgi145* mutant and

the *iGLV6/RPS5pro:RGI1:Venus/rgi145* line with and without estradiol compared to the *iGLV6* control (13 dag). f, Quantification of ELRs in the *rgi145* mutant compared to the wild type (14 dag) germinated on GLV10p (100nM). g, GLV6p-induced MPK6 phosphorylation is decreased in the *rgi145* triple mutant. h, Quantification of the ratio between the phosphorylated MPK6 or MPK3 (pMPK6/3) and the MPK6 or MPK3 protein signal shown in (g), respectively. Fold change relative to time 0 (wild type) is shown. This experiment was done three times with similar results. Different treatments for the same genotype are compared using a two-sided Student's *t*-test. Scale bars represent 20 μm in (a) and (d) and 0.5 cm in (c).

GLV and *RGI* expression are induced by auxin while *GLV6*[OE] negatively influences auxin accumulation/signaling

Auxin is known to be crucial for LR initiation as mutants in auxin signaling fail to initiate LRs (Fukaki et al., 2002; Okushima et al., 2005). *GLV6* and *10* expression patterns during LR initiation resemble those of auxin reporters containing the *DR5* promoter (Fig 1a) (Benkova et al., 2003; Dubrovsky et al., 2008; Fernandez et al., 2013). Therefore, we tested whether auxin induces *GLV6/10* and *RGI1/4/5* transcription. Indeed, after short treatments with the auxin analogue NAA all transcripts were induced and this was dependent on *ARF7*, *ARF19* and *IAA14*, which are components of auxin signaling known to be involved in LR initiation (Fig. 6a and Supplementary Fig. 7) (Fukaki et al., 2002; Okushima et al., 2005). We then tested if *GLV6*[OE] affected auxin accumulation and/or signaling. We crossed the *iGLV6* line to a *DR5pro:Luciferase* reporter (Moreno-Risueno et al., 2010) and quantified the *DR5pro:Luciferase* signal during prebranch site formation in mock or estradiol-induced roots. The results show that the *DR5pro:Luciferase* signal decreased upon *GLV6*[OE] indicating a negative effect of the GLV pathway on auxin accumulation and/or signaling (Fig. 6b-d).
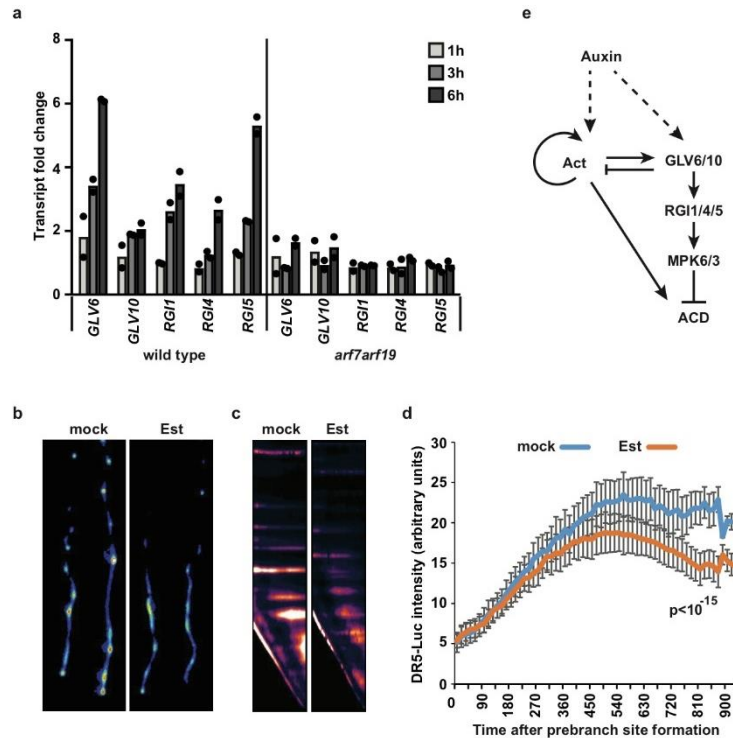
Figure 6. Model for GLV6/10 signaling restricting ACD during LR initiation. a, Quantification of *GLV6/10* and *RGI1/4/5* transcript fold change after treatment with 10 µM NAA relative to mock treatment for the indicated time points in wild type and *arf7arf19* mutants, detected by qRT-PCR. Bars show mean values of two independent replicates. b, *iGLV6xDR5pro:Luciferase* seedlings 14 hours after transfer to mock or estradiol treatment. c, Kymographs showing *iGLV6xDR5pro:Luciferase* signal of a representative root transferred to mock or estradiol treatment. d, Quantification of *iGLV6xDR5pro:Luciferase* signal in seedlings transferred to mock or estradiol treatment. Graph shows mean values ± s.e.m (n=8). t0 (9-11 hours after transfer) was normalized for all roots as the start of a prebranch site. An extra sum-of-squares F-test was performed to determine whether one or multiple model(s) could adequately describe the data for all conditions. A single model was not sufficient to describe the two datasets ($p < 10^{-15}$). e, GLV6/10 signals through the RGI1, 4 and 5 receptors and MPK6 to inhibit ACD. Auxin likely acts upstream of GLV signaling potentially via an activator gene (Act).

Discussion

Our suppressor screen identified MPK6 as a downstream effector of the GLV pathway during LR initiation. This is in line with previous reports showing that MPK6 acts downstream of peptide signaling in plant developmental processes (Cho et al., 2008; Jewaria et al., 2013). Although *mpk6* mutants suppressed the *GLV6^{OE}* phenotype to a large degree, MPK3 could act redundantly with MPK6 during LR initiation and contribute to a lesser extent to the GLV pathway. It is very likely that perception of GLV6 and 10 peptides upstream of MPK6 is mediated by the RGI1, 4 and 5 receptors. Although receptor-ligand binding assays need to be performed to confirm that RGIs are receptors for GLV6/GLV10, it was shown that both peptides can bind to RGI3 with high affinity (Song et al., 2016) and GLV10 competed for binding of GLV11/RGF1 to RGI1. Unfortunately, we were not able to successfully purify RGI ectodomains from heterologous systems. As the *glv6glv10* mutant, *rgi1* and *rgi4* mutants display increased ACD indicating that like GLV peptides, RGI1 and 4 are necessary to restrict ACD during the first steps of LR formation.

Our data point to GLV peptides acting as inhibitors to restrain excess of ACDs taking place after LR founder cell specification. Knocking out *GLV6* and *10* genes resulted in increased LR initiation indicating that more of the primed LR founder cells undergo the first ACD when GLV levels are low. A second ACD happened more frequently in *glv* mutants than in the wild type as well. Since *GLV6* and *10* are both transcribed in LR founder cells and expression seems stronger in the central cells after the first ACD (Fig. 1a) (Fernandez et al., 2015) it is tempting to think that principles of the Turing's reaction-diffusion (RD) model resulting in lateral inhibition apply during LR initiation (Turing, 1952). Turing mechanism has been used to explain the generation of patterns in living organisms such as the skin stripes in zebrafish, and stomata and trichome cell patterning in plants (Torii (2012). In the activator-inhibitor model proposed by Turing, the interaction between a self-activator and a diffusing inhibitor generates patterns from undifferentiated cells. In the case of LR initiation, a yet unknown activator would promote ACD in LR founder cells while cell-autonomous GLV signaling induced by the activator would counteract that effect. In the event that the first ACD proceeds and LR initiation takes place due to differences in levels of activator and inhibitor, GLV6 expression/secretion induced by the activator mainly in central cells, (trans-) inhibits flanking cells from undergoing a second ACD (Fig. 6e-f). In the frame of LR initiation, the generation of GLV gradients and the direction of signaling might be important for patterning as overexpression of *GLV6* equally in all cell layers results in pericycle cells undergoing symmetric divisions instead of no division at all (Fernandez et al., 2015). As in other biological systems, more complex regulation is probably at play during LR initiation and the presence of undiscovered factors has to be taken into account. However, based on the current knowledge of LR initiation we can speculate on a possible scenario. Most probably auxin acts upstream of both the activator and GLV6 signaling (Fig. 6e). In agreement with this the transcription of *GLV6, GLV10* and the *RGI1*, *4* and *5* receptors was induced by auxin treatment. Concurring also with our model, the *DR5pro:Luciferase* signal reporting auxin maxima was decreased during prebranch site formation after induction of *GLV6* overexpression (Fig. 6b-d), indicating a negative feedback of the GLV pathway on auxin accumulation/signaling.

Interestingly a recent publication points to another signaling peptide that regulates LR spacing. The TARGET OF LBD SIXTEEN 2 (TOLS2)/PAMP-INDUCED SECRETED PEPTIDE-LIKE 3

(PIPL3) peptide transcription is induced in LR founder cells and signals to the cells flanking the nascent primordium through the RLK7 receptor (Toyokura et al., 2019). In contrast, we found that *RGI* receptors are transcribed in all xylem-pole pericycle cells (*RGI1*) or in LR founder cells (*RGI5*) where LRs initiate. Therefore, the TOLS2/PIPL3-RLK7 pathway could be activated downstream or concomitantly with GLV6/10 signaling to spatially propagate lateral inhibition to the cells flanking the LR founder cells after they have been specified. It is fascinating that plants may deploy different signaling peptides to guarantee the correct LR formation and patterning. Different signaling peptide pathways likely contribute to LR formation at different stages, as it has been shown for the IDA peptide and its receptors, necessary for the separation of outer root cell layers during LR emergence (Kumpf et al., 2013). Remarkably, this IDA-HAE/HSL2-dependent cell separation also involves activation of MPK3 and 6 (Zhu et al., 2019).

How different signaling peptides that use a common downstream component result in specific developmental outputs, is a challenging but essential question that needs to be addressed in future studies to understand how signaling pathways operate during plant development.

Acknowledgements

Material and Methods

Plant material and growth conditions

Seedlings were sown on solid half MS medium (Duchefa Biochemie B.V.) supplemented with 1% of Sucrose (VWR), 0.1 g/L Myo-inositol (Sigma-Aldrich), 0.5 g/L MES (Duchefa Biochemie B.V.) and 0.8% Plant Agar (Lab M, MC029). Plates were stratified for 2 days at 4 °C and grown at 21 °C under continuous light conditions. For phenotypic analysis seedlings were germinated on mock (DMSO) or 2 µM estradiol unless otherwise specified.

The *iGLV6* line was generated by Gateway® LR recombination reaction using the *pEN-L1-GLV6-L2* (Fernandez et al., 2013) and the estradiol inducible pMDC7_B (pUBQ) vector (Barbez et al., 2012; Curtis & Grossniklaus, 2003). Seven independent single locus homozygous lines were obtained and all of them behave in a similar manner based on quantification of the ELR density and qRT-PCR. The transgenic lines display a decrease of 69,6%-89,8% in ELR relative to the mock treatment (DMSO), compared to a 15% decrease in the wild type treated with estradiol, which indicates that estradiol has a small effect on lateral root development. In addition, strong induction of *GLV6* expression in the transgenic lines was measured by qRT-PCR. The chosen *iGLV6* line was the one with the strongest lateral root phenotype (for the EMS mutagenesis suppressor screen).

To generate the *glv6* CRISPR mutants, three gRNA were designed targeting the first and fourth exons of the *GLV6* gene (Supplementary Table 1 and Supplementary M&M). The sextuple *glv* mutant was also generated by CRISPR/Cas9 (Peterson et al., 2016). This mutant was originally intended to knockout *GLV* genes transcribed in aerial tissues and therefore *GLV1*, *2*, *6*, *7*, *8* and *10* were targeted. The *CLE18* gene, encoding a precursor that contains a GLV motif in the C-term (Meng et al., 2012) was also mutated. Out of the six targeted *GLV* genes, only *GLV6* and *10* were found to be transcribed early during LR initiation. *GLV7* is transcribed from stage IV primordia on, *GLV2* and *8*, only in emerged LRs, while *GLV1* is not expressed at all in the root (Fernandez et al., 2013). *CLE18* expression has been reported in the primary root pericycle and vascular tissues of mature lateral roots (Jun et al., 2010), however we could not confirm *CLE18* transcription in primary root tissues after RNA-Seq experiments were performed in root segments of the young maturation zone (Jourquin *et al.*, unpublished results; Chen *et al.*, unpublished results).

The *glv6glv10* double mutant was obtained by crossing a *glv10* T-DNA insertion mutant (*Salk_048797*) with the *CRISPR glv6-2* line. Mutant lines were validated by (q)RT-PCR (Supplementary Fig. 8a and d, and Supplementary M&M).

iGLV6 EMS mutagenesis and mutation identification

8000 *iGLV6^OE* seeds were incubated for five minutes in 0.1 M phosphate buffer (pH=7.5) containing 0.05% Triton X-100. After washing with water, seeds were incubated for 7 hours in 0.3% ethyl methanesulfonate (EMS) in phosphate buffer (v:v) (final concentration= 30mM). Seeds were washed with $Na_2S_2O_3$ five times, then eight times with water. M1 seeds were planted on soil in pools of 50-70 plants/pool. The M2 population from each pool was harvested and screened (60 000 M2 seeds in total) on MS plates containing 2 µM of estradiol

for the presence of seedlings with ELRs. Mutants showing suppression of the $GLV6^{OE}$ LR phenotype were transferred to soil and the phenotype confirmed in the M3. Fifteen mutants totally or partially suppressing the $GLV6^{OE}$ ELR phenotype were confirmed in the M3. Of those, eight resulted in decreased $GLV6$ overexpression levels and one in a stop codon in the $GLV6$ coding sequence present in the transgene and were thus discarded. We also excluded one mutant with a limited suppression of the $GLV6^{OE}$ phenotype and exhibiting strong developmental defects. We ended up with five confirmed *sgps*.

The *TPST* gene was PCR-amplified and sequenced in *sgp1* and *2*. For next generation sequencing, *sgp3* and *4* were backcrossed to the unmutagenized *iGLV6* line and seedlings showing suppression of the $GLV6^{OE}$ phenotype were selected and pooled from the F2 segregating population. Nuclear DNA was isolated from 40-80 pooled seedlings. Next generation sequencing was performed with the Illumina Hi Seq 2500 platform (Eurofins) using paired-end sequencing and 36-fold genome coverage. Mutations were mapped with SHOREmap (Schneeberger et al., 2009) using the *Arabidopsis thaliana* genome as reference (TAIR10). The *iGLV6* parental line was not sequenced. Mutations that were found in all mutants were likely already present in the *iGLV6* line and were thus, discarded. Nine and three nonsynonymous candidate suppressive mutations were obtained for *sgp3* and *sgp4*, respectively (Supplementary Fig. 9). The only gene mutated in both lines was *MPK6*. Because *sgp3* and *4* are allelic in suppressing the $GLV6^{OE}$ phenotype (Supplementary Fig. 1e), we reasoned that the mutations found in *MPK6* must be responsible for the suppression of the $GLV6^{OE}$ phenotype.

The *sgp5* mutant was also studied using next generation sequencing. *sgp5* carries two candidate suppressive mutations in the *AT2G06050* and *AT2G22360* genes encoding for the OXOPHYTODIENOATE-REDUCTASE 3 (OPR3) involved in jasmonate biosynthesis, and the DNA J PROTEIN A6, respectively. Both mutations in *sgp5* generate a P to L change. It is not clear which of these is the suppressive mutation.

Light microscopy

When only ELRs were quantified, the analysis was performed in 12-14 days after germination (dag) seedlings grown on solid MS (except for GLV6p treatments assays) using a binocular microscope (Leica). Root length was measured with ImageJ. LR density was calculated by dividing the LR number by the primary root length.

For analysis of all LR developmental stages, 8-9 dag seedlings were collected and cleared using a modified Malamy and Benfey (Malamy & Benfey, 1997) protocol (see Supplementary M&M). All LR stages including primordia and emerged LRs were counted using an Olympus BX53 DIC microscope with a 400X magnification. Under our growth conditions the average distance between two primordia/LRs was 0.97 ± 0.24 mm (mean value ± s.e.m., n=5 roots, 22-28 primordia/root) in the wild type. Nearby primordia/LRs were counted if they could be observed together in the microscope view field using the 40X objective (distance between primordia equal or less than 0.5 mm). Pictures were taken with an Olympus BX53 DIC microscope or a VHX-7000 digital microscope (KEYENCE) equipped with a fully-integrated head.

mpk6 pleiotropic root phenotypes were classified according to Lopez-Bucio (Lopez-Bucio et al., 2014) Supplementary Fig 3b-c). *mpk6lr* roots were used for quantification of non-emerged primordia and emerged LRs.

For induction of LR primordia after primary root bending, 3 dag seedlings grown vertically on solid MS were gravistimulated for 6 hours, then transferred to mock or estradiol treatment for 44 hours. Seedlings were then mounted on chloral hydrate and the number and stage of primordia formed at the bend were scored under an Olympus BX53 DIC microscope.

Peptide treatments

The GLV6p: DY(SO3)RTFRRRRPVHN and rGLV6p: NRRY(SO3)RHRFTVDPR were synthesized as previously described (Whitford et al., 2012). rGLV6p has the same amino acid composition as GLV6p but the amino acid sequence is randomized. The GLV10p: DY(SO3)PKPSTRPPRHN was ordered from GenScript. For ELR counting, seedlings were germinated in liquid MS containing 2 µM of GLV6p for 7 days, then fixed with 90% acetone, followed by washing once with PBS buffer and finally mounted in lactic acid before ELR quantification under a binocular microscope. For mutant phenotype rescue, seedlings were grown on solid MS containing the GLV6p or GLV10p at the indicated concentrations.

Protein extraction and western blotting

Wild-type or mutant seedlings were germinated on solid half MS medium for 4 days. Then, 20-40 seedlings were transferred to multiwell plates containing 3 mL of liquid half MS. After one hour of conditioning the medium was supplemented with 1 µM of GLV6p or rGLV6p and seedlings were incubated with peptides for the indicated times, after which they were harvested and frozen in liquid N2. Alternatively, seedlings were germinated in liquid half MS medium. Then peptides were added to the medium and incubated for the indicated time points before sampling. Both methods yielded similar outcomes (Supplementary Fig 4a-b).

To detect MPK6/3 phosphorylation, an anti-phospho-p44/42 (Cell Signaling Technology; 1:2500) antibody was used. After stripping membranes were reblotted with anti-MPK6 antibody (Sigma-Aldrich; 1:8000) and anti-MPK3 antibody (Sigma-Aldrich; 1:2500). All blots were imaged in a ChemiDoc XRS+ imaging system (Biorad). For quantification of the relative pMPK6/pMPK3 signal, band intensity was measured with the ImageLab software (Biorad) and then divided by the MPK6/MPK3 signal for every time point. Afterwards, values were normalized by the time 0 values.

We need to point out that because MPK6/3 signaling can also be activated by wounding (Alves-Neubus *et al.*; unpublished results), we were not able to detect MPK6 phosphorylation induced by GLV6p specifically in root tissues. Therefore, the GLV6p activation of MPK6/3 reported here includes shoot as well as root-derived responses where *GLV* and *RGI* genes are also transcribed (Fernandez et al., 2013; Song et al., 2016).

DR5pro:Luciferase imaging and quantification

The *iGLV6* line was crossed to the *DR5pro:Luciferase* (Moreno-Risueno et al., 2010) and 5 dag double homozygous seedlings were transferred to mock (DMSO) or estradiol (2 µM) treatment. Seedlings were sprayed with D-Luciferin (Duchefa; 1mM D-Luciferin, 0.1% DMSO, 0.01% Tween-80) and kept in the growth room for three hours to induce *GLV6* expression. Seedlings were then imaged every 15 minutes with an exposure time of 10 min in a NightShade in vivo plant imaging system (Berthold). ImageJ was used for signal quantification as previously described (Xuan et al., 2018). t0 (9-11 hours after transfer to treatment) was normalized for all seedlings as the start of a prebranch site.

Statistical analysis

A two-sided Student's *t*-test was used for comparison of two conditions/genotypes. Comparison of root lengths between multiple genotypes was performed by one-way ANOVA. Other statistical analyses were performed in SAS (Version 9.4 of the SAS System for Windows7 64bit). For analysis of different lateral root developmental stages, a Generalized Estimation Equations (GEE) model was fitted to the primordium count rate with genotype and developmental stage, as well as the interaction, as fixed effects using a log link function and selecting a Poisson distribution. The log-transformed root length was used as offset. The correlations between the counts were modeled as exchangeable correlations. At each stage, we tested whether there was an equal primordium count rate in the mutant compared to the wild type, and if applicable, whether there was an equal primordium count rate between the mutant complemented with the peptide and the mutant without the peptide. The analysis was done with the genmod procedure. Contrast statements were set up with the plm procedure using the lsmestimate statement. A significance level of 0.05 was chosen. To correct for multiple testing, the maxT procedure was used as implemented in the plm procedure. Data on non-emerged, emerged and total lateral root densities as well as data on clustered lateral root primordia were analyzed by fitting a Generalized Linear Model (GLM) to the lateral root counts with the experimental condition (genotype + treatment) as a fixed effect, or if applicable, with genotype and treatment as well as the interaction term as fixed effects. A Poisson distribution was chosen, except when overdispersion was suspected, in which case we used a negative binomial distribution. A log link function was applied and log-transformed root length was used as an offset. Contrasts were set up with the plm procedure using the lsmeans statement. A significance level of 0.05 was chosen. To correct for multiple testing, a Tuckey correction was applied. All statistical tests used are two-sided.

For comparison of *DR5pro:Luciferase* between mock and estradiol treatments, second order polynomial models were fitted to the data via least squares regression using GraphPad Prism. An Extra sum-of-squares F-test was performed to determine whether one or multiple model(s) could adequately describe the data for all conditions. A single model was not sufficient to describe the two datasets ($p < 10^{-15}$).

Data availability

The data supporting the findings in this study are available from the corresponding author upon reasonable request.
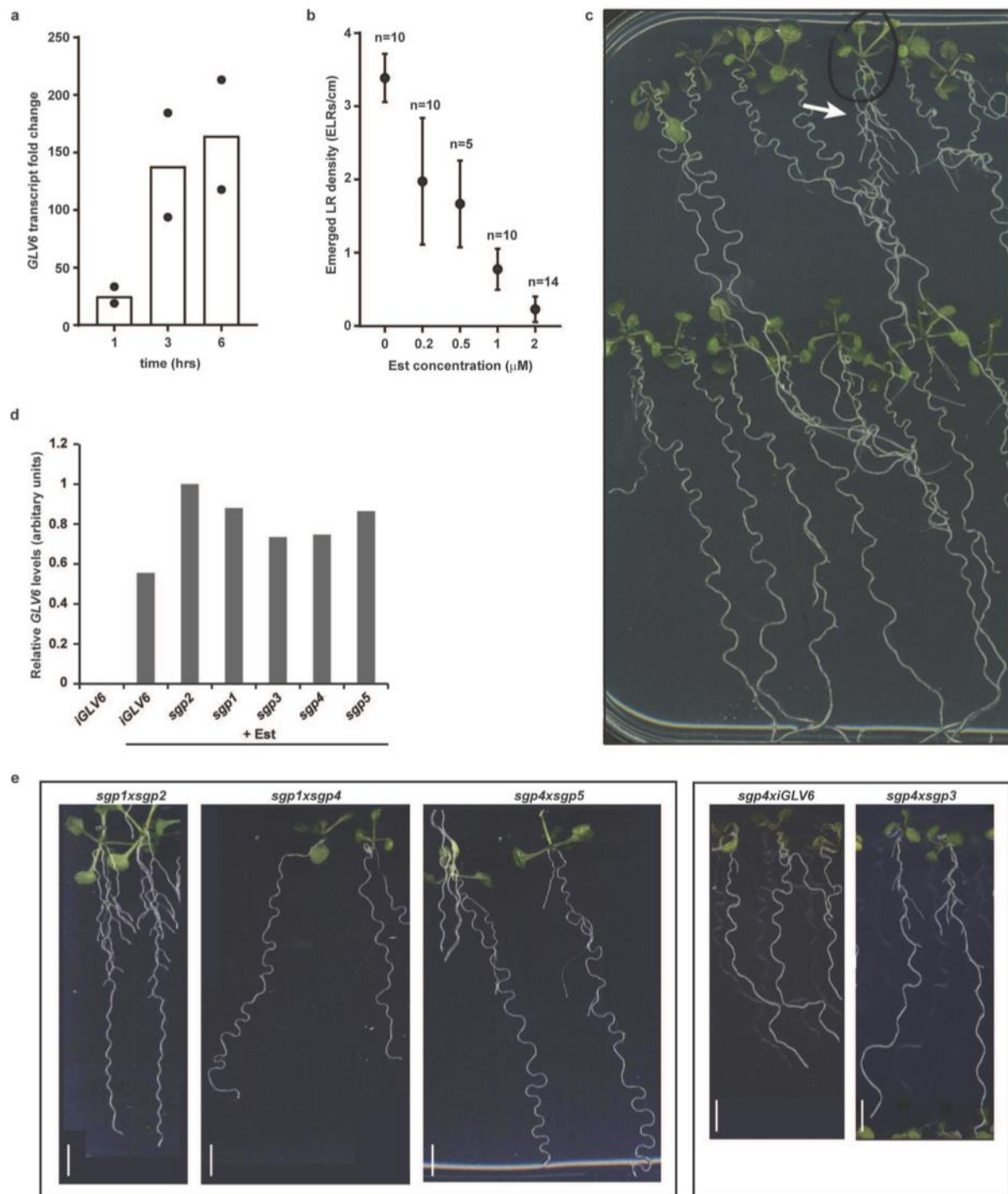
Supplemental Figure 1. Characterization of the *iGLV6* line and identification of suppressors of the *GLV6^OE* phenotype. a, induction of *GLV6* transcript in *iGLV6* seedlings after short estradiol treatment for different time points relative to t0. The mean and individual data points for two independent replicates are shown. b, ELR density of *iGLV6* seedlings germinated on different estradiol concentrations (12 dag). Data shows mean values ± SD. c, example of the screening performed to identify suppressors of the *GLV6^OE* LR phenotype in the mutagenized *iGLV6* line (M2 population). d, relative *GLV6* transcript levels in *sgp1-5* compared

to controls. Transcript levels are relative to the highest value (assigned value "1") and were calculated as previously described (Fernandez et al., 2013). e, F1 seedlings germinated on estradiol (2 µM) resulting from crosses between different *sgp* mutants or between *sgp4* and the *iGLV6* line. This experiment was done twice with similar results.
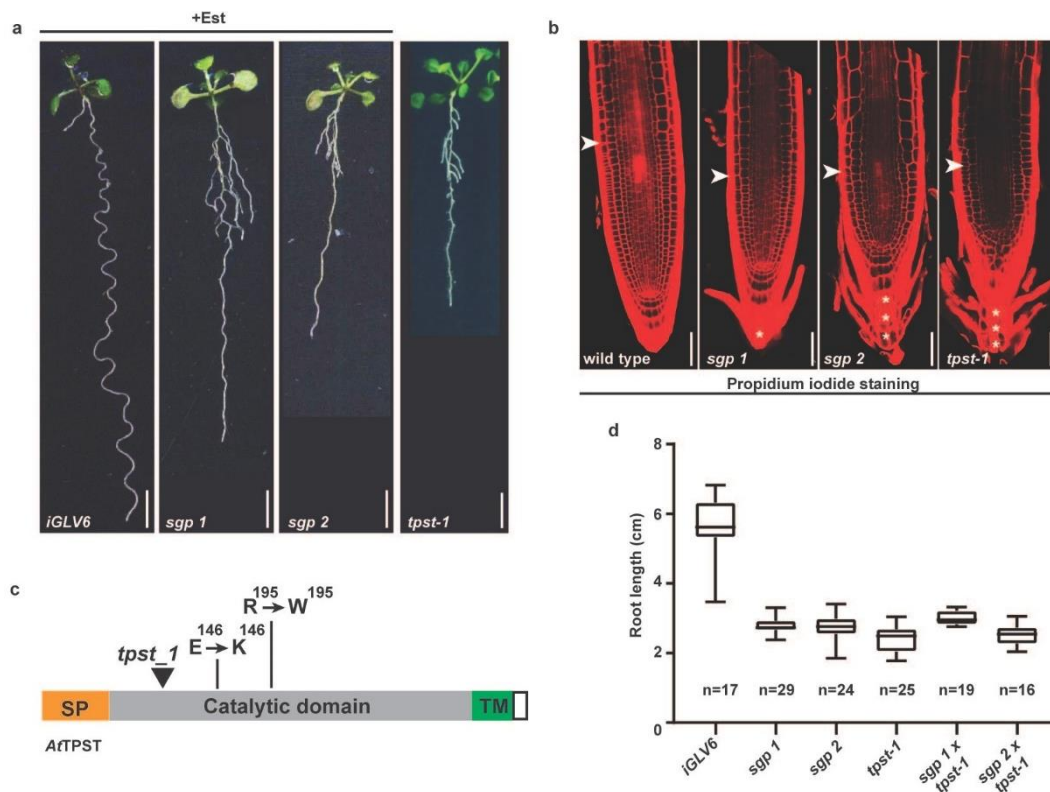

Supplemental Figure 2. *sgp1* and *2* have mutations in the *TPST* gene. a, *iGLV6* and *sgp1* and *2* seedlings grown on estradiol (2 µM), and *tpst-1* seedlings germinated on MS showing similar root phenotypes as *sgp1* and *2* mutants. b, short root apical meristem (indicated with arrowheads) and attached LRC layers (indicated with asterisks) in *sgp1* and *2*, and *tpst-1* mutants. Observations in (a) and (b) come from two independent experiments with similar results. c, schematic representation of the TPST protein showing amino acid changes caused by the mutations present in *sgp1* and *2.* d, quantification of root length in *sgp1* and *2*, *tpst-1* and F1 crosses of the *sgp1/2* mutants with *tpst-1*. All genotypes are significantly different from the wild-type p<0.0001. Root length was compared using one-way ANOVA. Scale bars represent 0.5 cm in A and 50 µm in B.
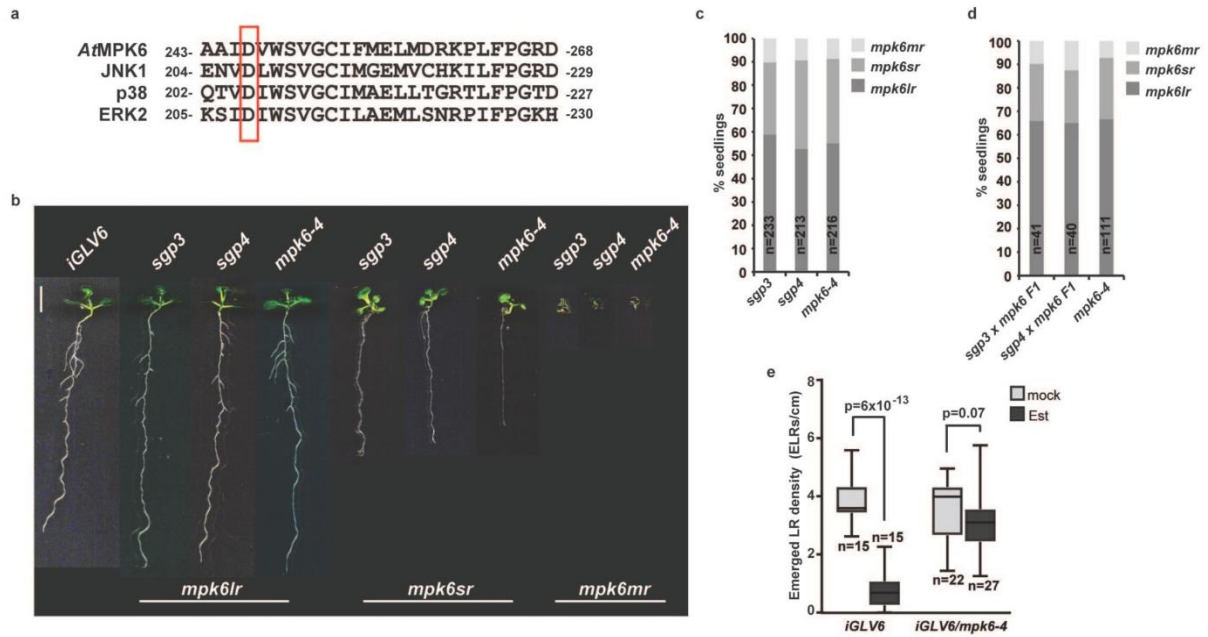
Supplemental Figure 3. *sgp3* and *4* have mutations in *MPK6*. a, fragment of MPK6 alignment with MAP kinases of other species (JNK1, UniProtKB - P45983 (MK08_HUMAN); p38 mouse, UniProtKB – P47811 (MK14_MOUSE); ERK2 rat, UniProtKB – P63086 (MK01_RAT)). The conserved D^{246} mutated in *sgp3* is indicated. b, pleiotropic root phenotypes observed in *sgp3*, *sgp4* and reported *mpk6* T-DNA mutants. *mpk6lr* (long roots), *mpk6sr* (short roots), *mpk6mr* (minus root) have been classified as previously reported (Lopez-Bucio et al., 2014). This experiment was performed twice with similar results. c-d, frequency of different root phenotypes in *sgp3*, and *sgp4* (c), and the F1 seedlings resulting from crossing both mutants to the *mpk6-4* line (d), compared to *mpk6-4* seedlings. e, quantification of ELRs in the *iGLV6/mpk6-4* seedlings (14 dag) compared to the *iGLV6* line with and without estradiol. A two-sided Student's *t*-test was used to determine significant difference between mock and estradiol treatment for the same genotype. Scale bars represent 0.5 cm.
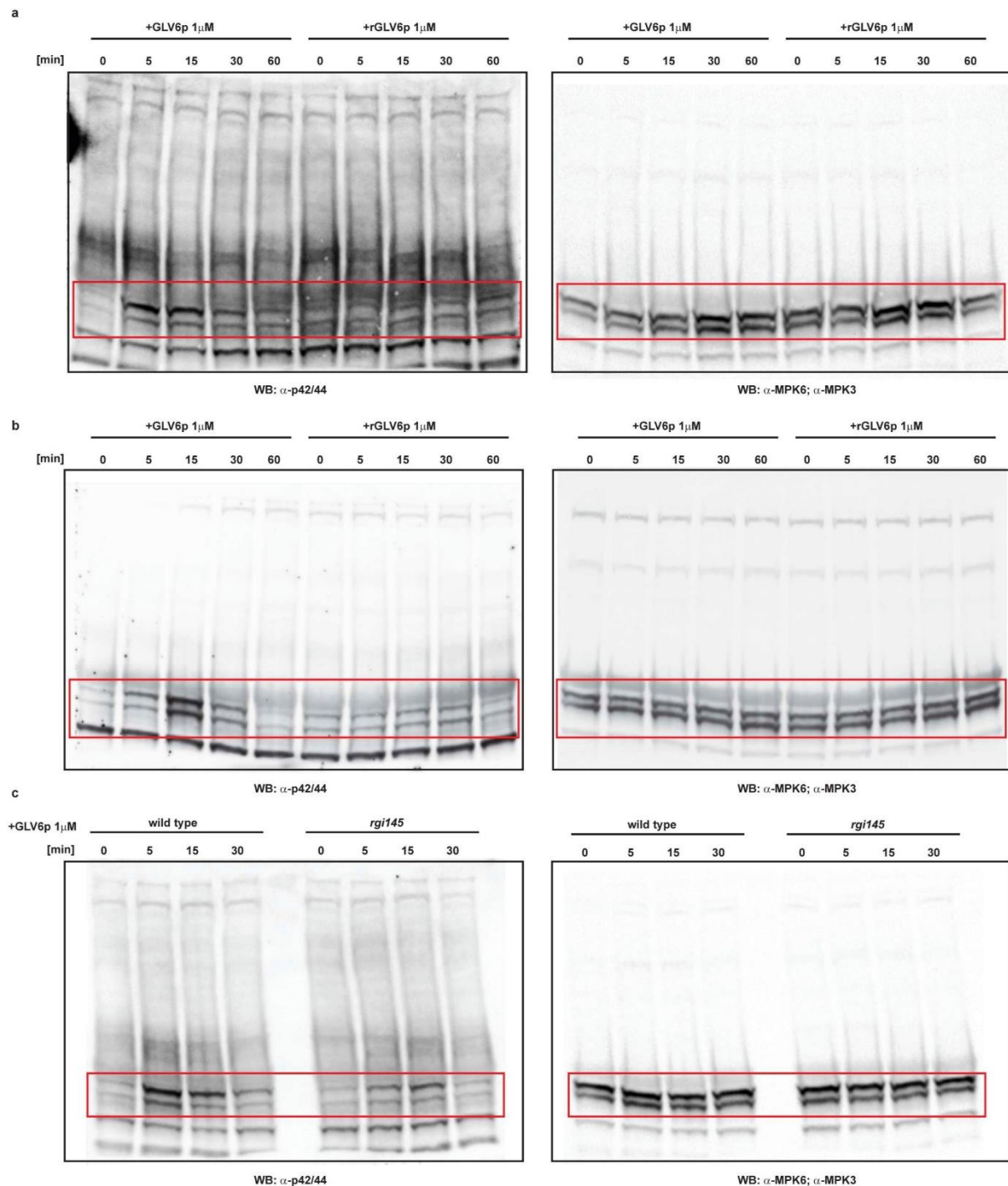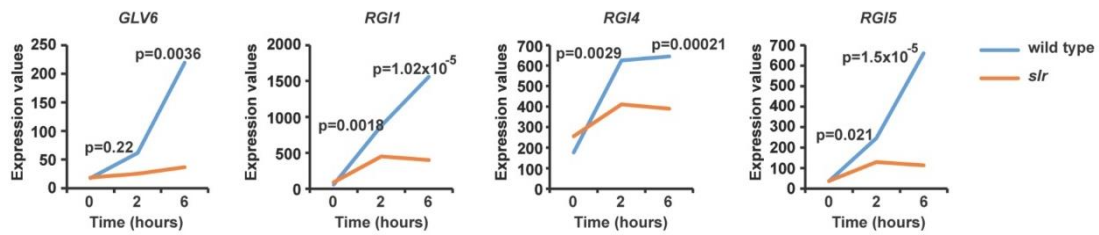
Supplemental Figure 4. GLV6p treatment induces MPK6 phosphorylation dependent on the RGI receptors. a-c, full blots showing MPK6 phosphorylation upon GLV6p treatment in the wild type or the *rgi145* mutant using anti-Phos 42/44 or anti-MPK6 antibodies. Seedling in (a) and (c) were transferred to liquid medium one hour prior to peptide treatment. The GLV6p: DY(SO3)RTFRRRRPVHN and rGLV6p: NRRY(SO3)RHRFTVDPR were synthesized as previously described (Whitford et al., 2012). rGLV6p has the same amino acid composition as GLV6p but the amino acid sequence is randomized. Seedlings in (b) were germinated in liquid medium. The framed area in (a) and(c) has been cropped shown in Fig 4a and Fig 5g, respectively. All experiments were done three times with similar results.
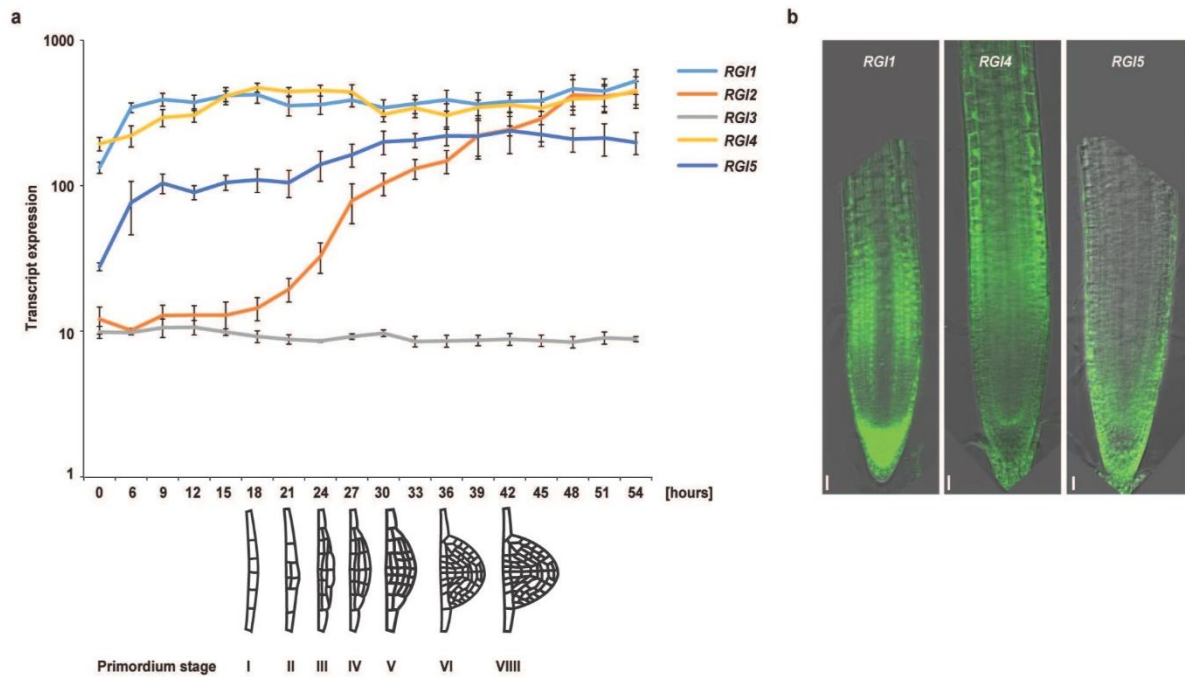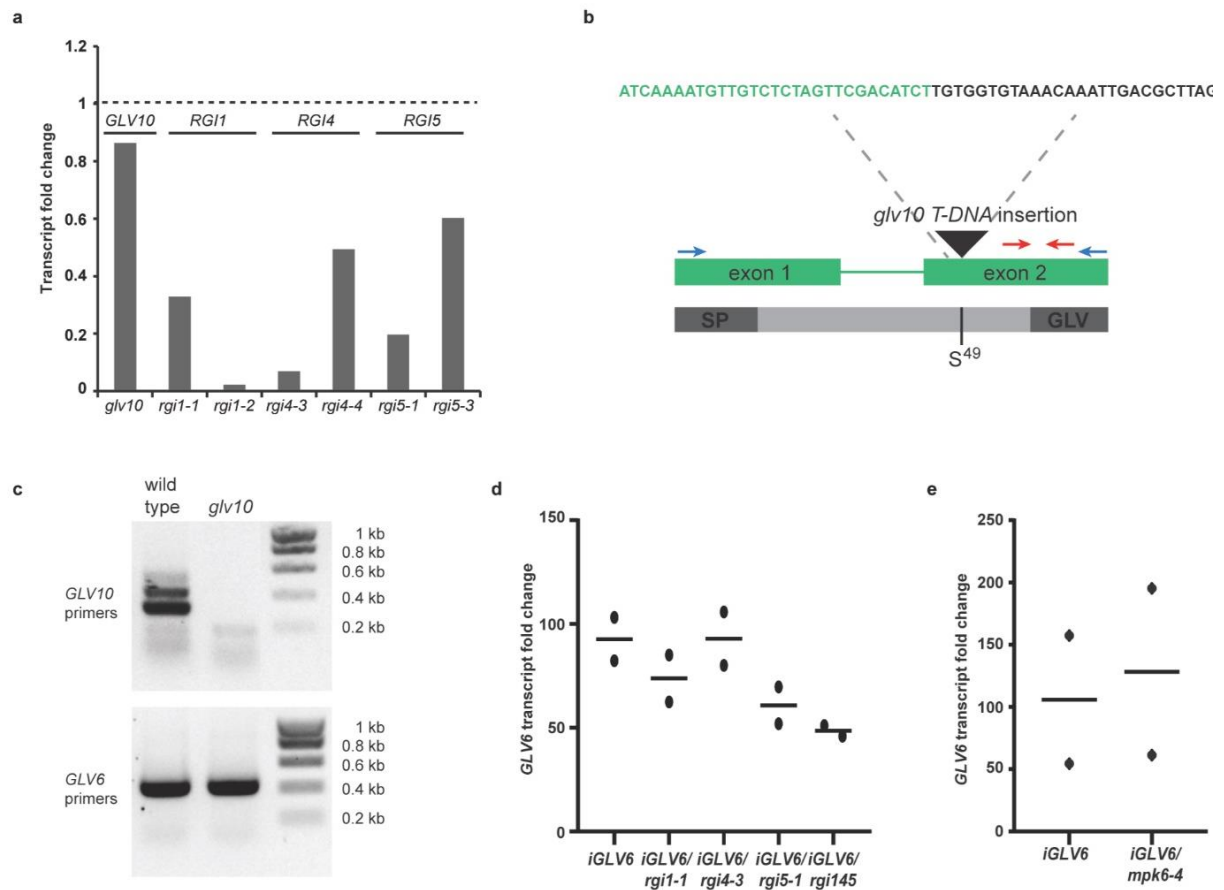
Supplemental Figure 5. *RGI1*, *4* and *5* are transcribed early during primordium development and in the root apical meristem. a, expression profiles of *RGI* genes in available transcriptomic data generated upon induction of LR formation by primary root bending (Peret et al., 2012; Voss et al., 2015) (n=4 independent replicates). Chart shows mean values ± s.e.m. b, *RGIpro-nls-2XGFP* signal showing: *RGI1* transcription in columella and the upper region of the root apical meristem, weak *RGI4* expression in the transition and the start of the elongation zone, and the *RGI5* expression in most root apical meristem cell layers with strongest expression in the lateral root cap and differentiated columella cells. Scale bars represent 20 μm. Expression patterns shown in (b) were observed in three to five independent homozygous single locus lines and at least two independent experiments with similar results.
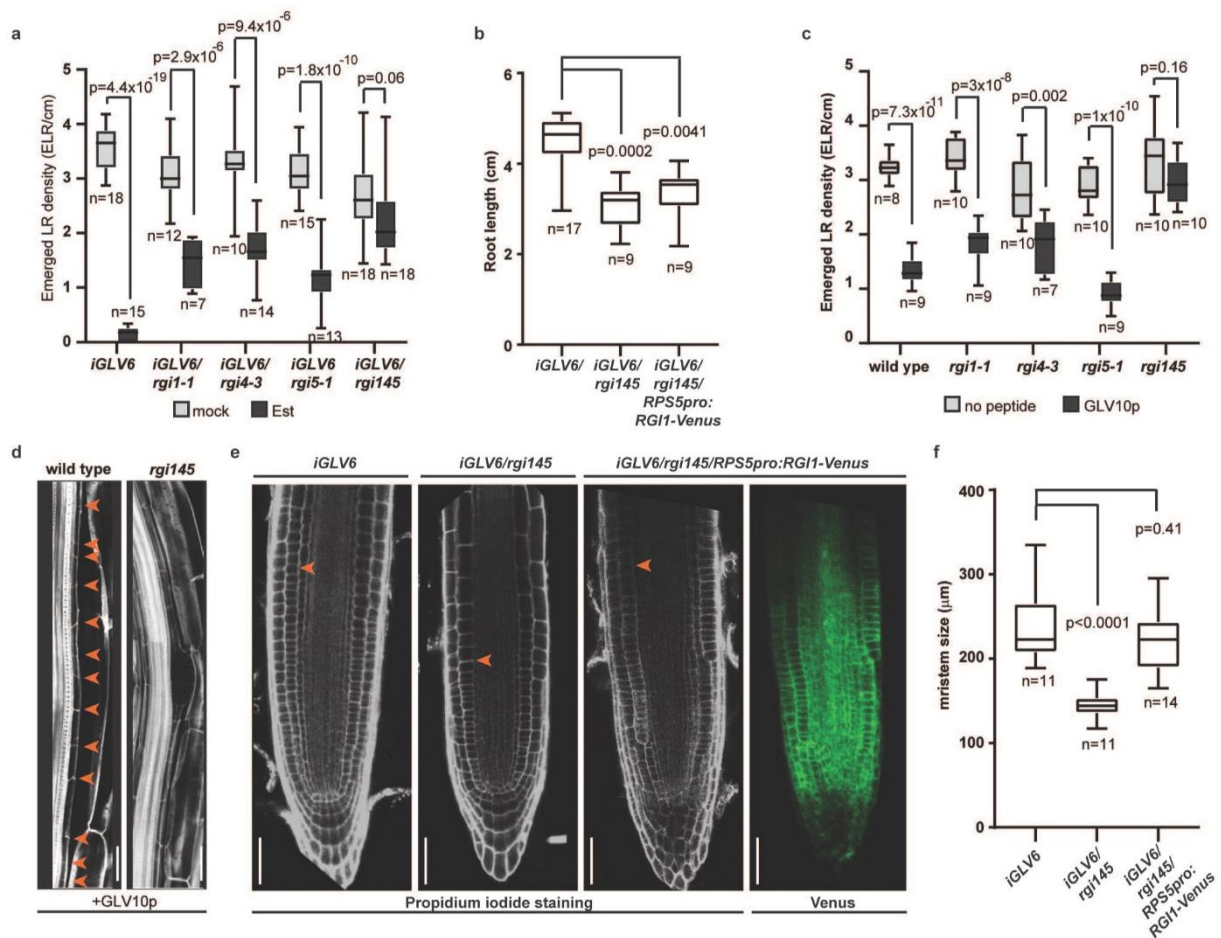
Supplemental Figure 6. *GLV6^{OE}* **phenotypes are suppressed in the** *rgi145* **mutant and partially rescued with an** *RPS5Apro:RGI1-Venus* **construct.** a, quantification of ELRs in the *iGLV6* in the wild type, single *rgi1*, 4 or 5 mutants or the triple *rgi145* mutant backgrounds with or without estradiol (13 dag). A two-sided Student's *t*-test was used to determine significant differences between mock and estradiol treatments for the same genotype. b, quantification of root length in *iGLV6*, *iGLV6/rgi145* and *iGLV6/rgi145/RPS5Apro:RGI1-Venus* seedlings. One-way ANOVA was used to determine significant differences. c, quantification of ELRs in the wild type, single *rgi1*, *4* or *5* mutants and the triple *rgi145* mutant germinated on 100 nM of GLV10p (14 dag). A two-sided Student's *t*-test was used to determine significant differences between peptide treatments and control for the same genotype. d, GLV10p (100 nM) treatment results in excessive anticlinal divisions in the wild type (indicated with arrowheads) and the phenotype is suppressed in the *rgi145* mutant. Representative images of two independent experiments with similar results are shown. e-f, the short root apical meristem size in the *rgi145* mutant is rescued in the *iGLV6/rgi145/RPS5Apro:RGI1-Venus* line. Note the disorganization of columella cells in *iGLV6/rgi145/RPS5Apro:RGI1-Venus* roots (6 dag). One-way ANOVA was used to determine significant differences. Scale bars represent 50 μm in (d) and (e).

Supplemental Figure 7. *GLV6* and *RGI1/4/5* transcript induction by auxin treatment is dependent on components of auxin signaling. Available microarray data on transcript induction using the lateral root inducible system. Wild type or *IAA14* dominant-negative mutant (*solitary-root*, *slr*) roots are germinated on the auxin efflux inhibitor NPA, then transferred to NAA for the indicated time points. *GLV10* is not represented in the *Arabidopsis* ATH1 microarray. The p-value was calculated with a two-way ANOVA that tested the interaction between genotyped and treatment at the indicated time points (n=2 independent replicates).

a

b

ATCAAAATGTTGTCTCTAGTTCGACATCT TGTGGTGTAAACAAATTGACGCTTAC

glv10 T-DNA insertion

exon 1   exon 2

SP   GLV

S^{49}

c

wild type   *glv10*

GLV10 primers

1 kb
0.8 kb
0.6 kb
0.4 kb
0.2 kb

GLV6 primers

1 kb
0.8 kb
0.6 kb
0.4 kb
0.2 kb

d

GLV6 transcript fold change

iGLV6   iGLV6/ iGLV6/ iGLV6/ iGLV6/
   rgi1-1 rgi4-3 rgi5-1 rgi145

e

GLV6 transcript fold change

iGLV6   iGLV6/
        mpk6-4

Supplemental Figure 8. Validation of *glv10* and *rgi* mutants. a, qRT-PCR showing *GLV10*, *RGI1*, *4* and *5* transcript levels relative to wild type (dashed line) in the respective mutants. The monitored transcript is indicated on top of the bars. b, schematic representation of the *GLV10* gene and the encoded pre-propeptide. The approximate location and the sequence of the T-DNA in the *glv10* mutant is shown. Primers in red and blue were used for qRT-PCR (a) or RT-PCR (c) respectively. c, RT-PCR performed in wild-type and *glv10* mutant cDNA using *GLV10* primers shown in (b). Primers at the beginning and end of the *GLV6* coding sequence were used as control of the cDNA integrity. Two independent replicates were performed with similar results. d, *GLV6* transcript levels on estradiol relative to mock conditions in the wild-type and *rgi* single and triple mutant backgrounds. e, *GLV6* transcript levels on estradiol relative to mock conditions in the wild-type and the *mpk6-4* mutant backgrounds. Charts (d-e) show mean values (line) and individual data points for two independent replicates.
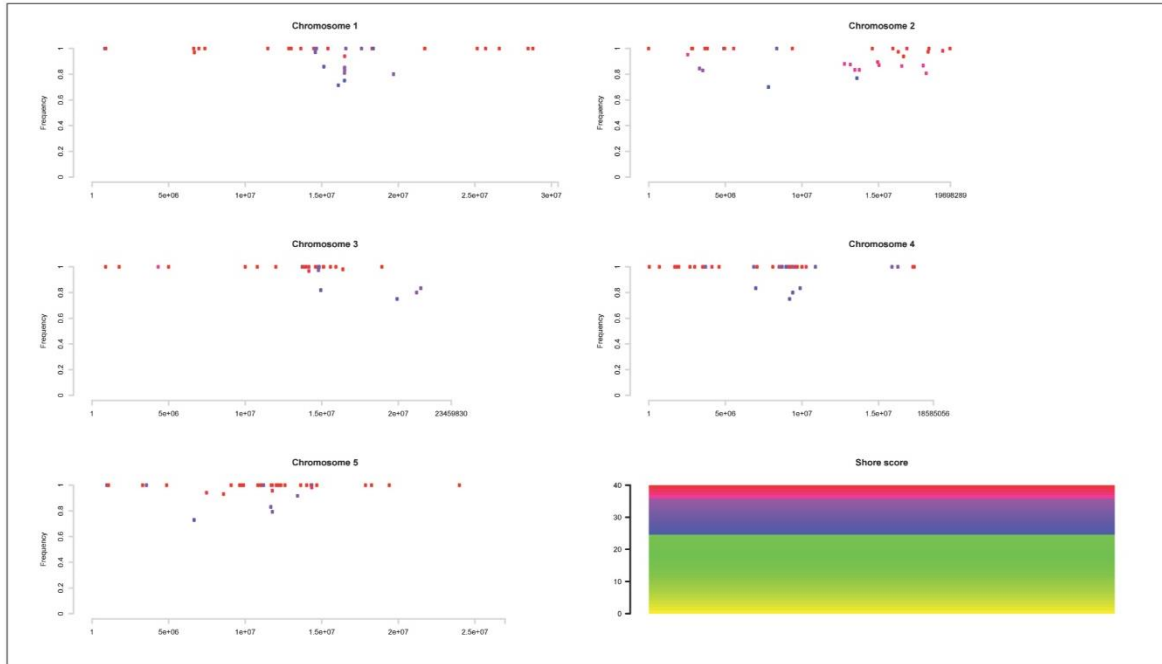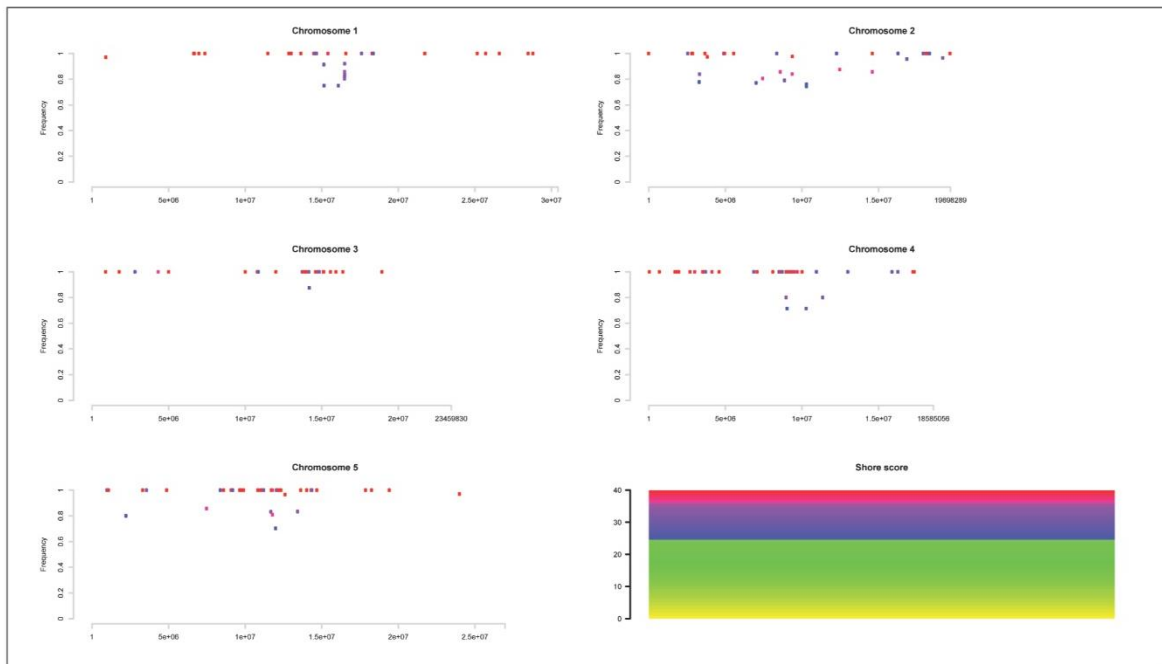
Supplementary Figure 9. Manhattan plots generated after SHOREmap analysis of the *sgp3* (a) and *sgp4* (b) mutants. The frequency and position of mutations is shown for each mutant. The mutations observed in chromosome 1 were present in all mutants and could indicated the position of the *iGLV6* construct.

Supplementary Table 1. Amino acid sequences predicted to be encoded in *CRISPR glv6* or *glv* mutants. The GLV6 pre-propeptide is shown as a reference. The presumed mature GLV6 peptide sequence is highlighted in bold, and stop codons are depicted as asterisks. Amino acid sequences different from the corresponding GLV wild-type precursor are italicized in the mutants.

Target	gRNA		Predicted protein sequence
GLV6		wildtype	MKLIRVTLFLCALAILLLVTPTSSLQLKHPYSSPSQGLSKKIVTKMATRKLMIISSEYVMTSTSHEGSSSEQLRVTSSGKSKDEEKKLASEEEEKKALAKYLSMD**YRTFRRRRPVHNK**ALPLDP*
	CCCTACTCATCCTCCTAGCCA	glv6-1	MKLIRVTLFLCALAILLLVTPTSSLQLKHPYSSPS*PRFKQKDCYENGDAKAHDHL**
	TGAACTTAATTACCTTGGCT	glv6-2	MKLIRVTLFLCALAILLLVTPTSSLQLKL*IAPKKLI**
	TCTAGCGAAATATCTATCGA	glv6-3	MKLIRVTLFLCALAILLLVTPTSSLQLKHPYSSPSQGLSKKIVTKMATRKLMIISSEYVMTSTSHEGSSSEQLRVTSSGKSKDEEKKLASEEEEKKALAKY*DGLSYV**

Target	gRNA	Genotype	Predicted protein sequence
GLV6	gctagtgcacaaagaaaga	Wildtype	MKLIRVTLFLCALAILLLVTPTSSLQLKHPYSSPSQGLSKKIVTKMATRKLMIISSEYVMTSTSHEGSSSEQLRVTSSGKSKDEEKKLASEEEEKKALAKYLSMD**YRTFRRRRPVHNK**ALPLDP*
	tggagttacaagcaataaaa	mutant	MKLIRVTL*YSLCTSHFIACNSNIFSTT*
GLV10	aaggatcattgaagcaaca	Wildtype	MSSIHVASMLLFLFLHHSDSRHLDNVHITASRFSLVKDQNVVSSSTSKEPVKVSRFVPGPLKHHRRPPLLFA**DYPKPSTRPPRHN***
	gataatctgcaataaagag	mutant	MSSIHVLQ**
GLV1	cttcttggacgtcttcaa	Wildtype	MSCSLRSGLVIVFCFILLLLSSNVGCASAARRLRSHKHHHHKVASLDVFNGGERRALGGVETGEEVVVM**DYPQPHRKPPIH**NEKS*
	gagaaaggaggcgggcgtt	mutant	MSCSLRSGLVIVFCFILLLLSSNVGCASAARRLRSHKHHHHKVASLDVF*QWVRKEAGSWVVESRQGKK**
GLV2	tgcgacgaggaaagacttg	Wildtype	MAIRVSHKSFLVALLLLFISSPTQARSLREVVRNRTLLVVEKSQESRKIRHEGGSSDVDGLMDM**DYNSANKKRPIHNR***
	aatagaacgctattggttg	mutant	MAIRVSHKSFLVALLLLFISSPTQARSLRE VVRNRTLLV*CGEESRESENKARRWIRK**
GLV7	tgatgaaaagatgatacg	Wildtype	MTTLSKILCVLILLLCFSFRYSLHEDGNQQSSRDFVSTAKAIKYGDVMKKMIRGRKLMMASGEKEEAETKMKRGNRETERNSSKSVEEDGLVAYTA**DYWRAKHHPPKNN***
	ctgaaacgaagatgaagag	mutant	MTTLSKILCVLILLLCFSFRYSLHEDGNQQSSRDFVSTAKAIKYGDVMKK--IRGRKLMMASGEKEEAETKMNERK**
GLV8	atcaatcccaaaaagaagaa	Wildtype	MKKWSYAKLMTSALLLVFLSIILLAFHGGSRGDNHLYDHVAIGTKDILMGRKLKDLKPKTESLKMINPKKKNGFEYSDQVSSDLSRQEVFVDMMAR**DYQGPKPRSKPLKNN***
	aagacaagcaataaagctg	mutant	MKKWSYAKLMTSAYCLSS**
CLE18	tcgaggaaacaatatcgac	Wildtype	MHLLKGGVVLIITLILFLITSSIVAIREDPSLIGVDRQIPTGPDPLHNPPQPSPKHHHWIGVEENNIDRSWNY**DYESHHAHSPIHN**SPEPAPLYRHLIGV*
	aaaacaatatcgaccggtct	mutant	MHLLKGGVVLIITLILFLITSSIVAIREDPSLIGVDRQIPTGPDPLHNPPQPSPKHHHWTG*LGIMWIMNLIMHIVLYITLLSLHHYIVI*

Supplementary Table 2. Statistical analysis of the primordia stages and LR density in *glv* and *mpk6* mutants compared to controls. *P* values indicating significant differences are highlighted in green. The Excel file is available upon request to the corresponding author.

Supplementary Table 3. Segregation analysis of *sgp1 to 4* mutants backcrossed to the *iGLV6* line. The presence of ELRs was scored in the F2 and a X^2 test was performed applying Yates correction and considering a recessive mutation as the null hypothesis, with one degree of freedom and p=0.05.

mutant	n	No. of seedlings with $GLV6^{OE}$ phenotype		No. of seedlings with suppressed $GLV6^{OE}$ phenotype		X^2
		observed	expected	observed	expected	
sgp1	222	175	165.5	47	55.5	1.54
sgp2	385	302	288.75	83	96.25	2.25
sgp3	184	150	138	34	46	3.83
sgp4	192	150	144	42	48	0.84

Supplemental experimental procedures

Plant material and growth conditions

To generate the CRISPR *glv6* mutants, three guide RNAs (gRNA1;2;3) were designed targeting the first and fourth exons of the *GLV6* gene (Table S1). Each gRNA was cloned in pEN-Chimera and subsequently recombined in pDe-Cas9 by Gateway® LR reaction (Fauser et al., 2014). The CRISPR T-DNA vectors (pDe-Cas9-gRNA1-*GLV6*, pDe-Cas9-gRNA2-*GLV6* and pDe-Cas9-gRNA3-*GLV6*) in *Agrobacterium tumefaciens* C58C1 were each transformed in wild-type *Arabidopsis thaliana* (ecotype Col-0) via the floral-dip method (Clough & Bent, 1998). T0 seeds were germinated on horizontal square plates with solid growth medium supplemented with 10 mg/L glufosinate-ammonium (Merck).

For each CRISPR T-DNA construct, 51 glufosinate-ammonium-resistant T1 seedlings were transferred to soil and genotyped. The presence of somatic mutations in the T1 plants was determined by harvesting one rosette leaf, DNA extraction, PCR amplification of the CRISPR-targeted DNA sequence (PCR primers for gRNA1 and gRNA2: Fw_tctcacttttgtgtttcgtg, Rv_ tgacatggtcaatgattcgt and for gRNA3: Fw_cctttctgggactttcaaac and Rv_gaacaaatcgtcttgactct), Sanger sequencing and TIDE analysis (http://shinyapps.datacurators.nl/tide/).

The progeny of the T1 plant with the highest mutation frequency (gRNA1: 36%; gRNA2: 13%; gRNA3: 48%) was screened for homozygous mutations in *GLV6* and absence of the CRISPR T-DNA construct. For each CRISPR T-DNA construct, 25 glufosinate-ammonium-sensitive T2 seedlings were rescued and transferred to soil and genotyped as described for the T1 generation.

The heritability of the CRISPR-generated mutation in *GLV6* and absence of the CRISPR T-DNA construct was validated in the T3 generation: 16 T3 seedlings were genotyped as described for previous generations. PCR amplification of a fragment of the CRISPR T-DNA vector was performed (PCR primers for the gRNA expression cassette present in the T-DNA: Fw_AtU6_ TCCCAGGATTAGAATGATTAGG and as reverse primer the Rv_spacer_gRNA1;2;3 for each CRISPR T-DNA construct respectively) to verify the absence of the CRISPR T-DNA vector.

The *glv10* mutant (*Salk_048797*) was obtained from the Nottingham Arabidopsis Stock Center (NASC). qRT-PCR analysis indicated a small change in *GLV10* transcripts levels relative to wild type (Supplementary Fig 8a). However the T-DNA insertion was anticipated to be in an exon. We confirmed by sequencing that the second exon in the *GLV10* open reading frame was interrupted by a T-DNA insertion (Supplementary Fig 8b). In agreement with this, RT-PCR experiments using primers at the beginning and end of the coding sequence identified *GLV10*-derived transcripts in wild type but not in *glv10* cDNA (Supplementary Fig 8c). Therefore, the *glv10* mutant is predicted to result in a truncated precursor after Ser[49] (Supplementary Fig 8b).

The *rgi1-1* (Salk_020659), *rgi1-2 (Salk_040393), rgi4-3* (Salk_037932), *rgi4-4 (Salk_089560), rgi5-1* (Salk_058918) and *rgi5-2 (Salk_014726)* mutant lines were used. *mpk6-3* and *-4* mutants have been previously reported (Bush & Krysan, 2007; Liu & Zhang, 2004). All mutants were ordered from NASC. The *iGLV6/rgi145* and the *iGLV6/mpk6-4* were obtained

by crossing the mutants and the *iGLV6* line. Mutant lines, as well as *GLV6* overexpression, were validated by (q)RT-PCR (Supplementary Fig 8).

The *GLV10pro:nls-2XGFP* line was previously reported (Fernandez et al., 2015). The *RGI1*, *4* and *5* promoters (2119, 1899 and 2054 bp upstream the ATG, respectively) were PCR amplified from genomic DNA and cloned into pEN-L4-R1. The resulting entry clone was used together with *pEN-L1-NF-L2* and *pEN-R2-F-L3* and the *pB7m34GW* destination vector to generate the *RGIpro:nls-2XGFP* expression clones. A 1689 bp *RPS5A* promoter was amplified and cloned into pDONR P4P1r (Invitrogen). The *RGI1* coding sequence flanked by *attL1* and *attL2* sites was synthesized with a BioXp 3200 system (SGI-DNA) and cloned into pGGA006 (Lampropoulos et al., 2013) by Gibson assembly. The *pEN-L4-RPS5Apro-R1*, *pEN-L1-RGI1-L2*, *pEN-R2-Venus-L3* (Mylle et al., 2013) and *pB7m34GW* –FAST vectors were recombined by LR recombination reaction to generate the *RPS5Apro:RGI1-Venus* cassette that was transformed into the *iGLV6/rgi145* line. Single locus *RPS5Apro:RGI1-Venus/iGLV6/rgi145* T2 GFP-positive seeds were selected and used for LR analysis.

Nuclear DNA extraction for next generation sequencing

Plant material was frozen in liquid N_2, ground and 3 volumes of HBM buffer (25 mM Tris-HCl pH 7.5, 440 mM sucrose, 10 mM $MgCl_2$, 0.1% Triton-X, 10 mM ß-mercaptoethanol, 2 mM spermine) were added and homogenized by vortexing. The homogenate was then filtered through Miracloth and spun at 3 000 rpm for 10 min at 4 °C. The pellet was resuspended in 0.5 mL of NIB buffer (20 mM Tris-HCl pH 7.5, 250 mM sucrose, 5 mM $MgCl_2$, 5 mM KCl, 0.1% Triton-X, 10 mM ß-mercaptoethanol) and loaded on top of a 15/50% percoll gradient. Samples were spun at 3 000 rpm for 10 min at 4 °C and the nuclei pellet was washed once with NIB buffer. DNA was extracted by resuspending the pellet in 500 μL of CTAB buffer (2% CTAB, 100 mM Tris.HCl (pH 8), 20 mM EDTA (pH 8) and 1,4 M NaCl) preheated at 60 °C, then incubated at 60 °C for 30 minutes with regular mixing steps. 500 μL of chloroform was then added and after gentle mixing, samples were spun at 7,000 g for 10 minutes at 4 °C. 0.5 μL of RNase A (100 mg/mL) was added to the soluble fraction and incubated 30 min at 37 °C. Then, 350 μL of isopropanol was added and samples were incubated at -20 °C for at least 1 h. Samples were spun at 13000 g for 6 minutes and the pellet washed twice in 70% EtOH before resuspending it in water.

Modified Malamy and Benfey protocol for root clearing

For analysis of all LR developmental stages, a modified Malamy and Benfey (Malamy & Benfey, 1997) protocol was used (See Supplementary M&M). 8-9 dag seedlings were collected in 6-well plates containing 90% acetone and kept at 4 ºC until all pigment was removed (usually 3-6 days and replacing once the acetone). Then, they were transferred to a new plate containing 0.5 M sodium phosphate buffer pH 7 for half an hour and incubated at 37 ºC. Buffer was replaced by clearing solution I (2% fuming HCL, 20% Methanol v/v) and incubated for 45 minutes at 60 ºC. Then, incubated at RT for 15 minutes in clearing solution II (7% NaOH m/v, 60% Ethanol v/v). Seedlings were rehydrated in 40, 20 and 10 % Ethanol (5 minutes/treatment). Then seedlings were incubated for 15 minutes or longer in 25% Glycerol/5% Ethanol (v/v) and finally mounted in 50% Glycerol (v/v). We processed maximum 20 seedlings in minimum 5 ml of solution as we found that increasing the solution/tissue

ratio yielded better cell separation necessary for precise counting of primordia at early developmental stages.

Protein extraction and western blotting

Frozen plant material was ground and the extraction buffer [50 mM Tris, pH 7.5, 200 mM NaCl, 1 mM EDTA, 10% (v/v) glycerol, 0.1% (v/v) Tween 20, 1 mM phenylmethylsulfonylfluoride, 1 mM DTT, 1× PhosSTOP™ (4906837001; Sigma-Aldrich) and 1× cOmplete™ ULTRA Tablets (5892791001; Sigma-Aldrich)] was added at the ratio of 2 μL per mg tissue (1:2 w:v). Samples were vortexed and centrifuged at 13 000 g for 30 minutes. Protein concentration was quantified in the supernatant using the Qubit protein assay kit (ThermoFischer Scientific). Equal amounts of proteins (30 μg) were separated on 7.5% SDS/PAGE and transferred onto a nitrocellulose membrane (Biorad). After blocking with 3% BSA, membranes were blotted overnight with primary antibodies against anti-phospho-p44/42 (Cell Signaling Technology; 1:2500). HRP-conjugated anti-rabbit secondary antibody (GE Healthcare; 1:10000) was used and signal detection was performed using SuperSignal™ West Femto Maximum Sensitivity Substrate (34095; Thermo Fisher Scientific). Antibodies were stripped in 1:1 (v:v) 10% SDS and 100 mM glycine-HCl (pH 2.5) solution, washed five times and reblotted with anti-MPK6 antibody (Sigma-Aldrich; 1:8000) and anti-MPK3 antibody (Sigma-Aldrich; 1:2500). HRP-conjugated anti-rabbit secondary antibody (GE Healthcare; 1:10000) was used and signal detection was performed using Western Lightning Plus ECL (NEL105001EA; PerkinElmer). All blots were imaged in a ChemiDoc XRS+ imaging system (Biorad). For quantification of the relative pMPK6/pMPK3 signal, band intensity was measured with the ImageLab software (Biorad) and then divided by the MPK6/MPK3 signal for every time point. Afterwards, values were normalized by the time 0 values.

qRT-PCR

To test *GLV* and *RGI* induction by auxin treatment, seedlings were germinated on solid MS on top of a mesh and 6 dag transferred to mock (DMSO) or NAA (10 μM) for the indicated time points. Then whole root was used for RNA extraction.

RNA was extracted with ReliaPrep RNA Miniprep System (Promega). First cDNA strand was synthesized using the iScript cDNA synthesis kit (Fermentas) or the qScript cDNA Supermix (Quantabio). qRT-PCR was performed using SyberGreen (Roche) and LightCycler real-time thermocycler (Roche). *CKIIα2* and *CDKA* were used as reference transcripts.

Confocal microscopy

For visualization of the root apical meristem, roots were stained with propidium iodide and observed under a Zeiss 710 confocal microscope with a 488 nm laser for excitation and 580-680 nm filter for detection. GFP was imaged using a 488 nm laser for excitation and 490- 550 nm for detection. Venus was imaged using a 514 nm laser for excitation and 540 nm for detection. For observation of LR primordia, the ClearSee protocol was employed as previously described (Ursache et al., 2018). Calcolfluor white M2R (Sigma) was used for staining of the cell wall and imaged with a 405 nm laser for excitation and 410-524 nm filter for detection.

References

Barbez, E., Kubes, M., Rolcik, J., Beziat, C., Pencik, A., Wang, B., Rosquete, M. R., Zhu, J., Dobrev, P. I., Lee, Y., Zazimalova, E., Petrasek, J., Geisler, M., Friml, J., & Kleine-Vehn, J. (2012). A novel putative auxin carrier family regulates intracellular auxin homeostasis in plants. *Nature, 485*(7396), 119-122. https://doi.org/10.1038/nature11001

Benkova, E., Michniewicz, M., Sauer, M., Teichmann, T., Seifertova, D., Jurgens, G., & Friml, J. (2003). Local, efflux-dependent auxin gradients as a common module for plant organ formation. *Cell, 115*(5), 591-602. http://www.ncbi.nlm.nih.gov/pubmed/14651850

Bush, S. M., & Krysan, P. J. (2007). Mutational evidence that the Arabidopsis MAP kinase MPK6 is involved in anther, inflorescence, and embryo development. *J Exp Bot, 58*(8), 2181-2191. https://doi.org/10.1093/jxb/erm092

Casimiro, I., Marchant, A., Bhalerao, R. P., Beeckman, T., Dhooge, S., Swarup, R., Graham, N., Inze, D., Sandberg, G., Casero, P. J., & Bennett, M. (2001). Auxin transport promotes Arabidopsis lateral root initiation. *Plant Cell, 13*(4), 843-852. http://www.ncbi.nlm.nih.gov/pubmed/11283340

Cho, S. K., Larue, C. T., Chevalier, D., Wang, H., Jinn, T. L., Zhang, S., & Walker, J. C. (2008). Regulation of floral organ abscission in Arabidopsis thaliana. *Proc Natl Acad Sci U S A, 105*(40), 15629-15634. https://doi.org/10.1073/pnas.0805539105

Curtis, M. D., & Grossniklaus, U. (2003). A gateway cloning vector set for high-throughput functional analysis of genes in planta. *Plant Physiol, 133*(2), 462-469. https://doi.org/10.1104/pp.103.027979

De Rybel, B., Vassileva, V., Parizot, B., Demeulenaere, M., Grunewald, W., Audenaert, D., Van Campenhout, J., Overvoorde, P., Jansen, L., Vanneste, S., Moller, B., Wilson, M., Holman, T., Van Isterdael, G., Brunoud, G., Vuylsteke, M., Vernoux, T., De Veylder, L., Inze, D., Weijers, D., Bennett, M. J., & Beeckman, T. (2010). A novel aux/IAA28 signaling cascade activates GATA23-dependent specification of lateral root founder cell identity. *Curr Biol, 20*(19), 1697-1706. https://doi.org/10.1016/j.cub.2010.09.007

De Smet, I., Lau, S., Voss, U., Vanneste, S., Benjamins, R., Rademacher, E. H., Schlereth, A., De Rybel, B., Vassileva, V., Grunewald, W., Naudts, M., Levesque, M. P., Ehrismann, J. S., Inze, D., Luschnig, C., Benfey, P. N., Weijers, D., Van Montagu, M. C., Bennett, M. J., Jurgens, G., & Beeckman, T. (2010). Bimodular auxin response controls organogenesis in Arabidopsis. *Proc Natl Acad Sci U S A, 107*(6), 2705-2710. https://doi.org/10.1073/pnas.0915001107

De Smet, I., Vassileva, V., De Rybel, B., Levesque, M. P., Grunewald, W., Van Damme, D., Van Noorden, G., Naudts, M., Van Isterdael, G., De Clercq, R., Wang, J. Y., Meuli, N., Vanneste, S., Friml, J., Hilson, P., Jurgens, G., Ingram, G. C., Inze, D., Benfey, P. N., & Beeckman, T. (2008). Receptor-like kinase ACR4 restricts formative cell divisions in

the Arabidopsis root. *Science, 322*(5901), 594-597.
https://doi.org/10.1126/science.1160158

Ditengou, F. A., Teale, W. D., Kochersperger, P., Flittner, K. A., Kneuper, I., van der Graaff, E., Nziengui, H., Pinosa, F., Li, X., Nitschke, R., Laux, T., & Palme, K. (2008). Mechanical induction of lateral root initiation in Arabidopsis thaliana. *Proc Natl Acad Sci U S A, 105*(48), 18818-18823. https://doi.org/10.1073/pnas.0807814105

Dubrovsky, J. G., Sauer, M., Napsucialy-Mendivil, S., Ivanchenko, M. G., Friml, J., Shishkova, S., Celenza, J., & Benkova, E. (2008). Auxin acts as a local morphogenetic trigger to specify lateral root founder cells. *Proc Natl Acad Sci U S A, 105*(25), 8790-8794. https://doi.org/10.1073/pnas.0712307105

Fauser, F., Schiml, S., & Puchta, H. (2014). Both CRISPR/Cas-based nucleases and nickases can be used efficiently for genome engineering in Arabidopsis thaliana. *The Plant Journal, 79*(2), 348-359. https://doi.org/10.1111/tpj.12554

Fernandez, A., Drozdzecki, A., Hoogewijs, K., Nguyen, A., Beeckman, T., Madder, A., & Hilson, P. (2013, Feb). Transcriptional and functional classification of the GOLVEN/ROOT GROWTH FACTOR/CLE-like signaling peptides reveals their role in lateral root and hair formation. *Plant Physiol, 161*(2), 954-970. https://doi.org/10.1104/pp.112.206029

Fernandez, A., Drozdzecki, A., Hoogewijs, K., Vassileva, V., Madder, A., Beeckman, T., & Hilson, P. (2015). The GLV6/RGF8/CLEL2 peptide regulates early pericycle divisions during lateral root initiation. *J Exp Bot, 66*(17), 5245-5256. https://doi.org/10.1093/jxb/erv329

Fernandez, A., Drozdzecki, A., Hoogewijs, K., Vassileva, V., Madder, A., Beeckman, T., & Hilson, P. (2015). The GLV6/RGF8/CLEL2 peptide regulates early pericycle divisions during lateral root initiation. *J Exp Bot, 66*(17), 5245-5256. https://doi.org/10.1093/jxb/erv329

Fukaki, H., Tameda, S., Masuda, H., & Tasaka, M. (2002). Lateral root formation is blocked by a gain-of-function mutation in the SOLITARY-ROOT/IAA14 gene of Arabidopsis. *Plant J, 29*(2), 153-168. http://www.ncbi.nlm.nih.gov/pubmed/11862947

Hofhuis, H., Laskowski, M., Du, Y., Prasad, K., Grigg, S., Pinon, V., & Scheres, B. (2013). Phyllotaxis and rhizotaxis in Arabidopsis are modified by three PLETHORA transcription factors. *Curr Biol, 23*(11), 956-962. https://doi.org/10.1016/j.cub.2013.04.048

Jewaria, P. K., Hara, T., Tanaka, H., Kondo, T., Betsuyaku, S., Sawa, S., Sakagami, Y., Aimoto, S., & Kakimoto, T. (2013). Differential effects of the peptides Stomagen, EPF1 and EPF2 on activation of MAP kinase MPK6 and the SPCH protein level. *Plant Cell Physiol, 54*(8), 1253-1262. https://doi.org/10.1093/pcp/pct076

Jun, J., Fiume, E., Roeder, A. H., Meng, L., Sharma, V. K., Osmont, K. S., Baker, C., Ha, C. M., Meyerowitz, E. M., Feldman, L. J., & Fletcher, J. C. (2010). Comprehensive analysis of CLE polypeptide signaling gene expression and overexpression activity in Arabidopsis. *Plant Physiol, 154*(4), 1721-1736. https://doi.org/10.1104/pp.110.163683

Komori, R., Amano, Y., Ogawa-Ohnishi, M., & Matsubayashi, Y. (2009). Identification of tyrosylprotein sulfotransferase in Arabidopsis. *Proc Natl Acad Sci U S A, 106*(35), 15067-15072. https://doi.org/10.1073/pnas.0902801106

Kumpf, R. P., Shi, C. L., Larrieu, A., Sto, I. M., Butenko, M. A., Peret, B., Riiser, E. S., Bennett, M. J., & Aalen, R. B. (2013). Floral organ abscission peptide IDA and its HAE/HSL2 receptors control cell separation during lateral root emergence. *Proc Natl Acad Sci U S A, 110*(13), 5235-5240. https://doi.org/10.1073/pnas.1210835110

Lampropoulos, A., Sutikovic, Z., Wenzl, C., Maegele, I., Lohmann, J. U., & Forner, J. (2013). GreenGate - A Novel, Versatile, and Efficient Cloning System for Plant Transgenesis. *PLoS One, 8*(12), e83043. https://doi.org/10.1371/journal.pone.0083043

Laskowski, M., Grieneisen, V. A., Hofhuis, H., Hove, C. A., Hogeweg, P., Maree, A. F., & Scheres, B. (2008). Root system architecture from coupling cell shape to auxin transport. *PLoS Biol, 6*(12), e307. https://doi.org/10.1371/journal.pbio.0060307

Liu, Y., & Zhang, S. (2004). Phosphorylation of 1-Aminocyclopropane-1-Carboxylic Acid Synthase by MPK6, a Stress-Responsive Mitogen-Activated Protein Kinase, Induces Ethylene Biosynthesis in Arabidopsis. *Plant Cell, 16*(12), 3386. https://doi.org/10.1105/tpc.104.026609

Lopez-Bucio, J. S., Dubrovsky, J. G., Raya-Gonzalez, J., Ugartechea-Chirino, Y., Lopez-Bucio, J., de Luna-Valdez, L. A., Ramos-Vega, M., Leon, P., & Guevara-Garcia, A. A. (2014). Arabidopsis thaliana mitogen-activated protein kinase 6 is involved in seed formation and modulation of primary and lateral root development. *J Exp Bot, 65*(1), 169-183. https://doi.org/10.1093/jxb/ert368

Lucas, M., Kenobi, K., von Wangenheim, D., Vobeta, U., Swarup, K., De Smet, I., Van Damme, D., Lawrence, T., Peret, B., Moscardi, E., Barbeau, D., Godin, C., Salt, D., Guyomarc'h, S., Stelzer, E. H., Maizel, A., Laplaze, L., & Bennett, M. J. (2013). Lateral root morphogenesis is dependent on the mechanical properties of the overlaying tissues. *Proc Natl Acad Sci U S A, 110*(13), 5229-5234. https://doi.org/10.1073/pnas.1210807110

Malamy, J. E., & Benfey, P. N. (1997). Organization and cell differentiation in lateral roots of Arabidopsis thaliana. *Development, 124*(1), 33-44. http://www.ncbi.nlm.nih.gov/pubmed/9006065

Matsuzaki, Y., Ogawa-Ohnishi, M., Mori, A., & Matsubayashi, Y. (2010). Secreted peptide signals required for maintenance of root stem cell niche in Arabidopsis. *Science, 329*(5995), 1065-1067. https://doi.org/10.1126/science.1191132

Meng, L., Buchanan, B. B., Feldman, L. J., & Luan, S. (2012). CLE-like (CLEL) peptides control the pattern of root growth and lateral root development in Arabidopsis. *Proc Natl Acad Sci U S A, 109*(5), 1760-1765. https://doi.org/10.1073/pnas.1119864109

Moreno-Risueno, M. A., Van Norman, J. M., Moreno, A., Zhang, J., Ahnert, S. E., & Benfey, P. N. (2010). Oscillating gene expression determines competence for periodic Arabidopsis root branching. *Science, 329*(5997), 1306-1311. https://doi.org/10.1126/science.1191937

Mylle, E., Codreanu, M.-C., Boruc, J., & Russinova, E. (2013). Emission spectra profiling of fluorescent proteins in living plant cells. *Plant Methods, 9*(1), 10. https://doi.org/10.1186/1746-4811-9-10

Okushima, Y., Overvoorde, P. J., Arima, K., Alonso, J. M., Chan, A., Chang, C., Ecker, J. R., Hughes, B., Lui, A., Nguyen, D., Onodera, C., Quach, H., Smith, A., Yu, G., & Theologis, A. (2005). Functional genomic analysis of the AUXIN RESPONSE FACTOR gene family members in Arabidopsis thaliana: unique and overlapping functions of ARF7 and ARF19. *Plant Cell, 17*(2), 444-463. https://doi.org/10.1105/tpc.104.028316

Ortiz-Morea, F. A., Savatin, D. V., Dejonghe, W., Kumar, R., Luo, Y., Adamowski, M., Van den Begin, J., Dressano, K., Pereira de Oliveira, G., Zhao, X., Lu, Q., Madder, A., Friml, J., Scherer de Moura, D., & Russinova, E. (2016). Danger-associated peptide signaling in Arabidopsis requires clathrin. *Proc Natl Acad Sci U S A, 113*(39), 11028-11033. https://doi.org/10.1073/pnas.1605588113

Ou, Y., Lu, X., Zi, Q., Xun, Q., Zhang, J., Wu, Y., Shi, H., Wei, Z., Zhao, B., Zhang, X., He, K., Gou, X., Li, C., & Li, J. (2016). RGF1 INSENSITIVE 1 to 5, a group of LRR receptor-like kinases, are essential for the perception of root meristem growth factor 1 in Arabidopsis thaliana. *Cell Res, 26*(6), 686-698. https://doi.org/10.1038/cr.2016.63

Peret, B., Li, G., Zhao, J., Band, L. R., Voss, U., Postaire, O., Luu, D. T., Da Ines, O., Casimiro, I., Lucas, M., Wells, D. M., Lazzerini, L., Nacry, P., King, J. R., Jensen, O. E., Schaffner, A. R., Maurel, C., & Bennett, M. J. (2012). Auxin regulates aquaporin function to facilitate lateral root emergence. *Nat Cell Biol, 14*(10), 991-998. https://doi.org/10.1038/ncb2573

Peterson, B. A., Haak, D. C., Nishimura, M. T., Teixeira, P. J., James, S. R., Dangl, J. L., & Nimchuk, Z. L. (2016). Genome-Wide Assessment of Efficiency and Specificity in CRISPR/Cas9 Mediated Multiple Site Targeting in Arabidopsis. *PLoS One, 11*(9), e0162169. https://doi.org/10.1371/journal.pone.0162169

Schneeberger, K., Ossowski, S., Lanz, C., Juul, T., Petersen, A. H., Nielsen, K. L., Jorgensen, J. E., Weigel, D., & Andersen, S. U. (2009). SHOREmap: simultaneous mapping and mutation identification by deep sequencing. *Nat Methods, 6*(8), 550-551. https://doi.org/10.1038/nmeth0809-550

Shinohara, H., Mori, A., Yasue, N., Sumida, K., & Matsubayashi, Y. (2016). Identification of three LRR-RKs involved in perception of root meristem growth factor in Arabidopsis. *Proc Natl Acad Sci U S A, 113*(14), 3897-3902. https://doi.org/10.1073/pnas.1522639113

Song, W., Liu, L., Wang, J., Wu, Z., Zhang, H., Tang, J., Lin, G., Wang, Y., Wen, X., Li, W., Han, Z., Guo, H., & Chai, J. (2016). Signature motif-guided identification of receptors for peptide hormones essential for root meristem growth. *Cell Res, 26*(6), 674-685. https://doi.org/10.1038/cr.2016.62

Torii, K. U. (2012). Two-dimensional spatial patterning in developmental systems. *Trends Cell Biol, 22*(8), 438-446. https://doi.org/10.1016/j.tcb.2012.06.002

Toyokura, K., Goh, T., Shinohara, H., Shinoda, A., Kondo, Y., Okamoto, Y., Uehara, T., Fujimoto, K., Okushima, Y., Ikeyama, Y., Nakajima, K., Mimura, T., Tasaka, M., Matsubayashi, Y., & Fukaki, H. (2019). Lateral Inhibition by a Peptide Hormone-Receptor Cascade during Arabidopsis Lateral Root Founder Cell Formation. *Dev Cell, 48*(1), 64-75 e65. https://doi.org/10.1016/j.devcel.2018.11.031

Turing, A. M. (1952). The Chemical Basis of Morphogenesis. *Philosophical Transactions of the Royal Society of London. Series B, Biological Sciences, 237*(641), 37-72.

Ursache, R., Andersen, T. G., Marhavý, P., & Geldner, N. (2018). A protocol for combining fluorescent proteins with histological stains for diverse cell wall components. *The Plant Journal, 93*(2), 399-412. https://doi.org/10.1111/tpj.13784

von Wangenheim, D., Fangerau, J., Schmitz, A., Smith, R. S., Leitte, H., Stelzer, E. H., & Maizel, A. (2016). Rules and Self-Organizing Properties of Post-embryonic Plant Organ Cell Division Patterns. *Curr Biol, 26*(4), 439-449. https://doi.org/10.1016/j.cub.2015.12.047

Voss, U., Wilson, M. H., Kenobi, K., Gould, P. D., Robertson, F. C., Peer, W. A., Lucas, M., Swarup, K., Casimiro, I., Holman, T. J., Wells, D. M., Peret, B., Goh, T., Fukaki, H., Hodgman, T. C., Laplaze, L., Halliday, K. J., Ljung, K., Murphy, A. S., Hall, A. J., Webb, A. A., & Bennett, M. J. (2015). The circadian clock rephases during lateral root organ initiation in Arabidopsis thaliana. *Nat Commun, 6*, 7641. https://doi.org/10.1038/ncomms8641

Whitford, R., Fernandez, A., Tejos, R., Perez, A. C., Kleine-Vehn, J., Vanneste, S., Drozdzecki, A., Leitner, J., Abas, L., Aerts, M., Hoogewijs, K., Baster, P., De Groodt, R., Lin, Y. C., Storme, V., Van de Peer, Y., Beeckman, T., Madder, A., Devreese, B., Luschnig, C., Friml, J., & Hilson, P. (2012). GOLVEN secretory peptides regulate auxin carrier turnover during plant gravitropic responses. *Dev Cell, 22*(3), 678-685. https://doi.org/10.1016/j.devcel.2012.02.002

Wu, T., Kamiya, T., Yumoto, H., Sotta, N., Katsushi, Y., Shigenobu, S., Matsubayashi, Y., & Fujiwara, T. (2015). An Arabidopsis thaliana copper-sensitive mutant suggests a role

of phytosulfokine in ethylene production. *J Exp Bot, 66*(13), 3657-3667. https://doi.org/10.1093/jxb/erv105

Xu, J., & Zhang, S. (2015). Mitogen-activated protein kinase cascades in signaling plant growth and development. *Trends Plant Sci, 20*(1), 56-64. https://doi.org/10.1016/j.tplants.2014.10.001

Xuan, W., Band, L. R., Kumpf, R. P., Van Damme, D., Parizot, B., De Rop, G., Opdenacker, D., Moller, B. K., Skorzinski, N., Njo, M. F., De Rybel, B., Audenaert, D., Nowack, M. K., Vanneste, S., & Beeckman, T. (2016). Cyclic programmed cell death stimulates hormone signaling and root development in Arabidopsis. *Science, 351*(6271), 384-387. https://doi.org/10.1126/science.aad2776

Xuan, W., Opdenacker, D., Vanneste, S., & Beeckman, T. (2018). Long-Term In Vivo Imaging of Luciferase-Based Reporter Gene Expression in Arabidopsis Roots. *Methods Mol Biol, 1761*, 177-190. https://doi.org/10.1007/978-1-4939-7747-5_13

Zhou, W., Wei, L., Xu, J., Zhai, Q., Jiang, H., Chen, R., Chen, Q., Sun, J., Chu, J., Zhu, L., Liu, C. M., & Li, C. (2010). Arabidopsis Tyrosylprotein sulfotransferase acts in the auxin/PLETHORA pathway in regulating postembryonic maintenance of the root stem cell niche. *Plant Cell, 22*(11), 3692-3709. https://doi.org/10.1105/tpc.110.075721

Zhu, Q., Shao, Y., Ge, S., Zhang, M., Zhang, T., Hu, X., Liu, Y., Walker, J., Zhang, S., & Xu, J. (2019). A MAPK cascade downstream of IDA-HAE/HSL2 ligand-receptor pair in lateral root emergence. *Nat Plants, 5*(4), 414-423. https://doi.org/10.1038/s41477-019-0396-x

Chapter 3: Lateral root-specific loss-of-function of *CYCLIN-DEPENDENT KINASES* reveals redundant function during lateral root organogenesis in *Arabidopsis*

Vangheluwe N., Jourquin J., Decaestecker W., Andrade Buono R., Pfeiffer M. L., Karimi M., Van Isterdael G., Njo M., Moritz N. K., Jacobs T. B. & Beeckman T.

Abstract

Cell cycle activity at the onset of lateral root initiation is essential for lateral root founder cells in the pericycle to undergo formative divisions resulting in the development of a lateral root primordium. Our study investigates the function of conserved components of the cell cycle machinery in formative divisions in *Arabidopsis* lateral root development. Functional analysis of *CYCLIN DEPENDENT KINASE* (*CDK*) *A;1* has been limited because of its central function in cell cycle progression. *CDKA;1* and *CDKB1;1* are both expressed at the onset of lateral root initiation and mutant analysis unveiled that B1-type CDK are involved in lateral root development. Moreover, lateral root-specific loss-of-function mutants revealed that *CDKA;1*, *CDKB1;1* and *CDKB1;2* kinases act redundantly and affect lateral root development soon after emergence. Finally, we reveal that morphogenesis of lateral roots is preserved despite the absence of intact cell cycle progression. Our data demonstrate that *A-* and *B1-*subtype *CDK*s are concomitantly essential for lateral root organogenesis and highlight the contribution of organ-specific genome editing to study gene function.

Authors contribution

TB designed the project. MN characterized the reporter lines for *CDKA;1, CDKB1;1* and *CDKB1;2*. NV phenotypically characterized loss-of-function and gain-of-function lines for *CDKA;1, CDKB1;1* and *CDKB1;2*. KM, WD and TBJ generated CRISPR constructs for lateral root-specific genome editing. NV generated and phenotypically characterized lateral root-specific *cdk* mutant lines with help from JJ. WD, MLP and GVI conducted CRISPR mutation analysis. JJ, RAB, and MKN performed confocal analysis of lateral root-specific *cdk* mutant lines. NV analysed crosstalk with auxin. NV prepared and performed expression analysis. NV carried out the statistical analysis. NV and TB wrote the manuscript. TB provided guidance and advice on the project, the experiments and the analysis of the results.

Introduction

The root system of terrestrial plants is responsible for anchorage to the substrate as well as for minerals and water supply. The capacity to fulfil these functions is highly dependent on its architecture. Root branching through lateral root formation is an important factor of the adaptability of the root system to its environment (Motte et al., 2019). In *Arabidopsis*, lateral roots initiate at regular intervals along the primary root in the pericycle adjacent to the xylem poles (Parizot et al., 2008). *GATA23* expression in subsets of xylem-pole pericycle cells marks the specification into lateral root founder cells (De Rybel et al., 2010). At the onset of lateral root initiation, founder cells undergo several rounds of anticlinal asymmetric divisions that generate files of small cells flanked by bigger cells referred to as a stage I lateral root primordium (LRP) (Malamy & Benfey, 1997). The subsequent round of division occurs periclinally rather than anticlinally, and yields a two-layered LRP (stage II). Additional divisions result in the formation of an LRP that progressively acquires the same tissue organisation as the primary root meristem and eventually emerges through overlying tissues of the primary root.

Regulation of cell cycle activity at the onset of lateral root initiation is essential for founder cells to undergo formative divisions (Beeckman et al., 2001; DiDonato et al., 2004; Himanen et al., 2002a; Jurado et al., 2010; Sanz et al., 2011; Vanneste et al., 2005). The transition of founder cells from G1 to S and subsequent cell cycle progression is stimulated by auxin. Disturbing the auxin response through inhibition of polar auxin transport is sufficient to inhibit lateral root initiation, whereas localized auxin production triggers lateral root initiation, indicating that auxin accumulation in xylem-pole pericycle cells is necessary for organogenesis (Casimiro et al., 2001; Dubrovsky et al., 2008; Himanen et al., 2002a; Vanneste et al., 2005). Auxin triggers lateral root initiation through the SOLITARY ROOT/(SLR)IAA14–ARF7–ARF19 auxin-signalling module (Fukaki et al., 2005; Fukaki et al., 2002; Vanneste et al., 2005). In the dominant-negative mutant *slr-1*, lateral root initiation is halted at the G1 to S transition and cannot be restored by exogenous auxin application. Interestingly, overexpression of genes regulating G1 to S transition induces pericycle cell division in *slr-1* but do not lead to formative cell divisions that normally precede the formation of an LRP, which indicates that the *SLR*-dependent auxin-signalling module is necessary both for cell cycle activation and for cell fate specification (Vanneste et al., 2005).

A plethora of highly conserved components of the cell cycle has been demonstrated to be important for lateral root initiation (Kajala et al., 2014). Activation and progression through the major phases of the cell cycle are governed by the control of cyclin-dependent kinases (CDKs). The activity of these CDKs can be modulated through interacting regulatory components, CDK subunits, inhibitory components, or through stimulatory and inhibitory phosphorylation (De Veylder et al., 2007; Joubès et al., 2000). It has been demonstrated that the auxin-mediated transition of founder cells from G1 to S is controlled by the INHIBITOR-INTERACTOR OF CDK/KINASE-INHIBITORY PROTEIN (KIP)-RELATED PROTEIN (ICK/KRP) family of proteins (Himanen et al., 2002a; Ren et al., 2008; Sanz et al., 2011). Upon auxin treatment, reduced *KRP2* expression and increased KRP2 protein turnover result in a transient increase in CDKA;1–CYCD2;1 activity and subsequent cell division, which positively regulates lateral root development (Ren et al., 2008; Sanz et al., 2011).

CDKA;1 is the central regulator of cell cycle progression in *Arabidopsis* and is functionally conserved among kingdoms (Scofield et al., 2014). The remaining *Arabidopsis CDK* members do not exhibit strong homology to *CDK* types in other organisms and hints that they are functionally specialized in plant-specific developmental processes (De Veylder et al., 2007; Joubès et al., 2000). This has been illustrated by the redundant control of embryo and gametophyte formation by *CDKA;1* and *CDKB1* kinases (Nowack et al., 2012). Moreover, it has been reported that cell proliferation in the stomatal lineage is controlled by *FOUR LIPS* (*FLP*)/*MYB124-MYB88-E2Fa* via modulation of CDKB1;1 and CDKB1;2 function (Boudolf et al., 2004; Xie et al., 2010). Interestingly, AUXIN RESPONSE FACTOR7 (ARF7) and the ARF7-regulated FLP transcription factors jointly form a coherent feed-forward motif that mediates the auxin-responsive *PIN3* transcription to steer the early steps of lateral root formation (Chen et al., 2015). These observations suggest a potential function of CDKB1 kinases in lateral root development.

It is currently unclear what the function is of CDKs in formative divisions essential for lateral root development. Functional analysis of *CDKA;1* and potential redundancy with other *CDK* members at the onset of lateral root initiation has been limited because loss-of-function of *CDKA;1* severely affects development (Nowack et al., 2012). Homozygous *cdka;1* mutant seedlings are not viable in soil but can be cultivated as sterile dwarf plants without a root system in liquid cultures (Nowack et al., 2012). This hurdle recurs for many fundamentally essential genes. Recently, a clustered regularly interspaced short palindromic repeats (CRISPR)-based tissue-specific knockout system (CRISPR-TSKO) was devised enabling the generation of somatic mutations in particular *Arabidopsis* cell types, tissues, and organs to overcome this limitation (Decaestecker et al., 2019; Wang et al., 2020).

Here, we report on the function of *A*- and *B1*-subtype *CDKs* during lateral root development through expression analysis and lateral root-specific loss-of-function studies using CRISPR mutagenesis. Our study demonstrates that *A*- and *B1*-subtype *CDKs* are concomitantly essential for lateral root organogenesis and reveals the striking observation that morphogenesis of lateral roots still occurs in the absence of intact cell cycle progression.

Results

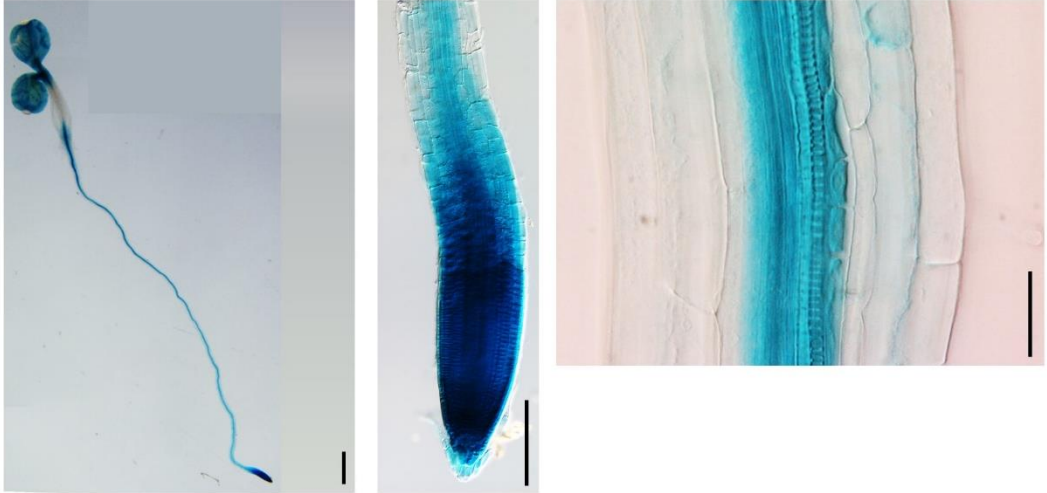*CDKA;1*, *CDKB1;1* and *CDKB1;2* root expression patterns reveal functional specification

The expression pattern during post-embryonic development of *CDKA;1, CDKB1;1* and *CDKB1;2* was analysed using transgenic lines expressing the GUS reporter under the regulation of their promoter (termed respectively *pCDKA;1::GUS, pCDKB1;1::GUS, pCDKB1;2::GUS*) (Figure 1). *pCDKA;1::GUS* activity was detected throughout whole seedlings with a prominent expression in the primary root meristem (Figure 1A; Figure S1A). It was further expressed in the vasculature and stage I lateral root primordia (Figure 1A) (Malamy & Benfey, 1997). The ubiquitous expression pattern of *CDKA;1* is in accordance with its function as central regulator of cell cycle progression in *Arabidopsis*. Interestingly, *pCDKB1;1::GUS* activity was confined to the vasculature and detected in stage I lateral root primordia (Figure 1B), while no expression of its close homolog *CDKB1;2* could be observed during post-embryonic development (Figure 1C).

Alternatively, transcriptional fold changes of *CDKA;1, CDKB1;1* and *CDKB1;2* were assessed in RNA-Seq experiments performed in primary root segments of the young maturation zone (Figure S1B) (Chen et al., unpublished; Perez et al., unpublished). In Chen *et al*. the lateral root inducible system was adapted, which enabled to detect differentially expressed genes in distinct early stages of lateral root development (Himanen et al., 2002a; Malamy & Benfey, 1997). Significant transcriptional fold changes were observed for *CDKB1;1* and *CDKB1;2* after 12 hours treatment with synthetic auxin, 1-naphthaleneacetic acid (NAA), which corresponds with the progression of Stage I lateral root primordium development (Figure S1B). In Perez *et al*. primary roots were treated for 2 hours with NAA or DMSO as control to detect auxin-dependent differential gene expression and revealed that transcription of *CDKB1;1* and *CDKB1;2* is significantly upregulated upon synthetic auxin treatment (Figure S1B).

The transition of lateral root founder cells from G1 to S and subsequent cell cycle progression is stimulated by auxin (Beeckman et al., 2001; Himanen et al., 2002a). To investigate the cell cycle progression during lateral root initiation, the expression of *CDKA;1* and *CDKB1;1* was analysed using GUS reporter lines and the lateral root inducible system (LRIS) (Himanen et al., 2002a). It has been demonstrated that expression of *CDKB1;1* is induced in the xylem-pole pericycle upon auxin treatment via the SLR/IAA14 auxin-signalling module, while expression of *CDKA;1* remains unaffected (Vanneste et al., 2005). These observations suggest that expression of the central regulator *CDKA;1* concomitantly with *CDKB1;1* expression in founder cells might be necessary to surpass a required threshold level of CDK activity for cell cycle progression at the onset of lateral root initiation.
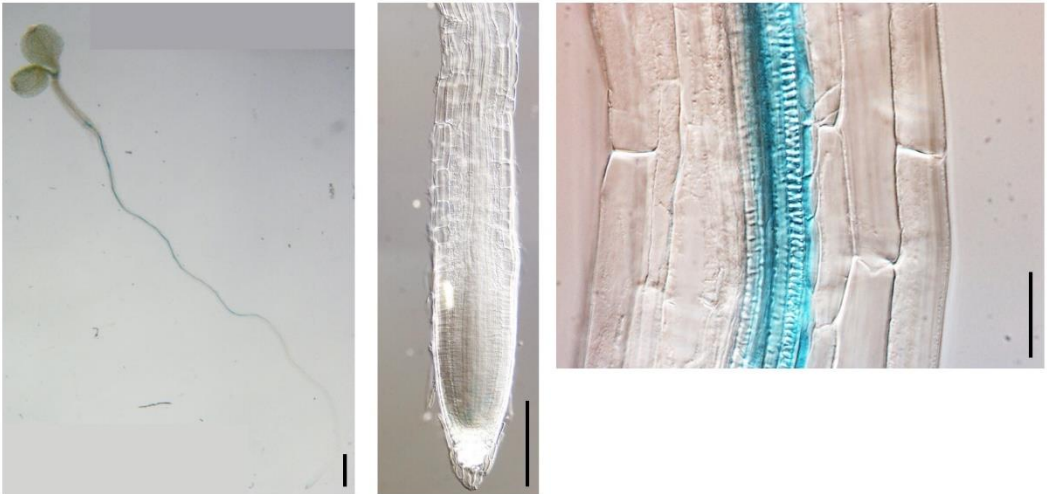
A

CDKA;1

B

CDKB1;1

C

CDKB1;2

Figure 1. *CDKA;1*, *CDKB1;1* and *CDKB1;2* root expression patterns reveal functional specification.

A. Expression pattern of *pCDKA;1::GUS* in the primary root tip and representative stage I lateral root primordium of 5-day-old *Arabidopsis* seedlings.

B. Expression pattern of *pCDKB1;1::GUS*.

C. Expression pattern of *pCDKB1;2::GUS*.

Scale bar left panel: 1 mm. Scale bar middle panel: 0,1 mm. Scale bar right panel: 20 µm.

Loss-of-function of *CDKA;1* severely affects development (Nowack et al., 2012). Homozygous *cdka;1* mutants are viable, although severely compromised and microscopic analysis revealed that they consist of fewer and larger cells compared to wild-type (Nowack et al., 2012). To evaluate the root system, homozygous *cdka;1* seedlings were grown on solid medium. Primary root growth was severely stunted, and no lateral roots could be observed (Figure 2C; Figure 2D) even after 3 weeks of growth (data not shown). The central role of *CDKA;1* during plant development precludes the study of its function in a post-embryonic organ-specific context.

Functional analysis of *CDKB1;1* and its closest homolog *CDKB1;*2 revealed a function in guard mother cell cytokinesis in stomatal development (Boudolf et al., 2004; Xie et al., 2010). *CDKB1;1* and *CDKB1;2* redundantly promote both the last division in the stomatal cell lineage as well as the number of stomata and stomatal cell lineages that form (Boudolf et al., 2004; Xie et al., 2010). The loss-of-function lateral root phenotypes of neither *CDKB1;1* nor *CDKB1;2* have been previously reported. Emerged lateral root density was quantified and no significant difference was observed in *cdkb1;1* mutant seedlings compared to wild-type, (Figure 2A; Figure 2C). By contrast, the lateral root density in *cdkb1;1-1;2* double mutant seedlings was significantly decreased compared to wild-type, while the average primary root length was unaffected (Figure 2A; Figure 2B). In addition, it was observed that the lateral roots in *cdkb1;1-1;2* double mutant seedlings are shorter compared to wild-type.

Alternatively, the lateral root phenotype of seedlings expressing the N161 dominant-negative kinase version of CDKB1;1 was analysed (Boudolf et al., 2004; Xie et al., 2010). The aspartic acid residue at the amino acid position 161 is required for correct ATP binding by the CDK kinases, and its mutation to an asparagine residue (N) results in loss-of-kinase activity (Figure S2A). Overexpression of mutant *CDKB1;1 N161* has a dominant-negative effect (Boudolf et al., 2004). Two independent lines 1.6 and 2.6 overexpressing wild-type *CDKB1;1* and two independent lines 1.2 and 9.2 overexpressing dominant-negative *CDKB1;1* (*N161*) were compared (Boudolf et al., 2004). The emerged lateral root density was significantly decreased in *N161* dominant-negative mutant seedlings compared to seedlings overexpressing wild-type *CDKB1;1* (Figure 3A; Figure 3B), while the average primary root length remained unaltered (Figure S2B). This phenotype might result from N161 interfering with the function of related kinases, such as *CDKB1;2*.

These results indicate that the kinase dead form of *CDKB1;1* (*N161*) likely mimics the *cdkb1;1-1;2* double mutant lateral root phenotype by interfering both with the function of *CDKB1;1* and *CDKB1;2*. Taken together, mutant analysis revealed that *CDKB1;1* and *CDKB1;2* act redundantly in lateral root development as a consequence of loss-of-activity of CDKB1 kinases, which results in decreased emerged lateral root density.
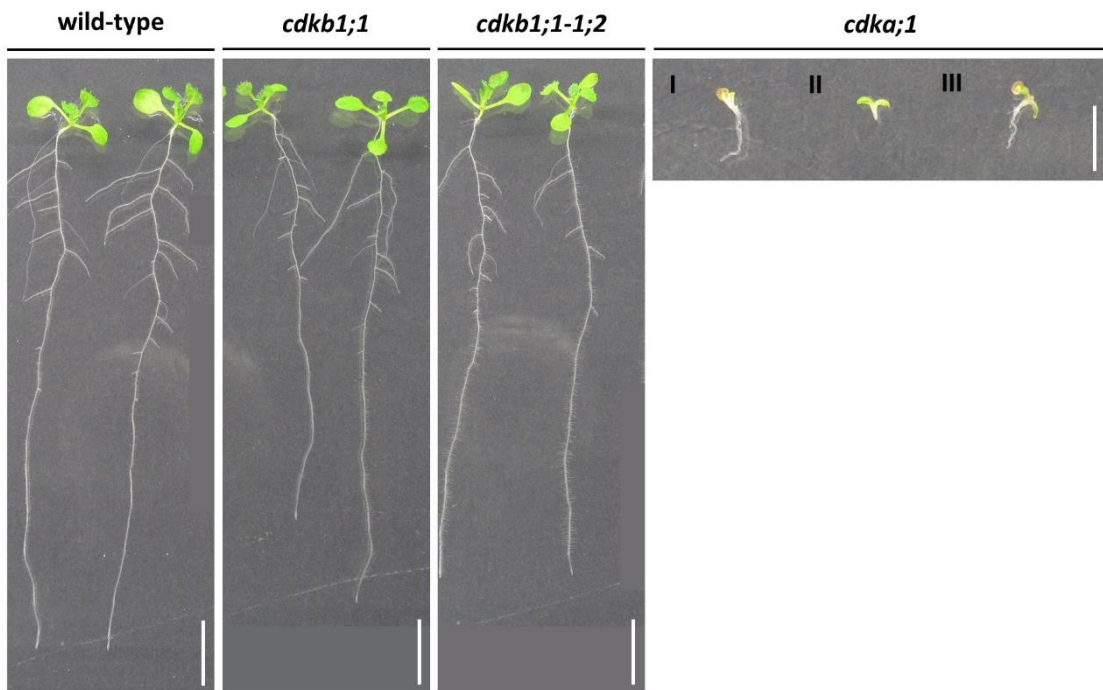
A

Emerged lateral root density

n =   21   19   16

B

Average primary root length

n =   21   19   16

C

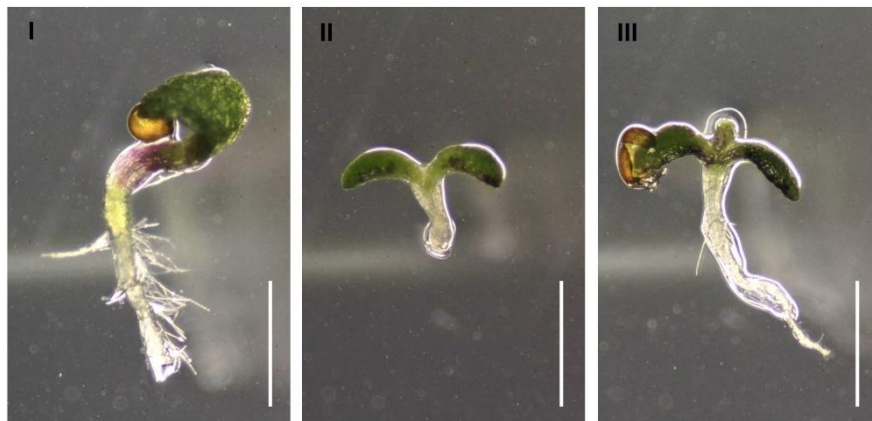| wild-type | *cdkb1;1* | *cdkb1;1-1;2* | *cdka;1* |
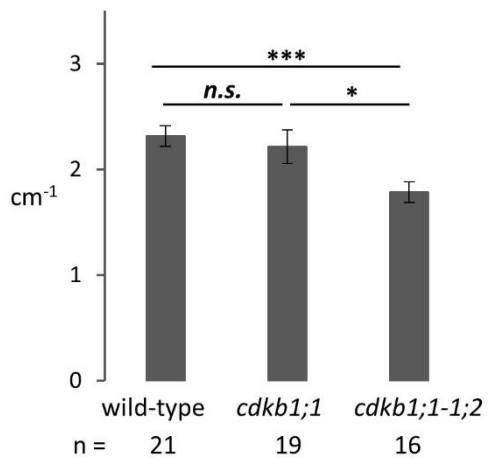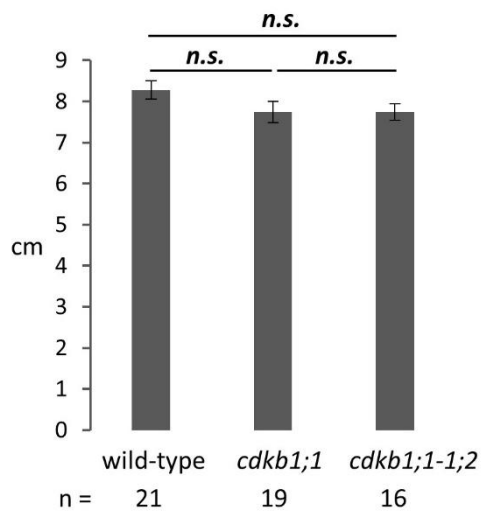
D

Figure 2. Loss-of-function mutants of *A*- and *B1*-subtype *CDKs* reveal function in lateral development in *Arabidopsis*.

A. Quantification of emerged lateral root density (ELR) (cm^{-1}) in 12-day-old *Arabidopsis* wild-type, *cdkb1;1* and *cdkb1;1cdkb1;2* (*cdkb1;1-1;2*) mutant seedlings. Chart represents mean value ± standard error. ELR was compared between wild-type and *cdkb1;1* and *cdkb1;1-1;2* using one-way ANOVA. n.s. indicates not significant with an α=0,05. * indicates p-values smaller than 0,05 *** indicates p-values smaller than 0,001. n indicates the number of seedlings analysed.
B. Quantification of average primary root length (cm) of the same seedlings as in A. No significant differences were found between mutants and wild type.
C. Representative images of 12-day-old *Arabidopsis* wild-type, *cdkb1;1*, *cdkb1;1-1;2* and *cdka;1* mutant seedlings. Scale bar: 1 cm.
D. *cdka;1* mutant seedlings from C represented at higher magnification and indicated with roman numerals. Scale bar: 0,5 cm.
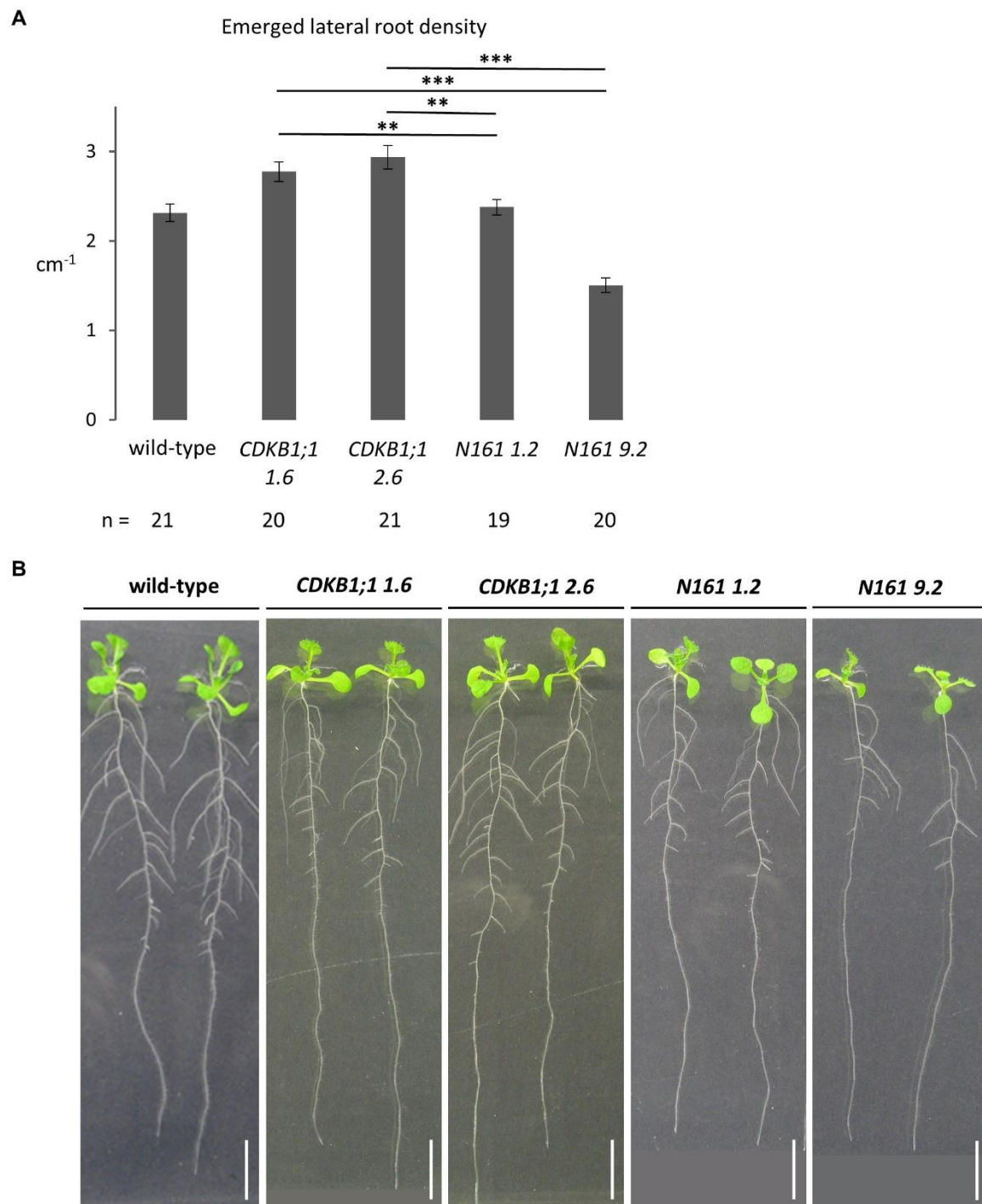
A

B

Figure 3. Dominant-negative mutant of *CDKB1;1* affects lateral root development in *Arabidopsis*.

A. Quantification of emerged lateral root density (ELR) (cm^{-1}) in 12-day-old *Arabidopsis* seedlings. Wild-type, two independent lines 1.6 and 2.6 overexpressing wild-type *CDKB1;1 p35S::CDKB1;1 D161* and two independent lines 1.2 and 9.2 overexpressing dominant-negative *CDKB1;1 p35S::CDKB1;1 N161* were analysed (Boudolf et al., 2004). Chart represents mean value ± standard error. ELR was compared between control line 1.6 and mutant lines 1.2 or 9.2 and between control line 2.6 and mutant lines 1.2 or 9.2 using a two-

sided Student's *t*-test. n.s. indicates not significant with an α=0,05. ** indicates p-values smaller than 0,01 *** indicates p-values smaller than 0,001. n indicates the number of seedlings analysed.

B. Representative images of 12-day-old *Arabidopsis* wild-type, transgenic lines 1.6 and 2.6 of *p35S::CDKB1;1 D161* and lines 1.2 or 9.2 of *p35S::CDKB1;1 N161*. Scale bar: 1 cm.

Functional analysis of CDKA;1 and potential redundancy with other CDK members at the onset of lateral root initiation has been limited because loss-of-function of CDKA;1 severely affects development (Nowack et al., 2012). The clustered regularly interspaced short palindromic repeats (CRISPR)-based tissue-specific knockout system (CRISPR-TSKO) was devised enabling the specific generation of somatic mutations in particular *Arabidopsis* cell types, tissues, and organs to overcome this limitation. We reasoned that by using tissue-specific, somatic promoters to drive Cas9 expression, CRISPR could be used to generate cell type-, tissue-, and organ-specific DNA mutations in plants (Decaestecker et al., 2019).

To facilitate the construction of CRISPR-TSKO reagents, a modular vector-cloning scheme based on the GreenGate system was developed (Figure 4A) (Lampropoulos et al., 2013). The modularity allows for the combination of Cas9, or any nuclease, with virtually any promoter sequence of choice. Furthermore, it is possible to produce Cas9 fusion proteins on the N- and C-termini, allowing for the use of a wide range of CRISPR technologies. The promoter, Cas9, N- and C-tags, and terminator modules can be combined with an "unarmed" gRNA cassette to generate an unarmed destination vector (Figure 4A).

The potential of CRISPR-TSKO was tested for generating mutant lateral roots in otherwise wild-type plants. To this end, we made use of the previously published promoter sequence of *GATA23,* a gene that marks the onset of lateral root organogenesis and is expressed in pericycle cells primed to become involved in lateral root formation in *Arabidopsis* (De Rybel et al., 2010). *GATA23* expression is transient and disappears prior to the emergence of the primordium from the primary root, except for some remaining expression at the base of the primordium (Figure 4B) (De Rybel et al., 2010).

The CRISPR system with a guideRNA targeting *GFP* and the promoter of *GATA23* driving expression of Cas9 translationally fused to mCherry (termed *pGATA23:*Cas9-mCherry;GFP-1) was transformed into a homozygous *Arabidopsis* line with ubiquitous expression of a nuclear-localized GFP and β-glucuronidase (GUS) fusion protein (*pHTR5:NLS-GFP-GUS*) (Ingouff et al., 2017). Transgenic seeds were selected based on the observation of a fluorescent seed coat. When targeting *GFP* with *pGATA23:*Cas9-mCherry;GFP-1, 20 out of 23 mCherry-positive T1 seedlings showed a complete or partial loss of GFP fluorescence in lateral roots while maintaining normal GFP expression in the primary root (Figure 4B; Figure 4C; Figure 4D). By contrast, lines with undetectable mCherry expression showed chimeric or normal GFP expression in lateral roots (Figure 4D).

Sequence analysis of lateral roots from six independent knockout events confirmed that >93% of the alleles were mutated in those organs (Figure S3A). Tracking of Indels by Decomposition (TIDE) analysis revealed that the mutation spectrum is predominantly a 1-basepair insertion (Figure S3A) (Brinkman et al., 2014). Taken together, specific expression of Cas9 in lateral root founder cells using the *GATA23* promoter results in entirely mutated lateral roots. CRISPR-TSKO enables to study the function genes in a lateral root development-specific context.

A

B

control   *pGATA23*:Cas9-mCherry;GFP-1

GFP

merged

C

control   *pGATA23*:Cas9-mCherry;GFP-1

Primary root   Primary root

D

	GFP signal in lateral roots		
mCherry	No	Chimeric	Normal
Positive	15	5	3
Negative	0	3	27
Total seedlings	15	8	30

101

Figure 4. CRISPR-TSKO in lateral root founder cells enables lateral root-specific loss-of-function.

A. Six entry modules are combined in a binary destination vector, containing a FAST screenable marker cassette, via Golden Gate assembly. The six entry modules contain a tissue-specific promoter, a cloning linker, the Cas9 nuclease, a fluorescent tag, a terminator and a module containing an *AtU6-26* promoter driving the expression of an unarmed gRNA scaffold. These modules replace the *ccd*B and *Cm*R selectable markers, allowing for the negative selection of the destination vector in *ccd*B-sensitive *E. coli* cells. The resulting vector can be directly 'armed' with one or two gRNAs, upon pre-digestion with AarI. Alternatively, the AarI restriction sites can be replaced by a PCR product containing two BsaI sites flanking *ccd*B and *Cm*R expression cassettes. In a single Golden Gate reaction, a pair of annealed oligonucleotides are cloned, resulting in an expression vector containing one gRNA. Alternatively, Golden Gate cloning of a PCR product containing a first gRNA attached to an *AtU6-26* promoter and the protospacer sequence of the second gRNA results in an expression vector containing two gRNAs.

B. Confocal images of lateral root primordia with nuclear marker *pHTR5:NLS-GFP-GUS* in 12-day-old *Arabidopsis* seedlings harbouring the CRISPR system *pGATA23*:Cas9-mCherry;GFP-1 or no CRISPR system as control. GFP in green, mCherry in magenta, and cell wall stained with calcofluor white displayed in cyan. White dashed line indicates morphology of the lateral root primordium. Scale bar: 100 μm.

C. Overlay of root morphology and nuclear marker *pHTR5:NLS-GFP-GUS* is shown for a representative control seedling and a T2 *pGATA23*:Cas9-mCherry;GFP-1 seedling. Arrowheads indicate GFP-negative lateral roots. Insets are the tip of primary roots. Scale bars: 1 mm for overview and 100 μm for inset.

D. GFP phenotype in lateral roots with nuclear marker *pHTR5:NLS-GFP-GUS* in 12-day-old *Arabidopsis* seedlings harbouring the CRISPR system *pGATA23*:Cas9-mCherry;GFP-1.

Lateral root-specific loss-of-function of *CDKA;1*, *CDKB1;1* and *CDKB1;2* inhibits progression of lateral root development

To determine the function of *CDKA;1* during lateral root initiation, lateral root-specific genome editing via the CRISPR-based tissue-specific knockout system (CRISPR-TSKO) was performed. Specific expression of Cas9 in lateral root founder cells using the *GATA23* promoter results in entirely mutated lateral roots. Transgenic lines harbouring the CRISPR system with a guideRNA targeting *CDKA;1* and the promoter of *GATA23* driving Cas9 expression specifically knockout *CDKA;1* during lateral root initiation. Emerged lateral root density of two independent T2 lines 1 and 2 targeting *CDKA;1* (termed *CDKA;1* line 1+ and line 2+) and their null-segregant siblings (*CDKA;1* line 1- and line 2-) was quantified (Figure 5A). Null-segregant siblings are segregants from T2 lines that do no longer contain the CRISPR system and were selected based on absence of a fluorescent seed coat.

Lateral root development was not severely affected. No significant difference in lateral root density was observed in lateral root-specific *cdka;1* mutant T2 seedlings compared to their null-segregant siblings (Figure 5A; Figure 5B). However, quantification of the average lateral root length revealed significantly shorter lateral roots in lateral root-specific *cdka;1* mutant T2 seedlings (Figure 6A). These observations suggest that other CDK homologs might compensate for the lack of CDKA;1 activity and we hypothesized that *B1*-subtype *CDKs* are likely candidates.

In a next step, we analysed transgenic lines harbouring the CRISPR system with guideRNAs targeting *CDKA;1*, *CDKB1;1* and *CDKB1;2* and the promoter of *GATA23* driving Cas9 expression to assess the redundant function of A – and B1-subtype CDK kinases during lateral root development. Macroscopically, the transgenic lines exhibited an apparent lack of lateral roots (Figure 5B). However, upon closer inspection, we observed that lateral roots did develop (Figure 5C; Figure 6C). Emerged lateral root density of two independent T2 lines 5 and 6 (termed *CDKA;1*, *CDKB1;1*, *CDKB1;2* line 5+ and line 6+) and their null-segregant siblings (*CDKA;1*, *CDKB1;1*, *CDKB1;2* line 5- and line 6-) was quantified (Figure 5A). The lateral root density was significantly decreased in lateral root-specific *cdka;1cdkb1;1cdkb1;2* mutant T2 seedlings compared to wild-type (Figure 5A; Figure 5B). Moreover, quantification of the average lateral root length revealed significantly shorter lateral roots in mutant T2 seedlings with an average of 0,1 cm compared to 0,63 cm in wild-type seedlings (Figure 6A), while the average primary root length was unaffected (Figure 6B).

These observations demonstrate that upon lateral root-specific loss-of-function of *CDKA;1*, *CDKB1;1* and *CDKB1;2* lateral roots develop and halt growth soon after emergence with only a small fraction of lateral roots that arrest before emergence (Figure 5C; Figure 6A; Figure 6C). These severely stunted lateral roots display the characteristic reduced number of cells and the presence of grossly enlarged epidermal and cortex cells in mutants severely affected in cell cycle progression (Nowack et al., 2012). Interestingly, the overall morphology of the few mutant lateral roots that develop is similar to wild-type lateral roots (Figure 5C; Figure 6C). Taken together, *de novo* generation of mutations concomitantly in *CDKA;1*, *CDKB1;1* and *CDKB1;2* during lateral root initiation inhibits progression of lateral root organogenesis.
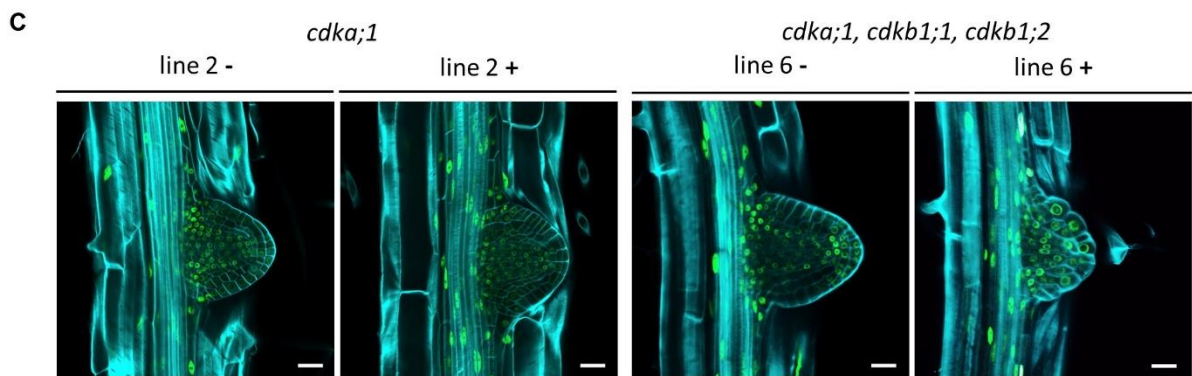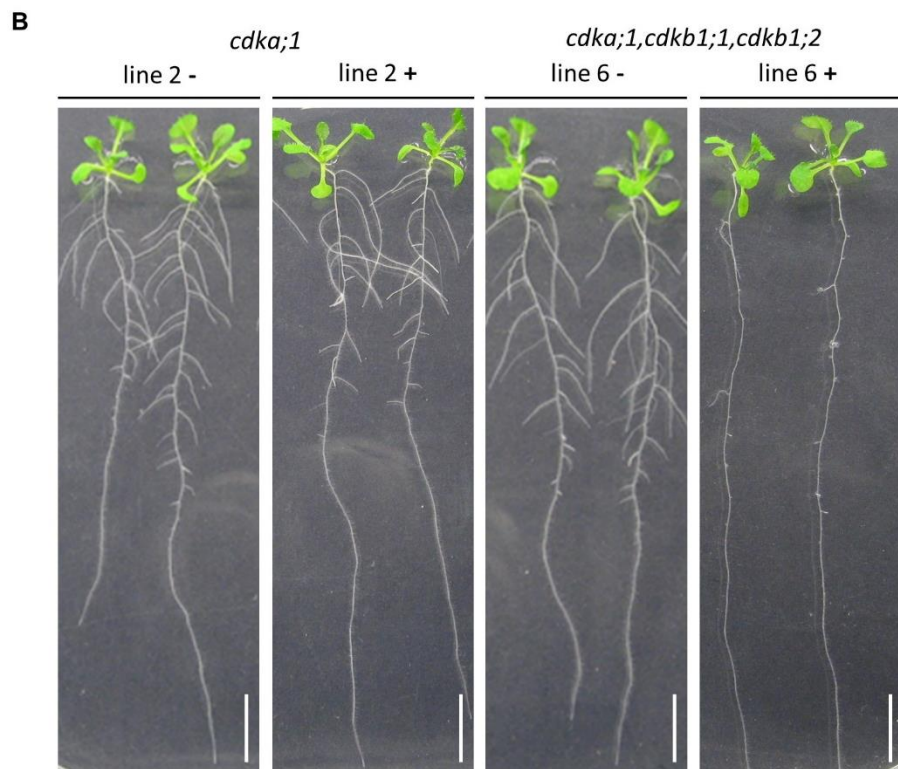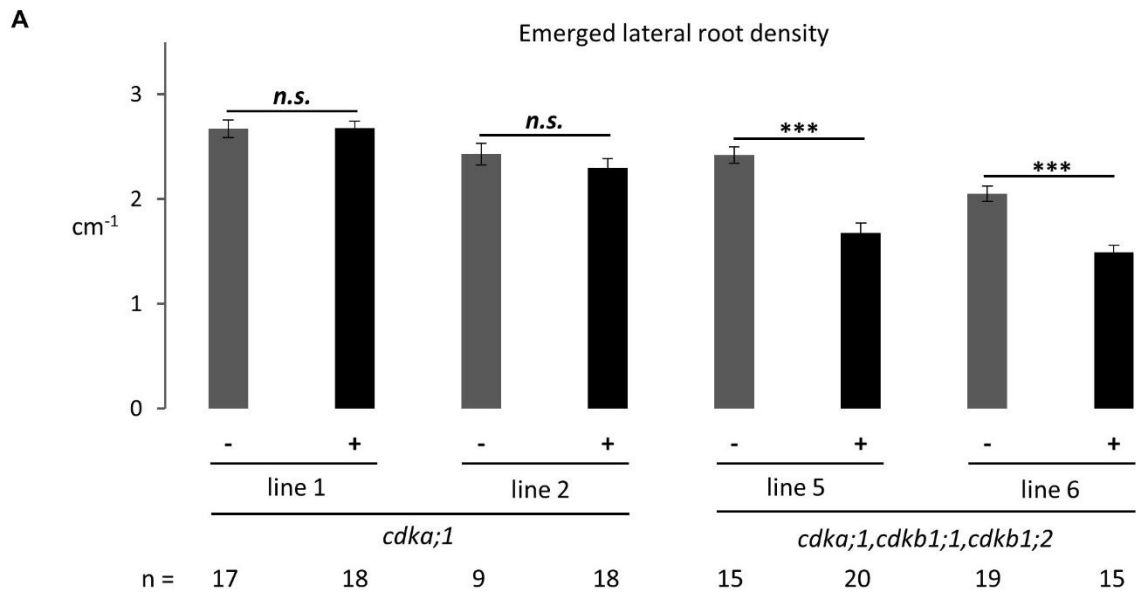
A

Emerged lateral root density

	cm^{-1}						
	n.s.		*n.s.*		***		***

	-	+	-	+	-	+	-	+
	line 1		line 2		line 5		line 6	
	cdka;1				*cdka;1,cdkb1;1,cdkb1;2*			
n =	17	18	9	18	15	20	19	15

B

cdka;1		*cdka;1,cdkb1;1,cdkb1;2*	
line 2 -	line 2 +	line 6 -	line 6 +

C

cdka;1		*cdka;1, cdkb1;1, cdkb1;2*	
line 2 -	line 2 +	line 6 -	line 6 +

Figure 5. Lateral root-specific loss-of-function of *A*- and *B1*-subtype *CDKs* affects lateral root development.

A. Quantification of emerged lateral root density (ELR) (cm^{-1}) in 12-day-old *Arabidopsis* wild-type and lateral root-specific *cyclin-dependent kinase* (*cdk*) mutant seedlings.
Two independent lines 1 and 2 targeting *CDKA;1* (*pGATA23::Cas9-mCherry;CDKA;1*) and two independent lines 5 and 6 targeting *CDKA;1*, *CDKB1;1* and *CDKB1;2* simultaneously (*pGATA23::Cas9-mCherry; CDKA;1, CDKB1;1 ,CDKB1;2*) were analysed. Chart represents mean value ± standard error. ELR was compared between the lateral root-specific *cdk* mutant (+) and corresponding null-segregant sibling (-) using a two-sided Student's *t*-test. n.s. indicates not significant with an α=0,05. *** indicates p-values smaller than 0,001. n indicates the number of seedlings analysed.
B. Representative images of 12-day-old *Arabidopsis* lateral root-specific *cdk* mutant (+) and corresponding null-segregant sibling (-) seedlings. Scale bar: 1 cm.
C. Confocal images of an emerged lateral root with nuclear marker *pHTR5:NLS-GFP-GUS* in 12-day-old *Arabidopsis* lateral root-specific *cdk* mutant (+) and corresponding null-segregant sibling (-) seedlings. *NLS-GFP-GUS* is displayed in green. Cell wall was stained with calcofluor white and is displayed in cyan. Scale bar: 20 μm.
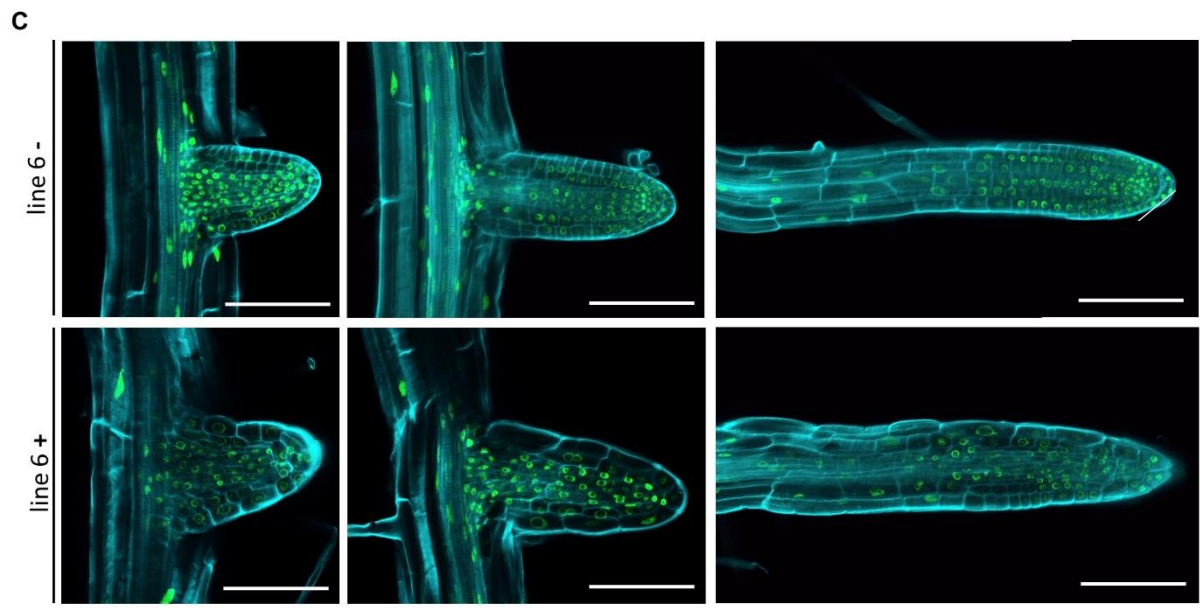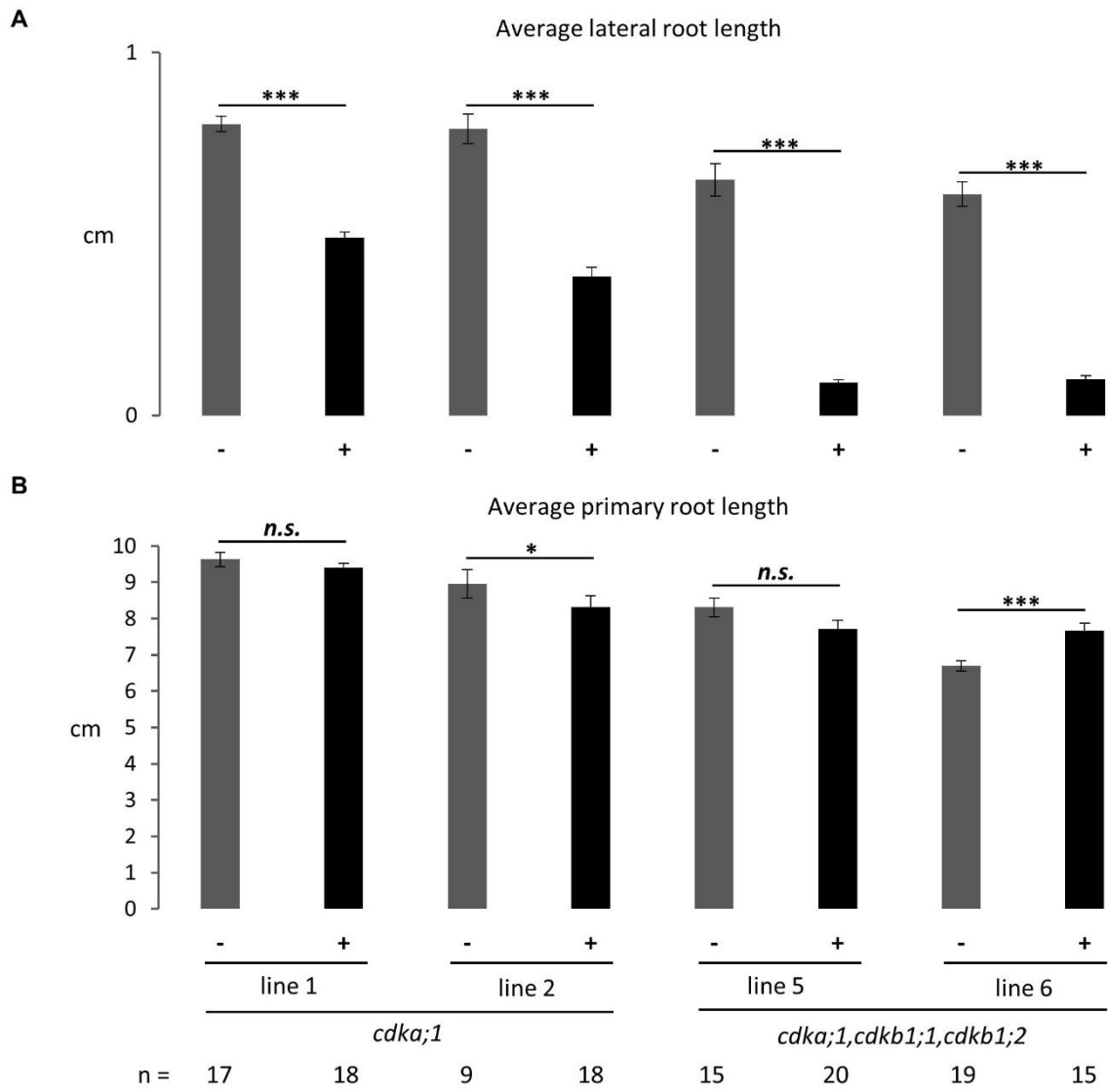
A

Average lateral root length

cm

B

Average primary root length

cm

	line 1		line 2		line 5		line 6	
	-	+	-	+	-	+	-	+
	cdka;1				*cdka;1,cdkb1;1,cdkb1;2*			
n =	17	18	9	18	15	20	19	15

C

line 6 -

line 6 +

Figure 6. Lateral root-specific loss-of-function of *A*- and *B1*-subtype *CDKs* inhibits progression of lateral root organogenesis.

A. Quantification of average lateral root length (cm) of the same seedlings as in Figure 5A: 12-day-old *Arabidopsis* wild-type and lateral root-specific *cyclin-dependent kinase* (*cdk*) mutant seedlings. Two independent lines 1 and 2 targeting *CDKA;1* (*pGATA23::Cas9-mCherry;CDKA;1*) and two independent lines 5 and 6 targeting *CDKA;1*, *CDKB1;1* and *CDKB1;2* simultaneously (*pGATA23::Cas9-mCherry; CDKA;1, CDKB1;1 ,CDKB1;2*) were analysed. ELR was compared between the lateral root-specific *cdk* mutant (+) and corresponding null-segregant sibling (-) using a two-sided Student's *t*-test. n.s. indicates not significant with an α=0,05. * indicates p-values smaller than 0,05. *** indicates p-values smaller than 0,001. n indicates the number of seedlings analysed.

B. Quantification of average primary root length (cm) of the same seedlings as in A and Figure 5A.

C. Confocal images of emerged lateral roots with nuclear marker *pHTR5:NLS-GFP-GUS* in 12-day-old *Arabidopsis* lateral root-specific *cdk* mutant (line 6 +) and corresponding null-segregant sibling (line 6 -) seedlings. *NLS-GFP-GUS* is displayed in green. Cell wall was stained with calcofluor white and is displayed in cyan. Scale bar: 0,1 mm.

Lateral root primordia (LRP) form through a highly ordered series of divisions that generates a structure with a radial organization similar to that of the mature root tip (Malamy & Benfey, 1997). We investigated whether lateral root-specific loss-of-function of *CDKA;1*, *CDKB1;1* and *CDKB1;2* affects the initial divisions at the onset of lateral root initiation and subsequent formation of an LRP. Microscopic analysis was performed on roots of lateral root-specific *cdka;1cdkb1;1cdkb1;2* mutant T2 seedlings and their null-segregant siblings and series of discrete developmental stages in LRP development could be observed (Figure 7A). Remarkably, distinct early and late LRP stages in the lateral root-specific *cdka;1cdkb1;1cdkb1;2* mutant were morphologically indistinguishable from wild-type and aberrant LRP consisting of fewer and larger cells were only rarely present (Figure 7A). These observations pinpoint that the defect during lateral root development primarily occurs after emergence.

To gain insights in the molecular lateral root regulatory framework upon lateral root-specific loss-of-function of *CDKA;1*, *CDKB1;1* and *CDKB1;2*, we quantified the expression of genes related to lateral root initiation in the lateral root-specific *cdka;1cdkb1;1cdkb1;2* mutant (Figure 7B) (De Rybel et al., 2010; De Smet et al., 2008; Fernandez et al., 2020; Hirota et al., 2007; Okushima et al., 2007). Relative expression levels of the selected lateral root regulatory genes were unaltered in the lateral root-specific *cdka;1cdkb1;1cdkb1;2* mutant compared to wild-type (Figure 7B). Only the expression of *ARABIDOPSIS CRINKLY 4* (*ACR4*) is significantly decreased in the mutant. In a next step, we quantified the expression of genes that are essential for LRP patterning and *de novo* meristem establishment (Figure 7C) (Du & Scheres, 2017). Relative expression levels of *WOX5* and *PLETHORA* (*PLT*) *1,3,5,7* were unaltered, while *PLT2* expression was slightly decreased in the lateral root-specific *cdka;1cdkb1;1cdkb1;2* mutant compared to wild-type (Figure 7C). In essence, essential gene expression programs for lateral root development are not affected upon lateral root-specific loss-of-function of *CDKA;1*, *CDKB1;1* and *CDKB1;2*.

Colchicine has been used to investigate the extent to which morphogenesis and growth can occur without completion of cell divisions in the early stages of organ development (Foard et al., 1965). It was shown that colchicine prevents completion of mitosis and cytokinesis, however *Triticum vulgare* L. roots can still initiate short lateral branches called primordiomorphs, which are entirely the result of cell expansion (Foard et al., 1965). To mimic in a complementary approach the lateral root defect present in the lateral root-specific *cdka;1cdkb1;1cdkb1;2* mutant, *Arabidopsis* seeds were germinated on solid growth medium supplemented with 0,03% colchicine in accordance with the protocol described in Foard, Haber, & Fishman. However, colchicine treatment arrested postembryonic root development after germination (data not shown) so alternatively 5-day old *Arabidopsis* seedlings were treated with 0,03% colchicine for 3 days in liquid culture. Analysis of progressing stages of LRP and lateral roots as well as the primary root tip revealed that colchicine steers root development to differentiation (Figure S4B; Figure S4C). Hence, colchicine treatment cannot mimic the lateral root defect observed in the lateral root-specific *cdka;1cdkb1;1cdkb1;2* mutant (Figure S4A).
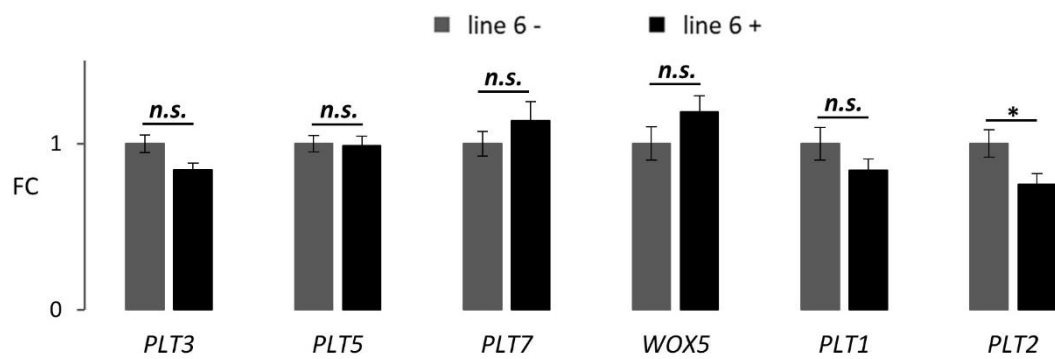
A
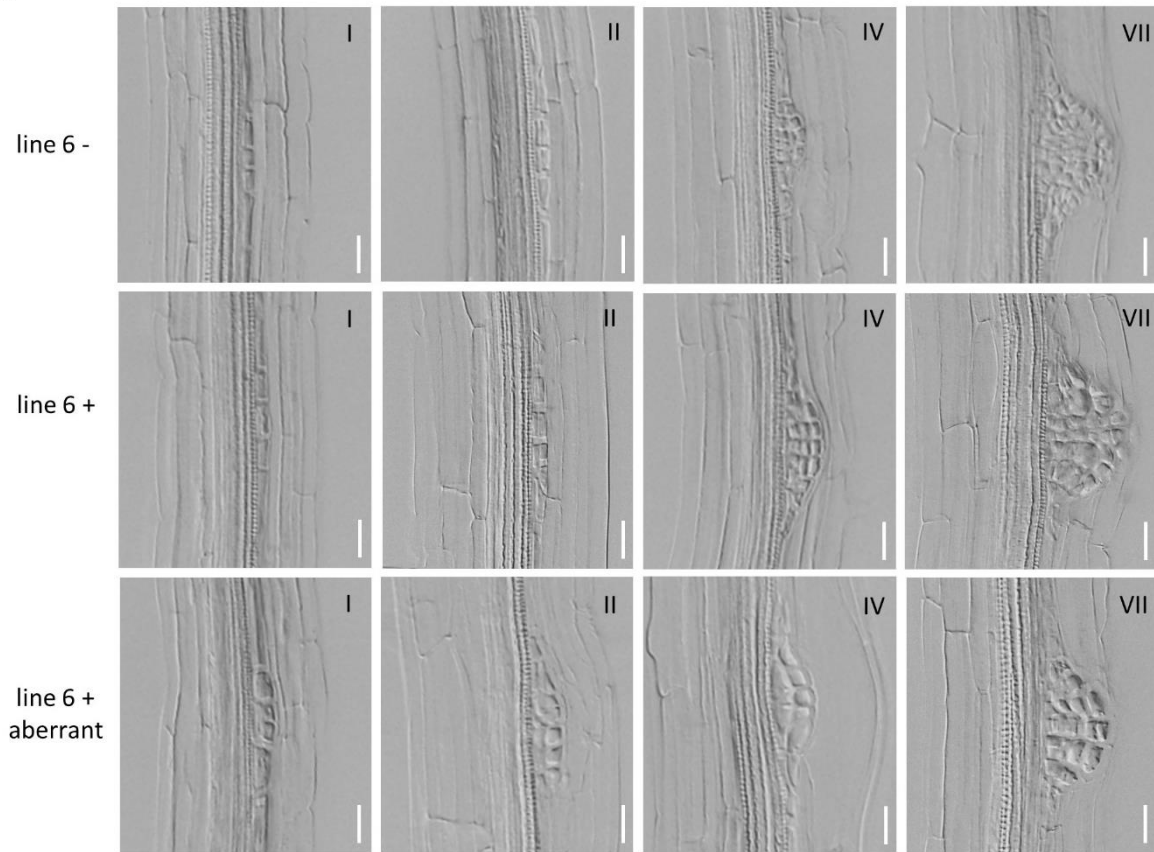
B
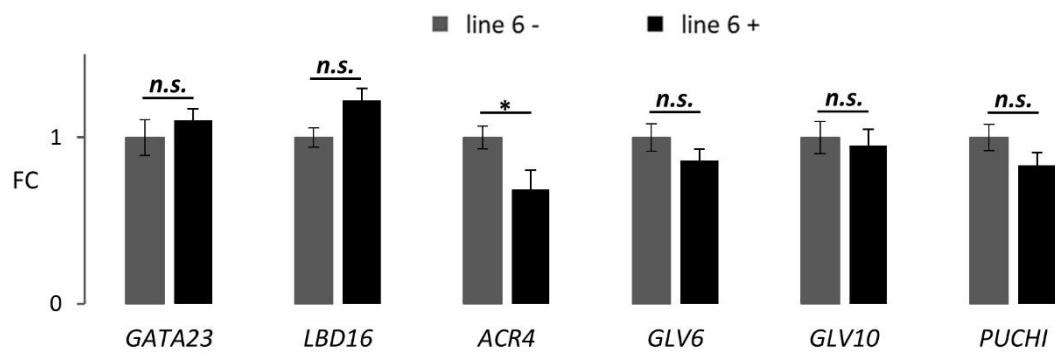
C

Figure 7. Lateral root-specific loss-of-function of *A*- and *B1*-subtype *CDKs* causes lateral root defect soon after emergence.

A. Images of representative lateral root primordium stages of 6-day-old *Arabidopsis* lateral root-specific *cdka;1cdkb1;1cdkb1;2* mutant (line 6 +) and corresponding null-segregant sibling (line 6 -) seedlings. Roman numerals indicate lateral root primordium stages as described in Malamy & Benfey, 1997. Scale bar: 20 µm.

B. Transcript fold changes (FC) of genes related to lateral root initiation in 5-day-old *Arabidopsis* roots of lateral root-specific *cdka;1cdkb1;1cdkb1;2* mutant (line 6 +) and corresponding null-segregant sibling (line 6 -) seedlings. The analysed genes are: *GATA23* (*AT5G26930*); *LBD16* (*AT2G42430*); *ACR4* (*AT1G69040*); *GLV6* (*AT2G03830*); *GLV10* (*AT5G51451*) and *PUCHI* (*AT5G18560*). Transcript fold changes were detected by quantitative real-time PCR. Chart represents mean values ± standard error of three independent replicates. FC was compared between lateral root-specific *cdka;1cdkb1;1cdkb1;2* mutant (line 6 +) and corresponding null-segregant sibling (line 6 -) roots using a two-sided Student's *t*-test. * indicates p-values smaller than 0,05. n.s. indicates not significant with an α=0,05.

C. Transcript fold changes (FC) of genes related to lateral root primordia patterning in 5-day-old *Arabidopsis* roots of lateral root-specific *cdka;1cdkb1;1cdkb1;2* mutant (line 6 +) and corresponding null-segregant sibling (line 6 -) seedlings. The analysed genes are: *PLT3* (*AT5G10510*); *PLT5* (*AT5G57390*); *PLT7* (*AT5G65510*); *WOX5* (*AT3G11260*); *PLT1* (*AT3G20840*) and *PLT2* (*AT1G51190*).
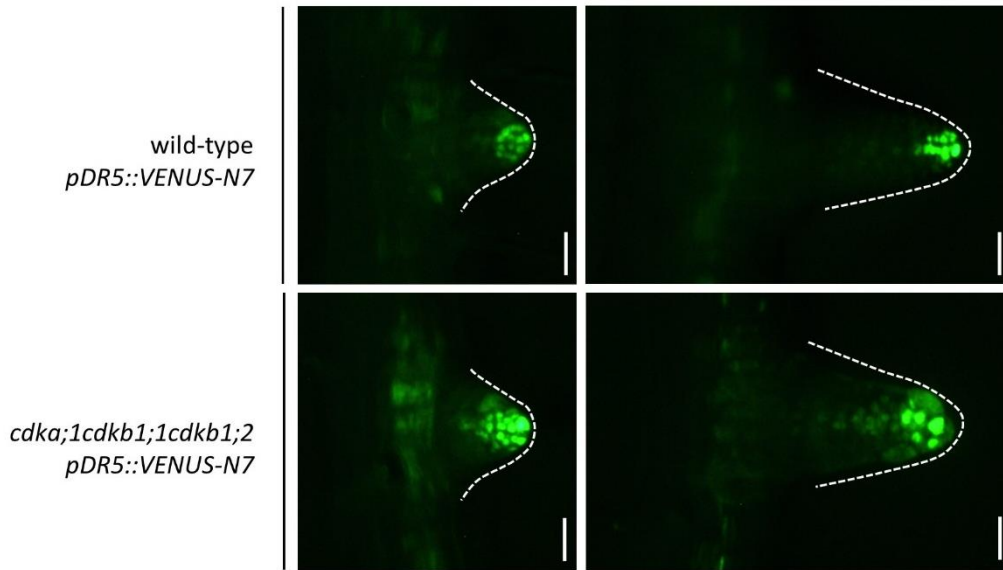
Auxin represents a key regulator of lateral root development (Lavenus et al., 2013). Polar auxin transport is used by plants to mobilize auxin from an auxin source in the shoot to basal sink organs including lateral roots (Casimiro et al., 2001). The transition of lateral root founder cells from G1 to S is stimulated by auxin and an auxin gradient is gradually established at later stages with its maximum at the LRP tip (Benková et al., 2003; Dubrovsky et al., 2008). The lateral root-specific CRISPR system with guideRNAs targeting *CDKA;1*, *CDKB1;1* and *CDKB1;2* was transformed in the reporter line *pDR5::VENUS-N7* to analyse the auxin response upon lateral root-specific loss-of-function of *CDKA;1*, *CDKB1;1* and *CDKB1;2* (Heisler et al., 2005). *DR5* activity was detected in lateral root-specific *cdka;1cdkb1;1cdkb1;2* mutant lateral roots and a similar expression pattern could be observed as in the null-segregant sibling (Figure 8A). Moreover, the *DR5* expression pattern in the primary root tip was unaltered (Figure 8D). This indicates that the auxin response in lateral root-specific *cdka;1cdkb1;1cdkb1;2* mutant roots resembles the response in wild-type.
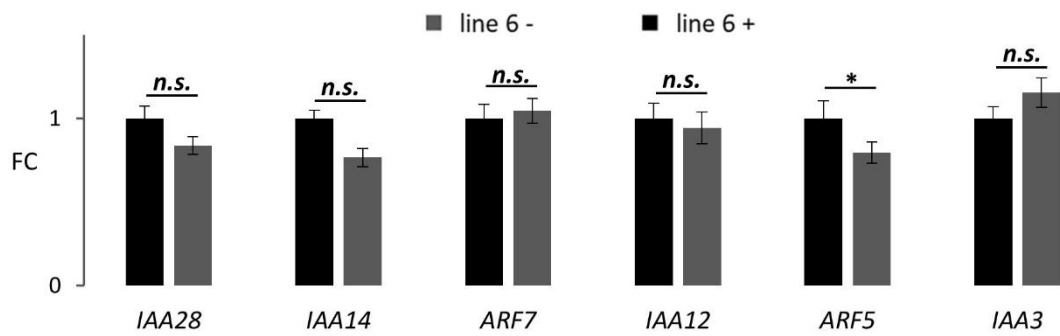
Different auxin signalling modules that consist of AUX/IAA and ARF factors act sequentially to control the various steps of lateral root formation (Lavenus et al., 2013). The *SOLITARY-ROOT* (*SLR*)/*IAA14–ARF7–ARF19* and *BODENLOS* (*BDL*)/*IAA12–MONOPTEROS* (MP)/*ARF5* module act during lateral root initiation, while the *SHORT HYPOCOTYL2* (*SHY2*)/*IAA3–ARF7* is necessary for lateral root emergence. To investigate the molecular auxin regulatory framework, we quantified expression of *IAA* and *ARF* genes in the lateral root-specific *cdka;1cdkb1;1cdkb1;2* mutant (Figure 8B). Relative expression levels of selected *IAA* and *ARF* genes were unaltered in the lateral root-specific *cdka;1cdkb1;1cdkb1;2* mutant compared to wild-type (Figure 8B). Only the expression of *ARF5* is significantly decreased in the mutant. This suggests that auxin signalling components essential for lateral root development are primarily unaffected upon lateral root-specific loss-of-function of *CDKA;1*, *CDKB1;1* and *CDKB1;2*.

Finally, it has been reported that lateral root initiation is blocked at the G1 to S transition in the dominant-negative *slr-1* mutant and the *arf7arf19* double mutant phenocopies *slr-1* (Fukaki et al., 2002; Okushima et al., 2005; Vanneste et al., 2005). Surprisingly, CRISPR-TSKO of *ARF7* and *ARF19* revealed that lateral root initiation is only mildly affected upon loss-of-function of *ARF7* and *ARF19* in *GATA23*-expressing pericycle cells (Decaestecker et al., 2019). As a complementary approach, functional analysis of *ARF7* and *ARF19* during lateral root initiation was conducted by crossing transgenic line 6 harbouring the CRISPR system and guideRNAs targeting *CDKA;1*, *CDKB1;1* and *CDKB1;2* with transgenic line 1 harbouring the CRISPR system and guideRNAs targeting *ARF7* and *ARF19*. The emerged lateral root density was significantly lower upon lateral root-specific loss-of-function of *CDKA;1*, *CDKB1;1* and *CDKB1;2* compared to lateral root-specific loss-of-function of *ARF7* and *ARF19* (Figure 8C). Analysis of F1 seedlings revealed that the emerged lateral root density approximates the density observed in lateral root-specific *cdka;1cdkb1;1cdkb1;2* mutant seedlings (Figure 8C). Hence, simultaneous lateral root-specific knockouts of *CDKA;1*, *CDKB1;1* & *CDKB1;2* and *ARF7* & *ARF19* does not synergistically affect lateral root development.

A

wild-type
pDR5::VENUS-N7

cdka;1cdkb1;1cdkb1;2
pDR5::VENUS-N7

B

■ line 6 -   ■ line 6 +

FC

n.s. *n.s.* *n.s.* *n.s.* * *n.s.*

IAA28 *IAA14* *ARF7* *IAA12* *ARF5* *IAA3*

C

wild-type
pDR5::VENUS-N7

cdka;1cdkb1;1cdkb1;2
pDR5::VENUS-N7

D

Emerged lateral root density

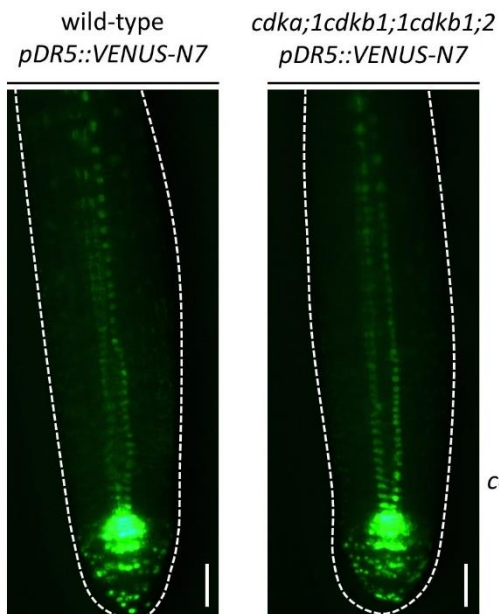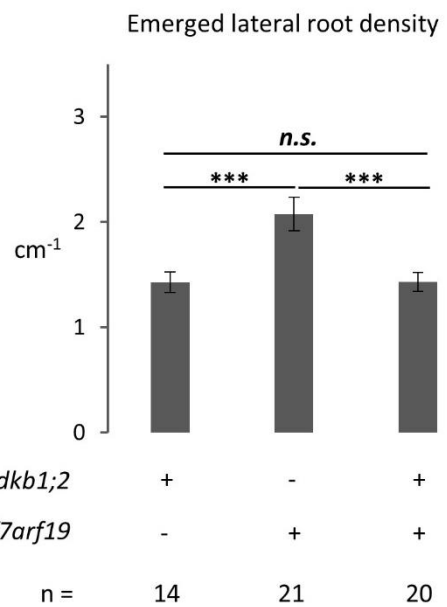|		
cdka;1cdkb1;1cdkb1;2	+	−	+
arf7arf19	−	+	+
n =	14	21	20

Figure 8. The auxin response is unaltered upon lateral root-specific loss-of-function of *CDKA;1, CDKB1;1* and *CDKB1;2.*

A. Expression pattern of *pDR5::VENUS-N7* (Heisler et al., 2005) in lateral roots of 6-day-old lateral root-specific *cdka;1cdkb1;1cdkb1;2* mutant and corresponding null-segregant sibling (wild-type) T2 seedlings. White dashed line indicates lateral root morphology. Scale bars: 20 µm.

B. Transcript fold changes (FC) of auxin signalling-related genes in 5-day-old *Arabidopsis* roots. The analysed genes are: *IAA28* (*AT5G25890*); *IAA14* (*AT4G14550*); *ARF7* (*AT5G20730*); *IAA12* (*AT1G04550*); *ARF5* (*AT1G19850*) and *IAA3* (*AT1G04240*). Transcript fold changes were detected by quantitative real-time PCR. Chart represents mean values ± standard error of three independent replicates. FC was compared between lateral root-specific *cdka;1cdkb1;1cdkb1;2* mutant (line 6 +) and corresponding null-segregant sibling (line 6 -) roots using a two-sided Student's *t*-test. * indicates p-values smaller than 0,05. n.s. indicates not significant with an α=0,05.

C. Expression pattern of *pDR5::VENUS-N7* (Heisler et al., 2005) in the primary root tip of 6-day-old lateral root-specific *cdka;1cdkb1;1cdkb1;2* mutant and corresponding null-segregant sibling (wild-type) T2 seedlings. White dashed line indicates primary root tip morphology. Scale bars: 20 µm.

D. Quantification of emerged lateral root density (ELR) (cm^{-1}) in 12-day-old *Arabidopsis* lateral root-specific *cdka;1cdkb1;1cdkb1;2* mutant, lateral root-specific *arf7arf19* mutant and F1 of lateral root-specific *cdka;1cdkb1;1cdkb1;2* and lateral root-specific *arf7arf19* mutant seedlings (Decaestecker et al., 2019). Chart represents mean value ± standard error. ELR was compared between the lateral root-specific mutants using one-way ANOVA. n.s. indicates not significant with an α=0,05. *** indicates p-values smaller than 0,001. n indicates the number of seedlings analysed.

Discussion

Plants have evolved sophisticated adaptive mechanisms that regulate how they pattern their root branching to explore heterogeneous soil environments. Root branching in *Arabidopsis* happens through the formation of new meristems out of a subset of pericycle cells inside the parent root also referred to as founder cells that enable the organogenesis of lateral roots. Regulation of cell cycle activity at the onset of lateral root initiation is essential for founder cells to undergo formative divisions (Beeckman et al., 2001; Himanen et al., 2002b; Vanneste et al., 2005). Loss-of-function of *CDKA;1* severely affects development (Nowack et al., 2012), and a better understanding of the function of CDKA;1 and potential redundancy with other CDK members in formative divisions during lateral root development has remained out of reach. Our study investigates the function of CDKA;1, and close homolog B1-type CDK kinases during lateral root organogenesis.

CDKA;1 is ubiquitously expressed, while *CDKB1;1* expression is confined to the stele and stage I LRP. The distinct expression pattern of *CDKB1;1* in the primary root corresponds with its reported specific expression in mitotic cells, from the S-phase into the G2 to M transition (Menges et al., 2005). Such cell-cycle-regulated expression is conventionally associated with the cyclin subunit of CDK rather than CDKs, and is a unique feature of the plant-specific CDKB class of CDKs (Scofield et al., 2014). In contrast, no *pCDKB1;2::GUS* activity of its close homolog *CDKB1;2* could be observed in roots, consistent with the reported absence of *CDKB1;2* expression in the epidermis compared with *CDKB1;1* (Xie et al., 2010) and with the reported lower abundance of *CDKB1;2* transcripts compared with *CDKB1;1* in synchronized *Arabidopsis* cell suspension cultures (Menges et al., 2005; Menges & Murray, 2002). Alternatively, transcription of *CDKB1;2* was detected in RNA-Seq experiments performed in primary root segments of the young maturation zone (Chen et al., unpublished; Perez et al., unpublished), which suggests that *CDKB1;2* is expressed in roots. Follow-up experiments are required to re-evaluate the *pCDKB1;2::GUS* line and determine the expression pattern of *CDKB1;2*.

In a next step, we analysed the function of *CDKB1;1* and *CDKB1;2* in lateral root development. Only *cdkb1;1-1;2* double mutant seedlings display a lateral root defect, while primary root growth is unaltered. It was observed that the lateral roots in *cdkb1;1-1;2* double mutant seedlings are shorter compared to wild-type. Quantification of the average lateral root length will be necessary to support this hypothesis. Furthermore, overexpressing the N161 dominant-negative kinase version of *CDKB1;1* (Boudolf et al., 2004) results in a similar lateral root phenotype, which revealed that *CDKB1;1* and *CDKB1;2* act concomitantly in lateral root development. This redundancy is in line with the reported function of *B1*-type *CDKs* in guard mother cell cytokinesis in stomatal development (Boudolf et al., 2004; Xie et al., 2010) and of CDKB1 and CDKA;1 kinases in embryo- and gametophyte formation (Nowack et al., 2012).

We further were able to carry out loss-of-function analysis of CDKA;1 and CDKB1 kinases during lateral root formation using lateral root-specific CRISPR mutagenesis (CRISPR-TSKO). Surprisingly, *de novo* generation of mutations in *CDKA;1* at the onset of lateral root initiation does not affect lateral root branching. This is a striking observation, considering the central function of *CDKA;1* in the progression of the cell cycle. However, simultaneous knockout of *CDKA;1*, *CDKB1;1* and *CDKB1;2* halts lateral root growth soon after emergence with only a small number of lateral roots that arrest before emergence. These severely stunted lateral

roots consist of a reduced number of extremely enlarged cells as a result of inadequate cell divisions and is reminiscent of mutants affected in cell cycle progression (Nowack et al., 2012). Quantification of the cell number -and size of lateral roots will contribute to pinpoint in which cells and tissues defects occur upon lateral root-specific loss-of-function of CDKA;1 and CDKB1 kinases.

Interestingly, the morphology and patterning of distinct LRP stages in the lateral root-specific *cdka;1cdkb1;1cdkb1;2* mutant is similar to wild-type and aberrant LRP consisting of fewer and larger cells are rarely present. Moreover, essential gene expression programs for lateral root initiation and patterning are maintained in lateral root-specific *cdka;1cdkb1;1cdkb1;2* mutant roots. In a next step, analysis of cell-type specific reporter lines in the mutant background will be required to establish the expression pattern at cellular resolution. Taken together, we were able to pinpoint that loss-of-function of *CDKA;1*, *CDKB1;1* and *CDKB1;2* results in a lateral root defect primarily after emergence. Interestingly, cell proliferation in the stele of these mutant lateral roots appeared to be less affected than in the epidermis and cortex.

Further research is needed to test if this is caused by the differential turnover of CDK transcript and/or proteins in distinct cell types or by the differential requirement of CDK activity in distinct tissues. As a complementary genetic approach, it will be interesting to evaluate if the lateral root defect can be phenocopied through lateral root-specific expression of *SIAMESE* which inhibits both CDKA;1- and CDKB1-containing CDK complexes (Wang et al., 2020). Alternatively, other CDK homologs might be able to partially compensate for *CDKA;1* and *CDKB1* loss-of-function in specific cell types (De Veylder et al., 2007; Joubès et al., 2000). The flexibility of the CRISPR system enables to assess the potential function of the remaining CDKs during lateral root organogenesis. CDKB2 kinases are likely candidates because they are closely related and it was observed that *CDKB2;1* is expressed during lateral root development (Engler et al., 2009).

Lateral root emergence is characterized by cell expansion of the basal cells of the LRP followed by divisions in cells at the apex of the LRP that constitute a lateral root apical meristem to drive lateral root growth (Laskowski et al., 1995; Malamy & Benfey, 1997). Hence, it is tempting to consider that activity of CDKA;1 and CDKB1 kinases is necessary to control the balance of cell division and elongation and/or to mediate the divisions once a lateral root meristem is established. It was shown that colchicine-treated *Triticum vulgare* L. roots initiate short LRP called primordiomorphs, which are entirely the result of cell expansion (Foard et al., 1965). Nevertheless, cell divisions occur in LRP and steers lateral root development towards differentiation after transfer of *Arabidopsis* seedlings to liquid culture supplemented with colchicine. Hence, colchicine treatment of *Arabidopsis* does not mimic the lateral root defect upon lateral root-specific loss-of-function of *CDKA;1*, *CDKB1;1* and *CDKB1;2* nor the primordiomorphs observed in *Triticum vulgare* L. roots.

The whole process of cell cycle progression and stimulation of the molecular pathway towards lateral root initiation is triggered by auxin (Vanneste et al., 2005). Subsequently, the establishment of a new auxin response maximum inside LRP is essential for organogenesis. Expression analysis revealed that the auxin response pattern in lateral root-specific *cdka;1cdkb1;1cdkb1;2* mutant lateral roots remains unaltered. However, a stronger intensity of *DR5* activity could be observed in the primary -and lateral root tips. This might be caused

by the progression of lateral roots is inhibited in the mutant, which are sink organs for auxin. Additional analysis of reporter lines for auxin signalling and transport in the lateral root-specific *cdka;1cdkb1;1cdkb1;2* mutant at cellular resolution will be necessary.

At the least our data revealed that morphogenesis of lateral root primordia is maintained upon deficient cell division and poses the question how the distribution of intrinsic determinants is preserved during lateral root organogenesis as it has been proposed that both coordinated cell cycle progression and cell identity specification is intertwined. Despite the absence of intact cell cycle progression, we hypothesize the presence of a "morphogenesis factor" that steers lateral root primordium development. This could be coordinated by auxin signalling and needs to be addressed in future studies to understand the role and control of coordinated cell divisions in organogenesis.

In summary, our data demonstrate that *A*- and *B1*-subtype *CDK*s are concomitantly essential for lateral root organogenesis and reveals the striking observation that morphogenesis of lateral roots still occurs upon absence of intact cell cycle progression. Through lateral root-specific knockouts of *CDKs* using CRISPR-TSKO, we provide a basis to unravel the role of CDKs in cell cycle progression during lateral root organogenesis. The developmental plasticity of plants is crucial for increasing the surface area of their root system to explore heterogeneous soil environments and cope with abiotic stresses.

Material and Methods

Plant materials

The *cdka;1* mutant (SALK_106809.34.90.x) was previously reported (Nowack et al., 2012). The mutant *cdkb1;1* (SALK_073457; N573457) and double mutant *cdkb1;1cdkb1;2* (SALK_073457 and SALK_133560; N66145) was obtained from the Nottingham Arabidopsis Stock Centre (Xie et al., 2010). The GUS reporter lines *pCDKA;1::GUS*, *pCDKB1;1::GUS* and *pCDKB1;2::GUS* as well as the dominant-negative *p35S::CDKB1;1-N161* mutant- and *p35S::CDKB1;1* control lines were gifts of Lieven De Veylder (VIB-UGent Center of Plant Systems Biology, Ghent, Belgium) (Boudolf et al., 2004). *pGATA23*-CRISPR-TSKO lines were previously reported (Decaestecker et al., 2019). CRISPR-TSKO lines contain the FASTR screenable marker so transgenic seeds were selected under a Leica M165FC fluorescence stereomicroscope.

The CRISPR-TSKO vector pFASTR-pGATA23-Cas9-P2A-mCherry-G7T-AtU6-CDKA1-1,CDKB1-1 in *Agrobacterium tumefaciens* C58C1 was transformed in the *pDR5:VENUS-N7* line (Heisler et al., 2005) via the floral-dip method (Clough & Bent, 1998). T1 transgenic seeds were selected under a Leica M165FC fluorescence stereomicroscope because the FASTR marker is present in the T-DNA vector. The lateral root-specific *cdka;1cdkb1;1cdkb1;2* mutant was confirmed in T2. All transgenic lines analysed in this study are in Col-0 background.

The F1 of lateral root-specific *cdka;1cdkb1;1cdkb1;2* and lateral root-specific *arf7arf19* mutant seedlings were obtained by crossing parental line, which are homozygous for the CRISPR-TSKO construct so as of consequence the expression cassette that drives Cas9 expression with the *GATA23* promoter is homozygous in the F1 crosses while the expression cassette that drives the gRNA expression is heterozygous.

Plant growing conditions

Arabidopsis thaliana seeds were surface sterilized, stratified for 2 days in the dark at 4°C, and grown on half-strength Murashige and Skoog (1/2 MS) medium (pH 5,7) solidified with 1% agar (Murashige & Skoog, 1962). For all phenotypic analyses, seedlings were vertically grown on square plates (Greiner Labortechnik) incubated in a growth chamber under continuous light (110 µE/m^2/s photosynthetically active radiation supplied by cool-white fluorescent tungsten tubes; Osram) at 21°C.

Histochemical and histological Analysis

GUS assays were performed as described previously. For microscopic analysis, samples were cleared by mounting in lactic acid saturated with chloralhydrate. For analysis of all LR developmental stages, 8-9 dag seedlings were collected and cleared using a modified Malamy and Benfey (Malamy & Benfey, 1997) protocol (Fernandez et al., 2020). All samples were analysed by differential interference contrast microscopy (Olympus BX51).

Quantitative real-time PCR confirmation

RNA was extracted with ReliaPrep RNA Miniprep System (Promega) from approximately 40

whole roots for each sample. First cDNA strand was synthesized using the qScript cDNA Supermix (Quantabio). Quantitative real-Time PCR was performed using SyberGreen (Roche) and LightCycler real-time thermocycler (Roche). *ACTIN 2* (*AT4G05320*) and *UBIQUITIN 10* (*AT4G05320*) were both used as reference transcripts. Analysis was conducted with in-house software only available at VIB-UGent Center for Plant Systems Biology. Primer sequences for quantification of gene expression are compiled in Supplemental Experimental Procedures. Two biological repeats were conducted and for each biological repeat, three technical repeats were performed.

Morphological characterization of roots

The number of emerged lateral roots was determined for every seedling using a binocular microscope, and root lengths were measured via ImageJ using digital images obtained by scanning the square plates. Lateral root density was calculated by dividing the emerged lateral root number by the primary root length.

In vivo root confocal imaging

Seedlings were cleared using the ClearSee protocol (Kurihara et al., 2015; Ursache et al., 2018) in combination with cell wall staining using Calcofluor White M2R (Sigma). Fluorescent images of lateral root primordia were acquired on a Leica SP8X confocal microscope. Calcofluor White was excited at 405 nm and acquired at 430 to 470 nm. GFP was excited at 488 nm and acquired at 500 to 525 nm. Fluorescent images of *VENUS-N7* signal in lateral root primordia were acquired with a Leica M165FC fluorescence stereomicroscope.

Statistical analysis

All values reported in this study are the means (± standard error) of at least two independent experiments with three replicates, unless otherwise stated. The significance of the results and statistical differences were analysed using Microsoft Excel for Office or GraphPad PRISM 8. A two-sided Student's t-test was used for comparison of two conditions/genotypes. Comparison of multiple genotypes was performed by one-way ANOVA. A p-value equal to or lower than 0,05 was considered statistically significant.

Accession numbers

The Arabidopsis Information Resource (TAIR) locus identifiers for the genes mentioned in this study are *AT5G26930* for GATA23, AT4G14550 for *SLR/IAA14*, *AT5G20730* for *ARF7*, *AT1G19220* for *ARF19*, AT3G48750 for *CDKA;1*, AT3G54180 for *CDKB1;1*, AT2G38620 for *CDKB1;2*, AT2G42430 for *LBD16*, AT1G69040 for *ACR4*, AT2G03830 for *GLV6*, AT5G51451 for *GLV10*, AT5G18560 for *PUCHI*, AT3G11260 for *WOX5*, AT3G20840 for *PLT1*, AT1G51190 for *PLT2*, AT5G10510 for *PLT3*, AT5G57390 for *PLT5*, AT5G65510 for *PLT7*, AT5G25890 for *IAA28*, *AT1G04550* for *IAA12*, *AT1G19850* for *ARF5*, *AT1G04240* for *IAA3/SHY2*, *AT4G05320* for *ACT2* and *AT4G05320* for *UBI10*.
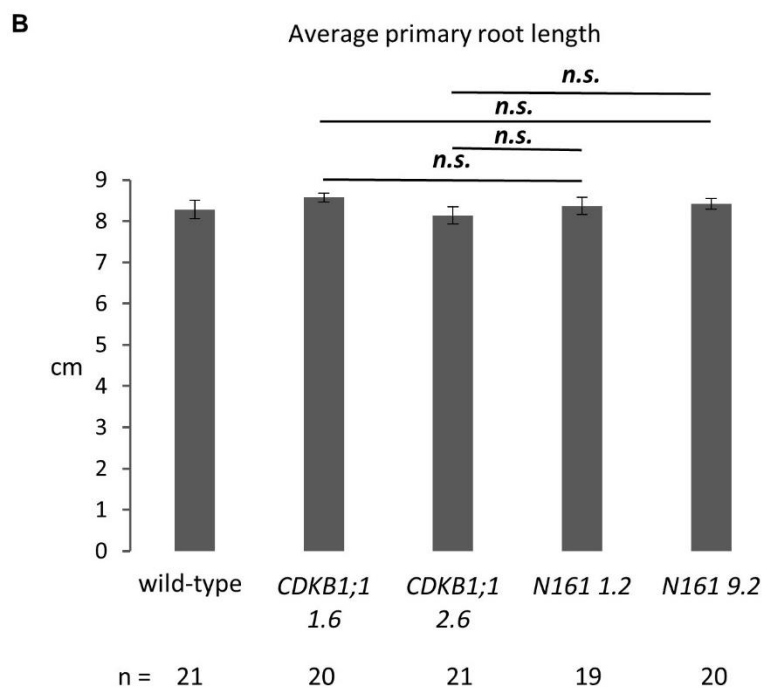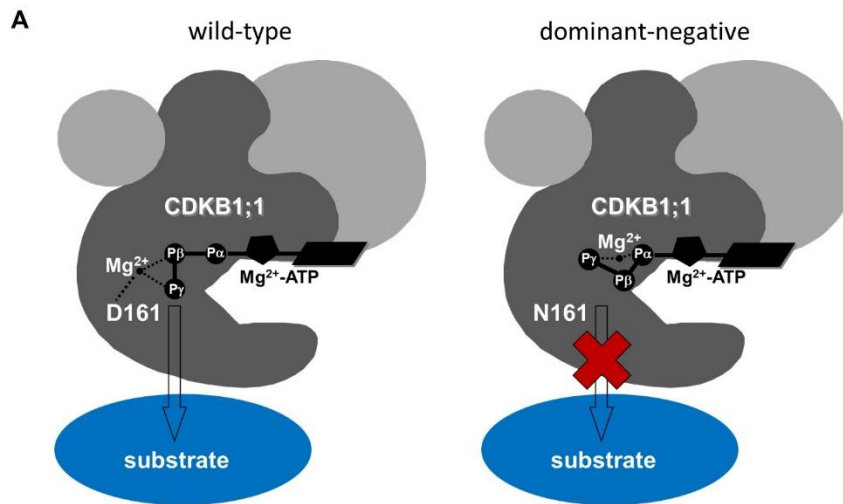
Supplemental information

A
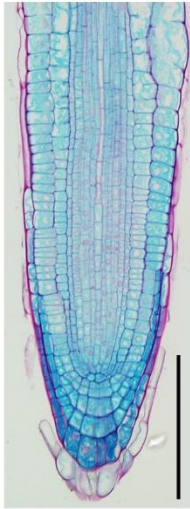
B

Arabidopsis gene	RNA-Seq	Chen *et al.*, unpublished			Perez *et al.*, unpublished
		Col-0 0-12 hours 10µM NAA Stage I	Col-0 12-18 hours 10µM NAA Stage II	Col-0 18-24 hours 10µM NAA Stage III	Col-0 2 hours DMSO-10µM NAA
CDKA;1	FC	1,035	-1,059	-1,024	1,179
(AT3G48750)	FDR	0,84	0,71	1	0,24
CDKB1;1	FC	**2,574**	**1,494**	**1,374**	**3,727**
(AT3G54180)	FDR	1,05 10^{-23}	6,06 10^{-06}	4,11 10^{-04}	1,48 10^{-14}
CDKB1;2	FC	**6,749**	1,179	1,213	**6,341**
(AT2G38620)	FDR	7,93 10^{-93}	0,11	0,05	4,84 10^{-09}

Supplemental Figure 1. Expression pattern and relative expression of *CDKA;1, CDKB1;1 and CDKB1;2* during root development in *Arabidopsis*.
A. Expression pattern of *pCDKA;1::GUS* in the primary root tip and primary root meristem of *Arabidopsis* seedlings 24 hours after germination. Scale bar: 0,1 mm.
B. Transcript fold changes (FC) of *CDKA;1*, *CDKB1;1* and *CDKB1;2* in primary root segments of the young maturation zone of *Arabidopsis*. Transcript fold changes were detected by RNA-Seq analysis. FC was compared between different time points (0, 12, 18, 24 hours) after treatment with 10µM synthetic auxin, 1-naphthaleneacetic acid (NAA), in the RNA-Seq of Chen *et al*., which enabled to detect differentially expressed genes in distinct early stages of lateral root development (Stage I, Stage II and Stage III respectively). FC was compared between treatment with 10µM NAA or DMSO for 2 hours in the RNA-Seq dataset of Perez et al., which enabled to detect auxin-dependent differential gene expression. The False Discovery Rate (FDR) is included for each FC and significant FC are indicated in bold.

A wild-type / dominant-negative

B Average primary root length

Supplemental Figure 2. Dominant-negative mutant of *CYCLIN-DEPENDENT KINASE B1;1* affects lateral root development in *Arabidopsis*.

A. Schematic representation of wild-type D161 (left) and dominant-negative mutant N161 (right) of CYCLIN-DEPENDENT KINASE B1;1 (CDKB1;1). The aspartic acid residue (D) at the amino acid position 161 is required for correct ATP binding by the CDK kinases, and its mutation results in loss of kinase activity. Overexpression of mutant *CDKB1;1 N161* has a dominant negative effect.

B. Quantification of average primary root length (cm) in 12-day-old *Arabidopsis* seedlings. Wild-type, two independent lines 1.6 and 2.6 overexpressing wild-type *CDKB1;1 p35S::CDKB1;1 D161* and two independent lines 1.2 and 9.2 overexpressing dominant-negative *CDKB1;1 p35S::CDKB1;1 N161* were analysed (Boudolf et al., 2004). Chart represents mean value ± standard error. ELR was compared between control line 1.6 and mutant lines 1.2 or 9.2 and between control line 2.6 and mutant lines 1.2 or 9.2 using a two-sided Student's *t*-test. n.s. indicates not significant with an α=0,05. n indicates the number of seedlings analysed.

A

T1 Line	GFP phenotype in lateral roots	R2	TIDE score	Indel Profile (%)																				
				-10	-9	-8	-7	-6	-5	-4	-3	-2	-1	0	1	2	3	4	5	6	7	8	9	10
13977.4	knockout	0,99	96,9%	0	0	0	0	0	0	0	2	0	13	2	82	0	0	0	0	0	0	0	0	0
13977.5	knockout	0,99	96,4%	0	0	0	0	0	0	1	3	2	10	2	79	0	1	0	0	0	1	0	0	0
13977.32	knockout	0,96	96,3%	0	0	0	0	0	0	0	0	0	17	0	77	0	0	0	0	0	0	0	0	2
13977.33	knockout	0,99	95,3%	0	0	0	0	0	0	0	0	0	0	4	95	0	0	0	0	0	0	0	0	0
13977.30	knockout	0,98	93,7%	0	0	0	0	0	0	0	0	0	2	5	91	0	0	0	0	0	0	0	0	0
13977.34	knockout	0,98	93,0%	2	0	0	0	0	0	0	0	0	5	5	86	0	0	0	0	0	0	0	0	0
13977.6	chimeric	0,93	29,4%	0	0	1	0	0	0	0	1	0	3	64	23	0	0	0	0	0	0	0	0	0
13977.7	wild-type	0,99	3,2%	0	0	0	0	0	0	0	0	0	0	96	1	0	0	0	0	0	0	0	1	0
13977.31	wild-type	0,99	1,7%	0	0	0	0	0	0	0	1	0	0	97	1	1	0	0	0	0	0	0	0	0

Supplemental Figure 3. Mutation profile of individual *pGATA23*:Cas9-mCherry;GFP-1 T1 lines.

A. TIDE (Tracking of Indels by Decomposition) analysis from the GFP-1 genotyping of pooled lateral roots (ca. 3-4). TIDE analysis (software version 3.2.0) was performed to determine the frequency and type of mutations generated with the CRISPR system (Brinkman et al., 2014). Significant values ($p < 0.001$) are highlighted in green.

Supplemental Figure 4. *Arabidopsis* **seedlings treated with cell cycle inhibitor colchicine steers root development towards differentiation.**

A. Representative image of a 8-day-old *Arabidopsis* wild-type seedling germinated in liquid growth medium and treated with 0,03% colchicine 5 days after germination. Scale bar: 1 cm.

B. Microscopic images of the primary root tip and lateral roots of a 8-day-old *Arabidopsis* wild-type seedling germinated in liquid growth medium and treated with 0,03% colchicine 5 days after germination. White dashed line indicates morphology of the lateral root primordium. Scale bars: 0,1 mm.

C. Microscopic images lateral root primordia of a 8-day-old *Arabidopsis* wild-type seedling germinated in liquid growth medium and treated with 0,03% colchicine 5 days after germination. Roman numerals indicate lateral root primordium stage according to Malamy & Benfey, 1997. Scale bars: 20 μm.

Supplemental experimental procedures

Primer sequences (5'-3') for quantitative real-time PCR analysis

Gene	Forward primer	Reverse primer
GATA23	ACCAATGTGGAGAGGTGGAC	AAGCTTTTGTGGCTGCGAAT
LBD16	TACAACGGCGGGGACAGGT	GCTGCGAATCTTGCTGCTCC
ACR4	GATCATAGTGCGGTCTGTTGG	AGGGATAGAAGCAGGGAAACC
GLV6	ACCCTCTTTCTTTGTGCACTAGCCA	TCATGAGCTTTCGCGTCGCCAT
GLV10	CCATTGAAGCACCACCATCG	TCAGTTATGGCGTGGAGGC
PUCHI	TCGGCTGCGTAACGACCCCA	CACCACCACAACCGGCGAGA
WOX5	GGCTAGGGAGAGGCAGAAAC	TCCACCTTGGAGTTGGAGTC
PLT1	ACGAAAACCAATCCAACCAC	ATTGGACGCTAGGCATCAAG
PLT2	GAGGTTCCAAAAGTGGCTGA	CGTTGGTTTGATGAATGTCG
PLT3	TCAGGAGGAAGAGTAGC	TCTTTGTTCCCAGCAACTCG
PLT5	ACATTTAGCACTCAAGAGG	ATCATATCGACTGATGTCG
PLT7	ACCTTTGCAACCGAAGAGG	AAGAACTATTCATGACAGC
IAA28	CATCATTCCTTTCCAATAACAG	GTTGTGCCGTTAGGTTTC
IAA14	TCAGAAGAGCGGCGAAGC	GACATCACCAACGAGCATCC
ARF7	AGAAAATCTTTCCTGCTCTGGAT	TGTCTGAAAGTCCATGTGTTGTC
IAA12	GGTACTACTTGTCGAGAAAAGGTTAAACC	CCCCTTCCTTATCTTCATAAGTGAGTAC
ARF5	ACAAGCTTTAAAGACTACGAGGAGCTA	CGAGCTTTGTGGGTGAGTTAGTAG
IAA3	TTAACCTCAAGGAAACAGAGCTG	CTCTCTCTTTTGCTTCACATACATTAT
ACT2	GGCTCCTCTTAACCCAAAGGC	CACACCATCACCAGAATCCAGC
UBI10	TACGCCTGCAAAGTGACTCG	CCCAACAGCTCAACACTTTCG

References

Beeckman, T., Burssens, S., & Inzé, D. (2001). The peri-cell-cycle in Arabidopsis. *Journal of Experimental Botany, 52*(suppl_1), 403-411. https://doi.org/10.1093/jexbot/52.suppl_1.403

Benková, E., Michniewicz, M., Sauer, M., Teichmann, T., Seifertová, D., Jürgens, G., & Friml, J. (2003). Local, Efflux-Dependent Auxin Gradients as a Common Module for Plant Organ Formation. *Cell, 115*(5), 591-602. https://doi.org/https://doi.org/10.1016/S0092-8674(03)00924-3

Boudolf, V., Barrôco, R., Engler, J. d. A., Verkest, A., Beeckman, T., Naudts, M., Inzé, D., & De Veylder, L. (2004). B1-Type Cyclin-Dependent Kinases Are Essential for the Formation of Stomatal Complexes in Arabidopsis thaliana. *The Plant Cell, 16*(4), 945. https://doi.org/10.1105/tpc.021774

Brinkman, E. K., Chen, T., Amendola, M., & van Steensel, B. (2014). Easy quantitative assessment of genome editing by sequence trace decomposition. *Nucleic Acids Research, 42*(22), e168-e168. https://doi.org/10.1093/nar/gku936

Casimiro, I., Marchant, A., Bhalerao, R. P., Beeckman, T., Dhooge, S., Swarup, R., Graham, N., Inzé, D., Sandberg, G., Casero, P. J., & Bennett, M. (2001). Auxin Transport Promotes Arabidopsis Lateral Root Initiation. *The Plant Cell, 13*(4), 843. https://doi.org/10.1105/tpc.13.4.843

Chen, Q., Liu, Y., Maere, S., Lee, E., Van Isterdael, G., Xie, Z., Xuan, W., Lucas, J., Vassileva, V., Kitakura, S., Marhavý, P., Wabnik, K., Geldner, N., Benková, E., Le, J., Fukaki, H., Grotewold, E., Li, C., Friml, J., Sack, F., Beeckman, T., & Vanneste, S. (2015, 2015/11/18). A coherent transcriptional feed-forward motif model for mediating auxin-sensitive PIN3 expression during lateral root development. *Nature Communications, 6*(1), 8821. https://doi.org/10.1038/ncomms9821

De Rybel, B., Vassileva, V., Parizot, B., Demeulenaere, M., Grunewald, W., Audenaert, D., Van Campenhout, J., Overvoorde, P., Jansen, L., Vanneste, S., Möller, B., Wilson, M., Holman, T., Van Isterdael, G., Brunoud, G., Vuylsteke, M., Vernoux, T., De Veylder, L., Inzé, D., Weijers, D., Bennett, M. J., & Beeckman, T. (2010). A Novel Aux/IAA28 Signaling Cascade Activates GATA23-Dependent Specification of Lateral Root Founder Cell Identity. *Current Biology, 20*(19), 1697-1706. https://doi.org/https://doi.org/10.1016/j.cub.2010.09.007

De Smet, I., Vassileva, V., De Rybel, B., Levesque, M. P., Grunewald, W., Van Damme, D., Van Noorden, G., Naudts, M., Van Isterdael, G., De Clercq, R., Wang, J. Y., Meuli, N., Vanneste, S., Friml, J., Hilson, P., Jürgens, G., Ingram, G. C., Inzé, D., Benfey, P. N., & Beeckman, T. (2008). Receptor-Like Kinase ACR4 Restricts Formative Cell Divisions in the Arabidopsis Root. *Science, 322*(5901), 594. https://doi.org/10.1126/science.1160158

De Veylder, L., Beeckman, T., & Inzé, D. (2007). The ins and outs of the plant cell cycle. *Nature Reviews Molecular Cell Biology, 8*(8), 655-665. https://doi.org/10.1038/nrm2227

Decaestecker, W., Buono, R. A., Pfeiffer, M. L., Vangheluwe, N., Jourquin, J., Karimi, M., Van Isterdael, G., Beeckman, T., Nowack, M. K., & Jacobs, T. B. (2019). CRISPR-TSKO: A Technique for Efficient Mutagenesis in Specific Cell Types, Tissues, or Organs in Arabidopsis. *The Plant Cell, 31*(12), 2868. https://doi.org/10.1105/tpc.19.00454

DiDonato, R. J., Arbuckle, E., Buker, S., Sheets, J., Tobar, J., Totong, R., Grisafi, P., Fink, G. R., & Celenza, J. L. (2004). Arabidopsis ALF4 encodes a nuclear-localized protein required for lateral root formation. *The Plant Journal, 37*(3), 340-353. https://doi.org/10.1046/j.1365-313X.2003.01964.x

Du, Y., & Scheres, B. (2017). PLETHORA transcription factors orchestrate de novo organ patterning during Arabidopsis lateral root outgrowth. *Proceedings of the National Academy of Sciences, 114*(44), 11709. https://doi.org/10.1073/pnas.1714410114

Dubrovsky, J. G., Sauer, M., Napsucialy-Mendivil, S., Ivanchenko, M. G., Friml, J., Shishkova, S., Celenza, J., & Benková, E. (2008). Auxin acts as a local morphogenetic trigger to specify lateral root founder cells. *Proceedings of the National Academy of Sciences, 105*(25), 8790. https://doi.org/10.1073/pnas.0712307105

Fernandez, A. I., Vangheluwe, N., Xu, K., Jourquin, J., Claus, L. A. N., Morales-Herrera, S., Parizot, B., De Gernier, H., Yu, Q., Drozdzecki, A., Maruta, T., Hoogewijs, K., Vannecke, W., Peterson, B., Opdenacker, D., Madder, A., Nimchuk, Z. L., Russinova, E., & Beeckman, T. (2020). GOLVEN peptide signalling through RGI receptors and MPK6 restricts asymmetric cell division during lateral root initiation. *Nature Plants, 6*(5), 533-543. https://doi.org/10.1038/s41477-020-0645-z

Foard, D. E., Haber, A. H., & Fishman, T. N. (1965). INITIATION OF LATERAL ROOT PRIMORDIA WITHOUT COMPLETION OF MITOSIS AND WITHOUT CYTOKINESIS IN UNISERIATE PERICYCLE. *American Journal of Botany, 52*(6Part1), 580-590. https://doi.org/10.1002/j.1537-2197.1965.tb06825.x

Fukaki, H., Nakao, Y., Okushima, Y., Theologis, A., & Tasaka, M. (2005). Tissue-specific expression of stabilized SOLITARY-ROOT/IAA14 alters lateral root development in Arabidopsis. *The Plant Journal, 44*(3), 382-395. https://doi.org/10.1111/j.1365-313X.2005.02537.x

Fukaki, H., Tameda, S., Masuda, H., & Tasaka, M. (2002). Lateral root formation is blocked by a gain-of-function mutation in the SOLITARY-ROOT/IAA14 gene of Arabidopsis. *The Plant Journal, 29*(2), 153-168. https://doi.org/10.1046/j.0960-7412.2001.01201.x

Heisler, M. G., Ohno, C., Das, P., Sieber, P., Reddy, G. V., Long, J. A., & Meyerowitz, E. M. (2005). Patterns of Auxin Transport and Gene Expression during Primordium Development Revealed by Live Imaging of the Arabidopsis Inflorescence Meristem.

Current Biology, 15(21), 1899-1911.
https://doi.org/https://doi.org/10.1016/j.cub.2005.09.052

Himanen, K., Boucheron, E., Vanneste, S., de Almeida Engler, J., Inzé, D., & Beeckman, T. (2002a). Auxin-Mediated Cell Cycle Activation during Early Lateral Root Initiation. *The Plant Cell, 14*(10), 2339. https://doi.org/10.1105/tpc.004960

Himanen, K., Boucheron, E., Vanneste, S., de Almeida Engler, J., Inzé, D., & Beeckman, T. (2002b). Auxin-Mediated Cell Cycle Activation during Early Lateral Root Initiation. *The Plant Cell, 14*(10), 2339-2351. https://doi.org/10.1105/tpc.004960

Hirota, A., Kato, T., Fukaki, H., Aida, M., & Tasaka, M. (2007). The Auxin-Regulated AP2/EREBP Gene PUCHI Is Required for Morphogenesis in the Early Lateral Root Primordium of Arabidopsis. *The Plant Cell, 19*(7), 2156. https://doi.org/10.1105/tpc.107.050674

Ingouff, M., Selles, B., Michaud, C., Vu, T. M., Berger, F., Schorn, A. J., Autran, D., Van Durme, M., Nowack, M. K., Martienssen, R. A., & Grimanelli, D. (2017). Live-cell analysis of DNA methylation during sexual reproduction in Arabidopsis reveals context and sex-specific dynamics controlled by noncanonical RdDM. *Genes & Development, 31*(1), 72-83. https://doi.org/10.1101/gad.289397.116

Joubès, J., Chevalier, C., Dudits, D., Heberle-Bors, E., Inzé, D., Umeda, M., & Renaudin, J.-P. (2000). CDK-related protein kinases in plants. In D. Inzé (Ed.), *The Plant Cell Cycle* (pp. 63-76). Springer Netherlands. https://doi.org/10.1007/978-94-010-0936-2_6

Jurado, S., Abraham, Z., Manzano, C., López-Torrejón, G., Pacios, L. F., & Del Pozo, J. C. (2010). The Arabidopsis Cell Cycle F-Box Protein SKP2A Binds to Auxin. *The Plant Cell, 22*(12), 3891. https://doi.org/10.1105/tpc.110.078972

Kajala, K., Ramakrishna, P., Fisher, A., C. Bergmann, D., De Smet, I., Sozzani, R., Weijers, D., & Brady, S. M. (2014). Omics and modelling approaches for understanding regulation of asymmetric cell divisions in arabidopsis and other angiosperm plants. *Annals of Botany, 113*(7), 1083-1105. https://doi.org/10.1093/aob/mcu065

Kurihara, D., Mizuta, Y., Sato, Y., & Higashiyama, T. (2015). ClearSee: a rapid optical clearing reagent for whole-plant fluorescence imaging. *Development, 142*(23), 4168. https://doi.org/10.1242/dev.127613

Lampropoulos, A., Sutikovic, Z., Wenzl, C., Maegele, I., Lohmann, J. U., & Forner, J. (2013). GreenGate - A Novel, Versatile, and Efficient Cloning System for Plant Transgenesis [Article]. *Plos One, 8*(12), 15, Article e83043. https://doi.org/10.1371/journal.pone.0083043

Laskowski, M. J., Williams, M. E., Nusbaum, H. C., & Sussex, I. M. (1995). Formation of lateral root meristems is a two-stage process. *Development, 121*(10), 3303. http://dev.biologists.org/content/121/10/3303.abstract

Lavenus, J., Goh, T., Roberts, I., Guyomarc'h, S., Lucas, M., De Smet, I., Fukaki, H., Beeckman, T., Bennett, M., & Laplaze, L. (2013). Lateral root development in Arabidopsis: fifty shades of auxin. *Trends in Plant Science, 18*(8), 450-458. https://doi.org/https://doi.org/10.1016/j.tplants.2013.04.006

Malamy, J. E., & Benfey, P. N. (1997). Organization and cell differentiation in lateral roots of Arabidopsis thaliana. *Development, 124*(1), 33. http://dev.biologists.org/content/124/1/33.abstract

Menges, M., De Jager, S. M., Gruissem, W., & Murray, J. A. H. (2005). Global analysis of the core cell cycle regulators of Arabidopsis identifies novel genes, reveals multiple and highly specific profiles of expression and provides a coherent model for plant cell cycle control. *The Plant Journal, 41*(4), 546-566. https://doi.org/10.1111/j.1365-313X.2004.02319.x

Menges, M., & Murray, J. A. H. (2002). Synchronous Arabidopsis suspension cultures for analysis of cell-cycle gene activity. *The Plant Journal, 30*(2), 203-212. https://doi.org/10.1046/j.1365-313X.2002.01274.x

Motte, H., Vanneste, S., & Beeckman, T. (2019). Molecular and Environmental Regulation of Root Development. *Annual Review of Plant Biology, 70*(1), 465-488. https://doi.org/10.1146/annurev-arplant-050718-100423

Murashige, T., & Skoog, F. (1962). A revised medium for rapid growth and bio assays with tobacco tissue cultures. *Physiologia plantarum, 15*(3), 473-497.

Nowack, Moritz K., Harashima, H., Dissmeyer, N., Zhao, X. A., Bouyer, D., Weimer, Annika K., De Winter, F., Yang, F., & Schnittger, A. (2012). Genetic Framework of Cyclin-Dependent Kinase Function in Arabidopsis. *Developmental Cell, 22*(5), 1030-1040. https://doi.org/https://doi.org/10.1016/j.devcel.2012.02.015

Okushima, Y., Fukaki, H., Onoda, M., Theologis, A., & Tasaka, M. (2007). ARF7 and ARF19 Regulate Lateral Root Formation via Direct Activation of LBD/ASL Genes in Arabidopsis. *The Plant Cell, 19*(1), 118. https://doi.org/10.1105/tpc.106.047761

Okushima, Y., Overvoorde, P. J., Arima, K., Alonso, J. M., Chan, A., Chang, C., Ecker, J. R., Hughes, B., Lui, A., Nguyen, D., Onodera, C., Quach, H., Smith, A., Yu, G., & Theologis, A. (2005). Functional Genomic Analysis of the AUXIN RESPONSE FACTOR Gene Family Members in Arabidopsis thaliana: Unique and Overlapping Functions of ARF7 and ARF19. *The Plant Cell, 17*(2), 444. https://doi.org/10.1105/tpc.104.028316

Parizot, B., Laplaze, L., Ricaud, L., Boucheron-Dubuisson, E., Bayle, V., Bonke, M., De Smet, I., Poethig, S. R., Helariutta, Y., Haseloff, J., Chriqui, D., Beeckman, T., & Nussaume, L. (2008). Diarch Symmetry of the Vascular Bundle in Arabidopsis Root Encompasses the Pericycle and Is Reflected in Distich Lateral Root Initiation. *Plant Physiology, 146*(1), 140. https://doi.org/10.1104/pp.107.107870

Ren, H., Santner, A., Pozo, J. C. d., Murray, J. A. H., & Estelle, M. (2008). Degradation of the cyclin-dependent kinase inhibitor KRP1 is regulated by two different ubiquitin E3 ligases. *The Plant Journal, 53*(5), 705-716. https://doi.org/10.1111/j.1365-313X.2007.03370.x

Sanz, L., Dewitte, W., Forzani, C., Patell, F., Nieuwland, J., Wen, B., Quelhas, P., De Jager, S., Titmus, C., Campilho, A., Ren, H., Estelle, M., Wang, H., & Murray, J. A. H. (2011). The Arabidopsis D-Type Cyclin CYCD2;1 and the Inhibitor ICK2/KRP2 Modulate Auxin-Induced Lateral Root Formation. *The Plant Cell, 23*(2), 641. https://doi.org/10.1105/tpc.110.080002

Scofield, S., Jones, A., & Murray, J. A. H. (2014). The plant cell cycle in context. *Journal of Experimental Botany, 65*(10), 2557-2562. https://doi.org/10.1093/jxb/eru188

Ursache, R., Andersen, T. G., Marhavý, P., & Geldner, N. (2018). A protocol for combining fluorescent proteins with histological stains for diverse cell wall components. *The Plant Journal, 93*(2), 399-412. https://doi.org/10.1111/tpj.13784

Vanneste, S., De Rybel, B., Beemster, G. T. S., Ljung, K., De Smet, I., Van Isterdael, G., Naudts, M., Iida, R., Gruissem, W., Tasaka, M., Inzé, D., Fukaki, H., & Beeckman, T. (2005). Cell Cycle Progression in the Pericycle Is Not Sufficient for SOLITARY ROOT/IAA14-Mediated Lateral Root Initiation in Arabidopsis thaliana. *The Plant Cell, 17*(11), 3035. https://doi.org/10.1105/tpc.105.035493

Wang, K., Ndathe, R. W., Kumar, N., Zeringue, E. A., Kato, N., & Larkin, J. C. (2020). The CDK inhibitor SIAMESE targets both CDKA;1 and CDKB1 complexes to establish endoreplication in trichomes. *Plant Physiology*, pp.00271.02020. https://doi.org/10.1104/pp.20.00271

Wang, X., Ye, L., Lyu, M., Ursache, R., Löytynoja, A., & Mähönen, A. P. (2020). An inducible genome editing system for plants. *Nature Plants, 6*(7), 766-772. https://doi.org/10.1038/s41477-020-0695-2

Xie, Z., Lee, E., Lucas, J. R., Morohashi, K., Li, D., Murray, J. A. H., Sack, F. D., & Grotewold, E. (2010). Regulation of Cell Proliferation in the Stomatal Lineage by the Arabidopsis MYB FOUR LIPS via Direct Targeting of Core Cell Cycle Genes. *The Plant Cell, 22*(7), 2306. https://doi.org/10.1105/tpc.110.074609

Chapter 4: Genome editing of *Nuclear Migration1* reveals function in nuclear migration and development in *Arabidopsis*

Vangheluwe N., Vassileva V., Njo M., Decaestecker W., Costa P., Goossens V., Drozdzecki A., Jacobs T., Audenaert D. & Beeckman T.

Abstract

The first visible event of lateral root initiation in *Arabidopsis* is the simultaneous migration of nuclei of neighbouring lateral root founder cells in the pericycle followed by asymmetric anticlinal cell divisions giving rise to cell diversity and tissue patterns resulting in the development of a lateral root primordium. Our study investigates the function of *Nuclear Migration1* (*NMig1*), an *Arabidopsis* homolog of the *Nuclear Distribution gene C* (*NudC*), which is structurally and functionally conserved in multicellular organisms and is essential for nuclear migration in fungal and mammalian cells. *NMig1* is specifically expressed during lateral root initiation and development, and is highly induced by auxin. Moreover, loss-of-function studies revealed that *NMig1* is essential for reproductive development and hints towards a function in lateral root development. Finally, we show that *NMig1* controls nuclear separation during cell division. Therefore, our data demonstrate that the *NudC* homolog *NMig1* could be considered as a potential essential gene for nuclear migration and asymmetric cell divisions in organogenesis.

Authors contribution

VV and TB designed the project. VV generated and characterized the reporter line *pNMig1::NLS-GFP-GUS* and crosstalk with auxin with help from MN. NV generated and characterized the *CRISPR nmig1-c1* mutant. PC performed the seed set score analysis. NV generated and characterized the *CRISPR* lateral root-specific *nmig1* mutants. WD and TJ generated the CRISPR construct for mutagenesis in PSB-D cell culture. NV, VG and AD executed analysis of the PSB-D cell culture with input from DA. VV prepared and performed the BiFC assay. NV and VV carried out the statistical analysis. NV, TB and VV wrote the manuscript. TB and VV provided guidance and advice on the project, the experiments and the analysis of the results.

Introduction

Lateral root formation is a major determinant of root systems architecture. In *Arabidopsis*, lateral roots arise from a subset of stem cells situated in the pericycle adjacent to the xylem poles (Parizot et al., 2008). The specification of this subset of xylem pole pericycle cells into lateral root founder cells is marked by expression of the transcription factor *GATA23* (De Rybel et al., 2010). Subsequently, the first visible event of lateral root initiation is the simultaneous migration of nuclei of neighbouring pericycle lateral root founder cells towards the common cell wall followed by an asymmetric anticlinal cell division giving rise to two small daughter cells and two larger flanking cells (De Rybel et al., 2010). In a next step, these cells undergo a series of anticlinal and periclinal cell divisions and differentiation steps to generate cell diversity and tissue patterns, resulting in the development of a lateral root primordium that eventually emerges through overlying tissues of the primary root (Malamy & Benfey, 1997).

Asymmetric cell divisions play a crucial role in enabling post-embryonic organogenesis including lateral root initiation and are fundamentally important in plant development (e.g. pollen and stomata development) (Kajala et al., 2014). These divisions are formative divisions that generate daughter cells of distinct identity. In lateral root initiation, the first asymmetric cell division is preceded by a nuclear migration event in lateral root founder cell pairs, which is an auxin-dependent process (De Rybel et al., 2010; De Smet et al., 2007). Several AUX/IAA–ARF factors have been identified that interact together. The *SOLITARY-ROOT* (*SLR*)/*IAA14*–*ARF7*–*ARF19* module regulates the coordinated nuclear migration (De Rybel et al., 2010; De Smet et al., 2007; Goh et al., 2012). In the *slr-1* and *arf7arf19* mutants with impaired lateral root formation no polar movement of nuclei could be observed (De Rybel et al., 2010). However, after prolonged auxin treatment, polar movement of nuclei and asymmetric cell division does occur, but only in single xylem-pole pericycle cells which will not result in formative divisions that normally precede the formation of a lateral root primordium (De Rybel et al., 2010).

Apart from the auxin module, little is known about the molecular mechanisms directing the simultaneous polar movement of the nuclei in lateral root founder cells resulting in the first asymmetric cell division (Kajala et al., 2014). In our quest of putative regulators, we searched for genes involved in nuclear migration and which are conserved in multicellular organisms. *Nuclear distribution C* (*NudC*) genes encode proteins with high structural and functional conservation in fungi, animals and plants (Fu et al., 2016). *NudC* has been originally identified in the filamentous fungus *Aspergillus nidulans* as an essential gene required for microtubule-dependent migration of nuclei and normal colony growth (Osmani et al., 1990). Depletion of *NudC* leads to the occurrence of multiple spindles during metaphase and induces lagging chromosomes during anaphase (Aumais et al., 2003; Zhou et al., 2003). Homologs of *NudC* from mammals, *Drosophila*, *Caenorhabditis elegans* and *Arabidopsis thaliana* complement the *nudC3* mutation in *A. nidulans*, and result in the normal movement of nuclei and colony growth (Cunniff et al., 1997; Dawe et al., 2001; Morris et al., 1997).

The CS domain -a domain shared by CHORD-containing proteins and SGT1- is conserved in the NudC family and has a similar molecular architecture with small heat shock chaperones, such as p23 and HSP20/alpha-crystallin proteins, which simultaneously interact with HSP90 and

specific proteins (Botër et al., 2007; Garcia-Ranea et al., 2002; Lee et al., 2004). The CS domain is considered as a binding module for HSP90, indicating that CS domain-containing proteins are involved in recruiting heat shock proteins to multiprotein complexes (Lee et al., 2004). Interestingly, a recent study describes the genetic connection between HSP90 and the MAPK signalling cascade component YODA in the regulation of stomata formation during heat stress conditions and hints for a function of HSP90 in cell-polarity establishment (Samakovli et al., 2020).

A. thaliana encodes three members of the family of NudC domain containing small heat shock proteins: *BOBBER1* (*BOB1*; *AT5G53400*), *BOB2* (*AT4G27890*) which is a duplicated gene of *BOB1* and *Nuclear Migration1* (*NMig1*; *AT5G58740*) (Jurkuta et al., 2009; Perez et al., 2009; Velinov et al., 2020). *BOB1* is required for the normal partitioning and patterning of the apical domain of the embryo (Jurkuta et al., 2009). Loss-of-function mutants of *BOB1* are embryo lethal. Analysis of the partial loss-of-function allele *bob1-3* revealed that BOB1 is required for plant thermotolerance and postembryonic development (Perez et al., 2009). Recently, a gain-of-function study of *NMig1* revealed that overexpression of *NMig1* results in increased primary root growth and increased density of both lateral root initiation events and emerged lateral roots (Velinov et al., 2020). In addition, overexpression of *NMig1* positively affects root growth and branching under abiotic stress conditions (Velinov et al., 2020). These observations indicate a potential regulatory function of *NMig1* in *Arabidopsis* primary and lateral root development, and tolerance to abiotic stress.

Here, we report on the function of *NMig1* during lateral root development through expression analysis and loss-of-function studies by generating inheritable or somatic mutations using CRISPR. Our study reveals that *NMig1* is essential for reproductive development and suggests a function in lateral root initiation. The molecular mechanism of *NMig1* in formative divisions points towards a function in nuclear migration.

Results

NMig1 is specifically expressed during root development

A transgenic line expressing the GFP and GUS reporters under the regulation of the *NMig1* promoter was generated (termed *pNMig1::NLS-GFP-GUS*), and its expression during the seedling stage was observed to be root specific (Figure 1C; Figure S1A). *pNMig1::NLS-GFP-GUS* activity was confined to the primary root tip with a prominent expression in the quiescent centre and early root cap cells (Figure 1C). It was further expressed throughout progressing stages of lateral root development with the earliest activity detected in stage I primordia (Figure 1A and 1B). At the tissue level, strong *pNMig1::NLS-GFP-GUS* expression was primarily observed in the central cells of developing lateral root primordia, which indicates that *NMig1* is primarily expressed in actively dividing stem cells (Figure 1A). Moreover, this expression pattern mimics the pattern of the auxin response during lateral root formation as visualized by the synthetic auxin responsive promoter *DR5* (Benková et al., 2003), and which has been associated with installation and maintenance of the root stem cell niche.

It has been earlier reported that a close homolog of *NMig1*, *BOB1* is expressed throughout the early embryo, which remains strong until the transition stage and is absent after the heart stage (Jurkuta et al., 2009). In a next step, *pNMig1::NLS-GFP-GUS* expression was analysed during embryogenesis. Interestingly, *pNMig1::NLS-GFP-GUS* activity was confined to the basal half of progressing embryo stages (from globular to heart), which consists of the cells that will give rise to the primary root stem cell niche (ten Hove et al., 2015) (Figure S1B). The embryonic and post-embryonic expression patterns thus suggest that *NMig1* is involved in primary and lateral root development with a putative role in root stem cell activity.

Auxin induces *SOLITARY-ROOT/ARF7ARF19* dependent expression of *NMig1*

When a local auxin concentration maximum is reached, the lateral root founder cells proceed to lateral root initiation (Dubrovsky et al., 2008). To investigate the function of *NMig1* during lateral root initiation, we made use of the lateral root inducible system (LRIS) (Himanen et al., 2002). This system enables highly controlled lateral root initiation to occur synchronously in the primary root based on successive treatments with the auxin transport inhibitor naphthylphthalamic acid (NPA) and synthetic auxin, 1-naphthaleneacetic acid (NAA) (Crombez et al., 2016). On NPA (72 hours after germination) *pNMig1::NLS-GFP-GUS* activity was restricted to the root apical meristem (Figure 2). When transferred from NPA to NAA, *NMig1* expression was induced after 6 hours in the xylem-pole pericycle along the entire primary root axis (Figure 2; Figure S2A). This observation indicates that auxin induces expression of *NMig1* in the xylem-pole pericycle at the onset of lateral root initiation because in the LRIS the 6 hours timepoint has been correlated with the first anticlinal divisions of the pericycle (Himanen et al., 2002; Vanneste et al., 2005) and our microscopical analysis confirmed *pNMig1::NLS-GFP-GUS* activity in the pericycle at this time point (Figure S2A).

The SLR/IAA14–ARF7–ARF19 module regulates the coordinated nuclear migration preceding the first asymmetric cell division during lateral root initiation (De Rybel et al., 2010; De Smet et al., 2007). In *slr-1* and *arf7arf19* mutants no simultaneous polar movement of nuclei in neighbouring xylem-pole pericycle cells could be observed (De Rybel, Vassileva et al. 2010).

We analysed whether *NMig1* expression is *SLR/IAA14* and/or *ARF7ARF19* dependent. Relative *NMig1* expression levels in roots of wild-type and *slr-1* or *arf7arf19* mutant seedlings in response to synthetic auxin (NAA) were compared. Interestingly, *NMig1* expression does not significantly increase in *slr-1* or *arf7arf19* in response to auxin compared to wild-type (Figure S2B). Taken together, auxin induces expression of *NMig1* in a *SLR/ARF7ARF19* dependent manner.
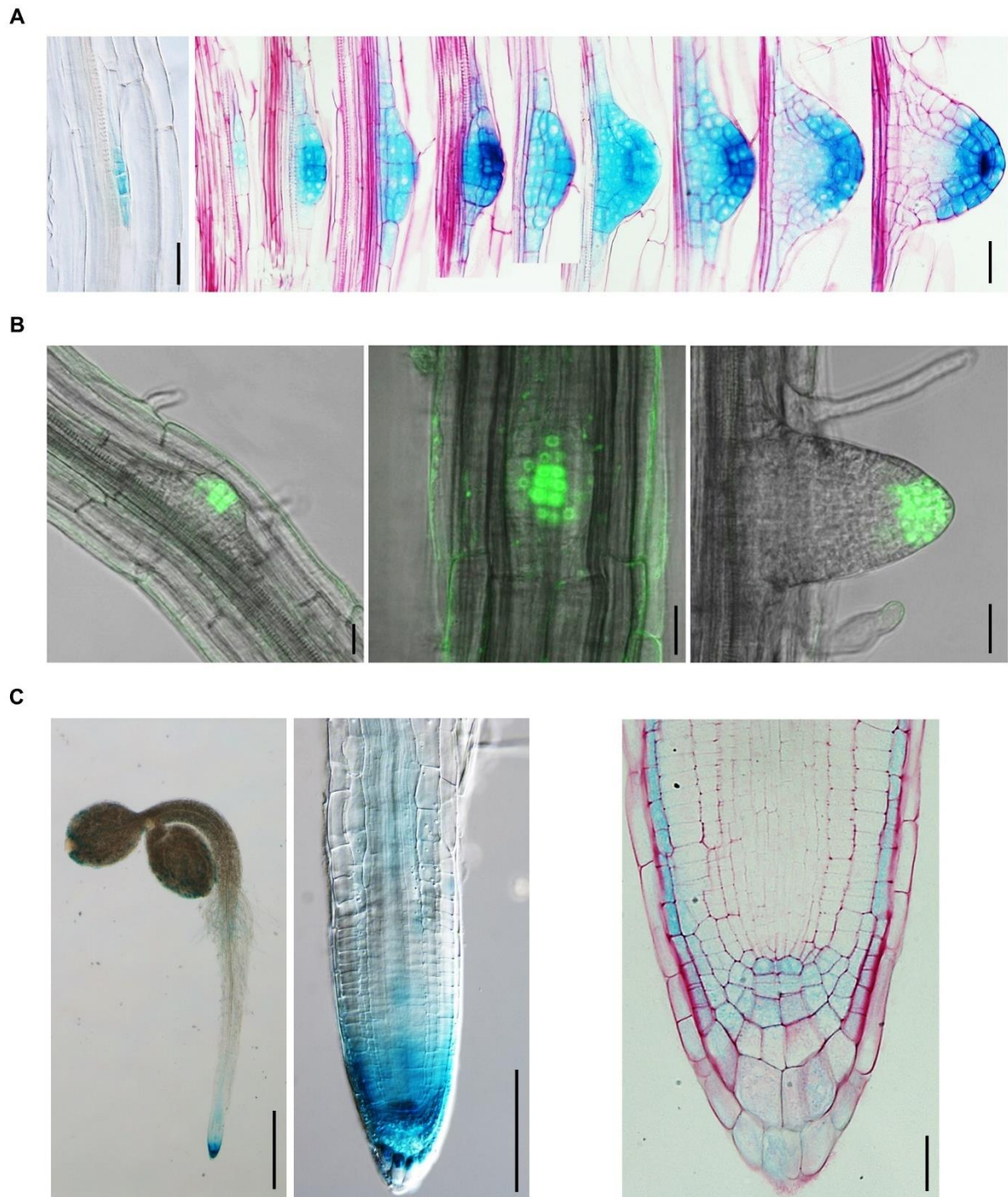
Figure 1. *NMig1* is expressed during lateral root development in *Arabidopsis*.
A. Expression pattern of *pNMig1::NLS-GFP-GUS* in representative lateral root primordium stages of 5-day-old *Arabidopsis* seedlings. Scale bars: 20 μm.
B. Representative confocal images of *pNMig1::NLS-GFP-GUS* during lateral root development of 5-day-old *Arabidopsis* seedlings. *NLS-GFP-GUS* is displayed in green. Scale bars: 20 μm.
C. Expression pattern of *pNMig1::NLS-GFP-GUS* in the primary root tip and primary root meristem of *Arabidopsis* seedlings 24 hours after germination. Scale bar left panel: 1 mm. Scale bar middle panel: 0,1 mm. Scale bar right panel: 20 μm.
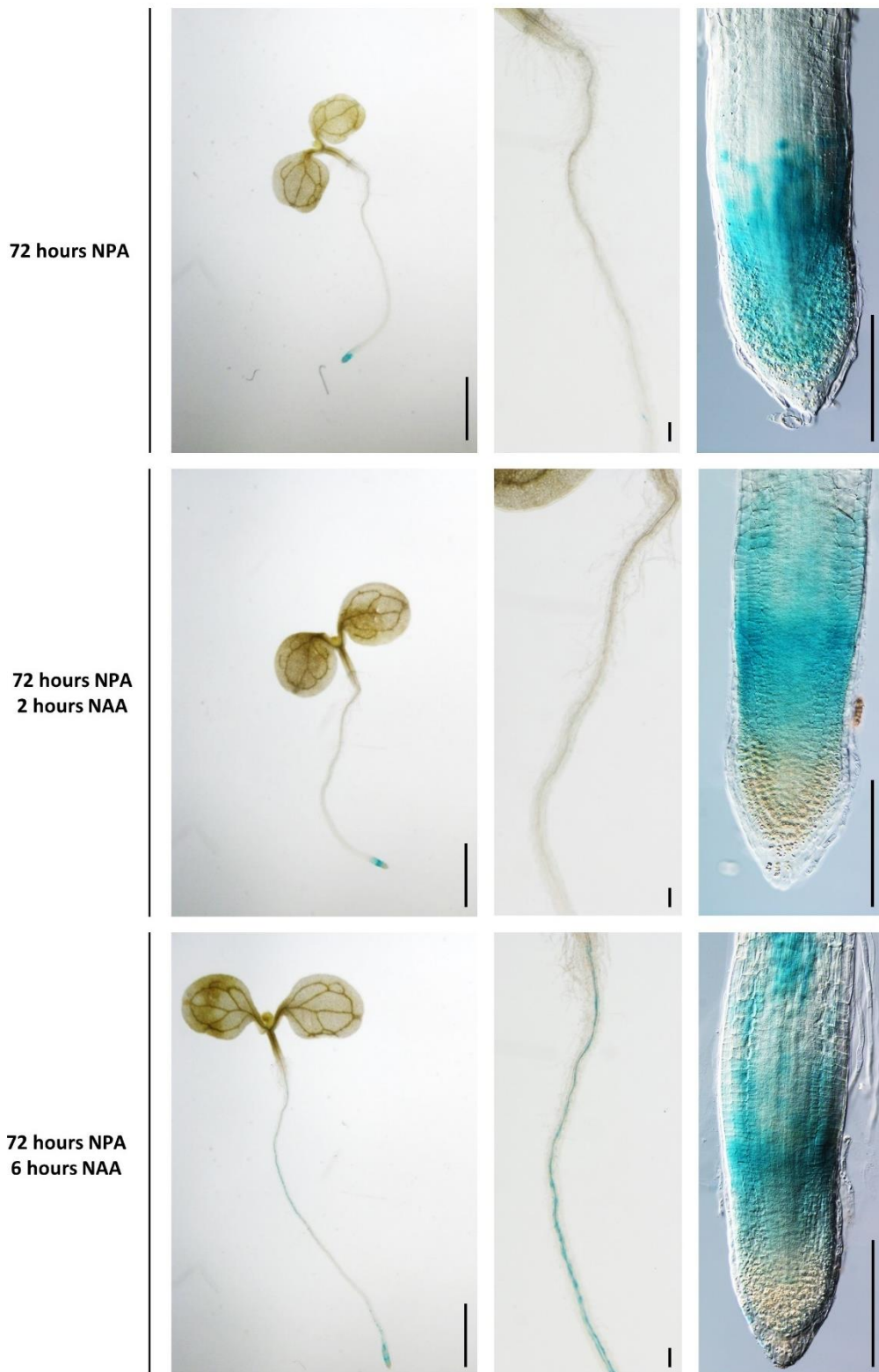
Figure 2. Synthetic auxin 1-naphthaleneacetic acid induces expression of *NMig1* at the onset of lateral root initiation. Expression pattern of *pNMig1::NLS-GFP-GUS* in 3-day-old *Arabidopsis* seedlings germinated on growth medium supplemented with 10 µM naphthylphthalamic acid (NPA) and subsequently treated for 2 or 6 hours with 10 µM of synthetic auxin 1-naphthaleneacetic acid (NAA). Scale bar left panels: 1 mm. Scale bar middle and right panels: 0,1 mm.

CRISPR-generated loss-of-function mutant of *NMig1* reveals function in reproductive development

Loss-of-function analysis of *NMig1* is hindered due to the lack of mutants in the available *Arabidopsis* mutant collections. The only identified transgenic lines contain insertions in the last exon of *NMig1* and are likely not affecting the gene function as the conserved *NudC* domain is encoded in upstream exons (Figure 3A). As an alternative strategy, knockdown lines were generated using artificial microRNAs and RNA interference. However, downregulation of *NMig1* expression severely affected development and hindered seed production (data not shown).

In a next step, the CRISPR system was employed with the aim to generate heritable mutations in *NMig1* (Fauser et al., 2014). Transgenic lines harbouring two guideRNAs that simultaneously target the 5'untranslated region (UTR) and exon 2 of *NMig1* were generated (Figure 3A). The progeny of T1 plants was screened for inherited mutations. In the 5'UTR, homozygous and heterozygous mutations were identified, while in exon 2 only a heterozygous mutation was detected (Figure 3A). The deletion of 40 base pairs in exon 2 causes a frameshift mutation and results in a hypothetical truncated protein that encodes only 4 amino acids of the conserved *NudC* domain (Figure S3A). We refer to this CRISPR-generated mutant allele of *NMig1* as *nmig1-c1*.

Progeny of the heterozygous mutant *nmig1-c1+/-* was genotyped in order to identify homozygous mutants. For a total of 84 seedlings, only wild-type or heterozygous mutants were detected (Figure 3C). To evaluate the effect of the mutation, emerged lateral root density was quantified in heterozygous *nmig1-c1+/-* seedlings. No significant difference in lateral root density was observed compared to wild-type (Figure 3B; Figure 3D). Interestingly, the ratio of wild-type and heterozygous mutants is close to 1:1, which lead us to postulate that loss-of-function of *NMig1* might cause a defect in reproductive development.

To investigate reproductive defects, we scored the seed set in siliques of the heterozygous mutant *nmig1-c1+/-* (Figure S3B). Wild-type siliques show full seed set and each developing seed is relatively plump and green, while *nmig1-c1+/-* mutant siliques exhibit a significant proportion of unfertilized ovules, which are shrivelled and grey (Figure S3B; Figure S3C). Moreover, the unfertilized ovules are randomly distributed along the axis of the silique, which hints towards a female gametophytic defect (Noble & Palanivelu, 2020). The observation of unfertilized ovules in the heterozygous mutant *nmig1-c1+/-* as well as the absence of homozygous mutants in its progeny provides evidence that *NMig1* is essential in reproductive development.

Moreover, in the screening of the progeny of T1 plants for inherited mutations, seedlings that lack basal body structures were observed, which resemble mutants with patterning defects in the embryo (Figure 3E) (Mayer et al., 1991). Quantitative assessment of CRISPR-generated mutations in these seedlings revealed a mixture of CRISPR-generated mutations with a total proportion varying between 62% and 77% in the genotyped seedlings (Figure 3F). Interestingly, all seedlings have the deletion of 40 base pairs in exon 2 with a proportion of approximately 50% (Figure S3D). We conclude that these seedlings are heterozygous chimeras because they contain the *nmig1-c1* allele and the Cas9 nuclease is actively inducing new mutations in the wild-type allele (Fauser et al., 2014). In addition, seedlings that lack basal body structures could no longer be observed in the progeny of the heterozygous mutant *nmig1-c1+/-* in which the CRISPR system is segregated out. Hence, we postulate that the chimeric pattern of mutations in *NMig1* causes patterning defects in the embryo, which may result in seeds with aberrant morphology and seedlings that lack basal body structures (Figure 3C; Figure S3E). This is in line with the reported phenotype for loss-of-function mutants of a close homolog of *NMig1*, *BOB1* which is required for the normal partitioning and patterning of the apical domain of the embryo (Jurkuta et al., 2009) and correlates with the basal expression pattern of *NMig1* during early embryogenesis (Figure S1B).

Lateral root-specific loss-of-function of *NMig1* affects lateral root development

To evaluate the function of *NMig1* during lateral root initiation, lateral root-specific genome editing via a CRISPR tissue-specific knockout (TSKO) system was conducted (Decaestecker et al., 2019). By expressing *Cas9* in *GATA23*-expressing pericycle cells, it is possible to generate seedlings with entirely mutated lateral roots (Decaestecker et al., 2019). Transgenic lines harbouring the CRISPR system with the guideRNA targeting exon 2 of *NMig1* and the promoter of *GATA23* driving Cas9 expression were generated. Emerged lateral root density was quantified in lateral root-specific *nmig1* mutant T1 seedlings. The lateral root density is significantly decreased in lateral root-specific *nmig1* mutant T1 seedlings compared to wild-type (Figure 4A). Moreover, quantification of the average lateral root length revealed significantly shorter lateral roots in lateral root-specific *nmig1* mutant T1 seedlings compared to wild-type (Figure 4B). These observations reveal that *de novo* generation of mutations of *NMig1* during lateral root initiation results in lateral root developmental defects. On the contrary, it has been reported that constitutive overexpression of *NMig1* results in increased density of emerged lateral roots (Velinov et al., 2020).
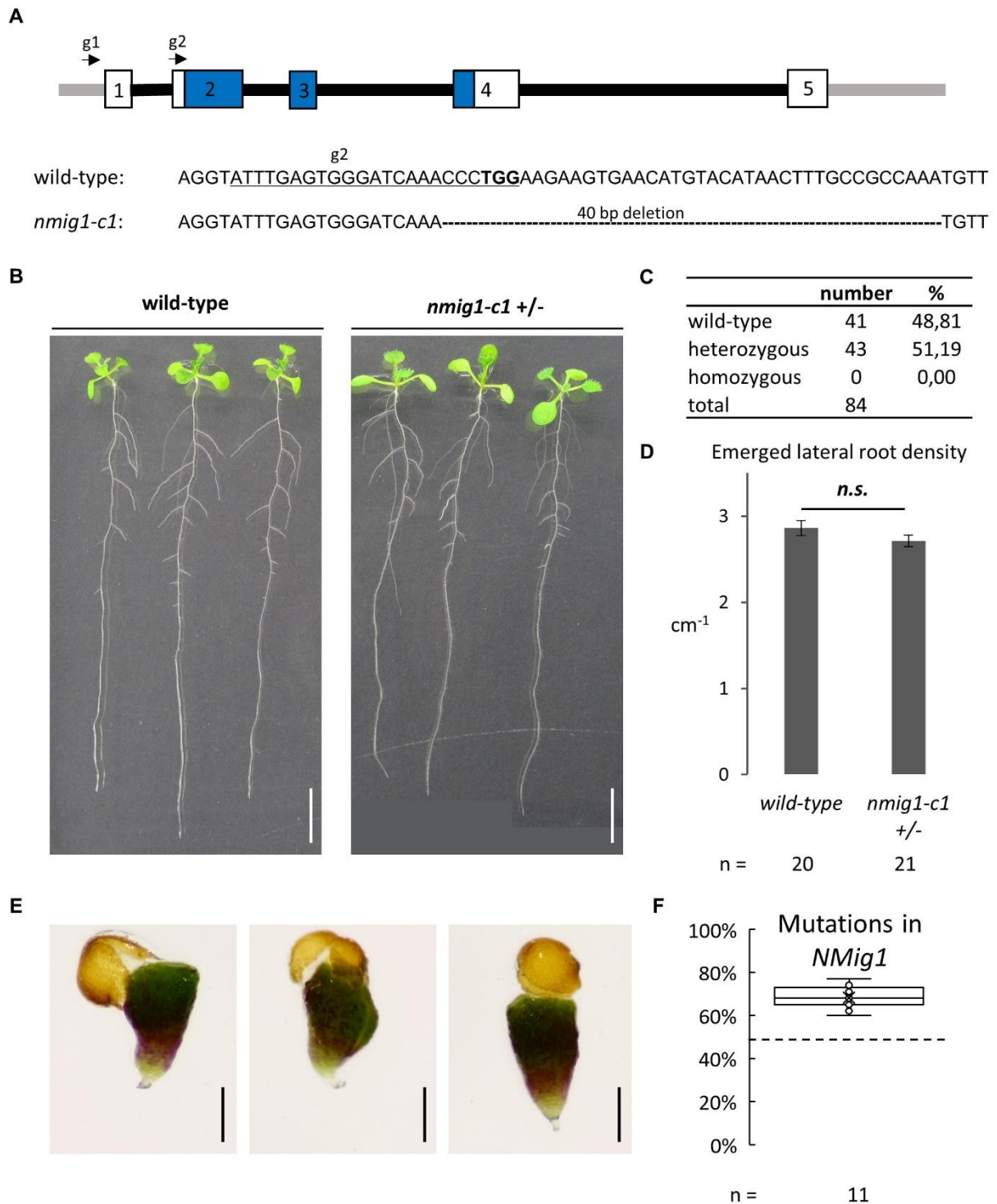
A

g1   g2

```
1    2    3    4    5
```

g2

wild-type: AGGT<u>ATTTGAGTGGGATCAAACCC</u>**TGG**AAGAAGTGAACATGTACATAACTTTGCCGCCAAATGTT

nmig1-c1:   AGGTATTTGAGTGGGATCAAA---------------------------40 bp deletion-------------------------------------TGTT

B

wild-type   *nmig1-c1 +/-*

C

	number	%
wild-type	41	48,81
heterozygous	43	51,19
homozygous	0	0,00
total	84	

D

Emerged lateral root density

n.s.

cm^{-1}

3

2

1

0

wild-type   *nmig1-c1 +/-*

n =   20   21

E

F

Mutations in *NMig1*

100%
80%
60%
40%
20%
0%

n =   11

Figure 3. CRISPR-generated loss-of-function mutant of *NMig1* reveals function in reproductive development in *Arabidopsis*.

A. Schematic representation of *NMig1* gene structure and guideRNA design for CRISPR mutagenesis. Rectangles: transcribed region and conserved *NudC* domain is coloured blue; Black lines: introns; Grey lines: untranslated regions; Arrows indicate the two guideRNAs (g1 and g2) that were simultaneously used for mutagenesis. CRISPR-generated mutant allele of *NMig1*: *nmig1-c1*. Underlined text: guideRNA 2 sequence; Bold text: PAM site; Dashed line: deleted sequence of 40 base pairs (bp).

B. Representative images of 12-day-old *Arabidopsis* wild-type and heterozygous (+/-) *nmig1-c1* mutant seedlings. Scale bar: 1 cm.

C. Segregation analysis of the progeny of a heterozygous (+/-) *nmig1-c1* mutant seedling.

D. Quantification of emerged lateral root density (ELR) (cm^{-1}) in 12-day-old *Arabidopsis* wild-type and heterozygous (+/-) *nmig1-c1* mutant seedlings. Chart represents mean value ± standard error. ELR was compared between wild-type and heterozygous (+/-) *nmig1-c1* mutant using a two-sided Student's *t*-test. n.s. indicates not significant with an α=0,05. n indicates the number of seedlings analysed.

E. Representative images of T2 seedlings that lack basal body structures observed in the progeny of *Arabidopsis* T1 plants harbouring the CRISPR T-DNA construct for mutagenesis. Scale bars: 1 mm.

F. Quantitative assessment of CRISPR-generated mutations (%) by TIDE analysis in T2 seedlings that lack basal body structures. The middle line of the boxplot indicates the median. The box indicates the lower and upper quartiles and the whiskers indicate the minimum and maximum values. Dashed line: 50% of total analysed sequences. n indicates the number of seedlings analysed.
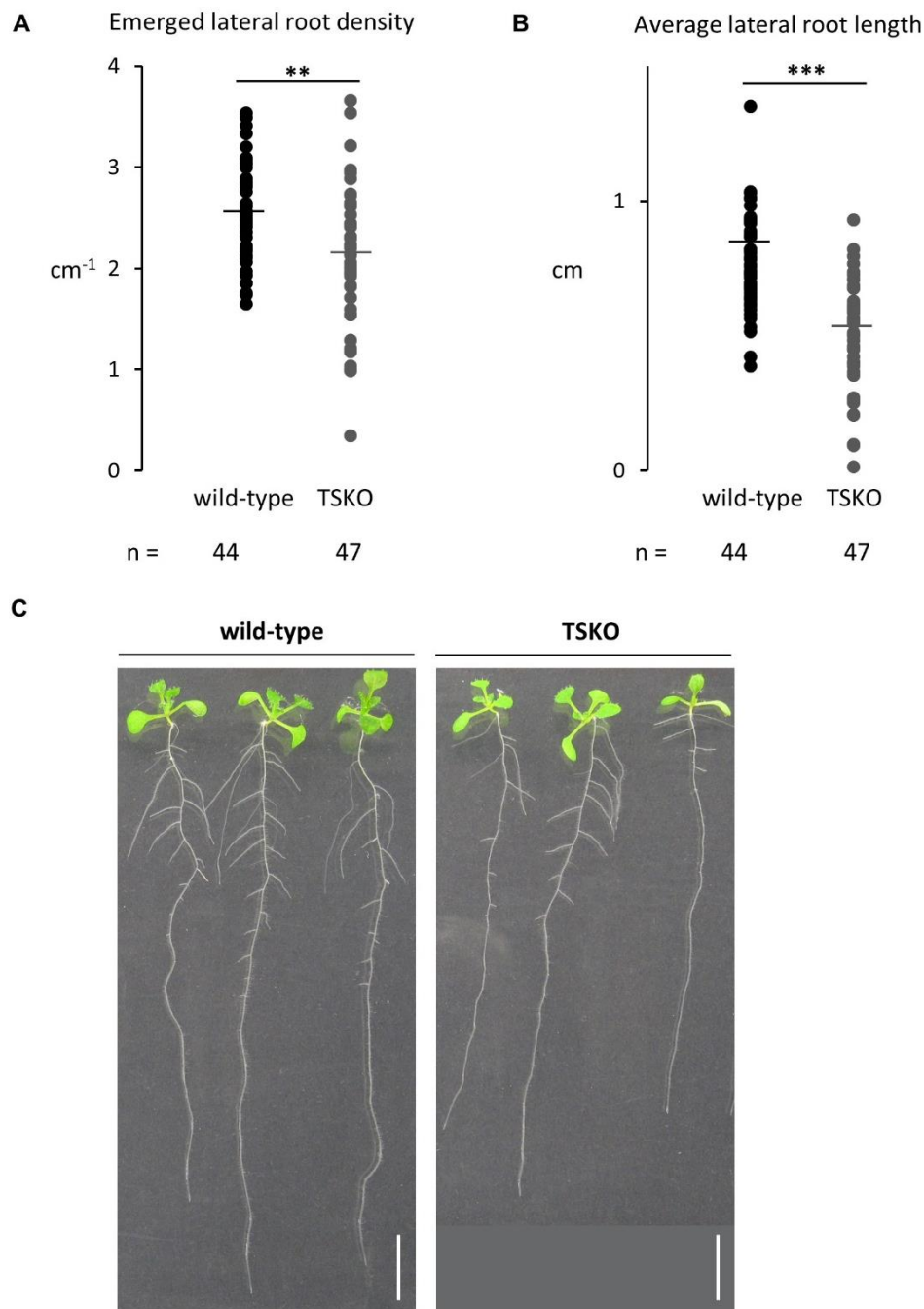
Figure 4. Lateral root-specific loss-of-function of *NMig1* affects lateral root development.

A. Quantification of emerged lateral root density (ELR) (cm^{-1}) in 12-day-old *Arabidopsis* wild-type and lateral root-specific *nmig1* mutant (referred to as TSKO) T1 seedlings (*pGATA23::Cas9-mCherry;NMig1*). Scatter plot represents mean value (horizontal bar) and individual values (dots). ELR was compared between wild-type and lateral root-specific *nmig1* mutant (TSKO) using a two-sided Student's *t*-test. ** indicates p-values smaller than 0,01 *** indicates p-values smaller than 0,001. n indicates the number of seedlings analysed.
B. Quantification of average lateral root length (cm) of the same seedlings as in A.
C. Representative images of 12-day-old *Arabidopsis* wild-type and lateral root-specific *nmig1* mutant (TSKO) T1 seedlings. Scale bar: 1 cm.

NudC, a mammalian homolog of *NMig1* plays multiple roles in mitosis and cytokinesis in cultured mammalian cells (Aumais et al., 2003). Downregulation of *NudC* inhibits cell proliferation and leads to an increase in the proportion of multinucleated cells (Aumais et al., 2003). Moreover, an increase in the number of cells connected to each other by cytoplasmic bridges was observed, indicating a delay or inhibition in cytokinesis (Aumais et al., 2003). To examine the function of *NMig1* in nuclear migration during cell division, PSB-D *Arabidopsis* cell suspension cultures were transformed with the CRISPR system and the guideRNA targeting exon 2 and the nuclear marker *p35S::mCherry-NLS*. As a control, cell suspension cultures were transformed with the CRISPR system targeting *GLABRA1*, which is required for the initiation of the differentiation of trichomes (Oppenheimer et al., 1991). Synthetic auxin naphthalene-1-acetic acid (NAA) was added to the growth medium to advance cell division.

Confocal live imaging of the nuclei revealed inhibition of nuclear separation during cell division suggesting a delay or inhibition in cleavage, cell separation or cytokinesis upon loss-of-function of *NMig1* in cultured plant cells (Figure 5B, Supplemental movie 1). This resembles the cytokinetic phenotype observed in mammalian cells upon NudC depletion (Aumais et al., 2003). However, it is difficult to pinpoint during which phase(s) of cell division defects occur upon loss-of-function of *NMig1* because cells of the PSB-D *Arabidopsis* cell suspension culture are heterogeneous in morphology and cell division phase. In the control line targeting *GLABRA1*, no nuclear separation defect was observed (Figure 5A, Supplemental movie 2). These observations indicate that *NMig1* is involved in nuclear separation during cell division.

In the NudC family, the CS domain is conserved which is considered as a binding module for HSP90, indicating that NudC is potentially involved in recruiting heat shock proteins to multiprotein complexes (Lee et al., 2004). Based on a database of known and predicted protein-protein interactions (STRING), putative interactors of NMig1 were selected and tested for interaction using bimolecular fluorescence complementation (Figure S4 and Figure S5). Analysis revealed that NMig1 interacts with HEAT SHOCK PROTEIN (HSP) 60-2, CDC5 which is a co-chaperone of HSP90, ACTIN7, RPN1a which is a subunit of the 26S proteasome and NRPD11, a non-catalytic subunit of nuclear DNA-dependent RNA polymerases. Taken together, these interactions provide evidence that NMig1 interacts with proteins involved in cell division and stress responses.
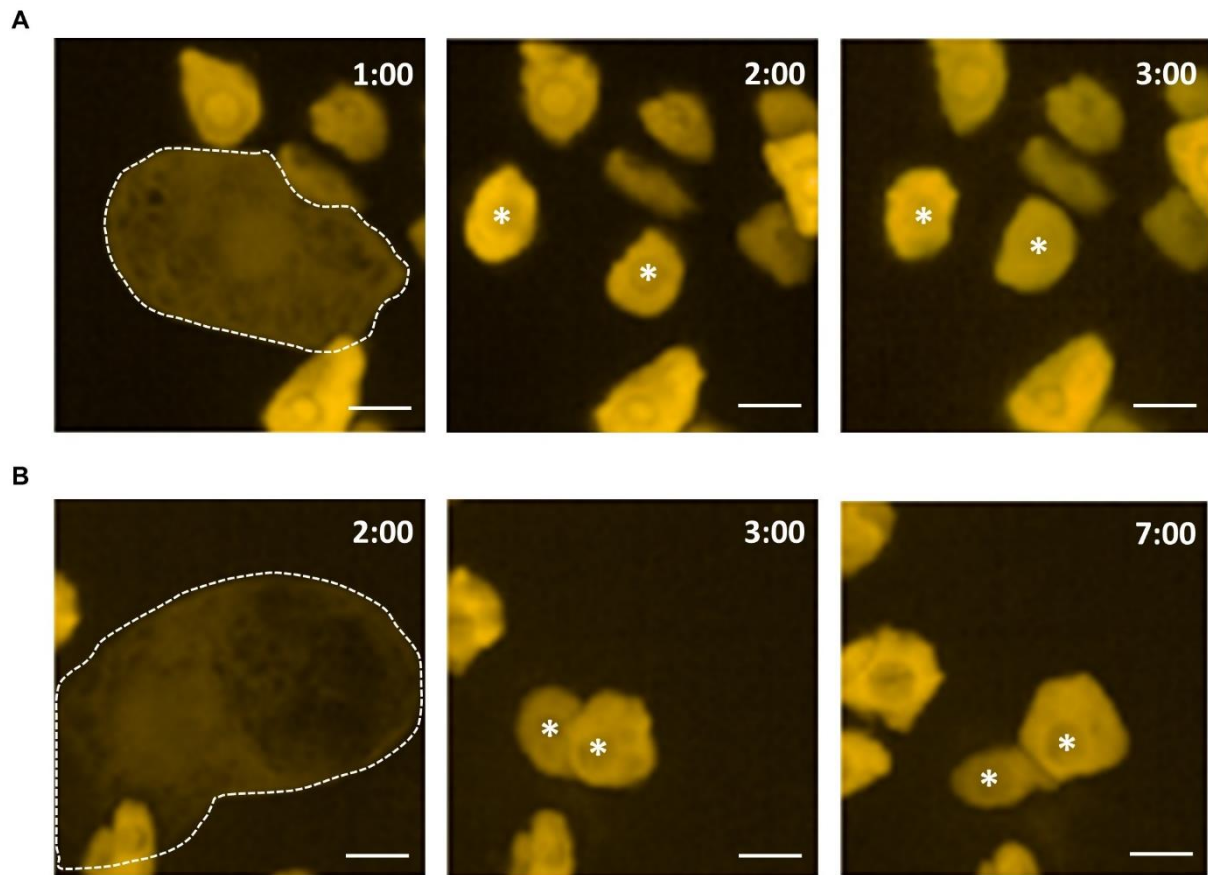
Figure 5. Nuclear separation defect occurs upon loss-of-function of *NMig1*.
A. Confocal live imaging of *Arabidopsis thaliana* cell suspension culture PSB-D transformed with a T-DNA vector for CRISPR mutagenesis of *GLABRA1* as control and nuclear marker *p35S::mCherry-NLS* treated with 1 µM synthetic auxin naphthalene-1-acetic acid (NAA). Time after NAA application (in hours) is indicated in the right top corner. Dashed line estimates cell morphology before cell division event. Asterisk indicates nucleus. *mCherry-NLS* is displayed in yellow. Scale bar: 10 µm.
B. Confocal live imaging of *Arabidopsis thaliana* cell suspension culture PSB-D transformed with a T-DNA vector for CRISPR mutagenesis of *Nmig1* and nuclear marker *p35S::mCherry-NLS* treated with 1 µM synthetic auxin naphthalene-1-acetic acid (NAA). Time after NAA application (in hours) is indicated in the right top corner. Dashed line estimates cell morphology before cell division event. Asterisk indicates nucleus. *mCherry-NLS* is displayed in yellow. Scale bar: 10 µm.

We next investigated whether similar defects during cell division occur in *slr-1* representing a gain-of-function in an upstream regulator of *NMig1*. It has been reported that in *slr-1* and *arf7arf19* only after prolonged auxin treatment, polar movement of nuclei occurs in single xylem-pole pericycle cells resulting in asymmetric cell division in a single cell (De Rybel et al., 2010) as opposed to the regular paired asymmetric cell divisions in wild type. *In vivo* time-lapse analysis of *slr-1* roots treated with 10 µM NAA using a transgenic line with plasmalemma marker *p35S::LTI6B-GFP* and nuclear marker *p35S::H2B-YFP* was performed and confirmed the abnormal nuclear migration and asymmetric cell divisions in the xylem-pole pericycle as described before (Figure 6A; Supplemental movie 3) (De Rybel et al., 2010).

Interestingly, striking abnormalities occurred during cytokinesis (Figure 6A; Figure 6B; Figure S6; Supplemental movie 4). More specifically, a delay or inhibition of the separation of nuclei during the division of xylem-pole pericycle cells was observed, which resembles the cytokinetic phenotype observed in the *Arabidopsis* cell suspension culture upon loss-of-function of *NMig1*. This result provides evidence that *NMig1* acts in the same pathway as *SLR* and represents an important factor controlling nuclear migration during lateral root initiation (Figure 6C).
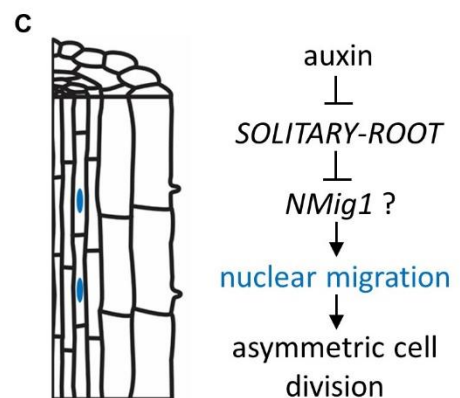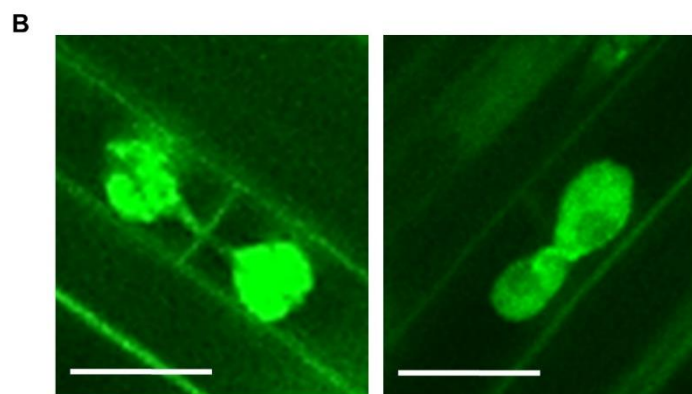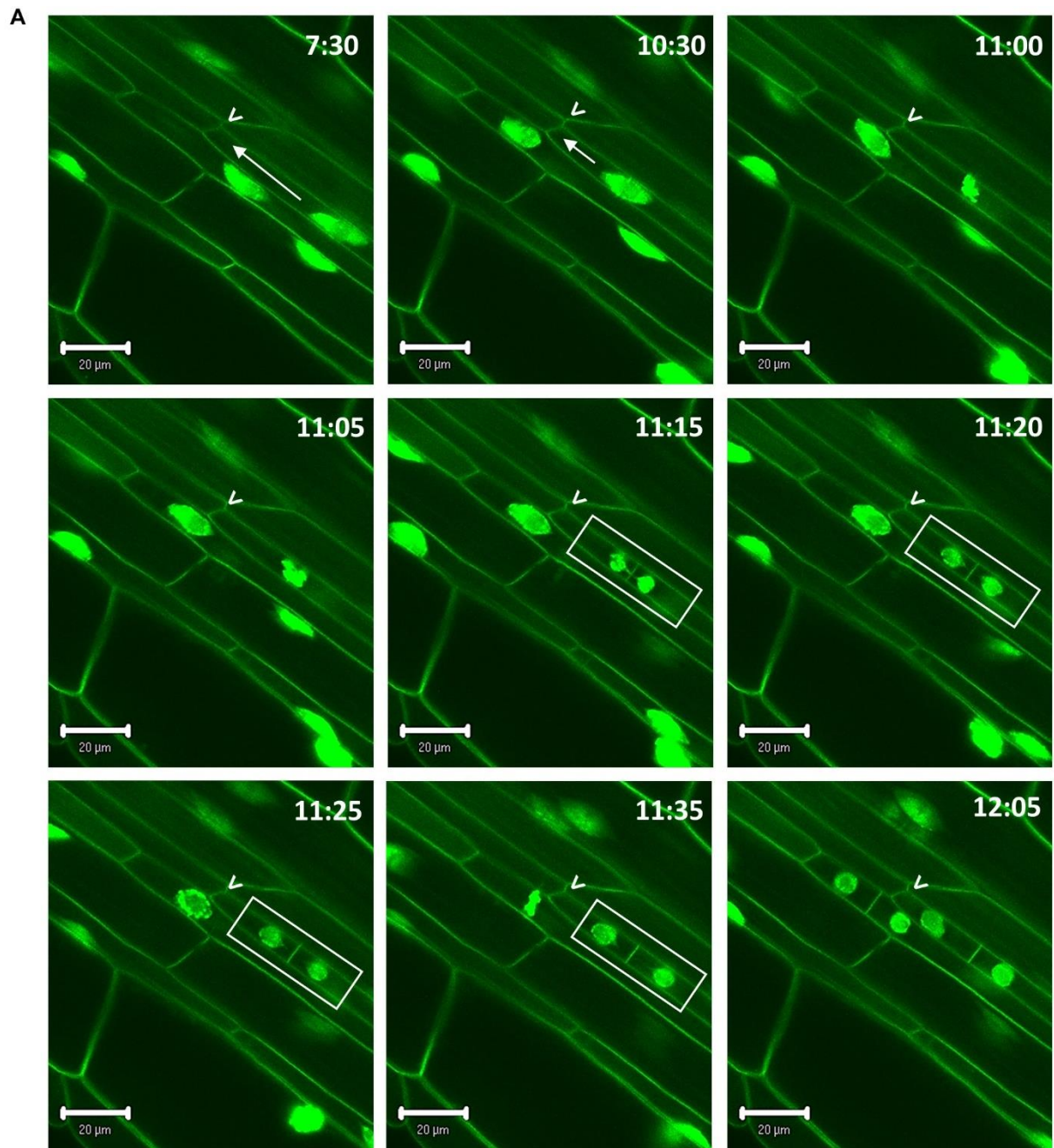
A

7:30   10:30   11:00
11:05   11:15   11:20
11:25   11:35   12:05

B

C

auxin

⊥

SOLITARY-ROOT

⊥

NMig1 ?

↓

nuclear migration

↓

asymmetric cell
division

Figure 6. Nuclear separation is affected in the lateral rootless mutant *solitary-root*.

A. Confocal live imaging of a nuclear migration event and subsequent cell division in the xylem-pole pericycle of *solitary-root* (*slr-1*) roots treated with 10 µM synthetic auxin naphthalene-1-acetic acid (NAA) using a transgenic line with plasmalemma marker *p35S::LTI6B-GFP* and nuclear marker *p35S::H2B-YFP*. Time after NAA application (in hours) is indicated in the right top corner. Arrow indicates movement of the nucleus; arrowhead indicates common cell wall; rectangle indicates nuclear separation defect. *GFP* and *YFP* is displayed in green. Scale bars: 20 µm.

B. Representative confocal images of nuclear separation defect in the xylem-pole pericycle of *solitary-root* (*slr-1*) roots treated with 10 µM synthetic auxin naphthalene-1-acetic acid (NAA) using a transgenic line with plasmalemma marker *p35S::LTI6B-GFP* and nuclear marker *p35S::H2B-YFP*. *GFP* and *YFP* is displayed in green. Scale bars: 10 µm.

C. Hypothetical model based on current observations: auxin likely acts upstream of *NMig1* in *SOLITARY-ROOT* dependent manner. *NMig1* might be necessary to mediate the nuclear movements (indicated in blue) necessary for asymmetric cell division at the onset on lateral root initiation. Formative cell divisions give rise to a new lateral root.

Discussion

Plants have evolved a wide range of strategies to take up plant growth-limiting resources, such as nitrogen, phosphorus, and water from the soil. The plasticity of roots to adapt to certain environmental conditions is phenomenal and relies on the availability of stem cells in the pericycle also referred to as founder cells that can form new lateral roots. Subsequent asymmetric cell divisions are essential to give rise to cell diversity and tissue patterns resulting in post-embryonic organogenesis. In lateral root initiation, the first asymmetric cell division is controlled by a nuclear migration event in lateral root founder cell pairs, which is an auxin-dependent process (De Rybel et al., 2010; De Smet et al., 2007).

In the absence of known regulators of nuclear migration in lateral root founder cells (apart from auxin signalling factors SLR/IAA14-ARF7-ARF19), a better understanding of this process has remained out of reach. Our study investigates the function of *Nuclear Migration1* (*NMig1*), an *Arabidopsis* homolog of the *Nuclear Distribution gene C* (*NudC*), which is structurally and functionally conserved in multicellular organisms and essential for nuclear migration (Fu et al., 2016). *NMig1* is specifically expressed in the primary root meristem and during lateral root development. Interestingly, *NMig1* is expressed in the basal half of progressing embryo stages, while a close homolog, *BOB1* is expressed primarily in the apical half which suggests a functional specialization during development (Jurkuta et al., 2009). Moreover, auxin induces expression of *NMig1* in het xylem-pole pericycle and is *SLR/IAA14-ARF7-ARF19* dependent. This expression pattern designates the function of *NMig1* at the onset of lateral root initiation.

In a next step, we were able to accomplish loss-of-function analysis of *NMig1* using CRISPR mutagenesis. Only heterozygous mutations could be detected in the open reading frame of *NMig1* and no homozygous mutants were identified in the progeny of the heterozygous mutant *nmig1-c1+/-* which pinpoints to a reproductive defect upon loss-of-function of *NMig1*. The involvement of *NMig1* in reproductive development is supported by the striking occurrence of unfertilized ovules in siliques of the *nmig1-c1+/-* mutant. Further research is needed, however, to determine whether the mutation is primarily affecting the male and/or female gametophyte. At least, for female gametogenesis, the importance of nuclei migration- and positioning for patterning the female gametophyte has been reported (Sprunck & Groß-Hardt, 2011).

Moreover, in the screening of the progeny of CRISPR plants for inherited mutations in *NMig1*, seedlings that lack basal body structures were observed which resemble mutants with patterning defects in the embryo. Genotyping provided evidence that these seedlings are heterozygous chimeras and appear to be correlated with severely obstructed embryogenesis. This is supported with the reported embryo-lethal phenotype for null alleles of *bob1* (Jurkuta et al., 2009) and the spatial expression pattern of *NMig1* in the basal half of progressing embryo stages. Complementary genetic approaches and in-depth analysis of the cell division patterns during embryonic development are needed to further elucidate the potential function of *NMig1* during embryogenesis.

Taken together, the defects upon loss-of-function of *NMig1* occur in developmental processes that strongly rely on correct asymmetric cell divisions. We further were able to carry out loss-

of-function analysis of *NMig1* during lateral root formation using lateral root-specific CRISPR mutagenesis (CRISPR-TSKO) (Decaestecker et al., 2019). *De novo* generation of mutations in *NMig1* at the onset of lateral root initiation results in lateral root developmental defects. This appears to be inversely correlated with the earlier reported positive effect on root growth and branching upon overexpression of *NMig1* (Velinov et al., 2020). Nevertheless, given the variability of CRISPR-TSKO in T1 seedlings, extensive analysis of lateral root phenotypic parameters in independent T2 lines is required to elucidate the function of *NMig*1 during lateral root development.

The molecular function of NMig1 hints towards a function as a scaffold protein by virtue of its molecular architecture that is similar to heat shock chaperones and its interaction with proteins involved in cell division and stress responses. In this respect, it is worth mentioning that a recent study hints for a function of HSP90 in cell-polarity establishment in the regulation of stomata formation (Samakovli et al., 2020). It will be interesting to study the function, interaction and regulation of these interactors specifically during lateral root initiation.

In a next step, we were able to specify more precisely the contribution of *NMig1* in nuclear migration during cell division through loss-of-function analysis of *NMig1* in *Arabidopsis* cell suspension culture using CRISPR mutagenesis. *In vivo* time lapse imaging revealed inhibition of nuclear separation during cell division suggesting a defect during exit from mitosis. This observation resembles the cytokinetic phenotype observed in mammalian cells upon NudC depletion (Aumais et al., 2003). Nevertheless, quantification of this observation is required to support the hypothesis that *NMig1* loss-of-function results in nuclear separation defects. Strikingly, similar defects occur during the division of xylem-pole pericycle cells in the lateral rootles mutant *slr-1*. In addition, auxin induces expression of *NMig1* in *SLR/IAA14-ARF7-ARF19* dependent manner. Therefore, it is tempting to consider that *NMig1* acts in the same pathway as *SLR* during lateral root initiation (Figure 6C).

In summary, our data demonstrate that the *NudC* homolog *NMig1* could be potentially considered as an essential gene for nuclear migration and asymmetric cell divisions in organogenesis. With the identification of *NMig1*, we provide a basis to decipher the molecular mechanisms that operate in the pericycle controlling the initial formative divisions essential for lateral root organogenesis. *De novo* formation of lateral roots is the let-off for plants to compensate their lack of mobility but to still be able to search for water and nutrients in the soil.

Acknowledgements

Material and Methods

Cloning and construction of expression vectors

To generate the *NLS-GFP-GUS* transcriptional reporter of *NMig1*, the promoter sequence of *NMig1* (1356 bp upstream of the start codon) was PCR-amplified and inserted into the donor vector pDONRP4-P1R (Invitrogen). The resulting Entry clone was subsequently recombined with the destination vector pEX-K7SNFm14GW (promoter-NLS-GUS/GFP) via the Gateway® LR reaction (Invitrogen) resulting in the Expression clone *pNMig1::NLS-GFP-GUS*, which consists of the *NMig1* promoter controlling the expression of a nuclear-localized GFP-GUS fusion protein (Karimi et al., 2007). The verified plasmid was then transferred into *Agrobacterium tumefaciens* strain C58C1 and the wild-type Col-0 plants were transformed using the floral dip method (Clough & Bent, 1998). Three independent homozygous T3 lines were identified by screening the transformants on medium containing kanamycin (50mg/L), and used for phenotypic analyses.

guideRNA design was conducted using the online available tool CRISPOR: http://crispor.tefor.net/. More information about the guideRNAs is available in supplementary experimental procedures. To generate the *nmig1-c1* mutant, oligos were annealed to build the spacer of the guideRNA targeting *NMig1*, which was cloned in the donor vector pEN-Chimera and subsequently recombined in the destination vector pDe-Cas9 by Gateway® LR reaction (Invitrogen) (Fauser et al., 2014).

To generate the CRISPR-TSKO vector, oligos were annealed to build the spacer of the guideRNA targeting *NMig1*, which was cloned via a Golden Gate reaction into pFASTR-pGATA23-Cas9-P2A-mCherry-G7T-AtU6-BsaI-CmR-ccdB-BsaI-gRNA scaffold (Decaestecker et al., 2019).

To generate the CRISPR vector for the *Arabidopsis* PSB-D cell suspension culture, oligos were annealed to build the spacer of the guideRNA targeting *Nmig1* or *GLABRA1*, which was cloned via a Golden Gate reaction into pK-mCherry-pPcUBI-Cas9-NLS-GreenGate-G7T-AtU6-26-BsaI-CmR-ccdB-BsaI.

Plant vectors were transformed in *Agrobacterium tumefaciens* C58C1 by electroporation. Transformation in wild-type or *pHTR5:NLS-GFP-GUS* was performed via the floral-dip method (Clough & Bent, 1998). For the constructs containing the FASTR marker, T1 transgenic seeds were selected under a Leica M165FC fluorescence stereomicroscope and for the construct containing an antibiotic selection marker, transgenic seedlings were selected on solid MS medium (Duchefa) with the appropriate selective agent.

Plant growing conditions and time-lapse experiments

Arabidopsis thaliana seeds were surface sterilized, stratified for 2 days in the dark at 4°C, and grown on half-strength Murashige and Skoog (1/2 MS) medium (pH 5,7) solidified with 1% agar (Murashige & Skoog, 1962). For all phenotypic analyses and time-lapse experiments, seedlings were vertically grown on square plates (Greiner Labortechnik) incubated in a growth

chamber under continuous light (110 µE/m^2/s photosynthetically active radiation supplied by cool-white fluorescent tungsten tubes; Osram) at 21°C.

Histochemical and histological analysis

GUS assays were performed as described previously (Fernandez et al., 2020). For microscopic analysis, samples were cleared by mounting in 90% lactic acid. All samples were analysed by differential interference contrast microscopy (Olympus BX51). For anatomical sections, GUS-stained samples were fixed overnight and embedded as described previously (De Smet et al., 2004).

Quantitative real-time PCR

Total RNA was extracted using the Trizol reagent (Invitrogen), followed by clean-up with RNeasy Mini Kit (Qiagen), including DNase I (Qiagen) treatment, according to the manufacturer's protocols. The quantity and quality of RNA samples were evaluated with Thermo Fisher Scientific NanoDrop 1000 Spectrophotometer. Complementary DNA (cDNA) was synthesized from 1 mg of total RNA with the iScript cDNA Synthesis Kit (Bio-Rad), according to the manufacturer's instructions. The quantitative PCR analysis was conducted using SyberGreen (Roche) and LightCycler real-time thermocycler (Roche). *EF1α* and *CDKA;1* were used as reference transcripts.

Quantitative assessment of CRISPR-generated mutations

The purified DNA samples were sent for Sanger sequencing (Eurofins Scientific) and TIDE (Tracking of Indels by Decomposition) analysis (software version 3.2.0) was performed to determine the frequency and type of mutations generated with the CRISPR system (Brinkman et al., 2014). In order to conduct PCR directly on plant samples, which was the case for the aberrant seedlings in the T2 generation as a result of CRISPR mutagenesis of *NMig1*, the Phire Plant Direct PCR Kit (ThermoFisher Scientific) was used.

Morphological characterization of roots

The number of emerged lateral roots was determined for every seedling using a binocular microscope, and root lengths were measured via ImageJ using digital images obtained by scanning the square plates. Lateral root density was calculated by dividing the emerged lateral root number by the primary root length.

Seed set score analysis

Seed set analysis was performed as described previously (Noble & Palanivelu, 2020).

In vivo root confocal Imaging

Fluorescent images were acquired on an inverted laser scanning confocal microscope Zeiss LSM 710 using the ZEN software package (Carl Zeiss, Germany) after excitation by a 488 nm

argon laser and detected using the bandpass 505–530 nm emission filter setting. Confocal images were processed with ImageJ software.

For long-term confocal observations, seedlings were placed into a chambered borosilicate cover glass system (Nalge Nunc International) with a block of agar over the roots. All supplements were added during the preparation of the agar blocks. The following transgenic lines was used in our observations: *slr-1* crossed with *p35S::LTI6B-GFP* and *p35S::H2B-YFP* (De Rybel et al., 2010). Temperature and light were kept as constant as possible during all observations. Fluorescence imaging of roots was performed with an Axiovert 100M confocal laser scanning microscope with software package LSM 510 version 3.2 (Zeiss). For excitation of GFP and YFP, the 488 nm line of an argon laser was used. Time-lapse series were typically collected at 4 minute intervals and lasted between 7 and 20 hours. Acquired images were processed and quantitatively analysed with ImageJ software.

In vivo cell culture confocal imaging

For long-term confocal observations, 50 µL of transformed *Arabidopsis* cell suspension culture PSB-D was transferred to a 96-well plate (Perkin Elmer Cell Carrier Ultra) and ½ diluted. All supplements were added to the wells in the 96-well plate (Perkin Elmer Cell Carrier Ultra). 10 µM of synthetic auxin 1-naphthaleneacetic acid. (NAA)

Temperature and light were kept as constant as possible during all observations. Fluorescence images of cells were acquired with the Opera Phenix in confocal mode. Image acquisition and analysis is performed with Harmony 4.9 (Perkin Elmer). For mCherry a 561 nm exitation laser and a bandpass 570-630 nm emission filter setting is used.

Statistical analysis

All values reported in this study are the means of at least two independent experiments with three replicates, unless otherwise stated. The significance of the results and statistical differences were analysed using Microsoft Excel for Office or GraphPad PRISM 8. The data were evaluated by multifactor analysis of variance and expressed as mean ± standard error. A p-value equal to or lower than 0,05 was considered statistically significant.

Accession numbers

The Arabidopsis Information Resource (TAIR) locus identifiers for the genes mentioned in this study are *AT5G58740* for *NMig1*, *AT5G53400* for *BOB1*, *AT4G27890* for *BOB2*, *AT4G14550* for *SLR/IAA14*, *AT5G20730* for *ARF7*, *AT1G19220* for *ARF19*, *AT5G26930* for *GATA23*, *AT3G27920* for *GLABRA1*, *AT3G45980* for *H2B*, *AT3G05890* for *LTI6B*, *AT1G07940* for *EF1α*, *AT3G48750* for *CDKA;1*, *AT3G52090* for *NRPD11*, *AT5G09810* for *ACTIN 7*, *AT2G20580* for *RPN1a*, *AT2G33210* for *HSP60* and *AT3G03773* for *CDC5*.

Supplemental information

A

B
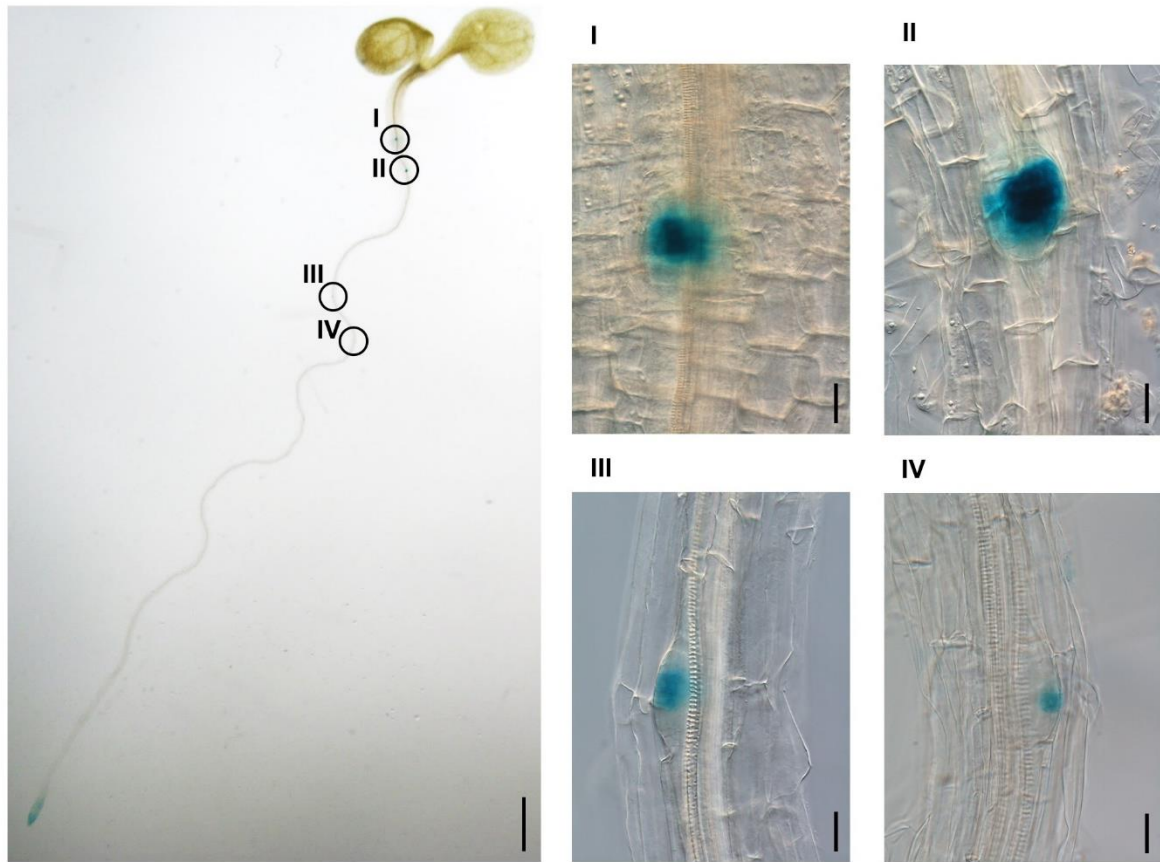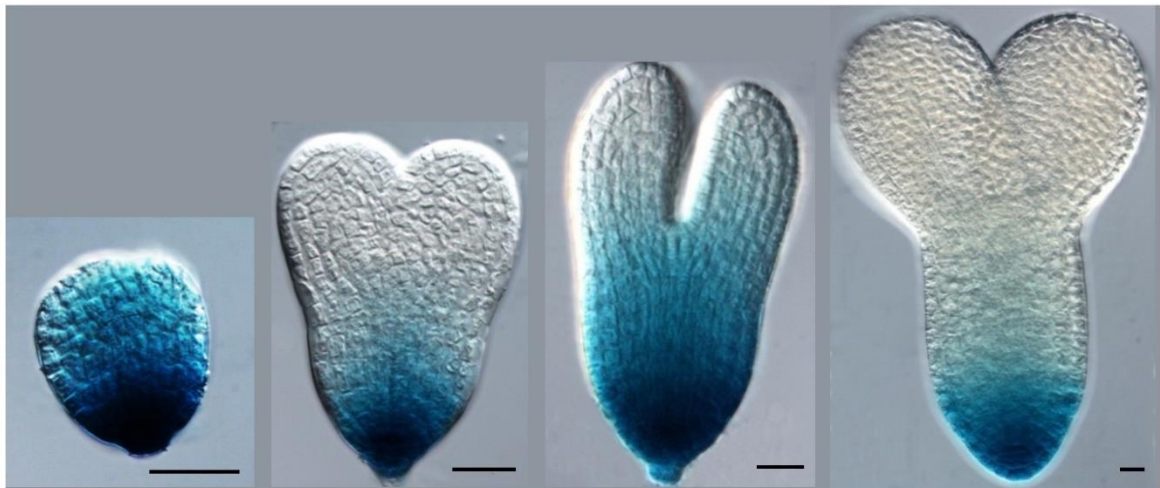
Supplemental Figure 1. *NMig1* is specifically expressed during lateral root development and embryogenesis in *Arabidopsis*.
A. Expression pattern of *pNMig1::NLS-GFP-GUS* in 5-day-old *Arabidopsis* seedling. Lateral root primordia presented at higher magnification are indicated with roman numerals. Scale bar left panel: 1 mm. Scale bars right panels: 20 μm.
B. Expression pattern of *pNMig1::NLS-GFP-GUS* in representative stages of embryogenesis in *Arabidopsis*. Scale bars: 20 μm.
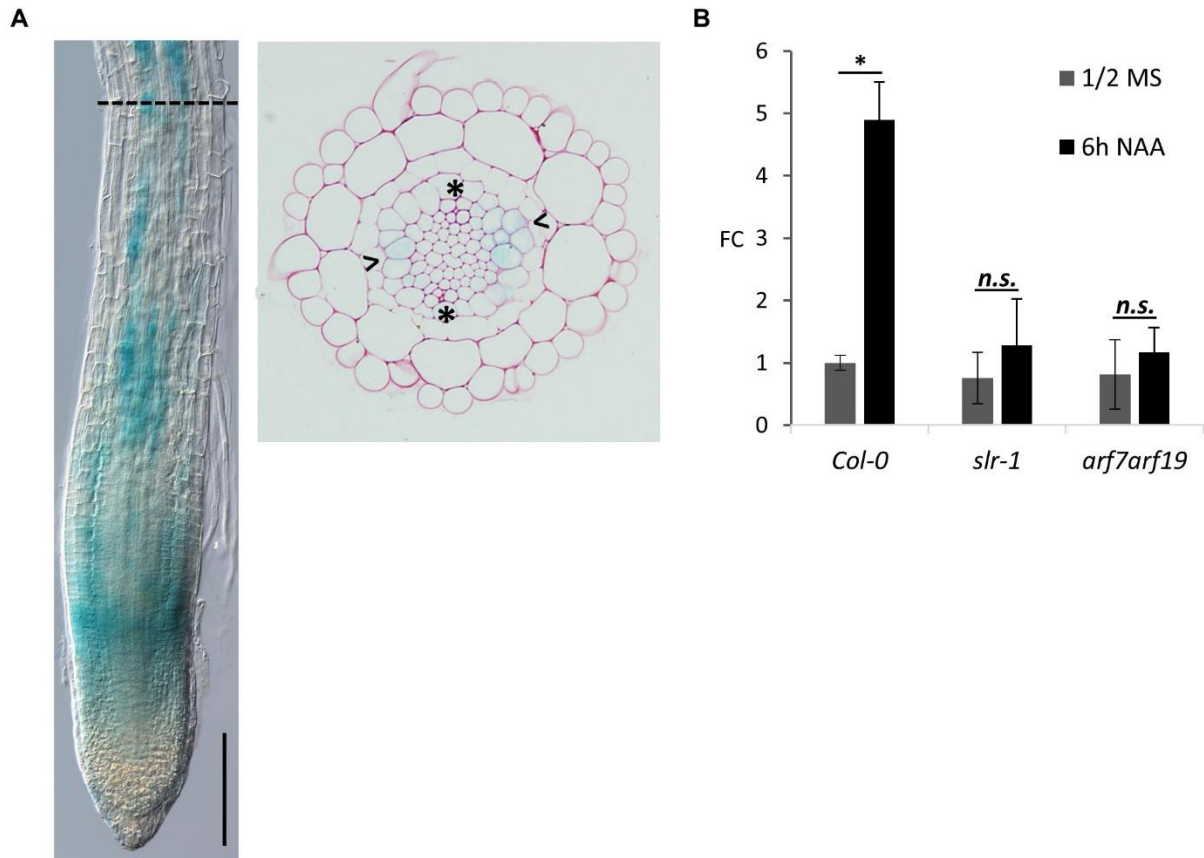
Supplemental Figure 2. Synthetic auxin 1-naphthaleneacetic acid induces *SLR/ARF7ARF19* dependent expression of *NMig1*.

A. Expression pattern of *pNMig1::NLS-GFP-GUS* in cross section of the primary root of 3-day-old *Arabidopsis* seedlings germinated on growth medium supplemented with 10 µM naphthylphthalamic acid (NPA) and subsequently treated for 6 hours with 10 µM of synthetic auxin 1-naphthaleneacetic acid (NAA). The horizontal black dashed line represents the location of the cross section. Asterisks and arrowheads indicate phloem pole and xylem-pole pericycle cells, respectively. Scale bar: 0,1 mm.

B. Transcript fold changes (FC) of *NMig1* in *Arabidopsis* roots of wild-type (Col-0), *slr-1* and *arf7arf19*. 3-day-old *Arabidopsis* seedlings (Col-0) germinated on ½ MS growth medium were treated for 6 hours (h) with 10 µM of synthetic auxin 1-naphthaleneacetic acid (NAA). Transcript fold changes were detected by quantitative real-time PCR. *EF1α* and *CDKA;1* were used as reference transcripts. Chart represents mean values ± standard error of two independent replicates. FC was compared between untreated and NAA-treated roots using a two-sided Student's *t*-test. * indicates p-values smaller than 0,05. n.s. indicates not significant with an α=0,05. n indicates the number of seedlings analysed.

A

**Wild-type NMig1**

MAEKLAPEKRHDFIHNGQKVFEWDQTLEEVNMYITLPPNVHPKSFHCKIQSKHIEVGIKGNPPYLNHDLSAPV
KTDCSFWTLEDDIMHITLQKREKGQTWASPILGQGQLDPYATDLEQKRLMLQRFQEENPGFDFSQAQFSGN
CPDPRSFMGGIRSD*

Hypothetical translated gene product nmig1-c1

MAEKLAPEKRHDFIHNGQKVFEWDQMFIQSHSTAKSSRNISKLASKATLPISITILVLL*RLIARSGL*RMI*CTLP
CRRGRKGKHGHHRFWDRVS*ILTPLILSRSGSCSRGFKKRTRDSTSRKLSSRVIVQIQGASWAVFVLT
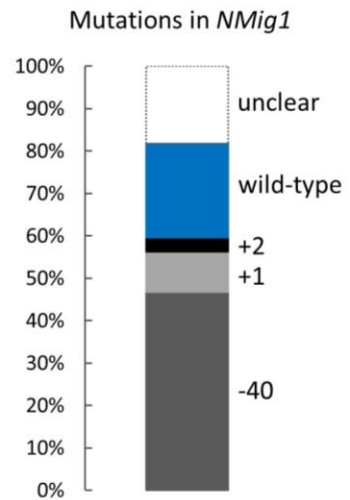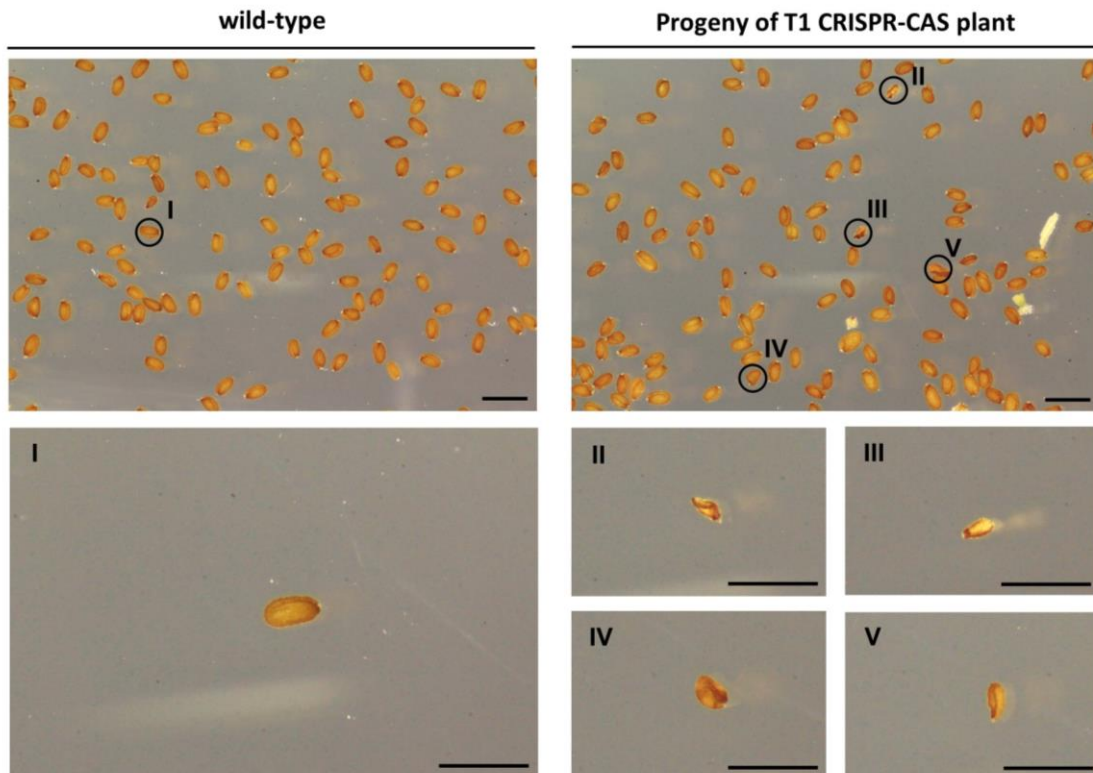
B

C

D

Mutations in *NMig1*

E
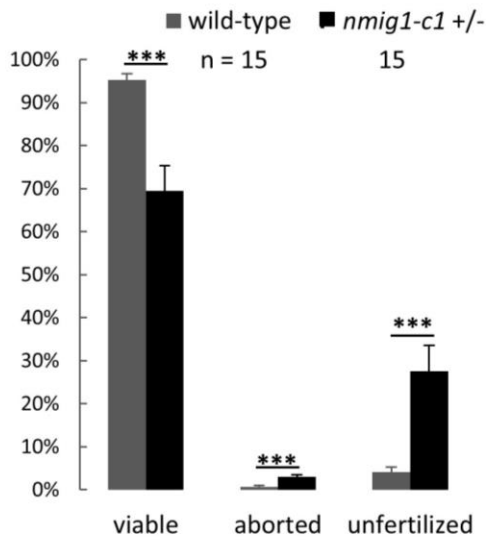
Supplemental Figure 3. CRISPR-generated loss-of-function mutant of *NMig1* reveals function in reproductive development in *Arabidopsis*.

A. Hypothetical protein sequence of CRISPR-generated *NMig1* mutant allele: *nmig1-c1*. Blue text: conserved NudC domain; Asterisk; stop codon; Strikethrough text: hypothetical untranslated amino acid sequence.

B. Quantification of seed set (unfertilized, viable or aborted) in siliques of *Arabidopsis* wild-type and heterozygous (+/-) *nmig1-c1* mutant seedlings. Chart represents mean value ± standard error. Seed set parameters were compared between wild-type and heterozygous (+/-) *nmig1-c1* mutant using a two-sided Student's *t*-test. *** indicates p-values smaller than 0,01. n.s. indicates not significant with an α=0,05. n indicates the number of siliques analysed.

C. Representative image of unfertilized (encircled) and viable ovules in a silique of *Arabidopsis* heterozygous (+/-) *nmig1-c1* mutant seedlings. Scale bar: 1 mm.

D. Quantitative assessment of CRISPR-generated mutations (%) by TIDE analysis of one of the T2 seedlings that lacks basal body structures. Chart represents proportion of wild-type –and CRISPR-generated mutant alleles. Note that a proportion of the sequences cannot be allocated ('unclear'). PCR confirmed that all T2 seedlings contain T-DNA construct (data not shown).

E. Images of seeds harvested of an *Arabidopsis* T1 plant harbouring the CRISPR T-DNA construct for mutagenesis of *NMig1*. Seeds presented at higher magnification are indicated with roman numerals. Scale bars: 1 mm.
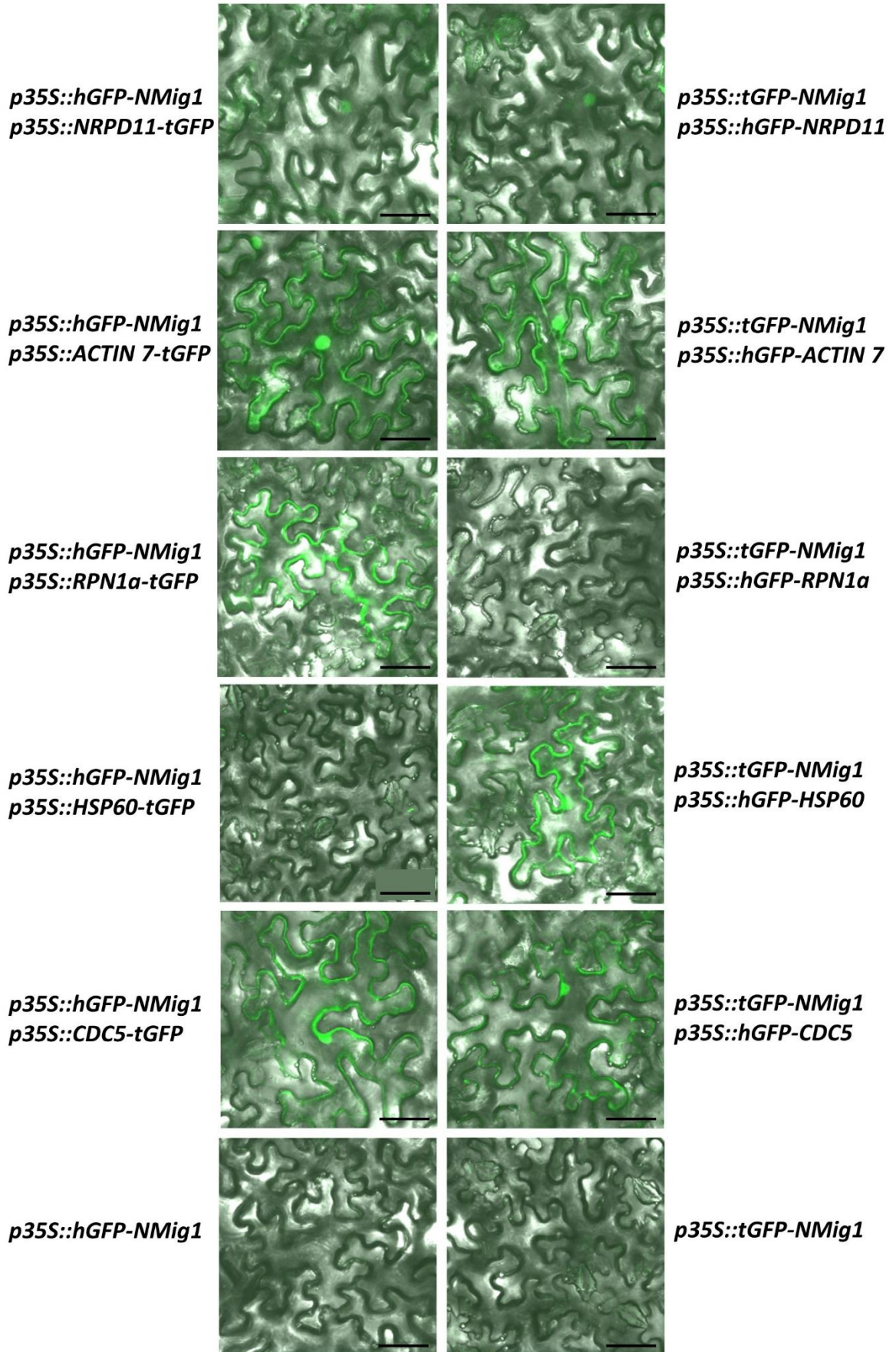
A
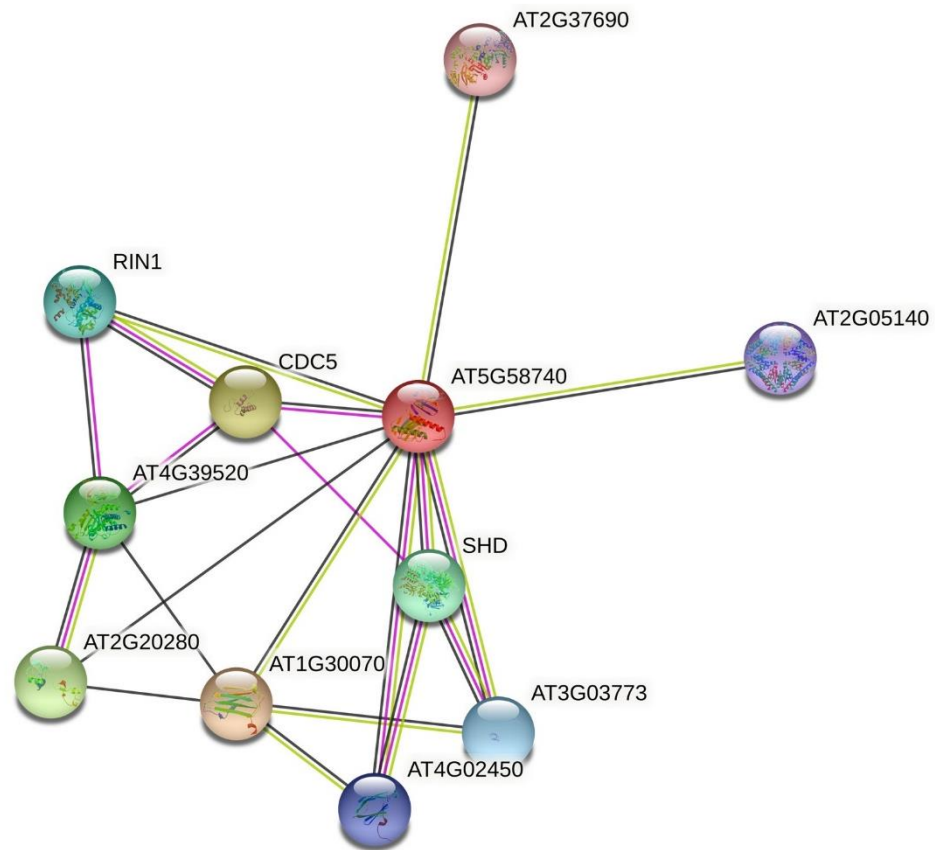
Supplemental Figure 4. STRING analysis of Nmig1.
A. Predicted network of protein-protein interactions of Nmig1 (*AT5G58740*) with NRPD11 (*AT3G52090*), ACTIN 7 (*AT5G09810*), RPN1a (*AT2G20580*), HSP60 (*AT2G33210*) and CDC5 (*AT3G03773*) using STRING analysis: https://string-db.org/.

A

p35S::hGFP-NMig1
p35S::NRPD11-tGFP

p35S::tGFP-NMig1
p35S::hGFP-NRPD11

p35S::hGFP-NMig1
p35S::ACTIN 7-tGFP

p35S::tGFP-NMig1
p35S::hGFP-ACTIN 7

p35S::hGFP-NMig1
p35S::RPN1a-tGFP

p35S::tGFP-NMig1
p35S::hGFP-RPN1a

p35S::hGFP-NMig1
p35S::HSP60-tGFP

p35S::tGFP-NMig1
p35S::hGFP-HSP60

p35S::hGFP-NMig1
p35S::CDC5-tGFP

p35S::tGFP-NMig1
p35S::hGFP-CDC5

p35S::hGFP-NMig1

p35S::tGFP-NMig1

Supplemental Figure 5. NMig1 interacts with proteins involved in cell division and stress responses. A. Confocal images of NMig1 interacting with NRPD11, ACTIN 7, RPN1a, HSP60 and CDC5 in *Nicotiana benthamiana* epidermal leaf cells using bimolecular fluorescence complementation. *Agrobacterium* containing p19 plasmid was co-infiltrated to enhance expression (Canto et al., 2006). *h/tGFP* is displayed in green. Panels at the bottom Scale bar: 50 μm.
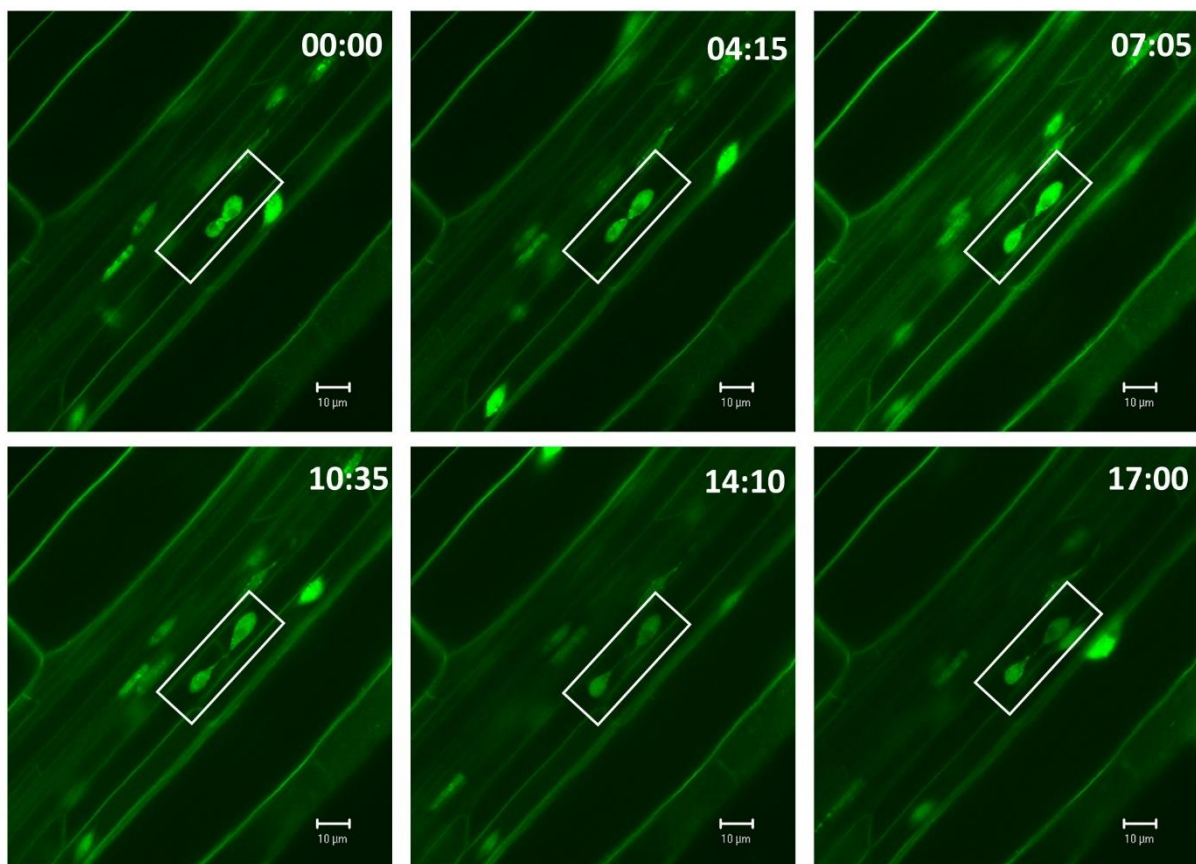
Supplemental Figure 6. Nuclear separation is affected in lateral rootles mutant *solitary-root*.
Confocal live imaging of a nuclear separation event in the xylem-pole pericycle of *solitary-root* (*slr-1*) roots treated with 10 μM synthetic auxin naphthalene-1-acetic acid (NAA) using a transgenic line with plasmalemma marker *p35S::LTI6B-GFP* and nuclear marker *p35S::H2B-YFP*. Time after auxin application (in hours) is indicated in the right top corner. Square indicates nuclear separation defect. *GFP* and *YFP* is displayed in green. Scale bar: 10 μm.

Supplemental movies are available upon request to the corresponding author

Supplemental movie 1: *In vivo* time-lapse recording of *Arabidopsis thaliana* cell suspension culture PSB-D transformed with a T-DNA vector for CRISPR mutagenesis of *GLABRA1* and nuclear marker *p35S::mCherry-NLS* treated with 1 µM synthetic auxin naphthalene-1-acetic acid (NAA). *mCherry-NLS* is displayed in yellow.

Supplemental movie 2: *In vivo* time-lapse recording of *Arabidopsis thaliana* cell suspension culture PSB-D transformed with a T-DNA vector for CRISPR mutagenesis of *NMig1* and nuclear marker *p35S::mCherry-NLS* treated with 1 µM synthetic auxin naphthalene-1-acetic acid (NAA). *mCherry-NLS* is displayed in yellow.

Supplemental movie 3. *In vivo* time-lapse recording of *solitary root* (*slr-1*) roots treated with 10 µM synthetic auxin naphthalene-1-acetic acid (NAA) using a transgenic line with plasmalemma marker *p35S::LTI6B-GFP* and nuclear marker *p35S::H2B-YFP*. *GFP* and *YFP* is displayed in green. Scale bar: 20 µm.

Supplemental movie 4. *In vivo* time-lapse recording of *solitary root* (*slr-1*) roots treated with 10 µM synthetic auxin naphthalene-1-acetic acid (NAA) using a transgenic line with plasmalemma marker *p35S::LTI6B-GFP* and nuclear marker *p35S::H2B-YFP*. *GFP* and *YFP* is displayed in green. Scale bar: 10 µm.

Supplemental experimental procedures

gRNA design

	spacer (5'-3')	target	strand	used for
gRNA1	gtgatcgatttcgccgggaa	5'UTR	forward	mutagenesis
gRNA2	ATTTGAGTGGGATCAAACCC	exon 2	forward	mutagenesis, TSKO, PSB-D cell culture

Primer sequences

Analysis CRISPR-generated mutations in *NMig1*:
Forward primer: gagtgttctactttggcgac
Reverse primer: CAGTCTTCACAGGAGCAC

Detection of T-DNA vector for CRISPR mutagenesis of *NMig1* in *Arabidopsis*:
Forward primer: TCCCAGGATTAGAATGATTAGG
Reverse primer: AAACGGGTTTGATCCCACTCAAAT

Analysis of potential off target mutations in *EMB2729***:**
Forward primer: GAAACGGCGCCTGGGAATC
Reverse primer: CAGAACCTGGACCCCAGTCC

Phire Plant Direct PCR protocol

20 µL PCR reaction: 1 µL forward primer (10 µM); 1 µL reverse primer (10 µM); 10 µL Phire Plant Direct PCR buffer; 8 µL PCR-grade water; 0,5 mm plant sample.

98 ˚C 5 minutes; (98 ˚C 5 seconds – 66 ˚C 5 seconds – 72 ˚C 20 seconds) 35 cycles; 72 ˚C final extension; 4 ˚C hold.

References

Aumais, J. P., Williams, S. N., Luo, W., Nishino, M., Caldwell, K. A., Caldwell, G. A., Lin, S.-H., & Yu-Lee, L.-y. (2003). Role for NudC, a dynein-associated nuclear movement protein, in mitosis and cytokinesis. *Journal of Cell Science, 116*(10), 1991. https://doi.org/10.1242/jcs.00412

Benková, E., Michniewicz, M., Sauer, M., Teichmann, T., Seifertová, D., Jürgens, G., & Friml, J. (2003). Local, Efflux-Dependent Auxin Gradients as a Common Module for Plant Organ Formation. *Cell, 115*(5), 591-602. https://doi.org/https://doi.org/10.1016/S0092-8674(03)00924-3

Botër, M., Amigues, B., Peart, J., Breuer, C., Kadota, Y., Casais, C., Moore, G., Kleanthous, C., Ochsenbein, F., Shirasu, K., & Guerois, R. (2007). Structural and Functional Analysis of SGT1 Reveals That Its Interaction with HSP90 Is Required for the Accumulation of Rx, an R Protein Involved in Plant Immunity. *The Plant Cell, 19*(11), 3791. https://doi.org/10.1105/tpc.107.050427

Brinkman, E. K., Chen, T., Amendola, M., & van Steensel, B. (2014). Easy quantitative assessment of genome editing by sequence trace decomposition. *Nucleic Acids Research, 42*(22), e168-e168. https://doi.org/10.1093/nar/gku936

Canto, T., Uhrig, J. F., Swanson, M., Wright, K. M., & MacFarlane, S. A. (2006). Translocation of Tomato Bushy Stunt Virus P19 Protein into the Nucleus by ALY Proteins Compromises Its Silencing Suppressor Activity. *Journal of Virology, 80*(18), 9064. https://doi.org/10.1128/JVI.00953-06

Clough, S. J., & Bent, A. F. (1998). Floral dip: a simplified method for Agrobacterium - mediated transformation of Arabidopsis thaliana. *The Plant Journal, 16*(6), 735-743. https://doi.org/10.1046/j.1365-313x.1998.00343.x

Crombez, H., Roberts, I., Vangheluwe, N., Motte, H., Jansen, L., Beeckman, T., & Parizot, B. (2016). Lateral Root Inducible System in Arabidopsis and Maize. *Journal of visualized experiments : JoVE*(107), e53481-e53481. https://doi.org/10.3791/53481

Cunniff, J., Chiu, Y.-H., Ron Morris, N., & Warrior, R. (1997). Characterization of DnudC, the Drosophila homolog of an Aspergillus gene that functions in nuclear motility. *Mechanisms of Development, 66*(1), 55-68. https://doi.org/https://doi.org/10.1016/S0925-4773(97)00085-3

Dawe, A. L., Caldwell, K. A., Harris, P. M., Morris, R. N., & Caldwell, G. A. (2001). Evolutionarily conserved nuclear migration genes required for early embryonic development in Caenorhabditis elegans. *Development Genes and Evolution, 211*(8), 434-441. https://doi.org/10.1007/s004270100176

De Rybel, B., Vassileva, V., Parizot, B., Demeulenaere, M., Grunewald, W., Audenaert, D., Van Campenhout, J., Overvoorde, P., Jansen, L., Vanneste, S., Möller, B., Wilson, M., Holman, T., Van Isterdael, G., Brunoud, G., Vuylsteke, M., Vernoux, T., De Veylder, L.,

Inzé, D., Weijers, D., Bennett, M. J., & Beeckman, T. (2010). A Novel Aux/IAA28 Signaling Cascade Activates GATA23-Dependent Specification of Lateral Root Founder Cell Identity. *Current Biology, 20*(19), 1697-1706. https://doi.org/https://doi.org/10.1016/j.cub.2010.09.007

De Smet, I., Chaerle, P., Vanneste, S., De Rycke, R., Inzé, D., & Beeckman, T. (2004). An easy and versatile embedding method for transverse sections. *Journal of Microscopy, 213*(1), 76-80. https://doi.org/10.1111/j.1365-2818.2004.01269.x

De Smet, I., Tetsumura, T., De Rybel, B., Frey, N. F. d., Laplaze, L., Casimiro, I., Swarup, R., Naudts, M., Vanneste, S., Audenaert, D., Inzé, D., Bennett, M. J., & Beeckman, T. (2007). Auxin-dependent regulation of lateral root positioning in the basal meristem of Arabidopsis. *Development, 134*(4), 681. https://doi.org/10.1242/dev.02753

Decaestecker, W., Buono, R. A., Pfeiffer, M. L., Vangheluwe, N., Jourquin, J., Karimi, M., Van Isterdael, G., Beeckman, T., Nowack, M. K., & Jacobs, T. B. (2019). CRISPR-TSKO: A Technique for Efficient Mutagenesis in Specific Cell Types, Tissues, or Organs in Arabidopsis. *The Plant Cell, 31*(12), 2868. https://doi.org/10.1105/tpc.19.00454

Dubrovsky, J. G., Sauer, M., Napsucialy-Mendivil, S., Ivanchenko, M. G., Friml, J., Shishkova, S., Celenza, J., & Benková, E. (2008). Auxin acts as a local morphogenetic trigger to specify lateral root founder cells. *Proceedings of the National Academy of Sciences, 105*(25), 8790. https://doi.org/10.1073/pnas.0712307105

Fauser, F., Schiml, S., & Puchta, H. (2014). Both CRISPR/Cas-based nucleases and nickases can be used efficiently for genome engineering in Arabidopsis thaliana. *The Plant Journal, 79*(2), 348-359. https://doi.org/10.1111/tpj.12554

Fernandez, A. I., Vangheluwe, N., Xu, K., Jourquin, J., Claus, L. A. N., Morales-Herrera, S., Parizot, B., De Gernier, H., Yu, Q., Drozdzecki, A., Maruta, T., Hoogewijs, K., Vannecke, W., Peterson, B., Opdenacker, D., Madder, A., Nimchuk, Z. L., Russinova, E., & Beeckman, T. (2020). GOLVEN peptide signalling through RGI receptors and MPK6 restricts asymmetric cell division during lateral root initiation. *Nature Plants, 6*(5), 533-543. https://doi.org/10.1038/s41477-020-0645-z

Fu, Q., Wang, W., Zhou, T., & Yang, Y. (2016). Emerging roles of NudC family: from molecular regulation to clinical implications. *Science China Life Sciences, 59*(5), 455-462. https://doi.org/10.1007/s11427-016-5029-2

Garcia-Ranea, J. A., Mirey, G., Camonis, J., & Valencia, A. (2002). p23 and HSP20/α-crystallin proteins define a conserved sequence domain present in other eukaryotic protein families. *FEBS Letters, 529*(2-3), 162-167. https://doi.org/10.1016/S0014-5793(02)03321-5

Goh, T., Joi, S., Mimura, T., & Fukaki, H. (2012). The establishment of asymmetry in Arabidopsis lateral root founder cells is regulated by LBD16/ASL18 and related LBD/ASL proteins. *Development, 139*(5), 883. https://doi.org/10.1242/dev.071928

Himanen, K., Boucheron, E., Vanneste, S., de Almeida Engler, J., Inzé, D., & Beeckman, T. (2002). Auxin-Mediated Cell Cycle Activation during Early Lateral Root Initiation. *The Plant Cell, 14*(10), 2339-2351. https://doi.org/10.1105/tpc.004960

Jurkuta, R. J., Kaplinsky, N. J., Spindel, J. E., & Barton, M. K. (2009). Partitioning the Apical Domain of the Arabidopsis Embryo Requires the BOBBER1 NudC Domain Protein. *The Plant Cell, 21*(7), 1957. https://doi.org/10.1105/tpc.108.065284

Kajala, K., Ramakrishna, P., Fisher, A., C. Bergmann, D., De Smet, I., Sozzani, R., Weijers, D., & Brady, S. M. (2014). Omics and modelling approaches for understanding regulation of asymmetric cell divisions in arabidopsis and other angiosperm plants. *Annals of Botany, 113*(7), 1083-1105. https://doi.org/10.1093/aob/mcu065

Karimi, M., Depicker, A., & Hilson, P. (2007). Recombinational Cloning with Plant Gateway Vectors. *Plant Physiology, 145*(4), 1144. https://doi.org/10.1104/pp.107.106989

Lee, Y.-T., Jacob, J., Michowski, W., Nowotny, M., Kuznicki, J., & Chazin, W. J. (2004). Human Sgt1 binds HSP90 through the CS domain and not the TPR domain. *Journal of Biological Chemistry*. http://www.jbc.org/content/early/2004/02/03/jbc.M400215200.short

Malamy, J. E., & Benfey, P. N. (1997). Organization and cell differentiation in lateral roots of Arabidopsis thaliana. *Development, 124*(1), 33. http://dev.biologists.org/content/124/1/33.abstract

Mayer, U., Ruiz, R. A. T., Berleth, T., Miséra, S., & Jürgens, G. (1991). Mutations affecting body organization in the Arabidopsis embryo. *Nature, 353*(6343), 402-407. https://doi.org/10.1038/353402a0

Morris, S. M., Anaya, P., Xiang, X., Morris, N. R., May, G. S., & Yu-Lee, L.-y. (1997). A Prolactin-Inducible T Cell Gene Product Is Structurally Similar to the Aspergillus nidulans Nuclear Movement Protein NUDC. *Molecular Endocrinology, 11*(2), 229-236. https://doi.org/10.1210/mend.11.2.9892

Murashige, T., & Skoog, F. (1962). A revised medium for rapid growth and bio assays with tobacco tissue cultures. *Physiologia plantarum, 15*(3), 473-497.

Noble, J. A., & Palanivelu, R. (2020). Workflow to Characterize Mutants with Reproductive Defects. In A. Geitmann (Ed.), *Pollen and Pollen Tube Biology: Methods and Protocols* (pp. 109-128). Springer US. https://doi.org/10.1007/978-1-0716-0672-8_8

Oppenheimer, D. G., Herman, P. L., Sivakumaran, S., Esch, J., & Marks, M. D. (1991). A gene required for leaf trichome differentiation in Arabidopsis is expressed in stipules. *Cell, 67*(3), 483-493. https://doi.org/10.1016/0092-8674(91)90523-2

Osmani, A. H., Osmani, S. A., & Morris, N. R. (1990). The molecular cloning and identification of a gene product specifically required for nuclear movement in Aspergillus nidulans. *Journal of Cell Biology, 111*(2), 543-551. https://doi.org/10.1083/jcb.111.2.543

Parizot, B., Laplaze, L., Ricaud, L., Boucheron-Dubuisson, E., Bayle, V., Bonke, M., De Smet, I., Poethig, S. R., Helariutta, Y., Haseloff, J., Chriqui, D., Beeckman, T., & Nussaume, L. (2008). Diarch Symmetry of the Vascular Bundle in Arabidopsis Root Encompasses the Pericycle and Is Reflected in Distich Lateral Root Initiation. *Plant Physiology, 146*(1), 140. https://doi.org/10.1104/pp.107.107870

Perez, D. E., Hoyer, J. S., Johnson, A. I., Moody, Z. R., Lopez, J., & Kaplinsky, N. J. (2009). BOBBER1 Is a Noncanonical Arabidopsis Small Heat Shock Protein Required for Both Development and Thermotolerance. *Plant Physiology, 151*(1), 241. https://doi.org/10.1104/pp.109.142125

Samakovli, D., Tichá, T., Vavrdová, T., Ovečka, M., Luptovčiak, I., Zapletalová, V., Kuchařová, A., Křenek, P., Krasylenko, Y., Margaritopoulou, T., Roka, L., Milioni, D., Komis, G., Hatzopoulos, P., & Šamaj, J. (2020). YODA-HSP90 Module Regulates Phosphorylation-Dependent Inactivation of SPEECHLESS to Control Stomatal Development under Acute Heat Stress in Arabidopsis. *Molecular Plant, 13*(4), 612-633. https://doi.org/https://doi.org/10.1016/j.molp.2020.01.001

Sprunck, S., & Groß-Hardt, R. (2011). Nuclear behavior, cell polarity, and cell specification in the female gametophyte. *Sexual Plant Reproduction, 24*(2), 123-136. https://doi.org/10.1007/s00497-011-0161-4

ten Hove, C. A., Lu, K.-J., & Weijers, D. (2015). Building a plant: cell fate specification in the early Arabidopsis embryo. *Development, 142*(3), 420. https://doi.org/10.1242/dev.111500

Vanneste, S., De Rybel, B., Beemster, G. T. S., Ljung, K., De Smet, I., Van Isterdael, G., Naudts, M., Iida, R., Gruissem, W., Tasaka, M., Inzé, D., Fukaki, H., & Beeckman, T. (2005). Cell Cycle Progression in the Pericycle Is Not Sufficient for SOLITARY ROOT/IAA14-Mediated Lateral Root Initiation in Arabidopsis thaliana. *The Plant Cell, 17*(11), 3035. https://doi.org/10.1105/tpc.105.035493

Velinov, V., Vaseva, I., Zehirov, G., Zhiponova, M., Georgieva, M., Vangheluwe, N., Beeckman, T., & Vassileva, V. (2020). Overexpression of the NMig1 Gene Encoding a NudC Domain Protein Enhances Root Growth and Abiotic Stress Tolerance in Arabidopsis thaliana [Original Research]. *Frontiers in Plant Science, 11*(815). https://doi.org/10.3389/fpls.2020.00815

Zhou, T., Aumais, J. P., Liu, X., Yu-Lee, L.-Y., & Erikson, R. L. (2003). A Role for Plk1 Phosphorylation of NudC in Cytokinesis. *Developmental Cell, 5*(1), 127-138. https://doi.org/10.1016/S1534-5807(03)00186-2

Chapter 5: Concluding remarks and future perspectives

Vangheluwe N. & Beeckman T.

Abstract

Lateral root branching in plants is crucial for increasing the surface area of their root system to explore heterogeneous soil environments and cope with various stresses. Lateral root initiation is the event in which two adjacent xylem-pole pericycle cells, also referred to as founder cells undergo coordinated asymmetric divisions giving rise to cell diversity and tissue patterns resulting in the development of new lateral roots. The first visible event of lateral root initiation is the simultaneous migration of nuclei in neighbouring founder cells. The plant signalling molecule auxin is a major regulator, however, little is known on the molecular mechanisms at play at the initiation of a new lateral root and functional analysis of redundant or fundamentally important genes has been impeded because of a lack of knockout mutant alleles or as a consequence of mutant pleiotropic phenotypes. Recently, loss-of-function studies through generating inheritable or somatic mutations using CRISPR technology has opened new avenues for discovering and analysing gene functions in lateral root initiation, which provides an excellent model to answer fundamental developmental questions such as coordinated cell division, growth axis establishment as well as specification of cell fate and cell polarity. In addition, the adoption of new technologies impacts not only scientific research, but also society. For that reason, we provide *in addendum* a Science & Society manuscript on the societal implications of genome editing technology in plants and the role of researchers in science communication.

Root branching through lateral root formation is a major component of the adaptability of the root system to its environment and contributes to the survival strategies of plants. Regular spacing of lateral roots, as well as initiation and development of lateral root primordia is tightly regulated in *Arabidopsis*. However, lateral root development is influenced by external signals, guaranteeing that the root system architecture is highly adaptable to various environmental conditions. To achieve such strict regulation while maintaining a high degree of flexibility, lateral root development relies on dynamic regulatory networks, mediated by the exchange of molecular messengers over both short and long distances. In a developmental context, the study of lateral root initiation is intriguing because this process requires tight interplay between cell division and cell fate respecification. Initiation of a new post-embryonic organ commences with the specification of competent xylem-pole pericycle cells into lateral root founder cells and subsequently encompasses the activation of coordinated nuclear migration in these cells to the first asymmetric cell division. Finally, lateral root initiation is defined as being finished when the first formative divisions are accomplished and the proper daughter cell fates are established.

Auxin acts as a common integrator to many endogenous and environmental signals regulating lateral root development (Lavenus et al., 2013). Auxin controls and coordinates both lateral root founder cell divisions and founder cell polarity/identity specification during lateral root initiation. How and which molecular mechanisms auxin regulates during lateral root development are still poorly understood. This can be partly attributed to the pleiotropic effects upon loss- or gain-of-function of auxin genes, which impede functional studies in a developmental-specific context. Auxin biosynthesis, transport, signalling and response controls numerous aspects of plant development and plant responses to the environment. Moreover, at the onset of lateral root initiation, fundamental processes including coordinated cell division & nuclear migration, specification of cell fate and cell polarity are implicated. Hence, the specific cellular defects caused by mutations in essential genes steering these processes are challenging to investigate due to lethality in the gametophyte or embryonic stage.

In plant development, peptide signals relay information coordinating cell proliferation and differentiation and a multitude of peptide-receptor signalling pathways have been identified mediating both stimulatory and inhibitory effects on lateral root initiation (Jourquin et al., 2020). Peptides are often encoded by gene families and bind to corresponding families of receptors. More than 1000 signalling peptides have been predicted in the genome sequence of *Arabidopsis* indicating that peptide-derived intercellular communication is an important signalling mechanism in plants. Peptide-encoding genes are relatively small and as of consequence, the availability of loss-of-function alleles in *Arabidopsis* mutant collections is rather limited. In addition, peptide families are relatively large and functional redundancy within peptide families has often been reported (Jourquin et al., 2020). Hence, most of our knowledge about the activity of these peptides is based on gain-of-function studies. Further elucidation of the function of redundant peptides during development will require the analysis of higher-order mutants.

Genome editing in plants, mainly through CRISPR technology is a new tool with great potential to address the abovementioned limitations in genetic studies. Most CRISPR efforts to date have focused on generating stable and heritable mutant alleles for reverse genetics approaches, which has substantially contributed to study redundant gene families or genes for which no or limited number of mutant alleles are available. However, CRISPR technology is versatile and the use of cell-type, tissue, organ-specific promoters driving Cas9 expression has enabled the study of genes in specific developmental contexts via conditional gene knockouts. Through collaboration, we have devised a CRISPR tissue-specific knockout (CRISPR-TSKO) vector system and tested the potential of conditional gene knockouts in particular plant cell types, tissues, and organs in *Arabidopsis* (Decaestecker *et al.*, 2019).

This dissertation depicts in every research chapter new findings and insights in lateral root initiation obtained through the use of genome editing with CRISPR. The reported results highlight that loss-of-function studies by generating inheritable or somatic mutations using genome editing has considerably improved our genetic toolbox for discovering and analysing gene functions in lateral root development.

In **Chapter 2**, we revealed that GOLVEN (GLV) peptides act redundantly as inhibitors to restrain excess of asymmetric cell divisions taking place after lateral root founder cell specification. To study the role of *GLV6* in lateral root initiation, CRISPR was employed to generate heritable mutant alleles, hence, no loss-of-function mutants were available (Fernandez et al., 2015). Unfortunately, *glv6* mutants did not display any difference in root system architecture compared to wild-type. Subsequently, an available sextuple *glv* mutant generated by CRISPR was analysed to investigate functional redundancy (Peterson et al., 2016). We revealed that knocking out *GLV6* and *GLV10* genes resulted in increased lateral root initiation indicating that more of the founder cells undergo the first asymmetric cell division when GLV levels are low. A second asymmetric cell division happened more frequently in *glv* mutants than in the wild type as well. Together with the observation that *GLV6* and *GLV10* are both transcribed in founder cells and expression seems stronger in the central cells after the first asymmetric cell division, we propose a function for GLV6/10 signalling to spatially propagate lateral inhibition to the cells flanking the lateral root founder cells after they have been specified. Thereafter, the generation of GLV gradients and the direction of signalling might be important for patterning of the lateral root primordium as overexpression of *GLV6* equally in all cell layers results in pericycle cells undergoing symmetric divisions instead of no division at all (Fernandez et al., 2015). Taken together, we revealed how secreted GLV peptides may restrict initial asymmetric cell divisions taking place during lateral root initiation.

CRISPR mutagenesis of *GLV* genes has contributed to break functional redundancy and revealed that *GLV6* and *GLV10* act redundantly as inhibitors to restrain excess of asymmetric cell divisions during lateral root development. Interestingly, a multitude of peptide-receptor signalling pathways have been identified that affect lateral root initiation. In addition, the involvement of signalling peptides in lateral inhibition seems to coincide with a role during lateral root initiation (Jourquin et al., 2020). It is not clear whether peptides and receptors from different families can also act redundantly with one another because peptide-receptor pathways have until now mainly been studied separately. Future research should determine

whether functional overlap and crosstalk between different peptide-receptor pathways is present in the regulation of lateral root development. Therefore, it will be important to unravel the mechanisms that are mediated downstream of each peptide-receptor pair during lateral root development, information that is currently lacking for most peptide signalling pathways.

Several peptides and receptors are not expressed in xylem-pole pericycle cells nor lateral root primordia, which leaves the question how they affect lateral root development (Jourquin et al., 2020). More in-depth knowledge of when and where peptides are secreted and perceived is required to understand how peptide-receptor pathways function as mechanisms for intercellular communication. Visualisation of GLV peptides in roots would greatly contribute to investigate the hypothesis that the generation of GLV gradients and the direction of signalling is important for patterning of the lateral root primordium. Technical advances in the field of receptor-ligand pairing and *in planta* visualization by means of chemically-labelled ligands are essential. Constant efforts are made to develop new tags and fluorophores with stronger signal, sensitivity and wider application (Sharma & Russinova, 2018). There is an important role for chemists and plant biologists to work closely together and to develop new chemical tools that can be used to study peptide-receptor signalling in plants.

It will be interesting to investigate the involvement of other peptide-receptor pathways in lateral root development. The *Arabidopsis* genome is estimated to encode more than 1000 signalling peptides and over 600 receptor-like kinases, of which only a fraction has been studied so far. CRISPR systems open avenues to knockout large, redundant gene families. In particular, the construction of large CRISPR libraries has driven the implementation of forward genetic screens in which mutations are permanently introduced at the genome-scale with high precision (Smith et al., 2017). However, the implementation of CRISPR screens to map and examine gene regulatory networks in plants has remained in its infancy. Many open questions persist on the best way to use and implement this technology. An overview of the current limitations that should be overcome, as well as some exciting possibilities that are not currently achievable with existing technologies was recently described (Gaillochet et al., 2020).

The generation of knockout plant lines via CRISPR genome editing technology has been widely adopted by researchers. Gene knockouts are efficiently obtained through CRISPR-induced deletions or frameshift mutations. The result of the introduced frameshift mutation is predicted based on the presence of a premature termination codon (PTC) in the expressed transcript, resulting in nonsense-mediated decay (NMD) of the messenger RNA (mRNA) and aberrant peptide products that are degraded. However, many current study designs do not further assess whether the induced frameshift mutation results in the complete loss of protein expression and activity that is expected. Recently, the effects of frameshift knockout mutations were systemically characterized in human cell lines and this analysis revealed that surprisingly about one third of the knockout lines still express the target protein, albeit the majority at reduced levels (Smits et al., 2019). In some cases, the detected protein products were truncated but preserved partial functionality (Smits et al., 2019). Two causal mechanisms have been identified: reinitiation of translation leading to N-terminally truncated target proteins or skipping of the edited exon leading to protein isoforms with internal sequence

deletions. The possible effects of frameshift knockout mutations on protein levels are summarized in the model below (Figure 1) (Smits et al., 2019). In summary, these findings highlight that the experimental design for CRISPR mutagenesis as well as the selection and validation of the generated mutant lines is pivotal for phenotype interpretation.
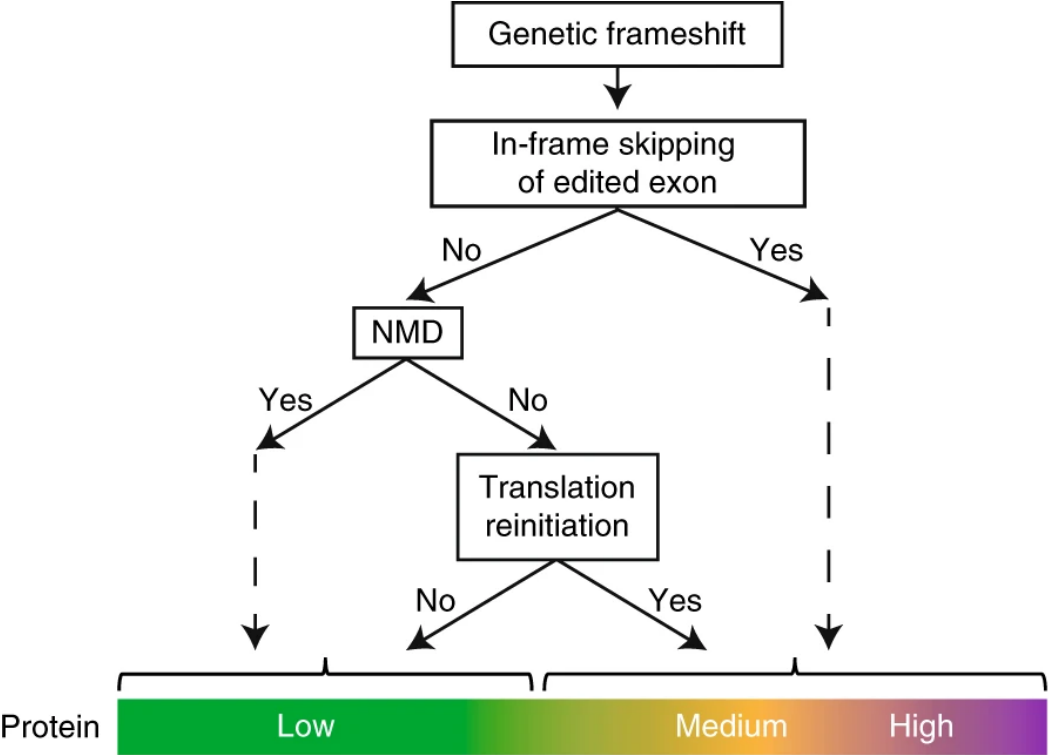

Figure 1. Model of the possible sequences of frameshift knockout mutations on protein levels. The first striking observation is the heterogeneity in nonsense-mediated decay (NMD) efficiency in the knockout lines. Both alternative splicing, which deletes the premature termination codon (PTC) from the transcript, and translation reinitiation appeared as causes for incomplete NMD efficiency. However, frameshift mutations can lead to full disruption of the protein despite no or weak NMD. The second striking observation is the residual protein expression observed in presumed knockout lines as a consequence of skipping of the frameshift mutation in the transcript by alternative splicing or as a consequence of translation reinitiation. Figure modified from Smits *et al*., 2019.

In **Chapter 3**, we demonstrated that A- and B1-subtype CYCLIN DEPENDENT KINASEs (CDKs) are concomitantly essential for lateral root organogenesis. Cell cycle activity at the onset of lateral root initiation is required for lateral root founder cells in the pericycle to undergo formative divisions resulting in the development of a lateral root primordium. Activation and progression through the major phases of the cell cycle are mediated by the control of CDKs. *CDKA;1* is the central regulator of cell cycle progression in *Arabidopsis*. Hence, loss-of-function of *CDKA;1* severely affects development and a better understanding of the function as well as potential redundancy with other CDK members has remained out of reach. Surprisingly, lateral root-specific CRISPR mutagenesis (CRISPR-TSKO) of *CDKA;1* did not affect lateral root branching (Decaestecker et al., 2019). This is a striking observation, considering the central function of CDKA;1 in the progression of the cell cycle. However, simultaneous knockout of *CDKA;1*, *CDKB1;1* and *CDKB1;2* arrested lateral root outgrowth soon after emergence. In addition, microscopic -and expression analysis revealed that morphogenesis of lateral roots is retained despite deficient cell cycle progression and poses the question how the distribution of intrinsic determinants is preserved during lateral root organogenesis. Conversely, it was shown that both cell cycle progression and cell identity specification is intertwined as overexpression of genes regulating G1 to S transition induces pericycle cell division in *solitary-root (slr)-1* but do not lead to formative cell divisions that normally precede the formation of a lateral root primordium (Vanneste et al., 2005). Through lateral root-specific knockouts of *CDKs* using CRISPR-TSKO, we present a tool to unravel the role of CDKs in cell cycle progression during lateral root organogenesis and address fundamental developmental questions such as coordinated cell division.

In **Chapter 4**, we investigated the function of *Nuclear Migration1* (*NMig1*). In lateral root initiation, the first asymmetric cell division is controlled by a nuclear migration event in lateral root founder cell pairs. We revealed that *NMig1* could be considered as a potential essential gene for nuclear migration in organogenesis. *NMig1* is specifically expressed in the primary root meristem and during lateral root development auxin treatment induces *SLR/IAA14-ARF7-ARF19*-dependent expression of *NMig1* in het xylem-pole pericycle. Loss-of-function analysis of *NMig1* was accomplished using CRISPR mutagenesis. Interestingly, only heterozygous mutants could be detected and no homozygous mutants were identified in the progeny. Moreover, a high number of unfertilized ovules in siliques of the heterozygous mutant were observed compared to wild-type. These observations indicate that *NMig1* is essential for reproductive development. In a next step, we were able to specify more precisely the contribution of *NMig1* in nuclear migration during cell division through CRISPR mutagenesis of *NMig1* in *Arabidopsis* cell suspension culture. *In vivo* time lapse imaging revealed inhibition of nuclear separation during cell division suggesting a defect during exit from mitosis. This resembles the cytokinetic phenotype observed in mammalian cells upon NudC depletion (Zhou et al., 2003). Strikingly, similar defects occur during the division of xylem-pole pericycle cells in the lateral rootles mutant *slr-1*. Although the data is preliminary, lateral root-specific CRISPR mutagenesis of *NMig1* indicates that *NMig1* is involved in lateral root development. Taken together, it is tempting to consider that *NMig1* acts in the same pathway as *SLR* during lateral root initiation. With the identification of *NMig1*, we provide a basis to decipher the

molecular mechanisms that operate in the pericycle controlling the initial formative divisions essential for lateral root organogenesis.

We have demonstrated that it is possible to knockout genes in entire lateral roots using the promoter sequence of *GATA23* to drive Cas9 expression (Decaestecker et al., 2019). Lateral root-specific knockouts of *CDKs* using CRISPR-mutagenesis revealed a redundant role for A- and B1-subtype CDKs in lateral root organogenesis. These mutant lines are convenient to investigate the cellular defects caused by depletion of CDK proteins in an easily accessible tissue. In addition, CRISPR-TSKO will contribute to study the function of *NMig1* in lateral root development, since we revealed that *NMig1* is essential in reproductive development. The CRISPR-TSKO system was developed and tested in collaboration with the research groups of Tom B. Jacobs and Moritz K. Nowack. We have experienced first-hand the advantages & limitations for the use of CRISPR-TSKO to study plant developmental processes.

An important consideration is that in the case of lateral roots, every *GATA23*-expressing founder cell will contribute individual mutations to the lateral root primordium. Therefore, unlike in ubiquitous, inheritable mutant approaches, no defined mutant alleles are generated. Most mutations are small insertions/deletions (indels) causing frame shifts and premature stop codons, but depending on the guideRNA, some will also lead to in-frame missense mutations. Despite this source of variation, we were able to observe knockout phenotypes of varying degrees for all of the genes investigated (Decaestecker et al., 2019). The indel spectrum was similar to those of the other tissue-types, with the 1 base pair insertion being the dominant repair outcome (Decaestecker et al., 2019).

CRISPR-TSKO enabled us to generate higher-order CDK mutant lateral roots with striking cell proliferation defects on otherwise wild-type plants. Interestingly, cell proliferation in the stele of lateral root-specific *cdka;1cdkb1;1cdkb1;2* mutant lateral roots appeared to be less affected than in the epidermis and cortex. Future research should determine whether this is caused by the differential turnover of CDK messenger RNA (mRNA) and/or proteins in different cell types or by the differential requirement of CDK activity in different root tissues. Alternatively, remaining CDK members might be able to partially compensate for *CDKA* and *CDKB1* loss-of-function in specific cell types. The versatility of CRISPR-TSKO allows to address these different scenarios (Decaestecker et al., 2019). In addition, many other central cell cycle or cell division regulators, of which no homozygous plants can be recovered, become amenable for detailed cellular investigation by CRISPR-TSKO.

Next to CDKs, auxin signalling factors *ARF7* and *ARF19* were targeted as lateral root initiation is strongly inhibited in *arf7arf19* double mutants. However, lateral root initiation was only mildly affected when *ARF7* and *ARF19* were knocked out in *GATA23*-expressing pericycle cells while an *arf7arf19* mutant is not capable in producing lateral roots (Decaestecker et al., 2019). This suggests that the function of ARF7 and ARF19 in lateral root founder cells is not essential for lateral root development and raises the question of when and in which cells of the primary root these ARFs are necessary for lateral root organogenesis. Alternatively, ARF7/ARF19 mRNA and/or protein may persist in *GATA23*-expressing cells long enough to promote lateral root initiation. This might be the case for the interpretation of the results for the CDKs as well because simultaneous lateral-root specific knockout of *CDKA;1*, *CDKB1;1* and *CDKB1;2* halts

lateral root development only soon after emergence. Future research should resolve this by testing other promoters active during lateral root development such as pXPP, which is specifically active in the xylem-pole pericycle (Schürholz et al., 2018) and by targeting fluorescently-tagged translational fusions to track their depletion upon knockout.

Nevertheless, these experiments demonstrated that conditional knockouts enable the functional study of genes in spatial and temporal contexts of plant development. As such, CRISPR-TSKO technology represents a powerful addition to the molecular genetics toolbox for plant biology research. Furthermore, an additional layer of conditionality was recently added by integrating the CRISPR technology with an XVE-based, cell-type-specific inducible system. This inducible CRISPR system enables efficient generation of target gene knockouts in desired cell types and at desired times in *Arabidopsis* (Wang et al., 2020). In summary, loss-of-function studies by generating inheritable or somatic mutations using genome editing opens avenues for discovering and analysing gene functions in lateral root development.

Decaestecker, W., Buono, R. A., Pfeiffer, M. L., Vangheluwe, N., Jourquin, J., Karimi, M., Van Isterdael, G., Beeckman, T., Nowack, M. K., & Jacobs, T. B. (2019). CRISPR-TSKO: A Technique for Efficient Mutagenesis in Specific Cell Types, Tissues, or Organs in Arabidopsis. *The Plant Cell, 31*(12), 2868. https://doi.org/10.1105/tpc.19.00454

Fernandez, A., Drozdzecki, A., Hoogewijs, K., Vassileva, V., Madder, A., Beeckman, T., & Hilson, P. (2015). The GLV6/RGF8/CLEL2 peptide regulates early pericycle divisions during lateral root initiation. *Journal of Experimental Botany, 66*(17), 5245-5256. https://doi.org/10.1093/jxb/erv329

Gaillochet, C., Develtere, W., & Jacobs, T. B. (2020). CRISPR Screens in Plants: Approaches, Guidelines, and Future Prospects. *The Plant Cell*, tpc.00463.02020. https://doi.org/10.1105/tpc.20.00463

Jourquin, J., Fukaki, H., & Beeckman, T. (2020). Peptide-Receptor Signaling Controls Lateral Root Development. *Plant physiology, 182*(4), 1645-1656. https://doi.org/10.1104/pp.19.01317

Lavenus, J., Goh, T., Roberts, I., Guyomarc'h, S., Lucas, M., De Smet, I., Fukaki, H., Beeckman, T., Bennett, M., & Laplaze, L. (2013). Lateral root development in Arabidopsis: fifty shades of auxin. *Trends in Plant Science, 18*(8), 450-458. https://doi.org/https://doi.org/10.1016/j.tplants.2013.04.006

Peterson, B. A., Haak, D. C., Nishimura, M. T., Teixeira, P. J. P. L., James, S. R., Dangl, J. L., & Nimchuk, Z. L. (2016). Genome-Wide Assessment of Efficiency and Specificity in CRISPR/Cas9 Mediated Multiple Site Targeting in Arabidopsis. *PLOS ONE, 11*(9), e0162169. https://doi.org/10.1371/journal.pone.0162169

Schürholz, A.-K., López-Salmerón, V., Li, Z., Forner, J., Wenzl, C., Gaillochet, C., Augustin, S., Barro, A. V., Fuchs, M., Gebert, M., Lohmann, J. U., Greb, T., & Wolf, S. (2018). A Comprehensive Toolkit for Inducible, Cell Type-Specific Gene Expression in Arabidopsis. *Plant physiology, 178*(1), 40. https://doi.org/10.1104/pp.18.00463

Sharma, I., & Russinova, E. (2018). Probing Plant Receptor Kinase Functions with Labeled Ligands. *Plant and Cell Physiology, 59*(8), 1520-1527. https://doi.org/10.1093/pcp/pcy092

Smith, I., Greenside, P. G., Natoli, T., Lahr, D. L., Wadden, D., Tirosh, I., Narayan, R., Root, D. E., Golub, T. R., Subramanian, A., & Doench, J. G. (2017). Evaluation of RNAi and CRISPR technologies by large-scale gene expression profiling in the Connectivity Map. *PLOS Biology, 15*(11), e2003213. https://doi.org/10.1371/journal.pbio.2003213

Smits, A. H., Ziebell, F., Joberty, G., Zinn, N., Mueller, W. F., Clauder-Münster, S., Eberhard, D., Fälth Savitski, M., Grandi, P., Jakob, P., Michon, A.-M., Sun, H., Tessmer, K., Bürckstümmer, T., Bantscheff, M., Steinmetz, L. M., Drewes, G., & Huber, W. (2019). Biological plasticity rescues target activity in CRISPR knock outs. *Nature Methods, 16*(11), 1087-1093. https://doi.org/10.1038/s41592-019-0614-5

Vanneste, S., De Rybel, B., Beemster, G. T. S., Ljung, K., De Smet, I., Van Isterdael, G., Naudts, M., Iida, R., Gruissem, W., Tasaka, M., Inzé, D., Fukaki, H., & Beeckman, T. (2005). Cell Cycle Progression in the Pericycle Is Not Sufficient for SOLITARY ROOT/IAA14-Mediated Lateral Root Initiation in Arabidopsis thaliana. *The Plant Cell, 17*(11), 3035. https://doi.org/10.1105/tpc.105.035493

Wang, X., Ye, L., Lyu, M., Ursache, R., Löytynoja, A., & Mähönen, A. P. (2020). An inducible genome editing system for plants. *Nature Plants, 6*(7), 766-772. https://doi.org/10.1038/s41477-020-0695-2

Zhou, T., Aumais, J. P., Liu, X., Yu-Lee, L.-Y., & Erikson, R. L. (2003). A Role for Plk1 Phosphorylation of NudC in Cytokinesis. *Developmental Cell, 5*(1), 127-138. https://doi.org/https://doi.org/10.1016/S1534-5807(03)00186-2

Acknowledgements

I am very happy that 6 years ago, I was accepted to take on the challenge as PhD candidate and teaching assistant to explore the hidden half of plants with the latest genetic tools. I would like to highlight that all the work described here is the result of the training, help, support and feedback I have received from many fellow researchers over the past years.

In a first step, I would like to thank my promoter Tom Beeckman to enable my roots to grow and develop as a person, lecturer, researcher and science communicator. You inspired me to open my scope, to work in a team, to present knowledge in creative narratives and to embrace not only your own but also other people's their strengths and weaknesses. In addition, I would like to thank Ana Fernandez for spending a considerable amount of her time to train and guide me. Your passion for science is phenomenal. Over the past years, many persons at VIB, UGent and in the Roots lab have come & gone and I am grateful that I could spend time together with you and built friendships.

I would also like to thank my parents, brother & sister and other family members for creating the environment that nurtured and stimulated my ambitions to undertake this journey. Last but not least, I would like to share that I am a very lucky guy to be together with you. Oana, you have been always there to have a good time with, to support, to give advice, to listen and to take care of me. Thank you with all my heart! And thank you to have welcomed Whitie to our home, her silly faces, meows and cuddles when she feels like it, bring us a lot of joy.

Additional publications

Lateral Root Inducible System in *Arabidopsis* and Maize

Crombez H., Roberts I., Vangheluwe N., Motte H., Jansen L., Beeckman T. & Parizot B.

Abstract

Lateral root development contributes significantly to the root system, and hence is crucial for plant growth. The study of lateral root initiation is however tedious, because it occurs only in a few cells inside the root and in an unpredictable manner. To circumvent this problem, a Lateral Root Inducible System (LRIS) has been developed. By treating seedlings consecutively with an auxin transport inhibitor and a synthetic auxin, highly controlled lateral root initiation occurs synchronously in the primary root, allowing abundant sampling of a desired developmental stage. The LRIS has first been developed for *Arabidopsis thaliana*, but can be applied to other plants as well. Accordingly, it has been adapted for use in maize (*Zea mays*). A detailed overview of the different steps of the LRIS in both plants is given. The combination of this system with comparative transcriptomics made it possible to identify functional homologs of *Arabidopsis* lateral root initiation genes in other species as illustrated here for the *CYCLIN B1;1* (*CYCB1;1)* cell cycle gene in maize. Finally, the principles that need to be taken into account when an LRIS is developed for other plant species are discussed.

CRISPR-TSKO facilitates efficient cell type-, tissue-, or organ-specific mutagenesis in Arabidopsis

Decaestecker W., Andrade Buono R., Pfeiffer M. L., Vangheluwe N., Jourquin J., Karimi M., Van Isterdael G., Beeckman T., Moritz N. K. & Jacobs T. B.

Abstract

Detailed functional analyses of many fundamentally important plant genes via conventional loss-of-function approaches are impeded by the severe pleiotropic phenotypes resulting from these losses. In particular, mutations in genes that are required for basic cellular functions and/or reproduction often interfere with the generation of homozygous mutant plants, precluding further functional studies. To overcome this limitation, we devised a clustered regularly interspaced short palindromic repeats (CRISPR)-based tissue-specific knockout system, CRISPR-TSKO, enabling the generation of somatic mutations in particular plant cell types, tissues, and organs. In Arabidopsis (*Arabidopsis thaliana*), CRISPR-TSKO mutations in essential genes caused well-defined, localized phenotypes in the root cap, stomatal lineage, or entire lateral roots. The modular cloning system developed in this study allows for the efficient selection, identification, and functional analysis of mutant lines directly in the first transgenic generation. The efficacy of CRISPR-TSKO opens avenues for discovering and analyzing gene functions in the spatial and temporal contexts of plant life while avoiding the pleiotropic effects of system-wide losses of gene function.

Overexpression of the *NMig1* Gene Encoding a NudC Domain Protein Enhances Root Growth and Abiotic Stress Tolerance in *Arabidopsis thaliana*

Velinov V., Vaseva I., Zehirov G., Zhiponova M., Georgieva M., Vangheluwe N., Beeckman T.& Vassileva V.

Abstract

The family of NudC proteins has representatives in all eukaryotes and plays essential evolutionarily conserved roles in many aspects of organismal development and stress response, including nuclear migration, cell division, folding and stabilization of other proteins. This study investigates an undescribed *Arabidopsis* homolog of the *Aspergillus nidulans NudC* gene, named *NMig1* (for *Nuclear Migration 1*), which shares high sequence similarity to other plant and mammalian *NudC*-like genes. Expression of *NMig1* was highly upregulated in response to several abiotic stress factors, such as heat shock, drought and high salinity. Constitutive overexpression of *NMig1* led to enhanced root growth and lateral root development under optimal and stress conditions. Exposure to abiotic stress resulted in relatively weaker inhibition of root length and branching in *NMig1*-overexpressing plants, compared to the wild-type Col-0. The expression level of antioxidant enzyme-encoding genes and other stress-associated genes was considerably induced in the transgenic plants. The increased expression of the major antioxidant enzymes and greater antioxidant potential correlated well with the lower levels of reactive oxygen species (ROS) and lower lipid peroxidation. In addition, the overexpression of *NMig1* was associated with strong upregulation of genes encoding heat shock proteins and abiotic stress-associated genes. Therefore, our data demonstrate that the *NudC* homolog *NMig1* could be considered as a potentially important target gene for further use, including breeding more resilient crops with improved root architecture under abiotic stress.

Give CRISPR a Chance: the GeneSprout Initiative

Vangheluwe N., Swinnen G., de Koning R., Meyer P., Houben M., Huybrechts M., Sajeev N., Rienstra J., Damian B.

Abstract

Did you know that a group of early-career researchers launched an initiative enabling open dialogue on new plant breeding techniques such as genome editing? We developed a wide-ranging initiative that aims to facilitate public engagement and provide a platform for young plant scientists to encourage participation in science communication.

Curriculum Vitae

Personalia

1 September 1991
Male, Belgian

Work experience

2014 – 2020   Doctoral researcher in the VIB-UGent Center For Plant Systems Biology (PSB)

- Fundamental research on lateral root development in *Arabidopsis thaliana*.
- Technical skills in advanced microscopy and genome editing with CRISPR.
- Trained in intellectual property and regulatory aspects of biotechnology.
- Research stay in Sofia (Bulgarian Academy of Sciences).
- Reviewed research proposals for funding at FWO and ERC.
- Coach of 4 Master students, 3 Bachelor students and 4 secondary school pupils.
- Lecturer of plant biodiversity, -developmental biology, -cell biology through workshops and practical sessions for Bachelor and Master students at UGent.
- Lab management: GLP standards and safety rules.

2013   Student worker in CropDesign NV. – a BASF Plant Science Company
Analysis of transformation events in rice using high-throughput PCR and Q-PCR.

Education

2012 – 2014   Master's Degree in Biochemistry and Biotechnology, great distinction
at the Faculty of Sciences, Ghent University

2009 – 2012   Bachelor's degree in Biochemistry and Biotechnology, distinction
at the Faculty of Sciences, Ghent University

Competences

Language skills		IT skills
Dutch	Mother tongue	Microsoft® Office 2019 Word with Endnote X9
English	C2	Microsoft® Office 2019 Excel
French	B2	Microsoft® Office 2019 PowerPoint
German	A2	Adobe Photoshop and ImageJ
Polish	A1	Basic programming in Unix for bioinformatics

Grants & awards

2019   Research Foundation Flanders (FWO) travel grant (K1A7519N) to attend the FASEB conference on the mechanisms in plant development, Olean (NY), US.

2017   Research Foundation Flanders (FWO) project (VS09516N) for research exchange of 10 days at the Bulgarian Academy of Sciences, Sofia, Bulgaria.

2017   Research Foundation Flanders (FWO) travel grant (K1C8917N) to attend the 5th European workshop on peptide signalling in plants, Helsingør, Denmark.

2014   Most meritorious student award: The Royal Flemish Chemical Society (KVCV) is the professional association of Flemish (bio)chemists and aims to bridge the gap between education, industry and society.

Participations

2019 –   Board member of the GeneSprout Initiative Belgium

2019 – 2020   Coach of practical sessions with PhD candidates and post-docs for the training Effective Oral Presentations hosted by Jean-Luc Doumont from Principae

2019   Presenter or exhibitor at science communication events: Fascination of Plants Day, Sound of Science, Pint of Science

2018 – 2020   Representative of the council of the Faculty of Sciences, Ghent University

2016 – 2018   Representative of the educational commission of Biotechnology, Ghent University

2014 – 2016   Chairman of the PhD committee in the VIB-UGent Center for Plant Systems Biology

2012 – 2014   Chairman of the student council of the Faculty of Sciences, Ghent University

2010 – 2014   Representative of the council of the Faculty of Sciences, Ghent University

2010 – 2014   Representative of the educational commission of Biotechnology, Ghent University

2010 – 2012   Volunteer worker in the youth, non-profit organisation "Kansen Voor Kinderen"

2008 – 2009   Chairman of the social-cultural organisation "Wereldcomité" at the secondary school Sint-Andreaslyceum Sint-Kruis (Brugge)

Conferences and workshops

2020	Invited speaker: "Crash introduction on genome editing". PlantEd training school: Regulatory Options for Genome Edited Plants, Brussels, Belgium.
2019	Invited speaker: "The potential of agricultural innovation to help adapting farming systems to climate change. The case of genome edited crops". European Parliament Farmers-Scientists network event, Brussels, Belgium.
2019	Invited speaker: "European research institutes jointly call for action: Give CRISPR a Chance!". 1st PlantEd conference (COST action CA18111), Novi Sad, Serbia.
2019	Presentation: "Lateral root specific gene knockouts through CRISPR/CAS". Lateral root workshop 2019, Louvain-La-Neuve, Belgium.
2019	Presentation: "Lateral root specific gene knockouts through CRISPR/CAS". FASEB conference on the mechanisms in plant development, Olean (NY), US.
2018	Poster: "Initiation of lateral root formation in Arabidopsis, one step at a time". 10th Symposium of the International Society of Root Research, Jerusalem, Israel.
2017	Presentation: "Unraveling the GOLVEN6 peptide signaling pathway during lateral root initiation in Arabidopsis". Lateral root workshop 2017, Montpellier, France.
2017	Presentation: "Peptide signalling during plant development, an emerging story from the roots". 5th EU workshop on peptide signalling in plants, Helsingør, Denmark.
2016	Presentation: "An EMS-mutagenesis screen to identify molecular components of the GOLVEN6 signalling pathway during lateral root initiation in Arabidopsis". 9th International PhD School Plant Development, Zellingen-Retzbach, Germany.
2016	Poster: "Generation of CRISPR/Cas9-mediated GLV6 knockouts in Arabidopsis". 4th EU workshop on peptide signalling in plants, Bischoffsheim, France.
2015	Presentation: "An EMS mutagenesis screen to identify molecular players of the GOLVEN6 signalling pathway during lateral root initiation in Arabidopsis". Lateral root workshop 2015, Heidelberg, Germany
2015	3rd EU workshop on peptide signalling in plants. Ghent, Belgium

-falowanie i spadanie-